



NBTE

Netherlands society for Biomaterials and Tissue Engineering

Program 30th Annual Meeting, 4 & 5 April 2022
at
Conference center De Werelt

Monday, 4th of April

Conference rooms: AIR (plenary) & FIRE (parallel)

09.00-9.50	<i>Conference assembly</i>
9.50-10.00	<i>Opening (room: AIR)</i>
10.00 – 10.45	<i>Good Morning NBTE with Rosanne Hertzberger (room: AIR) Panel discussion with NBTE pioneers and future authorities</i>

11.00 – 12.30 (10+2 min)	Oral Presentations Session 1 (AIR) <i>Supramolecular & Smart Polymeric Biomaterials</i> <i>Chair: Vasileios Trikalitis</i>	Oral Presentations Session 2 (FIRE) <i>Nanobiomaterials in Regenerative Medicine & Tissue Engineering</i> <i>Chair: Madison Ainsworth</i>
Topic Keynote (25+5 min)	Julieta Paez (University of Twente)	Sabine van Rijt (Maastricht University)
01 / 02	Laura Rijns Eindhoven University of Technology <i>Who wins? Synthetic supramolecular matrices based on the ureido- pyrimidinone (UPy) and benzene-1,3,5- tricarboxamide (BTA) motif</i>	Margo Terpstra UMC Utrecht <i>Bioink with cartilage ECM microfibers enables spatial control of capillary formation in 3D bioprinted constructs</i>
03 / 04	Celien Jacobs Eindhoven University of Technology <i>Osteoconductivity of UHMWPE fabric for a cervical artificial intervertebral disc - in vitro analysis</i>	Shivesh Anand MERLN - Maastricht University <i>Chitin Nanofibrils Modulate Mechanical and Inflammatory Response in Tympanic Membrane Scaffolds</i>
05 / 06	Martyna Nikody MERLN - Maastricht University <i>hMSCs response to polymer-calcium phosphate composite scaffolds containing zinc produced using additive manufacturing</i>	Lea Andrée Radboudumc, Nijmegen <i>The Effect of Surface Charge of Gelatin Nanoparticles on Cellular Internalization and Colloidal Gel Formation</i>

07 / 08	Marjan Hagelaars Eindhoven University of Technology <i>Directing Kidney Tubulogenesis Using Tunable Synthetic Matrices</i>	Ke Song MERLN - Maastricht University <i>Poly(lactic acid)Nano-hydroxyapatite Microcomposites for Bottom-Up Engineering of Bone Tissue</i>
09 / 10	Marc Falandt Utrecht University <i>Development of a thiol-ene gelatin-based bioresin for volumetric bioprinting</i>	Cansu Karakaya Eindhoven University of Technology <i>Mechanosensitive Notch Signalling is a Regulator of Strain-Mediated Changes in Vascular Smooth Muscle Cell Phenotype</i>

12.30 – 13.30	Lunch	
---------------	--------------	--

13.30 – 15.00	OPEN SCIENCE SESSION (AIR) <i>For early-stage researchers (PhD students & early post-docs)</i>	NBTE STAFF REUNION & POLICY (FIRE) <i>From mid-stage researcher onwards (post-docs and staff (AP, AOP, Prof))</i>
---------------	--	---

14.45 – 15.15	Coffee	
---------------	---------------	--

15.15 – 16.45 (10+2 min)	Oral Presentations Session 5 (AIR) <i>Biofabrication & Added manufacturing in Biomaterials & Tissue Engineering</i> <i>Chair: Johanna Husch</i>	Oral Presentations Session 6 (FIRE) <i>Enabling Technologies for Tissue Engineering & Regenerative Medicine</i> <i>Chair: Adrián Seijas Gamardo</i>
Topic Keynote (25+5 min)	Gosia Wlodarczyk-Biegun (University of Groningen)	Burcu Gumuscu Sefunc (Joining digitally) (Eindhoven University of Technology)
11 / 12	Alicia Damen Eindhoven University of Technology <i>Friction Reducing Ability of a Poly-L-Lysine and Dopamine Modified Hyaluronan Coating for Cartilage Resurfacing Implants</i>	Carlos Peniche Silva MERLN - Maastricht University <i>Establishment of a Rat Model for Enthesis Regeneration Studies</i>
13 / 14	Menghong Li University of Amsterdam <i>Biomimetic Calcium Phosphate coating on stainless steel</i>	Prasanna Padmanaban University of Twente <i>Revisiting ImageJ Automated quantification of vasculature properties using machine learning tools</i>
15 / 16	Paulina Núñez Bernal UMC Utrecht <i>Shaping hepatic organoids into functional metabolic biofactories through high-speed volumetric bioprinting</i>	Phanikrishna Sudarsanam Eindhoven University of Technology <i>High-throughput screening of topographies to mitigate fibrosis in glaucoma filtration surgery devices</i>
17 / 18	Magdalena Gladysz University of Groningen <i>Melt Electrowritten Artificial Trabecular Meshwork for Glaucoma Treatment</i>	Piotr Zielinski University of Groningen <i>Melt Electrowritten Scaffolds with Tunable Mechanical Properties for Interface Tissue Engineering</i>

19 / 20	Malin Becker University of Twente <i>Aqueous Two-Phase Enabled Low Viscosity 3D (LoV3D) Bioprinting of Living Matter</i>	Pardis Farjam University of Twente <i>Biomimetic Calcium Phosphate Coatings applied to poly(carbonate urethane) substrates</i>
16.50 – 17.15	Sponsor presentation Optics 11 Life (AIR) Mechanics Matter in 3D Biology	

18.00 – 20.00	<i>Dinner</i>
---------------	---------------

20.00 – 21.00	Evening lecture (AIR)
Dr. Arin Doğan (Mosa Meat) CULTURED MEAT	

21.00 – 22.00 (FIRE) <h1 style="margin: 0;">Pub-Quiz</h1>	
--	--

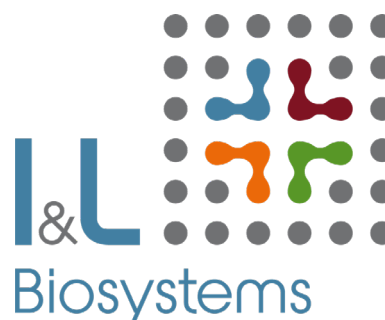
Gold sponsor:



Silver sponsors:



Miltenyi Biotec



Tuesday, 5 April

07.00 – 09.00	Breakfast & Poster mounting
09.00 – 09.45	Keynote Lecture: Dr. Britta Trappmann (AIR) Max Planck Institute for Biomolecular Medicine Bioactive Biomaterials

09.45 – 11.00	<i>Poster Session (AIR & FIRE)</i>
---------------	---

11.15 – 12.30 (10+2 min)	Oral Presentations Session 7 (AIR) <i>In vitro models in tissue engineering</i> <i>Chair: Lei Li</i>	Oral Presentations Session 8 (FIRE) <i>Biomaterials in Drug Delivery</i> <i>Chair: Sana Ansari</i>
Topic Keynote (25+5 min)	Silvia Mihaila (Utrecht University)	Daniela Wilson (Radboud University)
21 / 22	Esther Cramer Eindhoven University of Technology <i>Osteoclastic Differentiation in Human Osteochondral Explants cultured Ex Vivo</i>	Claire Polain MERLN - Maastricht University <i>Innervation In Bone Tissue Engineering Using Chemically Modified RNA</i>
23 / 24	Mike Broeders Erasmus MC, Rotterdam <i>Generation of a disease model for cartilage pathology in MPS VI</i>	Zhule Wang Radboudumc, Nijmegen <i>Dual-functional Porous Polymethylmethacrylate Cement Loaded with Cisplatin for Reconstruction of Segmental Bone Defect Kills Bone Tumor Cells</i>
25 / 26	Encheng Ji Erasmus MC, Rotterdam <i>Investigating The Effect Of Cartilage Maturation And Mineralisation On Angiogenesis In The Context Of Endochondral Ossification</i>	Jietao Xu Erasmus MC, Rotterdam <i>Delivery of Bone Morphogenetic Protein 2 and Platelet-Derived Growth Factor to improve the osteogenic properties of a collagenMagnesium-hydroxyapatite osteochondral scaffold</i>
27 / 28	Maria José Eischen-Loges MERLN - Maastricht University <i>Screening Osteogenic Properties of Calcium Phosphate Biomaterials with Inorganic Additives using a Multiplex Protein-Based Assay</i>	Claudia Del Toro Runzer MERLN - Maastricht University <i>Cellular Uptake and Activity of cmRNA and pDNA Lipid Complexes - Prospects for Gene Therapy and Tissue Engineering</i>

12.30 – 13.30	Lunch
---------------	--------------

13.30 – 14.30	SESSION FOR OPEN SCIENCE DEBATE (AIR)
---------------	--

14.30 – 15.00	Coffee	
15.00 – 16.30 (10+2 min)	Oral Presentations Session 9 (AIR) <i>Biomaterials associated infections and host response</i> <i>Chair: Esra Güben Kaçmaz</i>	Oral Presentations Session 10 (FIRE) <i>Small technologies, small tissues</i> <i>Chair: Melvin Gurian</i>
Topic Keynote (25+5 min)	Martijn Riool (Amsterdam UMC)	Massimo Mastrangeli (Delft University of Technology)
29 / 30	Leanne de Silva UMC Utrecht & Utrecht University <i>A Close Examination of the Bone Formation and Immune Response from a Devitalized Callus Mimetic</i>	Anika Schumacher MERLN - Maastricht University <i>Culture of stem cell-derived kidney organoids in physiological oxygen enhances amount and patterning of the endothelial network</i>
31 / 32	Jing Han Radboudumc, Nijmegen <i>Electrophoretic Deposition of Cu-doped Mesoporous Bioactive GlassChitosan Composite Coatings for Improved Sot Tissue Integration of Oral Implants</i>	Bas van Loo University of Twente <i>Ultra-High Throughput Production of Embryoid Bodies and Human Cardiac Organoids using In-Air Microfluidic generated Hollow Core-Shell Microcapsules</i>
33 / 34	Flurina Staubli UMC Utrecht <i>Effect of immune response on endochondral bone regeneration using partially mismatched allogeneic MSCs</i>	Michelle Vis Eindhoven University of Technology <i>Towards bone-remodeling-on-a-chip</i>
35 / 36	Rald Groven MERLN - Maastricht University <i>Profiling the microRNA fingerprint of the human fracture hematoma</i>	Meike Kleuskens Eindhoven University of Technology <i>Integration of Organoid- and Cell-filled Chondral Implants in Human Osteochondral Explants</i>
37 / 38	Devlina Ghosh University of Groningen <i>A universal nanogel-based coating approach for medical implants</i>	Niels Willemen University of Twente <i>Biochemical and biophysical tunable smart microbuilding blocks to instruct engineered living tissues</i>
16.40-17:00	Awards session & Closure of the meeting (AIR)	

Bronze sponsors:



**Monday,
4th April**

10.10-10.45

Biomaterial and Tissue Engineering across generations

In the 30 years that the society is existing many new developments in the field emerged and new technologies have been developed. But not only the fields as a scientific discipline has changed within this 30 years, also the vision, applications, social impact, and ethical views have been altered tremendously. During a panel discussion, led by Rosanne Hertzberger, 4 generations of scientists will engage in a discussion that will combine the early stage of the field, the emergence of Biomaterials and Tissue Engineering, with current perceptions and visions. An opening event for our anniversary conference that will resonate within the coming generation.

Oral Presentation

Session 1

Keynote session 1

Hydrogels with Engineered Crosslinks: Towards Tunable, Processable, and Adaptable Biomaterials for Cell Encapsulation

Dr. Julieta I. Paez
Faculty of Science and Technology
University of Twente



Cell-encapsulating hydrogels are used as extracellular matrix mimics for the basic study of cell function, high-throughput drug screening, and therapeutic delivery. In the fabrication of such biomaterials, the crosslinking chemistry plays a vital role in regulating several important properties of the system, such as gelation rate, mechanical strength, and bioactivity of the network. Despite the many covalent crosslinking strategies reported so far, they are often not economic, user-friendly, or tunable enough to facilitate the adaptability of the encapsulating system to a variety of biomedical scenarios.^[1, 2] In the first part of this presentation, our recent work on the development of bioinspired covalent chemistries for the fabrication of precisely tunable, cost-effective, and versatile hydrogels for 3D cell culture will be highlighted.^[3] Engineering the chemical crosslinks of hydrogel networks is also an important means to modulate their viscoelasticity, and in this regard, covalent dynamic networks have recently attracted great attention.^[4] For example, covalent dynamic crosslinks can confer self-healing and self-recovering properties to these networks, thus enabling their processing via additive manufacturing technologies. Additionally, a growing number of recent studies have shown that hydrogels with covalent dynamic crosslinks can mimic closely the dynamics and functions of natural extracellular matrix in soft tissues, thus enabling to study how cells sense and remodel their microenvironment. However, the palette of covalent dynamic crosslinks under physiological conditions is limited. In the second part of this presentation, novel hydrogels formed by covalent dynamic crosslinks will be presented. Our strategy enables straightforward engineering of hydrogels with hybrid static/dynamic crosslinks, for the fine-tuning of materials viscoelasticity.^[5] These adaptable biomaterials are expected to become valuable platforms to study cell function, as well as for the bioprinting of soft scaffolds.

References:

[1] J. I. Paez*, A. Farrukh, R. Valbuena-Mendoza, M. K. Włodarczyk-Biegun, A. del Campo*. *ACS Appl. Mater. Interfaces* 2020, 12, 8062. [2] J. I. Paez*, A. de Miguel-Jiménez, R. Valbuena-Mendoza, A. Rathore, M. Jin, A. Gläser, S. Pearson, A. del Campo*. *Biomacromolecules* 2021, 22, 7, 2874. [3] M. Jin, G. Kocer, J. I. Paez*, 2021 *in revision*. [4] K. Zhang, Q. Feng, Z. Fang, Z. Fan, L. Gu*, L. Bian*. *Chem. Rev.* 2021, 121, 18, 11149. [5] M. Jin, J. I. Paez*, *unpublished results*.

Biography:

Julieta obtained her PhD in Chemistry at the National University of Córdoba in Argentina, working on polymeric materials for sensing and antifouling applications. After her PhD, she moved to Germany to join the Dendritic Polymers group at the Freie Universität Berlin as a Postdoctoral Researcher for a short stay, working on biofunctional polymeric surfaces for protein microarrays. She then joined the Dynamic Biointerfaces group at the Max-Planck Institute for Polymer Research in Mainz, where she developed photoactivatable peptides for cell-instructive materials and catechol-functionalized polymers for tissue gluing applications. Afterwards, she moved to INM – Leibniz Institute for New Materials in Saarbrücken as Research Scientist and later as Project Leader funded by DFG, to develop coupling chemistries for bioconjugation and soft biomaterials fabrication under mild conditions. In April 2021, she moved to The Netherlands to join the Developmental BioEngineering Department at the University of Twente as Assistant Professor (Tenure Track). Her newly established team develops chemical strategies for the fabrication of smart hydrogels for diverse healthcare applications. Her main research interests involve hydrogels cell encapsulation, tissue adhesives, and biofabrication technologies.

Who wins?

Synthetic supramolecular matrices based on the ureido-pyrimidinone (UPy) and benzene-1,3,5-tricarboxamide (BTA) motif

L. Rijns^{1,2}, J.W. Peeters³, H.M. Janssen³, E.W. Meijer², P.Y.W Dankers^{1,2}

¹ Department of Biomedical Engineering, Laboratory for Cell and Tissue Engineering, Eindhoven University of Technology ² Institute for Complex Molecular Systems, Eindhoven University of Technology ³ SyMO-Chem B.V. Eindhoven University of Technology

Introduction: The extracellular matrix (ECM) is a dynamic, multicomponent network that provides both structural support and biochemical information to cells.¹ The constant interaction of the ECM with cells is essential for normal homeostasis and healthy functioning of tissue. However, as of today it is not completely clear how cells process the mechanical and biochemical cues of the ECM.² To better understand the cell-material interface, we propose synthetic, bioactive supramolecular assemblies to recapitulate all facets of the ECM in a modular, synthetic manner, such that the influence of distinct microenvironment components can be assessed individually. Here, we are comparing two different supramolecular hydrogel systems for culturing cells in terms of their mechanical, dynamical and bioactive properties; the ureido-pyrimidinone (UPy)³ versus the benzene-1,3,5-tricarboxamide (BTA)⁴ motif.

Materials and methods: UPy and BTA supramolecular hydrogels were prepared in a fixed molecular ratio of 80 monofunctional (M) to 1 bifunctional (B) molecules at 2.5 wt% concentrations. For cell adhesion studies, 1 mM of RGD-functionalized UPy or BTA was incorporated into the hydrogel as part of the M molecules. For the cell adhesion studies, renal proximal tubular epithelial cells (RPTECs) were seeded on top of the supramolecular hydrogels. RPTECs were fixed after 4 days of culture and then stained for its nucleus in blue and actin cytoskeleton in red. Strain sweep experiments were measured at 1 rad/s and stress relaxation tests at 7.5% strain by rheology at RT.

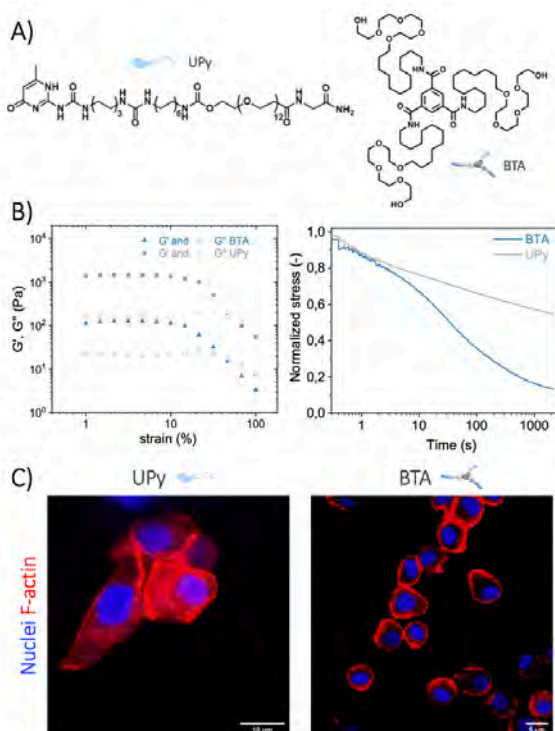


Figure 1: A) Chemical structures of M UPy and BTA molecules. B) Mechanical properties of UPy and BTA hydrogels as determined with a strain sweep plot at 1 rad/s, showing the storage (G') and loss modulus (G'') (left) and dynamical properties as measured by stress relaxation tests at 7.5% strain (right) at RT. C) Fluorescent images of RPTECs cultured on UPy (left) or BTA hydrogels (right), stained for the nucleus (blue) and actin (red). Scale bars are 10 μm (left) and 5 μm (right).

Results and discussion: The UPy and BTA-based supramolecular hydrogel systems were investigated for their ability to serve as synthetic ECM for culturing cells. First, we observed that the UPy hydrogels ($G' \sim 1$ kPa) are 10x stiffer than the BTA gels ($G' \sim 100$ Pa) at the 2.5 wt% concentrations as measured by rheology (Figure 1B, left). We hypothesize that this is caused by the stronger intermolecular interactions between the UPy monomers than between the BTA monomers. Besides, we found that the BTA hydrogels possess faster stress relaxation and recover more stress within the measured 1000 s time frame than the UPy hydrogels (Figure 1B, right). This indicates faster reorganization for both the BTA monomers within the BTA fibers and the BTA fibers within the whole BTA gel over the UPy system, again linked to its weaker intermolecular interactions. Lastly, we observed that renal epithelial cells remain small and round in morphology when cultured on the BTA gels and tend to spread more when cultured on the UPy gels. This could be attributed to the weaker stiffness and/or the faster dynamics of the BTA gels.

Conclusions: The UPy and BTA hydrogels were compared for their ability to act as a synthetic ECM for culturing cells. We found that the BTA gels are weaker and more dynamic than the UPy gels under similar concentrations and molecular conditions, indicating weaker intermolecular interactions between the BTA monomers than between the UPy monomers. Our study also showed that renal cells cultured on top of UPy gels spread well, while the cells tend to stay round and small in morphology when cultured on the BTA gels. Next, we investigate if this difference is caused by the weaker mechanical properties and/or the faster dynamics of the BTA gels. In conclusion, we, for now, recommend the UPy hydrogel to be a better candidate to act as a synthetic ECM for culturing cells, taking into account the gel's dynamic, mechanic and cell adhesion properties.

References:

1. Enemchukwu, N. O. *et al. J. Cell Biol.* **212**, 113–124 (2016).
2. Sapir, L. & Tzlil, S. *Seminars in Cell and Developmental Biology* **71**, 99–105 (2017).
3. Dankers P.Y.W. *et al. Adv. Mater.* **33**, 37 (2021).
4. Vereroudakis, E. *et al. ACS Cent. Sci.* **6**, 1401–1411 (2020).

Osteoconductivity of UHMWPE fabric for a cervical artificial intervertebral disc: in vitro analysis

C.A.M. Jacobs¹, E.E.A. Cramer¹, N. Davison², H. Smelt², S. Hofmann¹, K. Ito¹

¹Orthopaedic Biomechanics, Dept. of Biomedical Engineering, Eindhoven University of Technology, the Netherlands

²DSM innovation center, Chemelot campus gate 2, Urmonderbaan 22, 6167 RD Sittard-Geleen, The Netherlands

Introduction

Cervical artificial intervertebral discs (AIDs) have been developed as a mobility preserving alternative treatment for disc degeneration. First generation CDRs were based on traditional synovial joint arthroplasty designs, leading to a mismatch in kinematic behavior compared to a natural disc¹. It is hypothesized that mimicking the native structure of the intervertebral disc (IVD) would lead to appropriate biomechanical properties and less complications. Hence, a novel biomimetic AID was developed as shown in Fig. 1. The design contains a hydrogel core, representing the swelling nucleus pulposus, and an ultra-high-molecular-weight-polyethylene (UHMWPE) fiber jacket mimicking the annulus fibrosus. Although metal endplates with pins are used to achieve initial stabilization to the vertebrae, direct anchorage, or osseous integration of the UHMWPE fibers to the adjacent bony structures is required to achieve proper biomimetic function². A common approach to achieve a more stable and faster osseous integration is applying surface treatments. Therefore, the aim of this study was to determine the differences in osteoconductivity of different surface treatments of UHMWPE fabrics and fabrics made from a novel hydroxyapatite (HA) loaded UHMWPE fiber.

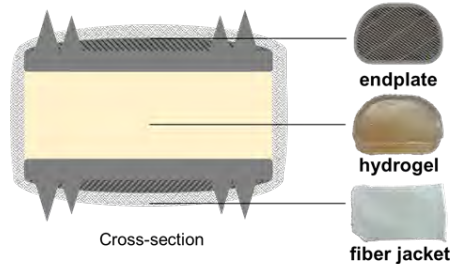


Figure 1: schematic representation of mimetic design.

Materials and Methods

Seven experimental groups (each n=6) were tested and compared i.e., 2D knitted fabrics made from: non-treated UHMWPE fibers (N), 10% HA loaded UHMWPE fibers (10%HA), 15% HA loaded UHMWPE fibers (15%HA), plasma treated UHMWPE fibers (PT), Plasma treated 10% HA UHMWPE fibers (PT-10%HA), Plasma treated 15%HA UHMWPE fibers (PT-15%HA) and hydroxyapatite coated UHMWPE fibers (OC). Osteoconductivity was graded based on three characteristics: cell viability and attachment, osteoblast differentiation and mineralization. To assess the differences based on these three characteristics, a static '2.5D' culture using mesenchymal stromal cells for 14 days was performed. After 2, 7 and 14 days, cell adherence on the surface was assessed using scanning electron microscopy (SEM), quantifying DNA content and cell viability with PrestoBlue assay. After 14 days, osteoblast differentiation was verified using alkaline phosphatase activity assay. Mineralization was assessed with SEM images and EDX analysis.

Results and Discussion

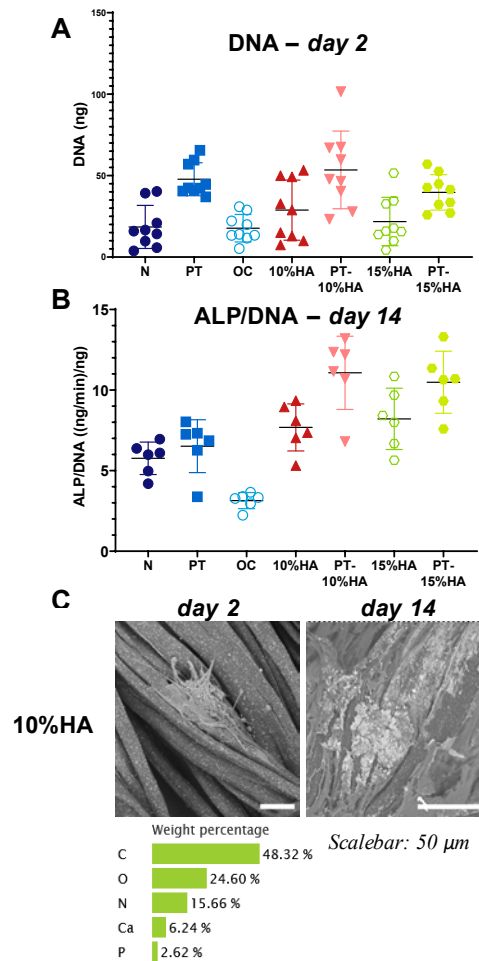


Figure 2: A: DNA content (ng). B: ALP normalized to DNA. C: representative SEM/EDX result of 10%HA group.

On day 2, both metabolic activity (not shown) and DNA content was upregulated for the groups that were plasma treated (PT, PT-10%HA and PT-15%HA) compared to the same surface without plasma treatment. Thus, it seems that plasma treatment, which makes the surface more hydrophilic, increases the initial cell adherence and viability³. SEM images also verify the cell adherence at day 2 for all groups. However, at day 7 and 14, this difference in metabolic activity and DNA content became non-significant (data not shown). At day 14, ALP activity results showed that the HA loaded, and plasma treated groups (PT-10%HA, PT-15%HA) have highest ALP activity. Moreover, SEM/EDX analysis at day 14 verified the presence of mineralization nodules for those groups. Based on these results, using HA loaded fibers that are plasma treated seem to provide the most promising surface for facilitating bony ingrowth.

References

1. Frost B *et al. Materials (Basel)*, 12(2):253,2019
2. Van Den Broek PR, TU Eindhoven 2012.
3. More *et al. S., Appl Surf Sci.*, 144665,2019

hMSCs response to polymer-calcium phosphate composite scaffolds containing zinc produced using additive manufacturing

Martyna Nikody^{1,2}, Jia ping Li^{1,2}, David Koper^{1,2,3}, Elizabeth Rosado Balmayor¹, Lorenzo Moroni², Pamela Habibovic¹

¹Department of Instructive Biomaterials Engineering, MERLN Institute for Technology-Inspired Regenerative Medicine, Maastricht University, Universiteitssingel 40, 6229 ER, Maastricht, the Netherlands

²Department of Complex Tissue Regeneration, MERLN Institute for Technology-Inspired Regenerative Medicine, Maastricht University, Universiteitssingel 40, 6229 ER, Maastricht, the Netherlands

³Department of Cranio-Maxillofacial Surgery, Maastricht University Medical Center, Maastricht, the Netherlands

Introduction

Currently available options for treating critical-sized cranial bone defects involve the use of either an autologous bone or a bioinert bone graft substitute. These approaches are far from an optimal solution as they often result in complications including donor site morbidity, lack of osteointegration ability, and a high risk of implant failure. To combat these limitations, we propose the use of a novel bioactive composite with high ceramic content composed of poly(ethyleneoxide terephthalate) poly(butylene terephthalate) (1000PEOT70PBT30, PolyActive, PA) and 50% beta-tricalcium phosphate (β -TCP) with the addition of zinc in a form of a coating of the β -TCP ceramic. Several inorganic ions have been shown to affect biochemical functions essential for different aspects of bone regeneration. Properties of one of such ions, zinc, have been evaluated by this study. Although zinc is found in the bone only in trace amounts, it plays an essential role in its remodelling, through stimulating the bone-forming process and inhibiting bone resorption. Therefore, we hypothesise that the addition of zinc to the β -TCP will result in enhanced osteogenic properties of additive manufactured polymer-ceramic composites.

Materials and Methods

Additively manufactured porous 3D scaffolds composed of 1000PEOT70PBT30, 1000PEOT70PBT30 and β -TCP in 1:1 ratio, 1000PEOT70PBT30- β -TCP composites with addition of 15 mM or 45 mM of zinc in a form of TCP coating were sterilised and seeded with bone marrow-derived human mesenchymal stromal cells (hMSCs). DNA content, alkaline phosphatase (ALP) activity, early cell attachment and extracellular matrix (ECM) formation were assessed on days 3, 7, 14 and 28.

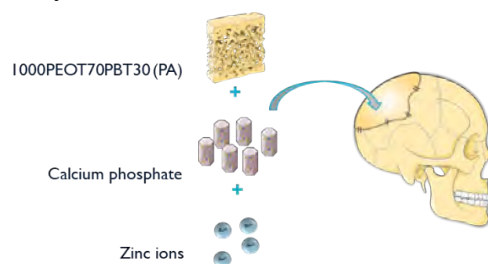
In addition, osteogenic gene expression was evaluated by qPCR analysis.

Results

Additively manufactured 3D composite scaffolds used in this study contained 50% of β -TCP, which is among the highest content of ceramic in a composite with a polymer achieved so far, without the need for the use of solvents. Regarding the *in vitro* assessment of the osteogenic properties of the porous 3D scaffolds, hMSCs cultured on all types of scaffolds proliferated and showed ALP activity. Higher cell growth and ALP production were observed on scaffolds containing β -TCP and β -TCP with the addition of zinc than on 1000PEOT70PBT30 scaffolds. Furthermore, ECM formation and cell attachment were observed on day 28 and day 1 respectively on all scaffolds except for 1000PEOT70PBT30. In addition, cells cultured on all types of scaffolds showed expression of osteogenic markers. Interestingly, preliminary results showed that the expression of late osteogenic markers such as osteocalcin and osteopontin was upregulated at day 3 when cells were cultured on composite scaffolds with zinc.

Conclusion

The addition of β -TCP with and without zinc to 1000PEOT70PBT30 resulted in higher cell proliferation, ALP activity, early cell attachment, and ECM formation. Furthermore, obtained results suggest that the addition of zinc to composite scaffolds increased the expression of osteogenic markers.



A schematic demonstration of the approach and application of the additive manufactured composite scaffolds.

Directing Kidney Tubulogenesis Using Tunable Synthetic Matrices

M.J. Hagelaars^{1,2*}, L. Rijns^{2,3*}, S. Loerakker^{1,2}, P.Y.W. Dankers^{2,3}, C.V.C. Bouten^{1,2}

1. Soft Tissue Engineering and Mechanobiology, Department of Biomedical Engineering, Eindhoven University of Technology, P.O. Box 513, 5600 MB Eindhoven, The Netherlands

2. ICMS, Eindhoven University of Technology, 5600 MB Eindhoven, The Netherlands

3. Biomedical Material and Chemistry, Department of Biomedical Engineering, Eindhoven University of Technology, P.O. Box 513, 5600 MB Eindhoven, The Netherlands

Introduction | Guided tissue morphogenesis has emerged as a novel method in the field of tissue engineering for functional organization of tissue replacements. In general, morphogenesis is a process of self-organization that is both triggered and steered by biological signals and cell-cell interactions. In the case of the mammalian kidney, epithelial morphogenesis plays a crucial role in the establishment of tubular structures that form the foundation of the nephrons, the functional subunits of the kidney. The self-assembly process of these tubes is a delicate interplay between both biological and physical factors originating from the renal epithelial cells and the extracellular matrix (ECM) [1].

Signals from the ECM that are regulated through integrin receptors are known to influence epithelial cell polarity allowing the emergence of an apical membrane at the interface between the cells, where the lumen can form and grow. Previous research has shown that Madin Darby Canine Kidney cells (MDCKs), a classic epithelial *in vitro* model, form cysts with a central lumen when grown in a 3D collagen gel. However, when these cells are cultured in suspension and thus in the absence of matrix, these cells invert the direction of their polarization and form aggregates or spheroids [2]. Inhibition or loss of $\beta 1$ integrins will result in the same inverted polarity. [3] These observations raise the question whether direct control of matrix properties, such as stiffness or bioactivity, influencing the integrin receptor, could steer the orientation of polarization and the following lumen formation.

The objective of this study is to investigate to which extent we could steer epithelial morphogenesis in a 3D environment using synthetic supramolecular hydrogels based on the ureido-pyrimidinone (UPy) motif; a dynamic material based on hydrogen bonding and π - π interactions that allows for full and independent control over stiffness and ligand concentration.

Materials and Methods | Madin Darby Canine Kidney II cells (MDCK) were resuspended after trypsinization and encapsulated in 3D UPy hydrogels of variable weight percentages (0.6, 1.25 and 2.5 wt%). The UPy hydrogels with variable weight percentages were fabricated by mixing monofunctional UPy-glycinamide and bifunctional UPy₂-PEG_{10k} in a fixed molecular ratio of 80 to 1, respectively. UPy-hydrogels were supplemented with 1 mM of UPy-cRGDfK as bioactive ligand. Mechanical properties of the UPy hydrogels were determined using rheology. MDCKs were fixed after ten days of culture. Samples were analyzed using IF staining to characterize the formed cellular structures.

Results and Discussion | The bulk modulus extracted from frequency sweep and strain sweep measurements for the 0.6, 1.25 and 2.5 wt% yielded 0.1 kPa, 1 kPa and

3 kPa gels respectively. Encapsulation of MDCKs in synthetic supramolecular hydrogels resulted in the formation of three different types of 3D structures: aggregates with no lumen (i), multi-lumen structure (ii) and cysts with a central lumen (iii) (Figure 1A). The orientation of polarization, marked by the apical protein podocalyxin, shifts from an inverted state in case of aggregates, to organized in case of cysts. We found that higher weight percentages primarily lead to the formation of cysts with a central lumen, while the low weight percentage hydrogel lead primarily to cell aggregation (Figure 1B). The results suggest a direct relation between the amount of matrix offered and the orientation and organization of MDCKs. YAP quantification suggests that the stiffness of the matrix does not play a role in the aforementioned process.

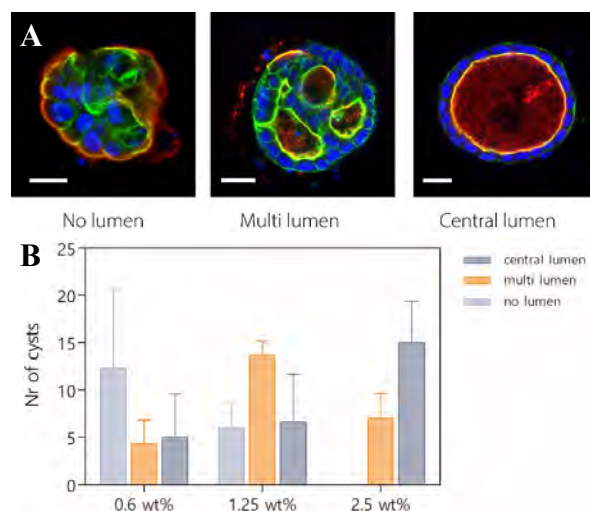


Figure 1: A) Representative fluorescent images of the different structures formed by MDCKs in UPy hydrogels with different weight percentages. The cells were stained for podocalyxin (red), actin (green) and the nucleus (blue). Scale bars are 20 μ m. B) Quantification of 3D structures formed by MDCKs in UPy hydrogels of different weight percentages.

Conclusion and Outlook | Our study demonstrates that tunable, synthetic supramolecular biomaterials based on the UPy motif can be used as a tool to direct epithelial morphogenesis. MDCKs have a different organization and orientation of polarity that depends on the weight percentage of the hydrogel. Next, we intend to test what the role of the bioactivity is to the epithelial morphogenesis, by varying the UPy-cRGDfK concentration at a constant weight percentage.

[1] R. Cruz-Acuña *et al.*, *J. Cell Sci.*, vol. 132, no. 20, Oct. 2019.

[2] A. Z. Wang, *et al.*, *J. Cell Sci.*, vol. 95, no. 1, 1990.

[3] W. Yu *et al.*, *Mol. Biol. Cell*, vol. 16, no. 2, Feb. 2005.

This work was performed under the framework of RegMed XB and the MDR Gravitation Program.

Development of a thiol-ene gelatin-based bioresin for volumetric bioprinting

M. Falandt¹, M. Schweiger², J. Malda^{2,1}, T. Vermonden³, R. Levato^{1,2}

¹Dept. of Clinical Sciences, Faculty of Veterinary Medicine, Utrecht University, 3584 CT, Utrecht, The Netherlands.

²Dept. of Orthopaedics, University Medical Center Utrecht, Utrecht University, 3584 CX, Utrecht, The Netherlands.

³ Dept. of Pharmaceutics, Faculty of Science, Utrecht University, 3508 TB, Utrecht, The Netherlands.

Introduction: The field of tissue engineering has rapidly progressed and opened new opportunities in 3D bioprinting techniques that permit the production of geometrically complex structures embedding living cells. In this project, we investigate a novel 3D bioprinting technique termed volumetric printing (VP). In VP, the entire gel construct is printed in a matter of seconds with resolution in the range of tens of micrometers. According to a tomographic algorithm, a digital micromirror device shapes visible light patterns into a filtered back-projection of the object to be printed. The projections are sent to a volume of a photoresponsive material at specific angles, and their combination allows selective crosslinking of the resin into the desired 3D object.¹ A fundamental component of the successful 3D printing of these constructs is the choice of materials used to print and subsequent culture of living cells. In this project, gelatin, functionalized with norbornene groups (GelNOR), is investigated as a bioresin combined with a thiolated crosslinker. To date, common photoresins rely on the use of methacrylate groups, which form hydrogels via chain-growth polymerization. In this work, GelNOR is investigated due to its faster crosslinking kinetics and superior potential to control the reproducibility of the hydrogel network.² This thiol-ene crosslinking reaction is a step-growth crosslinking method, in which the properties of the hydrogel can be influenced by either changing the type of thiolated crosslinker used. For tissue engineering, this step-growth mechanism is more beneficial since the mesh size of the formed polymer construct can be more easily controlled, as opposed to the completely randomized chain-growth mechanisms used in previous studies. The goal is to design a novel material which displays faster and more influenceable properties than previous gelatin based bioresins to utilize in VP for the printing of complex 3D constructs.

Experimental methods: GelNOR was synthesized in a pH-controlled buffer (PBS or CB buffer) with (sequential) the addition of carbic anhydride (CA) to the reaction mixture. To obtain macromers with different degrees of functionalization (DOF), multiple reaction conditions were used, namely changing the reaction time or molar concentration of the reactants. The resulting DOF was then measured by using a 2,4,6-trinitrobenzenesulfonic acid (TNBSA) assay and ¹H-NMR. GelNOR was used in the presence of LAP (0.1 w/v%) and a thiolated crosslinker (DTT and ethyleneglycol dithiol) to prepare the bioresin used in the volumetric printer. A Dynamic Mechanical Analyzer (DMA) was operated to determine the compression modulus (Young's modulus) and the elasticity ratio of the crosslinked hydrogels. Photorheological analysis was applied to study the kinetics of the crosslinking mechanism and find the storage and loss modulus of different bioresins concentrations upon crosslinking. Cylindrical disks for mechanical testing (width 5 mm, height 2 mm) and geometrically complex 3D

architectures were obtained via volumetric printing performed with a Tomolite device (Readily3D).

Results and discussion: In this study, we started with the optimization of the synthesis of the material. A first challenge was in removing the excess of CA from the reaction product, since its residual load in the material inhibited the actual crosslinking of the GelNOR constructs. For the synthesis, 3 concentrations were tried, **A:** 10 g of gelatin against 18 g of CA for 24 hours, **B:** 10 g of gelatin against 2 g of CA for 2 hours, **C:** 10 g of gelatin against 2 g of CA for 4 hours. Where condition A gave the highest DOF, it also showed on NMR that the excess of CA was the largest. With conditions B and C the DOF was lower, but no excess of CA was found. The excess of CA was removed by dialysis against water. Changing the reaction time and the amount of CA in the reaction made it possible to achieve different DOFs of GelNOR ranging from 50% to 85%. Thus, providing a synthesis protocol for the GelNOR material within 4 hours instead of the previously used 24 hours reaction. Secondly, the mechanical properties of the material were optimized. By modifying the length of the thiolated crosslinker (~5.4 Å or ~11.3 Å) and the thiol to norbornene molar ratio, a wide range of stiffness of the resulting hydrogel could be achieved, varying from ~1 kPa to 20 kPa. Even at a lower polymer concentration (5 w/v%). The GelNOR material proved to be possible to print multiple complex 3D objects (such as hollow discs, the Venus of Milo, and a gyroid structure) in a time and cost-efficient manner, using the volumetric printer.

Conclusion: We found a cost-efficient and scalable method to synthesize the GelNOR material used for printing complex 3D objects with optimized synthesis conditions. The ease in changing the mechanical properties by changing the thiol-based crosslinkers, the DOF of GelNOR, or the gel w/v% could open many possibilities, especially for printing with cells and for future applications in tissue engineering. These hydrogels based on thiol-norbornene photo-click reaction could contribute to creating constructs via light-based bioprinting with highly controllable physico-chemical properties.

Acknowledgments

This project received funding from the European Research Council (ERC) under the European Union's Horizon 2020 research and innovation program (grant agreement No. 949806, VOLUME-BIO)

References

1. Bernal, P. N. *et al.* Volumetric Bioprinting of Complex Living-Tissue Constructs within Seconds. *Adv. Mater.* **31**, 1904209 (2019).
2. Muñoz, Z., Shih, H. & Lin, C.-C. Gelatin hydrogels formed by orthogonal thiol-norbornene photochemistry for cell encapsulation. *Biomater. Sci.* **2**, 1063–1072 (2014).

Oral Presentation
Session 2

Keynote session 2

How inorganic nanoparticles can enhance regenerative approaches

Dr. Sabine Van Rijt
MERLN Institute for Technology-Inspired
Regenerative Medicine, Maastricht University



Abstract

Inorganic nanomaterials such as mesoporous silica, calcium phosphate and gold nanoparticles have unique physical properties and, in addition, are highly modifiable, making them versatile platforms for a range of medical applications including within regenerative medicine. In this talk I will highlight some of the ways these inorganic nanoparticles can be used to enhance regenerative strategies. For example, inorganic nanoparticles can be used as building blocks to create new types of nanocomposite biomaterials that have important properties for tissue regeneration such as self-healing, cell responsiveness, injectability, controllable drug delivery and moldable properties. Moreover, inorganic nanoparticles can also be used as instructive coatings or as 2D biointerfaces to study the effect of surface chemistry, nanotopography, biochemical cue and ligand presentation on stem cell behavior. Finally, inorganic nanoparticles can be designed as multimodal imaging probes capable of tracking stem cells in the body while providing functional information at the (sub)cellular level. Such tools enable critical information about the mechanisms of stem cell therapy and tissue regeneration.

In summary, with this talk I aim to give you a flavor of this rapidly evolving field using inorganic nanoparticles for the development of new generations of biomaterials with changeable features at the nanoscale.

Biography:

Sabine van Rijt is an assistant professor at the MERLN institute of technology inspired regenerative medicine at Maastricht University, working in the field of nanomaterials for tissue regeneration. In this position she aims to develop new types of responsive nanomaterials that can induce tissue regeneration, and allow (simultaneous) cell and tissue tracking. In the past years, together with her team, she developed cell imaging probes by modular design of nanoparticles and are currently developing these nanoparticles further within several consortia to improve our understanding of stem cell mediated tissue regeneration. Specifically, within a ZonMW TOP grant (VISION, granted in 2017) together with clinical partners, she is investigating limbal stem cell distribution over cornea to elucidate stem cell mediated corneal regeneration. As co-applicant in two EU grants PREMSTEM and JOINTPROMISE (both granted in 2019) she uses nanoparticles to study stem cell distribution and mechanism of action in 3D cell cultures and in vivo models. Next to cell imaging, together with her team, she used nanoparticles as building blocks to develop 2D and 3D materials for tissue regeneration applications, such as instructive coatings and responsive composite materials as part of the NWO gravitation consortium "materials driven regeneration" (www.mdr.nl). She has a large international scientific network and is active in several societies including NBTE, ESB and TERMIS. Next to leading her research group she also teaches and coordinates several courses in regenerative medicine and is curriculum committee member of the biomedical sciences master, in the Faculty of Health Medicine and Life Science of Maastricht University. She has recently been elected chair of the faculty PhD committee for a term of 3 years.

Bioink with Cartilage Extracellular Matrix Microfibers Enables Spatial Control of Capillary Formation in 3D Bioprinted Constructs

M.L. Terpstra¹, J. Li², A. Mensinga³, M. de Ruijter¹, M.H.P. van Rijen¹, C. Androulidakis^{4,5}, C. Galiotis^{4,5}, I. Papantoniou^{5,6,7}, M. Matsusaki², J. Ma lida^{1,3}, R. Levato^{3,1}

¹Department of Orthopaedics, University Medical Center Utrecht, Utrecht, The Netherlands. ²Division of Applied Chemistry, Graduate School of Engineering, Osaka University, Suita, Osaka, Japan. ³Department of Clinical Sciences, Faculty of Veterinary Medicine, Utrecht University, Utrecht, The Netherlands. ⁴Composites & Nanostructured Materials Lab, Department of Chemical Engineering, University of Patras, Patras, Greece. ⁵Institute of Chemical Engineering Sciences, Foundation for Research and Technology - Greece (FORTH), Patras, Greece. ⁶Skeletal Biology & Engineering Research Centre, Department of Development and Regeneration, KU Leuven, Leuven, Belgium. ⁷Prometheus the translational division of Skeletal Tissue Engineering, KU Leuven, Leuven, Belgium.

INTRODUCTION Microvasculature is essential for the exchange of gas and nutrient for most tissues in our body. Some tissue structures such as the meniscus presents spatially confined blood vessels adjacent to non-vascularized regions. In biofabrication, mimicking the spatial distribution of such vascular components is paramount, as capillary ingrowth into non-vascularized tissues can lead to tissue matrix alterations and subsequent pathology. Multi-material three-dimensional (3D) bioprinting strategies have the potential to resolve anisotropic tissue features, although building complex constructs comprising stable vascularized and non-vascularized regions remains a major challenge to date.

MATERIALS AND METHODS In this study, we developed endothelial cell-laden pro- and anti-angiogenic bioinks, supplemented with bioactive matrix-derived microfibers (MFs) that were created from type I collagen sponges (col-1) and cartilage decellularized extracellular matrix (CdECM), respectively. As a proof of concept, the bioinks were bioprinted into an anatomical meniscus shape with a biomimetic vascularized outer and non-vascularized inner region, using a gellan gum microgel suspension bath. These 3D meniscus-like constructs were cultured up to 14 days, with in the outer zone the HUVEC- and col-1 MF laden pro-angiogenic bioink, and in the inner zone meniscus progenitor cell (MPC)- and CdECM MF-laden anti-angiogenic bioink. To co-facilitate both microvessel formation and MPC-derived matrix formation, we formulated cell culture medium conditions that included a temporal switch.

RESULTS HUVEC-driven capillary networks started to form two days after bioprinting. Supplementing cartilage-derived MFs to endothelial-cell laden bioinks reduced the total length of neo-microvessels by 29%, and the number of microvessel junctions by 37% after 14 days, compared to bioinks with pro-angiogenic col-1 MFs (Figure 1). The 3D bioprinting of the zonal meniscus construct revealed successful spatial confinement of the vascular network only in the outer zone (Figure 2). To co-culture both endothelial-MSCs and the fibrochondrocytic MPCs, a successful combination of endothelial cell culture medium (EGM-2) and chondrogenic differentiation medium (CD medium) with TGF- β was formulated. Rather than one culture medium formulation during 14 days, a switch after 7 days was necessary starting with EGM-2 medium, followed by a mixture with 10, or 25% v/v CD medium, to achieve formation of endothelial cell networks and MPC type I collagen deposition.

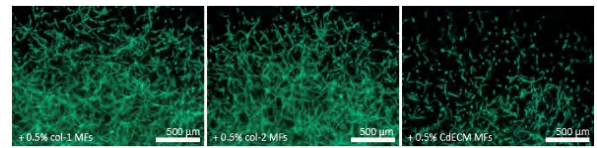


Figure 1: Supplementation of cartilage-derived microfibers (right) to a fibrin-based hydrogel resulted in a reduced endothelial network formation compared to col-1 (left), or col-2 MFs (middle).

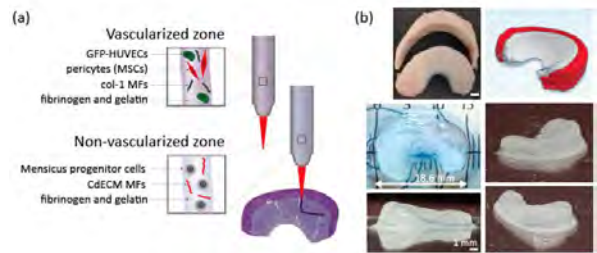


Figure 2: 3D bioprinted meniscus construct with biomimetic vascularized inner and non-vascular outer region. (a) Setup of 3D printed construct, (b) derived from an equine meniscus shape, and bioprinted with fibrin-gelatin bioinks.

CONCLUSION Overall, this study provides a new strategy to develop zonal biomimetic meniscal grafts. Moreover, the use of ECM-derived MFs to promote or inhibit capillary networks opens new possibilities for the biofabrication of tissues with anisotropic microvascular distribution. These have potential for many applications including in vitro models of vascular-to-avascular tissue interfaces, cancer progression, and for testing anti-angiogenic therapies.

ACKNOWLEDGEMENTS

The authors acknowledge L. Hao, L. de Silva, M. Rijkers, and J. Korpershoek for their help on the cell cultures. This project has received funding from the European Research Council (ERC) under the European Union's Horizon 2020 research and innovation programme (grant agreement No. 949806, No. 647426, and No. 814444), ReumaNederland (LLP-12 and 22), and R.L. acknowledges support from the 2019 Hofvijverkring Fellowship. The authors also acknowledge financial support by Mirai-Program (21-201031456) from JST and Grant-in-Aid for Scientific Research (A) (20H00665) from JSPS. The antibody against collagen type II, developed by T. F. Linsenmayer, was obtained from the Developmental Studies Hybridoma Bank, created by the NICHD and maintained at The University of Iowa, Department of Biology, Iowa City, IA 52242.

Chitin Nanofibrils Modulate Mechanical and Inflammatory Response in Tympanic Membrane Scaffolds

S. Anand¹, S. Danti², B. Azimi², A. Fusco³, G. Donnarumma³, L. Moroni¹, C. Mota¹

¹Complex Tissue Regeneration Department, MERLN Institute, Maastricht University, Maastricht, The Netherlands

²Department of Civil and Industrial Engineering, University of Pisa, Research Unit of INSTM, Pisa, Italy

³Department of Experimental Medicine, University of Campania Luigi Vanvitelli, Naples, Italy

Introduction: The human tympanic membrane (TM), or eardrum, is a thin concave tissue located at the end of the outer ear canal [1]. TM perforations are one of the most common eardrum injuries, resulting in a conductive hearing loss due to inept sound transmission. Conventional grafts applied for repairing the perforated TM often lack the requisite material characteristics, which leads to a suboptimal hearing restoration [2]. Therefore, there has been a growing interest to expand the current list of biomaterials available for treating the damaged eardrum. This work introduces the combination of chitin nanofibrils (CNs) with poly(ethylene oxide terephthalate)/poly(butylene terephthalate) (PEOT/PBT) to fabricate mechanically reinforced nanocomposites capable of modulating the inflammatory and immune response [3].

Materials and Methods: Melt blending was implemented as the key approach for the nanocomposite preparation. Poly(ethylene glycol) (PEG) was incorporated as a compatibilizing agent to improve the dispersion of CNs within the PEOT/PBT matrix. Different CN/PEG ratios, namely 50:50, 65:35, 70:30, and 75:25, were chosen in this regard. The biofabrication ability of the produced PEOT/PBT/CN formulations was examined with respect to electrospinning (ES) and melt extrusion based additive manufacturing (AM). The influence of CNs in the fabricated scaffolds was investigated by studying their surface morphologies, mechanical properties, degradability, and cytotoxicity. TM-specific mechanical characterizations were performed to assess the functional relevance of PEOT/PBT/CN composites. Finally, the expression of pro-inflammatory cytokines, such as IL-1, IL-6, IL-8, TNF- α , and TGF- β was evaluated for human dermal keratinocytes cultured on the TM constructs.

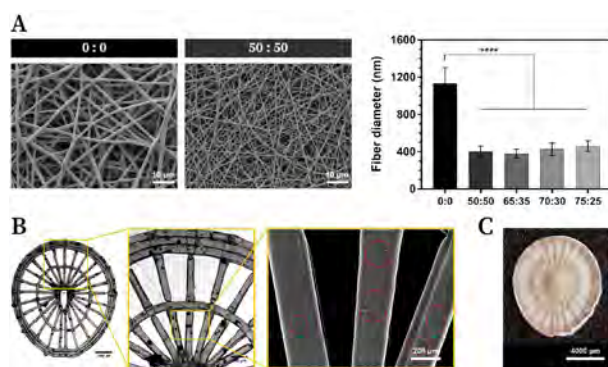


Figure 1. (A) Electrospun nanofibers obtained with pristine PEOT/PBT (0:0) and PEOT/PBT/CN composites (50:50, 65:35, 70:30, and 75:25). (B) Additive manufactured constructs highlighting the presence of CNs. (C) Dual-scale TM scaffolds fabricated by combining ES with AM (50:50).

Results and Discussions: The ES and AM studies conducted with the PEOT/PBT/CN composites validated their use for biofabrication of human eardrum scaffolds.

A three-fold reduction in the diameter of electrospun nanofibers was noted with the inclusion of CNs, although no significant differences were obtained among the different CN/PEG ratios (Figure 1A). In case of AM, reproducible constructs were created with 260 μ m and 184 μ m needles (Figure 1B); however, the 100 μ m needle failed to maintain a consistent extrusion due to formation of CN aggregates within its narrow channel. Tensile (Figure 2A) and indentation (Figure 2B) measurements confirmed the mechanical reinforcement offered by CNs to the fabricated membranes, but similar to the fiber diameters, no clear trend was detected with respect to the selected CN/PEG compositions. Finally, the immunomodulatory investigations performed with human dermal keratinocytes highlighted the efficacy of PEOT/PBT/CN scaffolds in downregulating the analyzed pro-inflammatory cytokines.

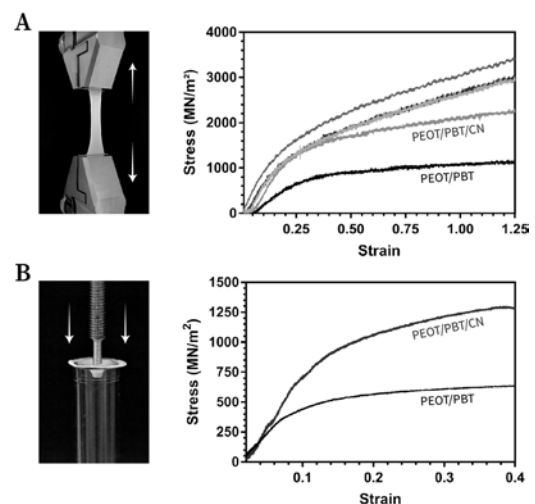


Figure 2. Mechanical characterization confirming the reinforcement offered by CNs. (A) Tensile tests performed on pristine PEOT/PBT scaffolds along with all the nanocomposite formulations (50:50, 65:35, 70:30, and 75:25). (B) Indentation measurements comparing the 50:50 composition with the unaltered copolymer.

Conclusions: This study validates CNs as a promising nanofiller for TM reconstruction, owing to their excellent reinforcement and immunomodulatory capabilities. It shows that the current gap in stiffness reported for PEOT/PBT scaffolds with respect to the native eardrum could be significantly minimized by the introduction of CNs within the polymer matrix.

Acknowledgements: This work is a part of the 4NanoEARDRM project, receiving funding from EuroNanoMed III, the ERA-NET Cofund Action on Nanomedicine under Horizon 2020.

References:

- [1] Mota, C. et al. *Biofab.* 2015: 7(2).
- [2] Anand, S. et al. *Adv. Healthc. Mater.* 2021: 10(11).
- [3] Danti, S. et al. *Pharmaceutics.* 2021: 13(9).

The Effect of Surface Charge of Gelatin Nanoparticles on Cellular Internalization and Colloidal Gel Formation

L. Andrée, J. Dodemont, P. Bertsch, N. Hassani Besheli, F. Yang, S. Leeuwenburgh

Department of Dentistry – Regenerative Biomaterials, Radboud Institute for Molecular Life Sciences, Radboudumc, Nijmegen, The Netherlands

Introduction: Gelatin, as a derivative of collagen, is inherently biocompatible, biodegradable and offers abundant cell attachment motifs. Depending on the extraction method, cationic (type A, IEP ~9) or anionic (type B, IEP ~5) gelatin can be obtained, making it a suitable carrier material for both positively and negatively charged cargos [1]. Gelatin nanoparticles (GNPs) have been recognized as powerful drug carriers due to their larger surface area compared to the conventional hydrogels. Additionally, nanoparticles can get internalized by cells, allowing intracellular drug delivery. Previously, GNPs have been used to assemble injectable, colloidal hydrogels [2]. Colloidal materials are based on aggregated (nano)particles that form a network of particle strands [3]. Yet, within this network structure, particles remain mobile [4]. By shedding of particles, colloidal biomaterials offer an interesting approach for long-term, intracellular drug delivery.

However, studies evaluating cellular uptake of GNPs have so far focussed on either of the two gelatine types, whereas the surface charge of nanoparticles is known to alter interactions with cells [5]. Moreover, the localization of GNPs within cells has not been addressed yet. Here, we investigate the effect of GNP surface charge on cell internalization, intracellular localization and colloidal gel formation.

Methods: GNPs were prepared by coacervation of type A or type B Rousselot gelatin, and characterized by scanning electron microscopy (SEM), dynamic light scattering (DLS) and zeta potential measurement. To yield GNPs with a positive surface charge (hereinafter referred to as type Am), type A GNPs were surface functionalized with ethylenediamine. Gel formation of GNP-based colloidal gels was confirmed using rheological frequency and time sweep measurements.

To study the internalization of differently charged GNPs into phagocytic and non-phagocytic cells, RAW264.7 macrophages and MC-3T3 preosteoblasts were cultured in the presence of fluorescently-labelled GNPs. After 24h, lysosomal compartments were stained with LysoTracker and the uptake of GNPs was visualized using live confocal microscopy.

Results: SEM showed spherical particles with a diameter of 118 ± 21 nm (type A) and 135 ± 36 nm (type B) in dry state. In swollen state diameters were 370 ± 92 nm (type A) and 285 ± 60 nm (type B). Zeta potential measurement revealed a surface charge of 1.0 ± 2.4 mV and -12.8 ± 1.2 mV for type A and type B GNPs, respectively. After surface amination, the Zeta potential of type Am GNPs was increased to 19.1 ± 0.5 mV. While DLS of modified type A GNPs showed an increased particle size in swollen state (427 ± 127 nm vs. 370 ± 92 nm), no significant change in particle size was observed in dry state (132 ± 28 nm vs. 118 ± 21 nm). Rheology confirmed gel formation with frequency-independent shear moduli and shear-thinning behaviour. Interestingly, using 10 w/v% gels, the combination of

oppositely charged type Am and type B GNPs did not lead to stronger gels compared to type Am or type B gels only (storage modulus G' : 6.4 kPa Am+B, ~10.5 kPa Am, ~2.3 kPa B). When reducing the electrostatic or hydrophobic interactions between particles using 1M NaCl and 1 vol% Tween 20, respectively, we saw that at higher solid contents (>10 w/v%), gel formation is mainly governed by hydrophobic interactions.

Confocal live imaging showed that all particle types, independent of their surface charge, get internalized into phagocytic and non-phagocytic cells. GNPs could be seen within the lysosomal compartments as well as in the cytosol. Although experiments have so far only been qualitatively, surprisingly, non-phagocytic MC-3T3 preosteoblasts seem to internalize more GNPs compared to RAW264.7 macrophages.

Conclusion: From the results, we found that gel formation and cell internalization are independent of the surface charge when using GNPs, indicating the flexibility of adopting GNPs compared to the other types of nanoparticles.

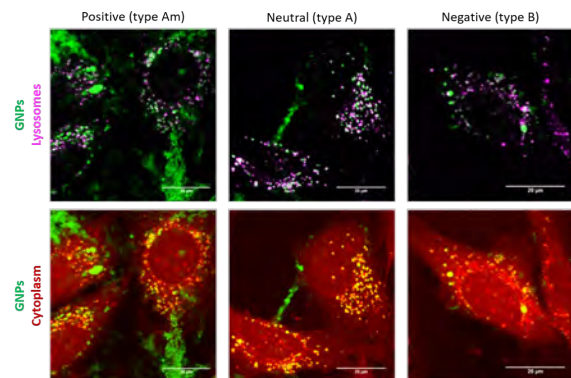


Figure 1 - Intracellular localization of gelatin nanoparticles in MC-3T3 preosteoblasts. Scale bar is 20 µm.

Acknowledgements: The authors would like to thank Rik Oude Egberink and Roland Brock for the helpful discussions and the Netherlands Organization for Scientific Research (NWO, project 17615) for funding.

Contact: lea.andree@radboudumc.nl

Bibliography:

1. Echave, M. C. *et al.* Recent advances in gelatin-based therapeutics. *Expert Opin. Biol. Ther.* **19**, 773–779 (2019).
2. Wang, H. *et al.* Oppositely charged Gelatin nanospheres as building blocks for injectable and biodegradable gels. *Adv. Mater.* **23**, 119–124 (2011).
3. Lu, P. J. *et al.* Gelation of particles with short-range attraction. *Nature* **453**, 499–503 (2008).
4. Landrum, B. J., Russel, W. B. & Zia, R. N. Delayed yield in colloidal gels: Creep, flow, and re-entrant solid regimes. *J. Rheol. (N. Y. N. Y.)* **60**, 783–807 (2016).
5. Augustine, R. *et al.* Cellular uptake and retention of nanoparticles: Insights on particle properties and interaction with cellular components. *Mater. Today Commun.* **25**, 101692 (2020).

Poly(lactic acid)/Nano-hydroxyapatite Microcomposites for Bottom-Up Engineering of Bone Tissue

K. Song, Z. Tahmasebi Birgani, P. Habibović, R. Truckenmüller

Department of Instructive Biomaterials Engineering, MERLN Institute for Technology-Inspired Regenerative Medicine, Maastricht University, Universiteitssingel 40, 6229 ER Maastricht, The Netherlands

Introduction: Bottom-up tissue engineering (TE) is based on the assembly of heterogeneous building blocks (e.g. cells and matrix mimicking components) into larger modular units. Early approaches in bottom-up TE have introduced cell-rich and cell-laden hydrogel assemblies¹⁻², which may not provide the stiffness required for load-bearing bone TE applications and the guidance for osteogenic differentiation. Here, we fabricated a series of microcomposites based on poly(lactic acid) (PLA) and nano-hydroxyapatite (HA), using a soft lithography method combined with (micro)particle replication in non-wetting templates³, to later participate in a cell-guided microparticle assembly and serve as a stiff matrix for cells in bone-like three-dimensional (3D) assemblies (Figure 1).

Materials and Methods: A polydimethylsiloxane (PDMS) intermediate mold containing squared protrusions (100 μm *100 μm *30 μm) was replicated from a SU-8 silicon mold, using a standard soft lithography method. Next, a photocurable perfluoropolyether (PFPE) solution containing 1-hydroxycyclohexyl phenyl ketone as photoinitiator (100/1 v/w) was poured onto the PDMS mold and photocured at 365 cm^{-1} in order to replicate squared indents in the PFPE to serve as non-wettable micromolds. Varying amounts of PLA and HA were respectively dissolved and suspended in acetonitrile (70/10, 50/30, 30/50, 10/70 in (w/v)/(w/v)), stirred overnight and cast onto the PFPE mold. After solvent evaporation, a sacrificial poly(vinyl alcohol) (PVA) film was cast on and then peeled off the mold to remove the microcomposites, and later dissolved in deionized water to release the microparticles. PLA microparticles as control. The microparticles were characterized with Fourier transform infrared spectroscopy (FTIR), Scanning electron microscopy (SEM) coupled with energy-dispersive X-ray spectroscopy (EDS) and laser scanning confocal profilometry.

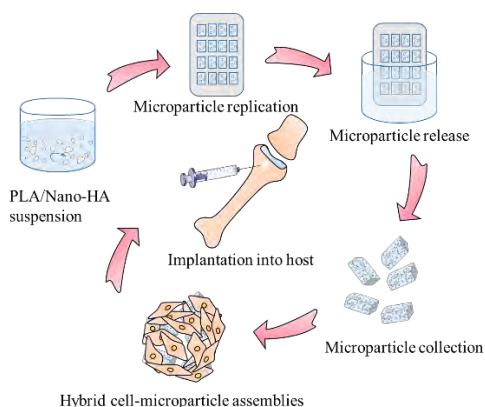


Figure 1. Fabrication of microcomposites and generation of hybrid cell-microcomposite assemblies

Results and Discussion: The particle replication method resulted in discrete and accurately shaped microcomposites with high replication fidelity (Figure 2A). Microparticles with either no or lower HA content had different extents of a meniscus shape on the top surface due to anisotropic solvent evaporation, as also seen before⁴. This effect was interestingly reduced or even eliminated at higher HA contents. EDS elemental maps presented a rather homogeneous distribution of HA throughout the microcomposites, indicating the efficiency of using a HA nanopowder and prolonged stirring time to obtain a uniform suspension. FTIR spectra showed only the bands of PLA and HA and the absence of the solvent residue (Figure 2B). Surface roughness varied between different microcomposites. A roughness anisotropy was also observed in the microparticles, where different roughness values were obtained from the front and the back sides of the microparticles (Figure 2C).

Conclusion: We developed a series of microcomposites with varying polymer/bioceramics ratios and pre-defined geometries. The fabrication process introduced a certain level of anisotropy to the properties of the microcomposites. Next, we plan to investigate the cell-guided assembly of the microcomposites to form hybrid cell-biomaterial spheroids, which ultimately can be used as modular units for bottom-up bone TE.

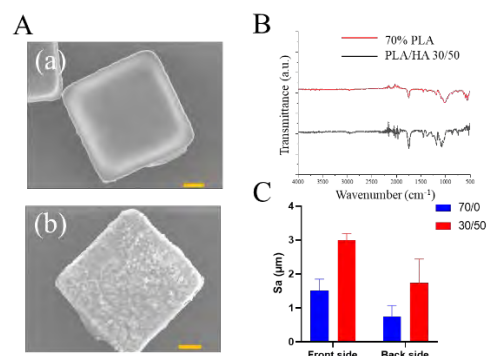


Figure 2. A) SEM images (scale bar: 20 μm) of (a) PLA and (b) PLA/HA 30/50 microparticles, their B) FTIR spectra and C) surface roughness of the front and the back sides.

- 1- Advanced Materials 32 (2020) 1903975.
- 2- Advanced Materials 26 (2014) 2592–2599.
- 3- Journal of Controlled Release 240 (2016) 541–543.
- 4- Advanced materials 33 (2021) 2007695.

Acknowledgements: This research was supported by the China Scholarship Council (CSC) from the Ministry of Education of P.R. China, the European Union Interreg Vlaanderen-Nederland project “BIOMAT on microfluidic chip), the Dutch Province of Limburg (program “Limburg INvesteert in haar Kenniseconomie/ LINK”), the NWO Gravitation Program (project “Materials-Driven Regeneration”) and the NWO Incentive Grant for Women in STEM (Project “Biotetris”).

Mechanosensitive Notch Signaling is a Regulator of Strain-Mediated Changes in Vascular Smooth Muscle Cell Phenotype

C. Karakaya^{1,2}, V.L. Visser¹, M. van Turnhout¹, T. Ristori¹, C.V.C. Bouten^{1,2}, C.M. Sahlgren^{1,2,3}, S. Loerakker^{1,2}

¹Department of Biomedical Engineering, Eindhoven University of Technology, The Netherlands

²Institute for Complex Molecular Systems, Eindhoven University of Technology, The Netherlands

³Faculty of Science and Engineering, Åbo Akademi University, Finland

Introduction: *In situ* vascular tissue engineering, which aims to transform biodegradable scaffolds into living tissues at the implantation site, has the potential to meet the clinical need for small-diameter vascular replacements. Despite the advances in strategies over the years, some fundamental questions, e.g. how the engineered tissues remodel after implantation, and how the native-like organization can be achieved to enable proper functionality, remain to be answered. To address these challenges, a mechanistic understanding of the processes regulating functional vessel growth and remodeling is needed. The understanding is crucial to steer and control the growth and remodeling of vascular tissue upon implantation of the scaffold.

Vascular growth and remodeling are mediated by vascular smooth muscle cells (VSMCs), in turn influenced by mechanical cues and cell-cell signaling. VSMCs obtain interchangeable synthetic and contractile phenotypes depending on the growth and remodeling state of the vessel, and this plasticity is controlled by mechanical cues and Notch signaling. Our computational models have recently predicted that this Notch mechanosensitivity can regulate the phenotypic switch in VSMCs and explain the establishment of homeostasis. Nevertheless, these computational findings are scarcely validated and the interaction between mechanical cues and Notch signaling in the remodeling of vascular tissues is poorly characterized. Validating this prediction and understanding the complex interaction between mechanical cues and Notch signaling in VSMCs will provide an opportunity to steer this interaction and control vascular growth and remodeling in engineered tissues.

Materials and Methods: Human coronary artery smooth muscle cells (Lonza) were cultured for 7 days in Medium 231 (Gibco) supplemented with either smooth muscle growth supplement (Gibco) to obtain synthetic VSMCs, or smooth muscle differentiation supplement (Gibco) to obtain contractile VSMCs. Bioflex culture plates (Flexcell) were coated with bovine fibronectin (Gibco) in the center of the wells. One day after cell seeding on the Bioflex plates, cells were either treated with the γ -secretase inhibitor DAPT (Sigma) to inhibit Notch signaling, or with the vehicle DMSO at a similar concentration as a control. In addition, the Jagged1 ligand was immobilized on the culture surface to continuously induce Notch signaling in a group of synthetic and contractile cells, respectively. Furthermore, cells were either cultured statically or equibiaxially stretched with the Flexcell Tension System at 1 Hz for 48 hours. The membranes of each well were marked and tracked with a camera. The displacement was analyzed, and the corresponding strain was calculated via digital image correlation.

Immunofluorescence (IF) imaging and quantitative polymerase chain reaction (qPCR) were conducted to characterize the changes in cell phenotype, ECM production and Notch signaling upon stretch. One-way ANOVA and post-hoc Tukey HSD were used to determine statistically significant differences between experimental groups (GraphPad Prism v8). The qPCR data were plotted as boxplot and differences were considered statistically significant for $p < 0.05$.

Results and Discussion: Synthetic and contractile VSMCs obtained different morphological features and gene expression. Contractile VSMCs expressed more α SMA and calponin compared to synthetic VSMCs, and they obtained fibrous stress fibers (Figure 1A). The induction of Notch signaling in synthetic VSMCs resulted in a contractile-like phenotype. The application of strain resulted in a transition in contractile VSMCs towards the synthetic phenotype. Contractile VSMCs lost their stress fibers (Figure 1A) and significantly decreased the expression of contractile markers to the level of synthetic VSMCs (Figure 1B). Furthermore, the phenotypic transition of contractile VSMCs with the application of strain was rescued by the activation of Notch signaling. On the other hand, gene and protein expression did not change in synthetic VSMCs upon stretch.

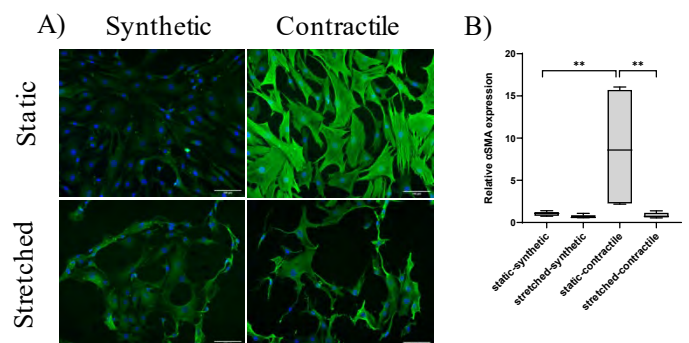


Figure 1: The representative IF images of α SMA (A) and gene expression (B) in static and stretched synthetic and contractile VSMCs. (green: α SMA, blue: DAPI. Scale bar: 100 μ m) (** $p < 0.01$, $n = 5$).

Conclusion: Our results suggest that Notch signaling has a key role in regulating strain-mediated changes in VSMC phenotype. The reduced Notch activity in stretched contractile VSMCs is responsible for the transition of contractile phenotype towards a more synthetic state.

Acknowledgements: This project has received funding from the European Research Council (ERC) under the European Union's Horizon 2020 research and innovation programme (Grant agreement No. [802967]).

Open Science

Dr Dennie Hebels
Project manager, data steward
MERLN Institute
Maastricht University



Abstract:

Open Science aims to make scientific research and its dissemination accessible to all levels of society, resulting in transparent and accessible knowledge. The FAIR principles of findability, accessibility, interoperability and reusability can be regarded as a set of standards to apply to openly shared research in order to maximize its use. However, even though Open Science and FAIR are being promoted by universities, funding organizations and publishers, there is still a lot of debate on these topics. Not everybody agrees on the merits of Open Science and FAIR and it is not always clear how to implement these practices either. In this two-part Open Science session, we will therefore present you with a set of dilemmas associated with FAIR and Open Science and invite you to discuss them in small groups. Provided the weather is good, you can do this during a walk in the woods around the conference centre and come up with suggestions on how to deal with these dilemmas. The next day, we will have a plenary discussion and provide you with information on how to tackle them.

Biography:

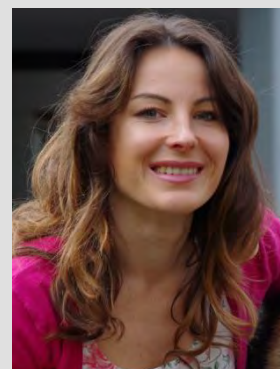
Open Science policy and the FAIR guidelines have formed an integral part of my work for more than 10 years. After a PhD and several post-doctoral positions in “big data” transcriptomics, a field that was one of the pioneers in creating FAIR data, I moved from doing research myself to supporting others with their research. In my current position at the MERLN Institute, I fulfil a hybrid role as a data steward and project manager. This includes coordinating MERLN’s data management activities (such as our internal data archiving procedures), the sharing of data in DataverseNL, and setting up an electronic lab notebook strategy for our researchers. My background in research often proves to be useful here since it allows me to better understand the needs of researchers. I also work as an Open Science ambassador in the Open Science Community Maastricht (OSCM, part of the International Network of OSCs: INOSC), where I help with setting up Open Science and FAIR-related lectures and workshops within our university to motivate people to adopt FAIR practices and be open with their science.

Oral Presentation
Session 5

Keynote session 5

3D printing for the reconstruction of hierarchical tissues: a matter of the design

Dr. Gosia Włodarczyk-Biegun
Faculty of Science and Engineering
University of Groningen



Abstract:

Native tissues are highly organized structures, with an intricate cellular microenvironment. They are non-homogeneous and typically exhibit functional gradients in the architecture and biochemical composition. Whereas it is challenging to produce biomimetic scaffolds using traditional manufacturing processes, 3D printing has emerged as a perfect tool to construct complex 3-dimensional objects with great precision.

In this lecture, I will present our work on 3D printing of hierarchical structures, obtained with high precision at very small scales using Melt Electrowriting (MEW). MEW is a biofabrication approach that combines principles of electrospinning with 3D printing, allowing to precisely deposit molten polymer as fibers with a diameter in the micrometer range, with high flexibility of the design. By alternating scaffolds architecture, the material systems with the structural, mechanical, and biological properties relevant for different tissues can be obtained. Particularly, I will present the utility of MEW for the reconstruction of the Human Trabecular Meshwork (membrane located in the eye), hard-soft tissue interfaces (e.g. connection between bone and tendon), and skin tissue, with the focus on the scaffold design. We envision that the proposed small-scale biomimetic scaffolds will serve in the future as high accuracy in-vitro testing models or implantable systems.

Biography:

Małgorzata Włodarczyk-Biegun is an Assistant Professor at the Silesian University of Technology, in Gliwice, Poland, and a Principal Investigator at The University of Groningen, The Netherlands. Her research is focused on applying 3D (bio)printing technique to generate complex hierarchical scaffolds of polymeric materials for advanced tissue regeneration. She is also interested in the rational design and development of novel polymer-based bioinks with tunable properties allowing to induce a specific cellular response, to produce systems with bio-instructive properties.

She has earned her Master degree in Poland, in Psychology, and in Biomedical Engineering. For her PhD, she decided to continue in the field of Biomedical Engineering. She obtained the title in January 2016, at Wageningen University and Research Center in the Netherlands, working on recombinant proteins for biomedical applications. In the years 2016-2020, she was employed at INM-Leibniz Institute for New Materials, in Germany as a postdoctoral researcher. There, she took on the challenge to set up from scratch and supervise the Bioprinting Lab. In 2017, she was awarded a UNESCO-L'Oréal for Women in Science Prize in recognition of her research qualities and ability to combine excellence in Science with being a mother. Currently, she is working in the Polymer Science group at the University of Groningen, where she has recently received 3 prestigious grants from NWO (Netherlands Organization for Scientific Research). She has also been awarded NAWA Polish returns grant (2019) intended to set-up her own research group in Poland, and the polish NCN Opus grant to further support her research. Combining all sources of funding, she is now building a young Research Group, located partially in the Netherlands and partially in Poland, to pursue international collaborative work.

Friction Reducing Ability of a Poly-L-Lysine and Dopamine Modified Hyaluronan Coating for Cartilage Resurfacing Implants

Alicia (A.H.A.) Damen¹, C.C. van Donkelaar¹, P.K. Sharma², K. Ito¹

1. Orthopaedic Biomechanics, Dept. Biomedical Engineering, Eindhoven University of Technology, the Netherlands
2. Dept. Biomedical Engineering, University Medical Center Groningen, the Netherlands

Ultralow friction and enhanced lubrication are essential features of healthy articular cartilage in the knee joint. When damaged cartilage is replaced by artificial biomaterials, the implant will articulate against cartilage, which disturbs the natural lubrication mechanism. Frictional properties of focal knee implants (FKIs) need to be sufficiently low to ensure that the opposing cartilage is not damaged during articulation. Ideally, the implant surface is able to recruit native lubricious molecules present in the synovial fluid (SF), like proteoglycan 4 (PRG4). A previous study by Wan *et al.* (2020) showed that a layer-by-layer (LbL) coating of poly-lysine (PLL) and dopamine-modified hyaluronan (HADN) on a polycarbonate urethane (PCU) surface was successful in reducing the friction between a PCU surface and opposing cartilage using SF as a lubricant. The present study determines the usage of this PLL-HADN coating on biodegradable polycaprolactone (PCL) as biomaterial for a novel FKI.

PCL disks (25 x 25 mm, n=10) were obtained by melting medical grade PCL granules in a Teflon mold. Half of the sample group (n=5) was coated with 4 layers of alternately PLL or HADN in phosphate buffered saline (PBS). Cartilage rings ($\sigma_{out} = 20$ mm, $\sigma_{in} = 12$ mm) were obtained from bovine patella (3-6 years-old). The coefficient of friction (CoF) was measured using a DHR3 rheometer extended with a ring-on-disk accessory using an intermitted loading protocol with one-minute steps with pressures and velocities of respectively 0 and 0.1 MPa and 0 and 6 mm/s, for 60 minutes in a row. PBS with 10 mg/ml bovine serum albumin (BSA), 3 mg/ml hyaluronic acid (HA) and 200 μ g/ml recombinant human (rh)PRG4 was used as lubricant in between the two contacting surfaces and kept at a constant temperature of 32° C. The water contact angle and surface roughness of the PCL disks was measured prior and after the coating procedure, using respectively an OCA30 contact angle goniometer and a Pl μ 2300 Sensofar and compared using an one-tailed paired t-test.

Besides a visible difference between bare and coated PCL surfaces using bright field microscopy (Fig. 1), the surface roughness significantly increased from 0.057 ± 0.009 μ m to 0.093 ± 0.015 μ m ($P=0.01$) due to the PLL-HADN coating. The water contact angle significantly decreased from $76.0 \pm 2.9^\circ$ to $52.2 \pm 3.8^\circ$ ($P<0.001$) indicating that the PLL-HADN coating made the surface more hydrophilic. Both the naked and the PLL-HADN coated PCL disks showed a decrease in CoF over time against the cartilage ring. The average CoF during the first minute of the friction experiment was twice as high for the naked disks compared to the PLL-HADN coated disks, respectively 0.23 ± 0.10 and 0.11 ± 0.02 (Fig. 2). All paired PCL disks, using the same cartilage ring,

showed a lower CoF for the coated PCL disk compared to the bare PCL disk after an hour of intermitted loading and rotation (Fig. 2).

Using a custom made sandwich enzyme-linked immunosorbent assay (ELISA) it was shown that PLL-HADN was effectively attracting rhPRG4 when diluted in PBS. The friction reduction is most likely the effect of PRG4 recruitment. To prove that PRG4 can also be selectively recruited from the lubricant solution despite the presence of albumin, another ELISA will be performed. Wan *et al.* (2020) showed that 8 layers of PLL-HADN had high adhesive strength to PCU and a high SF responsiveness. The present study shows that 4 layers of PLL-HADN are already enough to reduce friction between cartilage and a PCL surface.

In conclusion, the preliminary results of the present study show that PCL can effectively be coated with PLL-HADN. Additionally, this coating reduces the friction between PCL and cartilage with a SF-like lubricant which makes it a promising application to improve the clinical success of cartilage resurfacing implants, mimicking the lubricating surface of native cartilage.

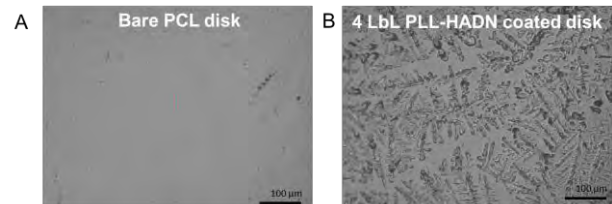


Figure 1: Bright field images of a (A) bare and (B) PLL-HADN coated PCL disk

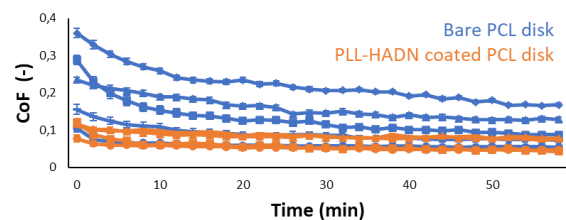


Figure 2: Coefficient of friction (CoF) over time for bare PCL (blue) and PLL-HADN coated PCL (orange) against cartilage

References: Wan *et al.* (2020) ACS Appl. Mater. Interfaces, 12, 23726–23736

Acknowledgements: This research was performed under the framework of Chemelot InSciTe, supported by the partners of Regenerative Medicine Crossing Borders and powered by Health-Hollands, Top Sector Life Sciences & Health. We acknowledge Tannin A. Schmidt for his contribution to the experimental design of the present study and L μ bris BioPharma for the kind donation of rhPRG4.

Biomimetic Calcium Phosphate Coating on Stainless Steel

M. Li, M. Wang, Y. Liu

Oral Cell Biology, Academic Center for Dentistry Amsterdam (ACTA), University of Amsterdam and Vrije Universiteit, Gustav Mahlerlaan 3004, 1081 LA, Amsterdam, Netherlands

Introduction:

Mini-screw implants (MSIs) made by stainless steel (SSL) have been widely used in orthodontic clinic to provide absolute anchorage to correct various orofacial deformities and malocclusions. However, its poor biocompatibility, particularly in teenagers, usually results in relatively high failure rates (1). In our previous study, biomimetic calcium phosphate (BioCaP) coating has been applied on Ti implants to sustain direct ossification and serve as a carrier system for bone growth factor bone morphogenetic protein 2 (BMP2) (2). In this study, we wish to achieve BioCaP coating incorporation with protein to increase the success rate of SSL MSIs.

Materials and Methods:

The roughness and chemical property of medical Ti and SSL plates were evaluated. Then the samples were immersed into five-fold simulated body fluid (SBF) at 37°C for 12h, 24h, 36h, 48h to form amorphous seeding layer (BMT). After this, an octacalcium phosphate (OCP) layer with or without bovine serum albumin (BSA) is obtained by immersing the abovementioned substrates in a supersaturated calcium phosphate solution for 48h at 37°C. Scanning electron microscopy (SEM) was used to verify the morphology of coatings. Contact angle was used to compare the wettability of the modified surface. Nanodrop was used to evaluate the amount of BSA incorporated. Cell seeding efficiency of different groups was also compared.

Results:

The roughness of Ti plates (1.4190 ± 0.0767) is almost 5 times more than SSL ones (0.2389 ± 0.0326).

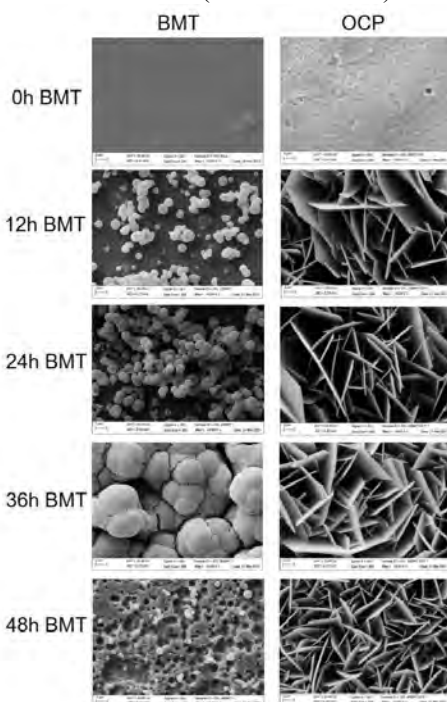


Fig.1 SEM of BMT and OCP coating on SSL. SEM results show that the OCP coating cannot be formed without BMT coating and density of crystalline coating has a positive relationship with BMT coating

period (Fig. 1). The OCP coating can decrease the contact angle of Ti and SSL (Fig. 2). The average amount of BSA incorporated per 5mm plate without seeding layer is 51.25ug (Fig. 3). It is significantly lower than other groups (more than 200ug). A significant increase of cell seeding efficiency can be observed after 36h and 48h BMT coating groups compared with uncoated SSL group (Fig. 4).

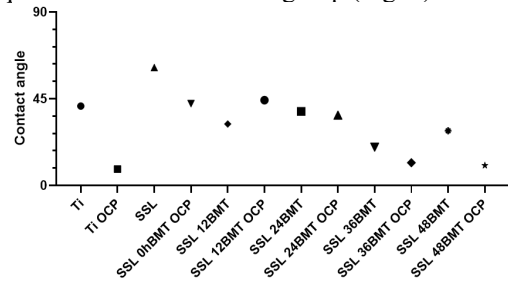


Fig.2 Contact angle of different groups.

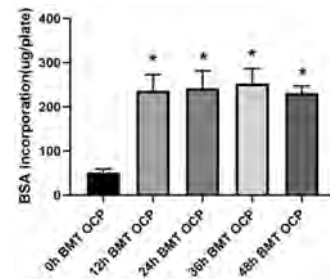


Fig.3 Amount of BSA incorporated.

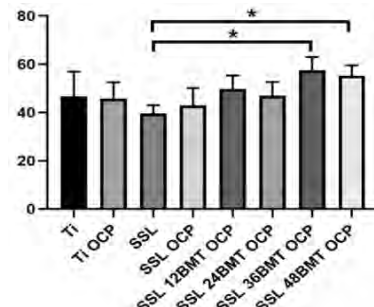


Fig.4 Cell seeding efficiency.

Conclusions:

1. OCP coating can be achieved on smooth SSL surface by extending BMT coating time to 36 hours.
2. OCP coating can increase hydrophilicity and cell seeding efficiency of SSL.
3. OCP coating can be a promising drug carrier and slow-release system.

References:

1. Gurdan, Z., and Szalma, J. Evaluation of the success and complication rates of self-drilling orthodontic mini-implants. *Niger J Clin Pract* **21**, 546, 2018.
2. Lin, X., Chen, J., Liao, Y., Pathak, J.L., Li, H., and Liu, Y. Biomimetic Calcium Phosphate Coating as a Drug Delivery Vehicle for Bone Tissue Engineering: A Mini-Review. *Coatings* **10**2020.

Shaping hepatic organoids into functional metabolic biofactories through high-speed volumetric bioprinting

P.N. Bernal¹, M. Bouwmeester², J. Madrid-Wolff³, M. Falandt², S. Florczak¹, N. Ginés Rodriguez¹, Y. Li¹, R.A. Samson², M. van Wolferen², P. Delrot⁴, D. Loterie⁴, J. Malda^{1,2}, C. Moser³, B. Spee², R. Levato^{1,2}

¹ Dept. of Orthopaedics, University Medical Center Utrecht, Utrecht University, 3584CX, Utrecht, The Netherlands.

² Dept. of Clinical Sciences, Faculty of Veterinary Medicine, Utrecht University, 3584CT, Utrecht, the Netherlands.

³ Laboratory of Applied Photonics Devices, École Polytechnique Fédéral Lausanne, CH-1015 Lausanne, Switzerland

⁴ Readily3D SA, EPFL Innovation Park, Building A, CH-1015 Lausanne, Switzerland

Introduction: The development of complex, multi-scale *in vitro* platforms for biomedical research remains a key challenge in tissue engineering. 3D bioprinting has greatly advanced this field given its ability to pattern cell-laden biomaterials into hierarchical, tissue-mimetic constructs. However, conventional biofabrication approaches carry important translational limitations, particularly i) challenges in mimicking convoluted architectures needed to modulate and enhance tissue-specific functions, and ii) long manufacturing times required to fabricate clinically relevant-sized constructs. The novel volumetric bioprinting (VBP) technique tackles these challenges through the ultra-fast, layerless biofabrication of viable and highly complex cell-laden structures^[1]. Herein, this nozzle-free approach was harnessed to pattern patient-derived human hepatic organoids into functional centimeter-scale biofactories, which are of great interest to create advanced *in vitro* models that capture salient features of the liver related to systemic homeostasis and detoxification.

Methods: Visible light back-filtered projections of a 3D object are sequentially directed towards a cell-laden bioresin (gelatin methacryloyl supplemented with visible-light photoinitiator lithium phenyl-2,4,6-trimethylbenzoyl-phosphinate). Upon sufficient light exposure, the hydrogel selectively crosslinks in a spatially controlled fashion in a single step process. VBP was carried out with patient-derived human hepatic organoids to evaluate tissue-specific function. Viability, metabolic activity and morphological characteristics of hepatic organoids were assessed, as well as hepatic differentiation capacity of VBP-printed constructs (hepatic markers, albumin secretion, and CYP enzyme activity) compared to extrusion bioprinted (EB) and casted constructs. Finally, organoid-laden, mathematically-derived complex architectures with different structural properties were printed and cultured under dynamic perfusion to evaluate the architecture-dependent liver-specific functionality of these constructs (Figure 1).

Results: VBP cm-scaled constructs were fabricated in under 20 seconds and exhibited high volume accuracy compared to CAD designs (5.71±2.31% variation from original design). Printing time remained constant for constructs scaled 2- and 3-fold in volume (up to 4.1 cm³). These prints resulted in extended fabrication times for EB (~30-90min). Hepatic organoids ranging from 100µm to 1mm in diameter were successfully printed via VBP with high printing accuracy, remained highly viable and sustained metabolic activity while exposed to differentiation media. Compared to EB-printed structures, in which organoids are fragmented pre-printing and subsequently exposed to shear stresses

during extrusion through a nozzle, VBP-printed organoids maintained their morphology and exhibited apicobasal polarity post-printing. Complex gyroid-like structures with different surface area to volume ratios, varying pore sizes and channel tortuosities, were printed in under 20 seconds and successfully integrated in a sterile fluidic system. These hydrogel-embedded organoids exhibited liver-specific enzyme and protein synthesis, as well as architecture-dependent rates of ammonia elimination, a key detoxification process carried out in the native liver.

Conclusion: This study established the feasibility of incorporating complex biological structures (hepatic organoids) into the VBP process. Organoids exhibited maintained viability and metabolism, unimpaired polarization, and hepatic differentiation capacity post-printing. Furthermore, sterile dynamic culture of complex VBP-printed structures was demonstrated. Through the selection of architectures with distinct structural properties, organoid metabolic function was successfully regulated, as seen through the architecture-dependent ammonia elimination rates exhibited by printed organoids. Overall, the combination of organoid technology with the ultra-fast printing times and freedom of design offered by VBP is a powerful tool that poses great promise for the development of more predictive and native-like platforms for personalized medicine, *in vitro* disease modeling, drug discovery and drug screening applications in the biomedical field.

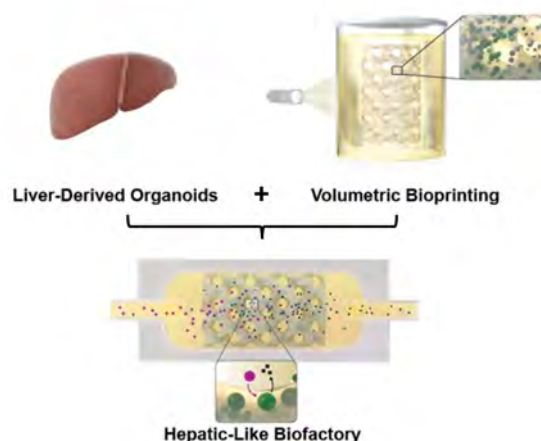


Figure 1. Volumetric bioprinting of human-derived hepatic organoids was employed to develop complex architecture biofactories able to carry out liver-specific metabolic functions.

Reference:

[1] P.N. Bernal, P. Delrot, D. Loterie, Y. Li, J. Malda, C. Moser, R. Levato. *Adv. Mater.* **2019.** 1904209, 1.

Melt Electrowritten Artificial Trabecular Meshwork for Glaucoma Treatment

M. Z. Gladysz^{1,2}, A. Hofman², A. Prus³, M. Koch⁴, M. Kamperman², M. K. Wlodarczyk-Biegun²

¹Groningen Research Institute of Pharmacy, University of Groningen, Antonius Deusinglaan 1, 9713 AV Groningen, The Netherlands,

²Polymer Science, University of Groningen, Nijenborgh 4, 9747 AG Groningen, The Netherlands

³Warsaw University of Technology, Pl. Politechniki 1, 00-661 Warsaw, Poland

⁴Leibniz Institute for New Materials, Campus D2 2, 66123 Saarbrücken, Germany

Contact: m.z.gladysz@rug.nl

Introduction: Trabecular meshwork (TM) is a structure situated in the eye around the base of the cornea. TM is a key structure responsible for forming a proper liquid drainage from the anterior chamber in the eye. When dysfunctional, leads to glaucoma - the fourth largest cause of vision loss according to the International Agency for the Prevention of Blindness¹. Glaucoma is predominantly driven by the increase in intraocular pressure when the permeability of TM is impeded. Currently, there is no satisfactory cure for glaucoma and in vitro models used for glaucoma treatment investigation lack the structural complexity characteristic for the native human TM. Therefore, new, adequate in vitro models of human TM are urgently needed.

Materials and Methods: Scaffolds were fabricated via melt electrowriting (MEW) printer (Spraybase, Ireland) with the use of polycaprolactone (PURASORB PC 12, Corbion). MEW is a 3D printing technique capable of fabricating highly detailed, precisely printed fibrous structures with micrometric resolution. Various designs (architecture, porosity, number of layers) were investigated and the optimal ones were identified for further experiments. Cell culture studies were performed with the use of NIH-3T3 cell line and the results were assessed via fluorescence imaging and scanning electron microscopy (SEM). Perfusion tests were performed with a gravity-based custom-made setup, using medium as a permeate.

Results and Discussion: MEW provided an extensive flexibility in design options and scaffolds were successfully printed with micron-scale resolution (Fig.1). The printed structures recapitulated hierarchical organization of native TM in more details than state-of-the-art approaches^{2,3}. The cells cultured on the scaffolds attach to the strands and proliferate during 15 days of experiment (Fig.2). SEM images show that the cells bridge the gaps between fibers and create a cellular network (Fig. 1). Their penetration capabilities will be optimized as a next step of the project. The liquid permeability is strongly dependent on the scaffold design and can be easily adjusted, providing a way to mimic the outflow of aqueous humor in both healthy and diseased model.

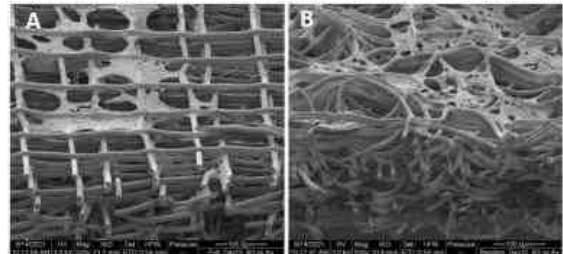


Fig. 1. SEM images of 3T3 cells cultured on scaffolds for 15 days, imaged at 60 °: (A) Square mesh; (B) Random design.

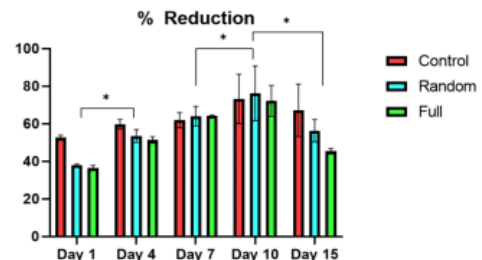


Fig. 2. The relative reduction of AlamarBlue for each design and time point; N = 3. A 2-way ANOVA analysis showed a significant difference ($P < 0,05$) between subsequent days.

Conclusions and Outlook: Human TM design manufactured via MEW has the ability to mimic, with unprecedented accuracy, the multi-layered native structure of the tissue, with its pore size gradient and various architecture of different TM regions. It also offers a good environment for cell attachment and growth. Our studies show a great promise of MEW for producing improved alternatives to current in vitro TM models.

References:

1. Focus on Glaucoma 2021 - The International Agency for the Prevention of Blindness. <https://www.iapb.org/learn/our-events/focus-on-glaucoma/>.
2. KY, T. *et al.* Bioengineered glaucomatous 3D human trabecular meshwork as an in vitro disease model. *Biotechnol. Bioeng.* **113**, 1357–1368 (2016).
3. M, O., SM, B., MB, P. & MD, K. Collagen and collagen-chondroitin sulfate scaffolds with uniaxially aligned pores for the biomimetic, three dimensional culture of trabecular meshwork cells. *Biotechnol. Bioeng.* **114**, 915–923 (2017).

Aqueous Two-Phase Enabled Low Viscosity 3D (LoV3D) Bioprinting of Living Matter

Malin Becker¹, Jeroen Leijten¹

¹ Leijten Lab, Dept. of Developmental BioEngineering, TechMed Centre, University of Twente, Enschede, NL

Introduction

Embedded bioprinting is a promising additive manufacturing technique that permits the fabrication of large-scale, freeform, complex 3D tissue constructs. During the development of new (bio)inks, the shape-stability of extruded strands plays a major role. To stabilize the strand after extrusion, while allowing for smooth extrusion with limited pressures, shear thinning inks are commonly employed. For these inks, the printing resolution is dictated by nozzle diameter¹, while shear stresses within the nozzle during extrusion determine cell viability², which thus limits bioprinting resolution and speed. Here, we report on a low viscosity 3D (LoV3D) liquid printing approach, which is enabled by the innovative use of an aqueous-two phase system (ATPS). LoV3D allows for the highly rapid bioprinting with high cell viability, while allowing for continuous on-the-fly tuning of filament diameter, which ranges from millimetric down to single cell resolution using a single nozzle in a nozzle-diameter independent manner.

EXPERIMENTAL METHODS

Alginate was functionalized with tyramine (TA) groups via DMTCM coupling to form a photo crosslinkable embedding bath. For 3D printing of several inks, a Cellink Inkredible+ printer was combined with a syringe pump to allow for printing at set speeds and extrusion rates. Various mammalian cell types including 3T3 mouse fibroblasts were used to investigate LoV3D's cytocompatibility.

RESULTS AND DISCUSSION

The suitability of a variety of established (bio)polymer solutions for loV3D printing was confirmed and Dex-TA/PEG as well as Alginate-TA/PEG were chosen as model systems. The formation of a stable ATPS interface was substantiated by establishing the binodal curves of these systems. The use of low viscous solutions allowed for strand elongation (thinning) with increased printing speeds (Figure 1a). Comparing reported print diameters in literature for various nozzle sizes, we determined that LoV3D printing offers a substantially higher resolution printing regime, which can be equally accessed with all tested nozzle diameters (Figure 1b). The unique thinning of printed low viscosity strands was utilized to create prints with diameters ranging over two orders of magnitude down to single-cell resolution, all achievable with a single nozzle (Figure 2a). Conventional complex shapes such as spirals, tubes and grids could readily be created (Figure 2b,c) To investigate the influence of viscosity dependent shear stresses within the printing nozzle on cell viability, we combined simulation based data with extrusion experiments. Here, we were able to establish, that for a wide range of flow rates, low viscosity inks do not show any significant reduction of cell viability, while higher viscosity inks reduced the viability with increasing flow rates down to 50% (Figure

2d). Further, incorporation of cells within a sacrificial ink allowed for a one-step print and seed approach. Here, the liquid/liquid interface during printing facilitated additional surface modification, where covalent bonds between coating and channel wall could be formed more-effectively for ATPS liquid/liquid as compared to conventional solid/liquid interfaces.

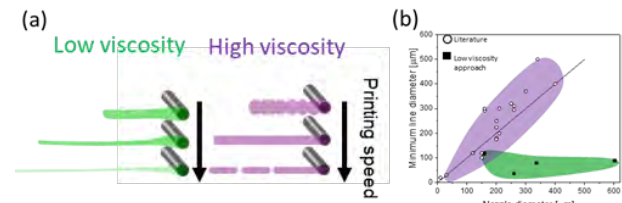


Figure 1: Filament thinning opens up a new high resolution printing regime. (a) Schematic filament shape of low and high viscosity aqueous solutions at different printing speeds and set extrusion rate. (b) Line diameters reported in literature with different nozzle sizes as compared to experimental data with low viscosity inks.

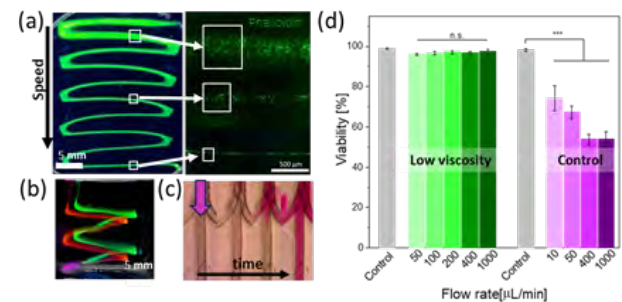


Figure 2: Low viscosity bio-inks allow for high cell viability while enabling high resolution and channel interconnection of prints. (a) Printing with increased speed thins filaments and decreases filament diameter down to single-cell resolution. (b) Multi-material 3D printing demonstrated with a printed spiral shape. (c) 3D printed perfusable branched capillary networks. (d) Cell viability after extrusion through a 25G nozzle at various flow rates.

CONCLUSION

In this study, we introduce loV3D bioprinting as a highly versatile and rapid bioprinting technique, which is inherently compatible with a wide range of biomaterials and crosslinking strategies, while offering on-the-fly tunable high resolution prints without compromising printing speed or cell viability. Future studies will focus on the cell incorporation within the channels, aiming for the creation of perfusable multiscale vascular networks.

REFERENCES

1. Jin Y. *et al.*, Mater. Sci. Eng., C. 80:313-325, 2017
2. Murphy, S.V. *et al.*, Nat. Biotechnol., 8:773-785, 2014

ACKNOWLEDGMENTS

Financial support was received from the European Research Council (ERC, Starting Grant, #759425) and the Dutch Research Council (NWO, Vidi Grant, #17522).

Contact:

Malin Becker, m.l.becker@utwente.nl

Oral Presentation
Session 6

Keynote session 6

MICROFLUIDIC ARRAYS FOR BIOCLINICAL AND ENGINEERING APPLICATIONS

Dr. Burcu Gümüřcü Sefünc
BiolInterface Science Research Group
Eindhoven University of Technology



Abstract:

Hydrogels are powerful soft materials that hold great promise for transformative technologies as well as hitherto unrealized fundamental studies. In the past decade, the synthesis of chemically and geometrically complex hydrogels created a surge of interest that is the pull from a wide range of applications including microfluidic biosensors for disease diagnosis, on-chip platforms for disease modeling. Such applications require a close link of the hydrogel function with chemical composition and morphology in microfabricated platforms. The integration of hydrogels in microfluidic platforms affords the ability to engineer material properties a priori and confer precise control of reactions and cell response at micron-sized environments. In this talk, I will (i) provide an overview of the recent advances in design and functionalization of microfabricated systems for hydrogel integration, (ii) highlight several applications including cancer diagnosis, next-generation biomolecule sequencing, organ-on-chip, and biomaterial discovery, and (iii) discuss the future directions of this emerging technology.

Biography:

Dr. Burcu Gümüřcü Sefünc is an assistant professor at BiolInterface Science Research Group. She strives for the development, fabrication, and application of smart biomaterials to realize high-precision processing in high-throughput microfluidic settings, especially for biomaterial discovery in regenerative medicine and immune-engineering. She also serves as a web writer at Royal Society of Chemistry in collaboration with the development editor of Lab on a Chip Journal. Previously, she was a postdoctoral fellow at University of California, Berkeley (USA), where she performed independent research on novel microfluidic biosensors for single-cell protein analysis. Dr. Gümüřcü Sefünc received her Ph.D. degree in bioengineering at BIOS Lab-on-a chip group at University of Twente in 2016. The focus of her Ph.D. project aimed at the design and development of microfluidic devices for next-generation sequencing, organ-on-chip, and water desalination on the microscale. She received the master's degree from Bilkent University Institute of Materials Science and Nanotechnology (TR) in 2012 and bachelor's degree from Hacettepe University Department of Biology (TR) in 2010. Dr. Gumuscu-Sefunc published over 35 high-impact scientific publications and patents. Dr. Gumuscu-Sefunc received University of Twente Sensing program to run independent research (2018), prestigious Pieter Langerhuizen Stipend given by KHMW (2019), Irene Curie Fellowship from TU/e (2020), and EAISI-AI for health grant (2021).

Establishment of a Rat Model for Enthesis Regeneration Studies

C. J. Peniche Silva¹, S.A. Müller², N. Quirk², R. E. De la Vega^{1,2}, C. H. Evans², E. R. Balmayor^{2,3}, M. van Griensven^{1,2}
¹cBITE, MERLN Institute for Technology-Inspired Regenerative Medicine, Maastricht University; Universiteitssingel 40, 6229 ER Maastricht, the Netherlands.

²Musculoskeletal Gene Therapy Laboratory, Rehabilitation Medicine Research Center, Mayo Clinic; 221 4th Ave, SW, 55905, Rochester, MN, USA.

³TBE, MERLN Institute for Technology-Inspired Regenerative Medicine, Maastricht University; Universiteitssingel 40, 6229 ER Maastricht, the Netherlands.

Introduction: Tendon attaches to bone through a highly specialized tissue called enthesis. Typically, these entheses can be described as a succession of four different zones: tendon, unmineralized fibrocartilage, mineralized fibrocartilage, and bone. However, the microstructure of the entheses, as well as their cellular composition and mechanical properties, vary depending on their anatomical localization. The patella (PT), Achilles tendon (AT), and Rotator cuff (RC) are among the most clinically relevant sites of enthesis injury. Yet, to develop efficient strategies to target enthesis regeneration upon injury, it is of paramount importance to establish an animal model for enthesis regeneration studies. Here, we aimed at the characterization of these three different entheses in terms of biomechanics, gene expression, and histology to select one enthesis as the ultimate model for enthesis regeneration studies.

Materials and Methods: The entheses samples from the PT, the AT, and the RC, were harvested from healthy adult Sprague Dawley rats. A custom-made, mechanical-testing machine was used to investigate the ultimate load, stiffness, and tangent modulus of each enthesis sample. Later, the mRNA was isolated and the expression of tenogenic, chondrogenic, and osteogenic markers was investigated by RT-qPCRs. Furthermore, the histological characterization of the samples was performed by Safranin O and Hematoxylin & Eosin staining in addition to the immunostaining for collagen 1, collagen 2, collagen 3, and collagen 10.

Results and Discussion: Biomechanical characterization (Figure 1) revealed similarities in terms of strength and stiffness between the PT and the AT entheses, while the RC was the weakest of the three, showing the highest values of stiffness. Additionally, the PT enthesis exhibited the largest cross-sectional area among the three entheses samples analyzed. Concomitantly, the AT enthesis had the longest associated tendon, closely followed by the PT enthesis. Interestingly, the RC enthesis featured the shortest associated tendon among all analyzed entheses. The analysis of the gene expression (Figure 2) exposed significant differences among each enthesis type. On the one hand, the AT enthesis showed significantly higher levels of expression of genes such as COL1a1, Mxkx, Tnmd, Sox9, Runx2, and COL10a1 than the other two entheses. The expression of Sox9 was also higher in the RC than in the PT enthesis, while the expression of COL3a1 was higher in AT and PT entheses when compared to the RC enthesis. On the other hand, the PT and AT entheses showed very similar expression of COL2a1 and COL10a1, and in both cases, the expression was higher than in the RC enthesis. The histological characterization allowed to visualize important

differences at the insertion site for each enthesis. The PT enthesis showed a large cartilaginous area at the tendon-to-bone interphase whilst this interphase was smaller in the RC enthesis specimens. Furthermore, the AT enthesis exhibited a more abrupt transition from tendon to bone. In all cases, a zone rich in collagen 2 was present in between the tendon and the bony ends of the entheses. Additionally, the tendon and bony zones were positively stained for collagen 1 in the three entheses.

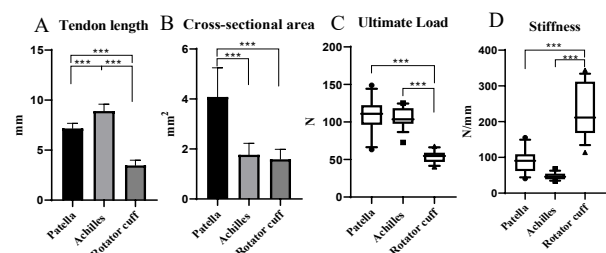


Figure 1: Biomechanical characterization of the three native entheses. (A) Tendon length, (B) Cross-sectional area, (C) Ultimate load, (D) Stiffness. ***p < 0.001

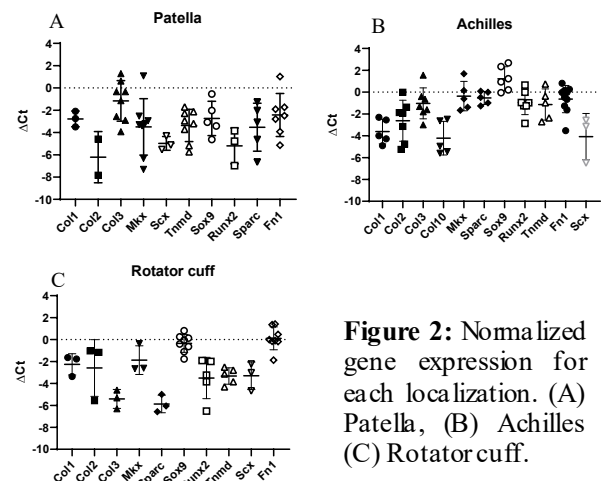


Figure 2: Normalized gene expression for each localization. (A) Patella, (B) Achilles (C) Rotator cuff.

Conclusions: Overall, the data presented herein provide valuable insights for a better understanding of three entheses at relevant anatomic sites. On the one hand, the gene expression analysis allowed the identification of clinically relevant genes that showed to be specific to each enthesis localization. On the other hand, biomechanical evaluations revealed that the PT enthesis featured the highest ultimate load resistance combined with the lowest stiffness. Furthermore, the large cross-sectional area of this enthesis and the convenient surgical accessibility to the PT region, allowed us to conclude this specific enthesis site as ultimate for the development of a preclinical model for enthesis regeneration studies in rats.

Revisiting ImageJ : Automated quantification of vasculature properties using machine learning tools

P. Padmanaban¹, T. Busink^{1,*}, T.M. Paquaij^{1,*} and J. Rouwkema¹

¹Department of Biomechanical Engineering, Technical Medical Centre, Faculty of Engineering Technology, University of Twente, The Netherlands

*these authors share equal contributions

Motivation

To include effective perfusable multiscale tubular structures within engineered tissues, the knowledge about spatiotemporal changes of vasculature properties such as diameter, branching density, erythrocyte velocity, etc. within a developing model organism is very important [1]. However, quantitative assessment of these rapidly changing vasculature properties is hampered by the lack of software analysis tools with automated protocols [2] and fast computation of complex multiscale structures [3].

Methods

Here, we developed a machine learning based algorithm and U-net (a convolutional neural network) segmentation strategy for the accurate and fast quantification of changes in vessel diameter and erythrocyte velocities. Particle tracking is implemented in MATLAB and vessel diameter detection in Python. We employed nearest neighbour method (for erythrocyte tracking) and an additional prediction algorithm (for diameter estimation) to increase the accuracy and decrease the processing time, thereby making it possible to perform a customized analysis of microscopic videos and static images. A graphical user interface (GUI) was developed to minimize the quantification process and for easy user access (Figure 1).

Results and discussion

We have validated both the particle tracker and vessel diameter detection application packages using videos and images of developing chick vasculature, the flow of fluorescent microbeads and microscopic images from literature database. For better segmentation results, the raw image is divided into multiple region of interest (ROI). The U-net uses those ROI for the prediction of the vessel's diameter. Every ROI can individually be selected, inside the GUI, for precise examination. An extraction button makes it possible to export every ROI to the user's computer, which makes it easier for comparing different stages of the vascular development. For optimal validation multiple ROI's with different vascular structures have been selected. Both the manual segmentation as the U-net model have their limitations. Results of the the Particle Tracker applications were compared with Fiji's tracking plug-ins to highlight the advantages of the developed customized tracking application.

Conclusions and Future directions

In conclusion, our user friendly application package (Particle tracker and Vascular properties detector) offers quick, precise and reproducible quantification of vascular properties from microscopic images. Future work will focus on combining these quantification packages into a single standalone application with customized options.

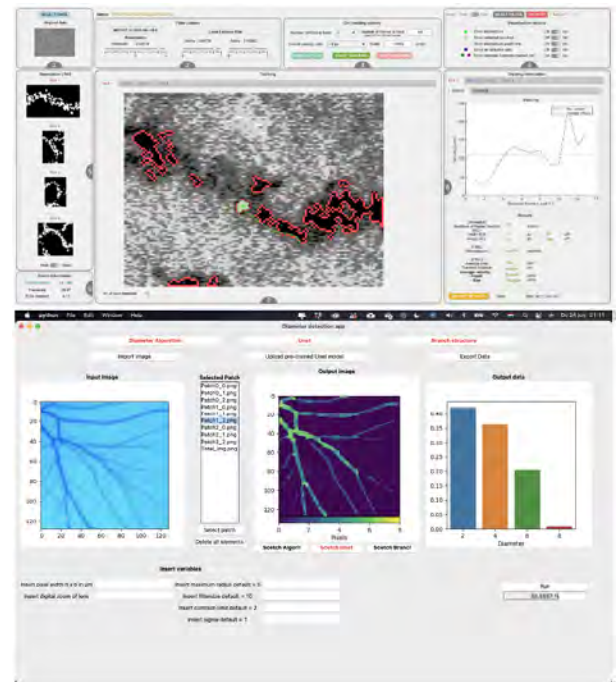


Figure 1. Graphical User Interface for (top panel) erythrocyte tracking and velocity measurement (bottom panel) vessel diameter quantification

References

- [1] Padmanaban P et al. **2021** *Sci. Rep* 11: 18251
- [2] Tinevez JY et al. **2017** *Methods* 115: 80-90
- [3] Guedri H et al. **2017** *Biomedicines* 5, 12

Acknowledgements

This work is supported by an ERC Consolidator Grant under grant agreement no 724469.

High throughput screening of topographies to mitigate fibrosis in glaucoma filtration surgery devices

P.K. Sudarsanam¹, Tim J.M. Kuijpers¹, Jarno E.J. Wolters², Theo G.M.F. Gorgels², Leonard Pinchuk³, Henny J.M. Beckers² and Jan de Boer¹

¹Eindhoven University of Technology, Department of Biomedical Engineering and Institute for Complex Molecular Systems Eindhoven, the Netherlands

²University Eye Clinic Maastricht, School for Mental Health and Neuroscience, Maastricht, the Netherlands

³InnFocus Inc., Miami, Florida, USA

Contact: p.k.sudarsanam@tue.nl, Ph. no: +31 (0) 617623600

Introduction

Glaucoma is one of the leading causes of irreversible blindness. It is caused by high intraocular pressure due to imbalance in the flow of aqueous humor, which is the clear liquid under the cornea. Severe glaucoma is treated by use of glaucoma filtration surgery devices, which drain the liquid from the eye into a bleb formed between the Tenon's capsule and sclera. A frequently occurring problem with this treatment is the formation of a dense fibrous tissue at the outlet that blocks the outflow of aqueous humor and thus causes implant failure. Macrophages and fibroblasts are known to be involved in implant-related fibrosis and respond to the physical and chemical nature of biomaterials, so we set out to identify surface topographies that attenuate the fibrotic process.

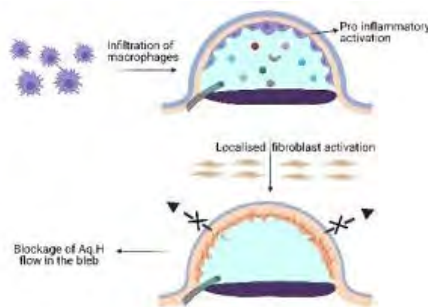


Figure 1: shows the scheme of events after the surgery which can lead to thick tissue formation due to the fibrotic process

Methods

We fabricated poly (styrene-block-isobutylene-block-styrene) (SIBS) TopoChips using hot embossing of a glass mould containing 2176 distinct topographies. Primary Tenon fibroblasts were grown on the TopoChip, and we quantified expression of the trans-differentiation marker alpha-smooth muscle actin (α -SMA) and proliferation through EdU staining by automated image analysis. We ranked topographies based on the relevant parameters and used the machine learning package XGBclassifier to correlate the topography design parameters to the biological response.

Results and discussion

Visual observation showed that the topographies have a strong effect on Tenon fibroblast morphology and stress fiber formation (see Fig 2(a)) relative to flat control surfaces. We ranked top and bottom hits based

on the imaging data and noticed that α -SMA and EdU show a 4-fold differences between top and bottom hits (Figure 2(b)). For both markers we identified topographies that were either higher or lower than cells on a flat surface.

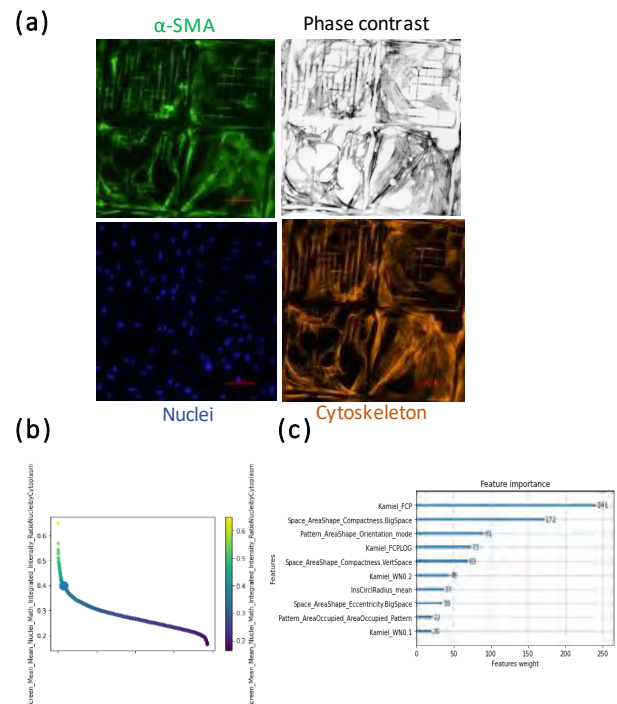


Figure 2: (a) Section of α -SMA TopoChip screen with zoomed in images of topographies with flat surface on right bottom corner (b) ranking of the SMA expression of topographies from the screen (Flat on bold dot). (c) feature descriptors which have highest difference in cell phenotype

Machine learning models based on either EdU, or α -SMA and the topography design features were able to predict with an accuracy of 0.85 and 0.92 respectively, meaning that there is a correlation between topographical design and cell response. Some of the descriptors are presented in Figure 2 (c).

Future Work

Based on the screening results, we will investigate topographies that are low in α -SMA and low in EdU and are favourable in a macrophage screen in an *in vivo* rabbit model.

Acknowledgements

This research was conducted under the framework of the Chemelot Institute for Science & Technology (InSciTe).

Melt Electrowritten Scaffolds with Tunable Mechanical Properties for Interface Tissue Engineering

Piotr Zielinski¹, Marleen Kamperman¹, Malgorzata Wlodarczyk-Biegun^{1,2}

¹Polymer Science - Zernike Institute for Advanced Materials, University of Groningen, Nijenborgh 4, 9747 AG Groningen, The Netherlands

²Biofabrication and Bio-Instructive Materials- Biotechnology Center, Silesian University of Technology, B. Krzywoustego 8, 44-100 Gliwice, Poland
Contact: p.s.zielinski@rug.nl

Introduction:

Soft-hard tissue interfaces are bone-ligament or bone-tendon connections. They are prone to injuries as they make up the region where stress concentration occurs [1]. Due to the poor healing process, these injuries are the leading contributor to disability worldwide [2]. Regeneration is difficult since the interface tissues are complex structures with mechanical and biochemical properties changing in a gradual manner. It is still a challenge to produce synthetic systems mimicking the native gradients. Therefore, this project aims at developing scaffolds with gradient architecture for soft-hard tissue interfaces.

Materials and methods:

The medical polycaprolactone (PURASORB PC 12, Corbion) scaffolds were fabricated using 3D printing method called Melt Electrowriting (MEW). Homogenous and gradient scaffolds with different designs (number of layers, architecture) were printed (Fig. 1). Stiffness of the scaffolds was investigated with the use of tensile testing device, and cyclic testing was performed using rheometer in a tension mode. To predict the mechanical properties of the scaffolds computer simulations in COMSOL Multiphysics have been used.

Results:

Various designs, both homogeneous and gradient, were successfully printed with good accuracy, and average fiber diameter of $16 \pm 2 \mu\text{m}$.

The tensile test revealed that different designs show different mechanical behavior (Fig. 2). The number of layers did not influence Young's Modulus of the scaffold in tensile mode, but altered the maximum force before breaking. Gradient scaffolds have shown to have also more complex, gradual response to the tensile loading (Fig. 2).

Cyclic testing revealed that square mesh can withstand 1% of strain without permanent changes while the radial and rhombus <138 designs endure more than 20% and 50% strain, respectively. Computer simulations allowed predicting mechanical properties of printed scaffolds.

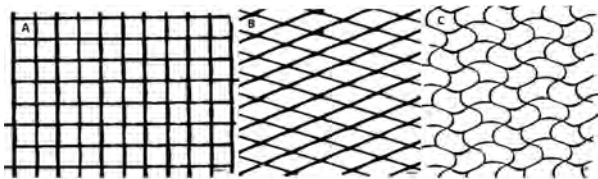


Fig. 1 Light microscope images of printed scaffolds with 8 layers: (A) square $200 \times 200 \mu\text{m}$, (B) rhombus <138, (C) radial. Scale bar: $100 \mu\text{m}$.

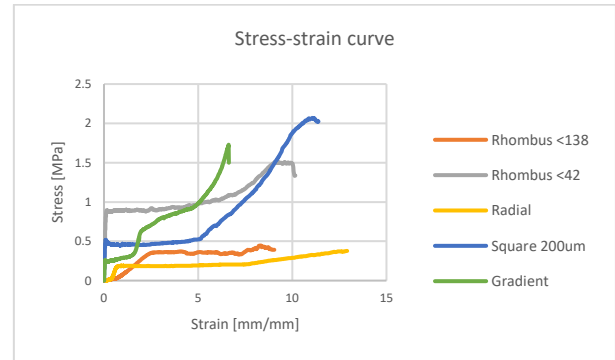


Fig.2 Stress-strain curves for different designs.

Summary and conclusions:

MEW allows to printing gradient scaffolds with exceptional accuracy. The printed scaffolds showed architecture-dependent mechanical properties, in the range relevant for interfacial tissues. We envision that MEW-printed scaffolds are suitable to obtain structures mimicking gradient interfacial tissues.

In the future, computer simulation will be used for more complex scaffolds. Cell culture studies will be performed to investigate cell behavior on both homogeneous and gradient scaffolds. The designs will be improved accordingly, to closely recapitulate biological and mechanical responses of hard-soft tissue interfaces.

References:

1. Benjamin, M., et al., Where tendons and ligaments meet bone: attachment sites ('entheses') in relation to exercise and/or mechanical load. (0021-8782 (Print)).
2. Blyth, F.M., et al., The Global Burden of Musculoskeletal Pain-Where to From Here? American journal of public health, 2019. 109(1): p. 35-40.

Biomimetic Calcium Phosphate Coatings Applied to Poly(carbonate urethane) Substrates

P. Farjam, J. Rouwkema, E.E.G. Hekman, G.J. Verkerke

Department of Biomechanical Engineering, University of Twente, Drienerlolaan 5, 7522 NB Enschede, The Netherlands

Introduction The use of polyurethane in medical applications has been reported and evaluated by several authors. For use in orthopaedics, there is particularly one member of the polyurethane family, polycarbonate-urethane (PCU), which has great potential. PCU demonstrated promising characteristics to be used in orthopaedic implants (Khan *et al.*, 2005). These include: good biocompatibility and mechanical properties, similarities to natural cartilage, and good wear properties. This makes the use of polycarbonate-urethane in orthopaedic applications compelling. The material can be involved in a diverse range of orthopaedic implants including but not limited to joint replacement implants. Success in the application of an orthopaedic implant depends on multiple factors. Implant design, surface configuration, fixation method and surgical procedure play critical roles to decrease the failure rate of implantation. An insufficient fixation technique may cause serious issues such as movement, delamination, deformation and detachment of an implant which leads to failure of the implant and thus the requirement for additional treatment. Tissue ingrowth techniques are reliable methods for long-term fixation of orthopaedic implants. One promising technique would be the addition of a bone-like apatite coating to improve integration of implant into the bone tissue. We currently are designing a novel joint replacement prosthesis, built from PCU. A bioactive, osteo-conductive coating could contribute to its long-term fixation to bone.

Purpose In this study we will identify the optimized osteo-conductive calcium phosphate (CaP) coating parameters for deposition on PCU.

Materials and Methods Extruded PCU foil (Carbothane AC-4085 A) with thickness of 150 μ m was obtained from our project partners at the Fraunhofer Institute for Manufacturing Engineering and Automation (Stuttgart, Germany). Square specimens of \sim 1 cm² were used. The specimens were thoroughly cleaned with 70% ethanol and distilled water, and then dried with N₂ gas. They were placed in a plasma oven to expose to oxygen plasma for 40S at 0.5Torr with intensity of 50W. The plasma treated specimens were suspended in simulated body fluid (SBF) and 5XSBF (Costa *et al.*, 2012) for 4 h, 8 h, 24 h and 6 days (with solution replenishment each 24 h) at a temperature of 20 °C, 37 °C or 50 °C. The coated specimens were thoroughly washed with distilled water and dried with N₂ gas.

Results Apatite coatings deposited by suspension in SBF did not form a homogenous layer across the PCU surface even after 6 days of incubation (Figure 2). Non-homogenous porous star-like crystals were formed on the surface of samples treated in SBF at 37 °C after 24 h (Figure 1). Increasing the temperature from 37 °C to 50 °C changed the star-like crystals into a block-like morphology. Increasing the incubation time from 24 h to

6 days reduced the density of nucleated apatite but enlarged the size of the star-like crystals (Figure 1). Increasing the concentration of the solution from SBF to 5XSBF led to the formation of a continuous multilayer porous structure with cracks.

Conclusion This study shows that a calcium phosphate coating can be formed on PCU films. Future research will focus on the optimization of the coating and the investigation of the stability of the coating.

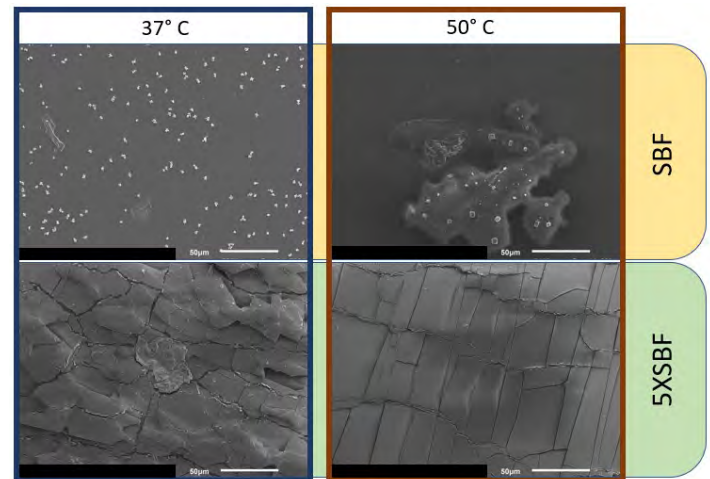


Figure 1. SEM micrographs of CaP coatings on PCU films after immersion in various SBF solutions and temperatures for 24 h

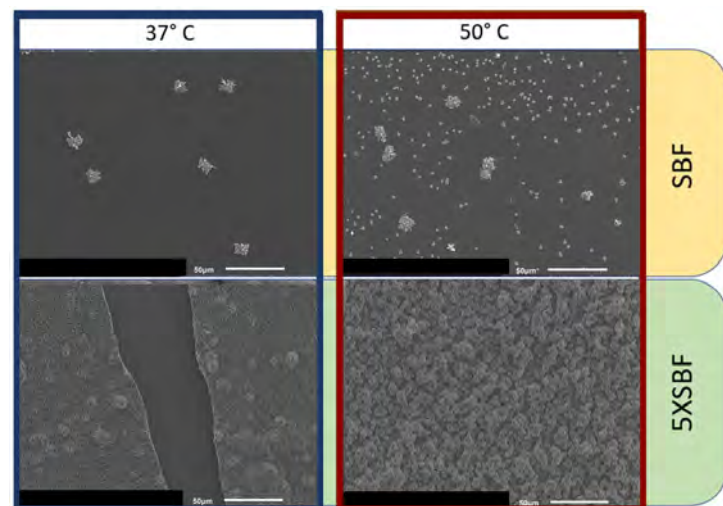


Figure 2. SEM micrographs of CaP coatings on PCU films after immersion in various SBF solutions and temperatures for 6 days

Costa, D. O. *et al.* (2012) 'Control of Surface Topography in Biomimetic Calcium Phosphate Coatings'. doi: 10.1021/la203224a.

Khan, I. *et al.* (2005) 'Analysis and evaluation of a biomedical polycarbonate urethane tested in an in vitro study and an ovine arthroplasty model. Part II: In vivo investigation', *Biomaterials*, 26(6), pp. 633–643. doi: 10.1016/j.biomaterials.2004.02.064.

20.00-21.00

Cultured meat

Prof. Mark Post

Maastricht University



Abstract:

Since the start of scientific development of cultivated meat in 2005 major steps have been made to convert this medical technology into a food production process. Whereas some of the developments remain based on results and concepts derived from the far larger and better funded regenerative medicine research, additional challenges force the cultivated meat society to pursue divergent routes. The unimaginable scale of cell/tissue production and need for low-cost production are challenges of technical and logistic nature. Not only rigorous optimization of existing processes but also novel scientific development is required to overcome these challenges. Biomaterials and coatings play a big role in this innovation, as will manufacturing. They are currently necessary as scaffolds for cell and tissue production, and their use will be extended when more complex tissues are being created. To reduce the cost of production, feedstock that is traditionally pharma-grade will be exchanged for food-grade substitutes and likely cruder hydrolysates. Consumer related challenges of a more ethical nature are also different between medical and food applications. The need for animal-component free culture of cells and tissues, abstinence of antibiotics and, for some consumers, genetic modification severely limit the solution-space available to developers of cultivated meat and for materials needed. At the same time, consumers are increasingly willing to accept alternative sources of meat, giving the field an appreciable tailwind. Given the huge potential for improvement and extension of applied tissue engineering for food, this will be an exciting scientific endeavor for the next couple of decades.

Biography:

Mark Post is an MD, PhD and professor of Sustainable Industrial Tissue Engineering at Maastricht University. His main research includes engineering of tissues for medical applications and consumer products, which has led to the development of cultured beef from bovine skeletal muscle stem cells. In August 2013, he presented the world's first hamburger from cultured beef. He is CSO and co-founder of two companies, MosaMeat and Qorium that will commercialize cultured meat and cultured leather.

**Tuesday,
5th April**

9.00-9.45

Regulation of angiogenesis by the extracellular matrix – a biomaterials approach

Dr. Britta Trappmann

**Max Planck Institute for Biomolecular
Medicine**



Abstract:

A major challenge in the field of tissue engineering is the generation of new materials that can support angiogenesis, wherein endothelial cells from existing vasculature invade the surrounding matrix to form new blood vessels. To proceed, material design criteria based on natural tissue characteristics are needed, but currently lacking because we do not know how extracellular matrix (ECM) properties affect angiogenic sprouting and ultimately, blood vessel formation. Due to the complex nature of native ECMs, it is difficult to identify the role of individual matrix properties. Here, we have developed synthetic hydrogels with independently tunable properties, which are integrated into a microfluidic platform that mimics the process of angiogenesis in vitro. In this talk, I will present our efforts to understand how matrix stiffness, adhesiveness and degradative properties jointly regulate angiogenic sprouting, and importantly, vascular lumen formation.

Biography:

After her studies in Chemistry at the University of Dortmund, Germany, Dr. Britta Trappmann did her PhD in the groups of Prof. Wilhelm Huck and Prof. Fiona Watt in Cambridge, UK, studying the role of matrix stiffness on epidermal stem cell differentiation. She then moved to the lab of Prof. Christopher Chen, first at the University of Pennsylvania and later at Boston University and the Harvard Wyss Institute, USA, for a postdoc in Biomedical Engineering, where she developed tools to investigate cell-ECM interactions. Since 2016, Dr. Trappmann has been a Max Planck Research Group Leader at the MPI for Molecular Biomedicine in Muenster, Germany. Her research aims for a better understanding of how biochemical and mechanical properties of the native tissue microenvironment regulate cell function, in particular in the context of angiogenesis.

Oral Presentation
Session 7

Keynote session 7

The domino effects of kidney failure: an in vitro perspective of modeling kidney diseases and their associated comorbidities

Dr. Silvia Mihaila
Department of Pharmaceutical Sciences,
Utrecht University



Abstract:

Kidney is complex organ with multiple functions. Besides cleansing the blood of endo- and exogenous compounds, it is also responsible of activating vitamin D and maintaining water and electrolyte balance, and with that it remotely sustains the activity of other organs. Specialized cells decorated with transporters and receptors are highly sensitive to environmental changes and, as a result, adapt their functions to maintain body's homeostasis. When kidneys fail, due to acquired or genetic conditions, a chain of biochemical events leads to metabolic disturbances in distant organs, and just like a domino effect, they become diseased leading to life changing comorbidities. Using functional tissue replicates, *via* tissue engineering approaches, we can reconstruct the pathological conditions associated with the kidney diseases and pursue the elucidation of those mechanisms that lead to disease progression and identify druggable targets. In her talk, Silvia will focus on the use of advanced *in vitro* models to replicate kidney diseases and the inter-communication between the kidneys and other organs (such as gut and bone), to highlight the complex pathophysiology associated with kidney diseases.

Biography:

Silvia Mihaila obtained her bachelor degree in chemistry and physics in Romania. She then pursued her PhD degree at the University of Minho (Portugal) under the prestigious MIT-Portugal Program focusing on TE strategies for bone vascularization (2015). After that, she continued her academic trajectory as a Marie Curie postdoc fellow at the Department of Urology of Radboud UMC (Nijmegen, NL) where she used synthetic biomimetic matrix to stir the differentiation potential of stem cells. In 2017, she moved to UMC Utrecht to embark in a project related to the development of a bioartificial kidney unit based on bioengineered hollow membranes. Since March 2021, Silvia is an assistant professor of *in vitro* models of disease at the Department of Pharmacology of Utrecht University. Her work aims to develop humanized *in vitro* models to replicate pathological complications associated with kidney injury failure in the pursuit of unraveling mechanisms of disease and potential therapeutic targets.

Osteoclastic Differentiation in Human Osteochondral Explants cultured *Ex Vivo*

E.E.A. Cramer (1), J.G.E. Hendriks (2), K. Ito (1), S. Hofmann (1)

1. Orthopaedic Biomechanics, Department of Biomedical Engineering and Institute for Complex Molecular Systems, Eindhoven University of Technology, 5600 MB Eindhoven, the Netherlands 2. Orthopaedic Center Máxima, Dept of Orthopaedic Surgery & Trauma, Máxima Medical Center Eindhoven-Veldhoven, 5631 BM Eindhoven, The Netherlands.

Introduction: Bone remodeling consists of bone formation and resorption which involves many cell types including osteocytes, osteoblasts, osteoclasts, and their progenitors MSCs and monocytes. The preservation of tissue specific cells in their native 3D ECM in bone explants provides a unique platform to study remodeling [1]. Up until now, studies involving bone explant cultures showed a clear focus on achieving bone formation and neglected osteoclast activity and resorption [2]. Consequently, culture medium often contains supplements to stimulate osteogenic differentiation, but might suppress osteoclast activity [3]. The aim of this study was to induce osteoclastogenesis in human osteochondral cores during *ex vivo* culture with medium that stimulates differentiation towards osteoclasts. Because vascularization is absent *ex vivo*, which limits the source of monocytes, and the average lifespan for osteoclasts is 14 days, it was evaluated whether addition of peripheral blood mononuclear cells (PBMCs), containing monocytes, could enhance osteoclastogenesis.

Materials and Methods: Osteochondral cores (Ø10 mm) were isolated from human femoral heads of 2 patients (62-69y, female) undergoing total hip replacement, approved by the Local Medical Ethical Committee (METC, number N16.148). These explants were cultured in chambers comprised of two separated media compartments [4,5]. On day 4, PBMCs extracted from a human buffy coat (Sanquin) were seeded in a defect created in the bone (Ø3 x 3 mm). Explants with and without PBMCs (n=4) were cultured for 20 days in α MEM medium supplemented with RANKL and M-CSF (50 ng/ml) in the bone compartment and α MEM without supplements in the cartilage compartment. Osteoclast activity was evaluated with a TRAP assay on medium samples taken every two days. Histology (H&E) and immunohistochemistry, using antibodies against osteoclast markers CD61 and TRAP, were performed on paraffin sections of decalcified explants.

Results: In response to isolation, TRAP release decreased for both groups up to day 4. Addition of PBMCs showed a significant increase in TRAP activity on day 20 compared to day 4 (Fig. 1). From day 12, TRAP levels seemed to stabilize when PBMCs were added, whereas a decreasing trend was observed for the

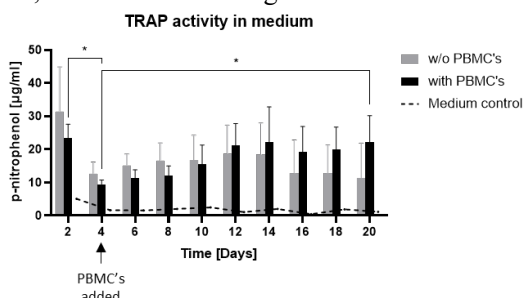


Figure 2 – TRAP release into medium of osteochondral explants measured during culture. Mean \pm SD are depicted.

samples without PBMCs, but did not reach statistical significance between groups. Samples without PBMCs showed multinucleated cells in the bone marrow (Fig. 2A) but no cells positive for osteoclast marker CD61 were found (Fig. 2C). In explants with PBMCs multinucleated cells were seen close to the bone surface (Fig. 2B) and they were positive for CD61 (Fig. 2D).

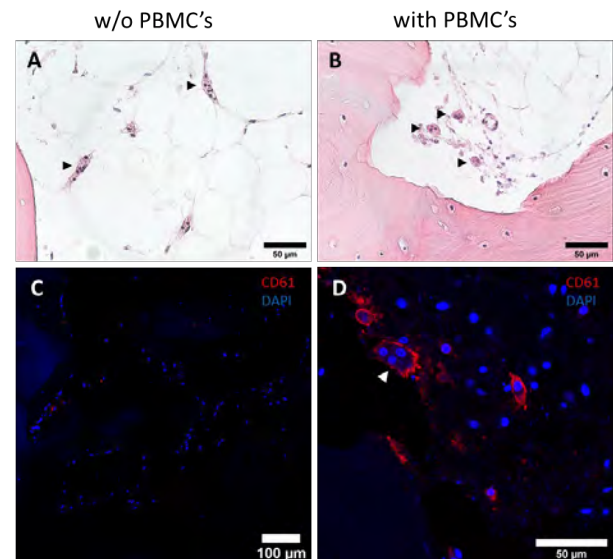


Figure 1 – Multinucleated cells (black arrowhead) in explants without (A) and with (B) PBMCs stained with H&E on day 20. Immunohistochemical staining for CD61 (red) in explants after 20 days culture without (C) and with (D) PBMCs. White arrowhead: osteoclast.

Discussion: Addition of PBMCs as a source of monocytes was necessary to achieve multinucleated cells positive for CD61 and TRAP, which were identified as osteoclasts, in explants after 20 days of culture *ex vivo*. Since osteoclasts' main function is bone resorption, it should be evaluated whether these osteoclasts are reactive and show resorption, for example with μ CT analysis. The TRAP activity in the medium showed a trend towards an increased osteoclast activity when PBMCs were added. However, only two human donors were included, and large donor variation was observed. More donors need to be included to obtain greater sample sizes to analyze whether the trends observed in both groups are statistically different.

Conclusion: In this study, osteoclast differentiation was induced after the addition of PBMCs in bone explants cultured *ex vivo*. This is a first step in incorporating osteoclast activity and resorption as key element of bone remodeling in *ex vivo* explant culture systems.

- [1] Marino et al., BoneKey reports, 5: 818, 2016;
- [2] Cramer et al., Curr Osteoporos Rep, 19(1): 75–87, 2021;
- [3] Kim et al, Arch Pharm Res, 29(8):691-698, 2006;
- [4] De Vries-van Melle et al., Tissue Eng Part C Methods, 18:45-53, 2012;
- [5] Schwab et al., ALTEX, 34:267-277, 2017;

Generation of a disease model for cartilage pathology in MPS VI using patient-derived and isogenic gene-corrected hiPSCs

M Broeders^{1,2,3,8}, JGJ van Rooij⁴, E Oussoren^{1,3}, TJM van Gestel^{1,2,3}, CA Smith⁵, SJ Kimber⁵, RM Verdijk⁵, MAEM Wagenmakers^{3,4}, JMP van den Hout^{1,3}, AT van der Ploeg^{1,3}, R Narcisi⁷, WWMP Pijnappel^{1,2,3*}

1: Department of Pediatrics, Erasmus MC University Medical Center, Netherlands; 2: Department of Clinical Genetics, Erasmus MC University Medical Center, Netherlands; 3: Center for Lysosomal and Metabolic Diseases, Erasmus MC University Medical Center, Netherlands; 4: Department of Internal Medicine, Erasmus MC University Medical Center, Netherlands; 5: Division of Cell Matrix Biology and Regenerative Medicine, School of Biological Sciences, Faculty of Biology Medicine and Health, University of Manchester; Manchester 6: Department of Pathology, Erasmus MC University Medical Center, Netherlands; 7: Department of Orthopaedics and Sports Medicine, Erasmus MC University Medical Center, Netherlands;

INTRODUCTION: Mucopolysaccharidoses type VI (MPS VI) is a severe metabolic disease caused by Arylsulfatase B (ARSB) enzyme deficiency leading to intralysosomal accumulation of glycosaminoglycans (GAGs). MPS VI is a multisystemic disease and progressive and severe cartilage pathology is a common symptom in MPS VI. Although cartilage is one of the major affected tissues in MPS VI patients, the development of cartilage pathology remains poorly understood. In-depth studies to unravel the mechanisms leading to the disease progression in human cartilage tissue affected by MPS VI are required.

METHODS: To develop an *in vitro* model system to study the cartilage pathology in MPS, we have generated four hiPSC lines from four patient-derived fibroblast using lentiviral expression of Oct4, Sox2, Klf-4, and C-Myc. We have adapted an previously published protocol^{1,2} for gene editing for the application to MPV VI: we generated isogenic lines from all hiPSCs using CRISPR-Cas9 in order to control for the high variability between genetic backgrounds of human individuals. Isogenic hiPSCs were differentiated into chondrogenic cells using an adapted version of a differentiation protocol published by Oldershaw et al.³ This differentiation protocol is based on the sequential activation of signaling pathways that operate during embryonic development of cartilage using growth factors and small molecules in chemically defined culture media. Chondrogenic cells were harvested and polysaccharides (such as GAGs) in enlarged lysosomes were visualized using periodic acid–Schiff (PAS) staining of cytopins. RNA sequencing analysis was used to compare genome wide changes in mRNA expression between chondrogenic cells from all 4 isogenic pairs.

RESULTS: High expression of pluripotency genes was observed in hiPSCs. The expression of *ARSB* was successfully restored by the introduction of a healthy copy into a safe location of the genome. Key chondrogenic genes were expressed after 14 days of differentiation including collagen II, Sox5 and Sox9 and *ARSB* RNA expression in chondrogenic cells was 2 to 12-fold increased in gene-corrected cells. Quantification of the number of PAS positive cells showed a reduction in all four gene edited lines to levels comparable to the levels in a healthy control. Genome wide mRNA expression analysis of the isogenic pairs showed the dysregulation of several processes including cell growth

and apoptosis, bone and cartilage development, Wnt signaling and metabolic processes.

DISCUSSION & CONCLUSIONS: In this study, we have generated a personalized *in vitro* disease model for MPS VI with isogenic controls and used this to obtain insight in early stages of disease pathology in chondrogenic cells. Using the differentiated isogenic pairs, we showed enlarged lysosomes at day 14 of differentiation, indicating accumulation of GAGs. Genome-wide mRNA expression analysis further indicated that chondrogenic cells develop MPS VI-related pathology at an early stage of development and support the conclusion of an early disease phenotype in cartilage. These results indicate that chondrogenic cells display strong disease hallmarks, and sheds novel light on the disease mechanisms involved in MPS VI. This approach may lead to identification of novel targets for therapy, and it enables personalized testing of future therapies designed to treat the cartilage symptoms in MPS VI.

REFERENCES:

- ¹ van der Wal et al. (2018) *Large-Scale Expansion of Human iPSC-Derived Skeletal Muscle Cells for Disease Modeling and Cell-Based Therapeutic Strategies*. Stem Cell Reports doi: 10.1016/j.stemcr.2018.04.002.
- ² in 't Groen et al. (2021) *CRISPR-Cas9-Mediated Gene Editing in Human Induced Pluripotent Stem Cells*. *CRISPR-Cas Methods*. Springer Protocols Handbooks. doi: 10.1007/978-1-0716-1657-4_16
- ³ Oldershaw et al. (2010) *Directed differentiation of human embryonic stem cells toward chondrocytes*. Nat Biotechnol doi: 10.1038/nbt.1683.

Investigating The Effect Of Cartilage Maturation And Mineralization On Angiogenesis In The Context Of Endochondral Ossification

E.Ji¹, L. Leijsten¹, J. Witte-Bouma¹, A. Rouchon², N. Di Maggio², A. Banfi², E. Farrell¹, A. Lolli¹

1: Department of Oral and Maxillofacial Surgery, Erasmus MC University Medical Center, Rotterdam, NL
2: Department of Biomedicine, Basel University Hospital, CH

Introduction. Endochondral ossification is the process of bone development via a cartilage template. It involves multiple stages, including chondrogenesis, mineralization and angiogenesis. To study this process, our laboratory has previously developed an *in vivo* model using human mesenchymal stem cells (hMSCs) to mimic bone formation. hMSC pellets are chondrogenically differentiated and implanted subcutaneously in nude mice where they undergo endochondral bone formation. To better characterize the interaction between hMSC-derived cartilage and blood vessels we now aimed to develop an *in vitro* co-culture model including cartilage pellets that undergo mineralization and endothelial cells. In this study, we employed a migration assay to assess the pro-angiogenic effect of conditioned medium produced from these pellets. Finally, we co-cultured the pellets and endothelial cells in a fibrin gel to develop a comprehensive system to study cartilage vascularization.

Materials and methods. Chondrogenic hMSC pellets were generated by culture with chondrogenic medium containing Transforming Growth Factor- β 3 (TGF- β 3), ascorbic acid and dexamethasone for 28 days. In the case of Mineralized pellets, BGP was added from day 7 and TGF- β 3 was withdrawn on day 14 (Fig.1A). On days 7, 14, 21 and 28, conditioned media were produced by culturing the pellets for 24h in basal medium. Then, the pellets were harvested for gene expression and histological analysis (N=3 hMSC donors). Thionin and Von Kossa staining were performed to analyse the glycosaminoglycan (GAG) production and calcium deposits, respectively. Transwell migration assays were employed to evaluate the effect of conditioned medium on human umbilical vein endothelial cell (HUVEC) migration. To generate a vascular network in the presence of chondrogenic or mineralized pellets, HUVECs, ASCs and the pellets were co-cultured in a fibrin hydrogel for 14 days. The vessel structures were visualised by immunofluorescence staining for Laminin(LAM), which indicates the basement membrane of vessels.

Results. Thionin and von kossa staining evidenced successful *in vitro* cartilage formation and mineralization, respectively. BGP exposure led to the formation of mineralized deposits which appeared on day 14 and increased in time, while GAG staining progressively decreased. In the absence of BGP exposure, no calcification was observed (Fig.1). In mineralized pellets the expression of osteogenic (ALPL, IBSP) and angiogenic markers (VEGFA, MMP13) showed the highest levels on d14 and then decreased during the late stages of mineralization. Initial data obtained from transwell migration assays showed that conditioned medium from both chondrogenic and mineralized pellets can stimulate HUVEC migration, with a maximum response on day 14. Finally, by co-

culturing ASCs/HUVECs in a fibrin hydrogel, we achieved successful formation of a 3D vascular network as visualised by confocal imaging (Fig.2). Vascular network formation was maintained in the presence of chondrogenic or mineralized pellets.

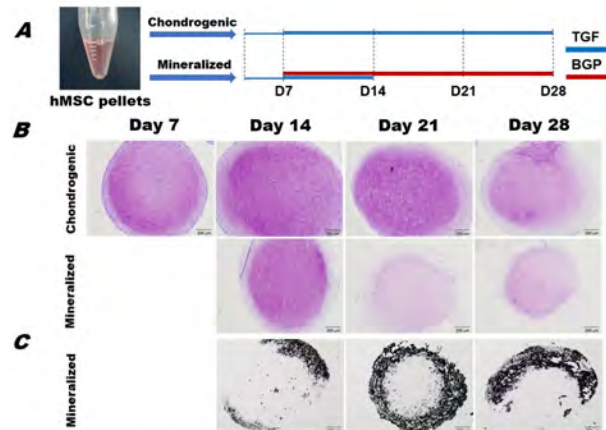


Figure 1. A: The 28-day culture plan of chondrogenic and mineralized pellets is shown. B: Thionin staining evidenced GAG presence in the pellets C: Von Kossa staining evidenced calcium deposits appearing in mineralized pellets from day 14 onwards.

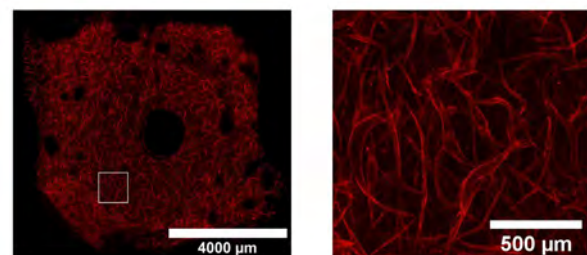


Figure 2. Confocal imaging of vessel-like structures in a 3D fibrin hydrogel system. Red signal indicates Laminin staining.

Conclusions: In this study, we achieved several goals towards the establishment of an *in vitro* model of cartilage vascularisation during endochondral ossification: 1) We succeeded in generating cartilage that undergoes mineralization *in vitro*. 2) By characterising mineralizing pellets culture, we found that the expression of pro-angiogenic markers and pro-migratory effect towards endothelial cells is maximum during early mineralization and then decreases. 3) We developed a 3D *in vitro* model of vascular network formation in the presence of chondrogenic or mineralized pellets. Based on these findings, we speculate that the developed 3D co-culture model can potentially recapitulate cartilage vascularization during endochondral ossification, and can further be used for mechanistic studies in bone formation and repair.

Acknowledgements: The study was supported by the European Union Horizon 2020 Research and Innovation Program under grant agreement 801159.

Screening Osteogenic Properties of Calcium Phosphate Biomaterials with Inorganic Additives using a Multiplex Protein-Based Assay

M. Eischen-Loges, Z. Tahmasebi Birgani, Y. Alaoui Selsouli, V. LaPointe and P. Habibović

MERLN Institute for Technology-Inspired Regenerative Medicine, Universiteitssingel 40, 6229 ER Maastricht, the Netherlands

Introduction: Critical-sized bone defects go beyond the intrinsic healing capacity of bone tissue. Off-the-shelf-available and synthetic bone graft substitutes such as calcium phosphate (CaP)-based biomaterials are already widely used for bone regeneration applications.¹ The properties and clinical performance of these biomaterials remain however inferior to an autologous bone graft, which is still considered as the gold standard treatment for these defects.² Doping CaPs with inorganic additives such as strontium, copper and magnesium, is considered a promising method to improve their performance.³ Here, we propose a targeted protein multiplex assay to improve the *in vitro* evaluation of such materials and to gain a better understanding of their effect on osteogenic differentiation.

Materials and methods: Cell culture microplates were coated with CaP doped with a range of inorganic additives including Sr²⁺ (CaP+Sr), Mg²⁺ (CaP+Mg), Mn²⁺ (CaP+Mn), Cu²⁺ (CaP+Cu) and Zn²⁺ (CaP+Zn) as previously described and characterized.⁴ Human mesenchymal stem cells (hMSCs) were seeded on the coatings. hMSCs in basic medium (BM) and osteogenic induction medium (OM) were used as controls. An MTT assay determined cell metabolic activity, and cell morphology and adhesion were assessed. A multiplex protein assay to detect analytes related to osteogenesis, angiogenesis, and immunomodulation was performed. Osteogenic differentiation was confirmed by an alkaline phosphatase (ALP) assay and qPCR.

Results and discussion: Multiplex analysis showed differences in protein expression profiles between CaP biomaterials with inorganic additives (Fig. 1).

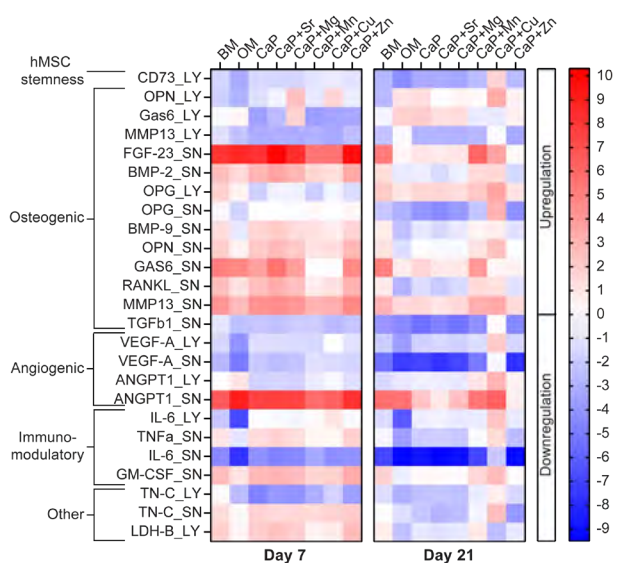


Figure 1. Multiplex protein analysis of hMSCs on CaP coatings at an early (day 7) and late time point (day 21) measured in the supernatant (SN) and lysate (LY). Protein content was normalized to housekeeping protein content and represented relative to respective protein expression at day 0. N=2.

The effect of different inorganic additives on hMSCs was detected in terms of hMSC stemness, osteogenic, angiogenic, immunomodulatory and other markers. Gene expression analysis showed an upregulation of the osteogenic transcription factor *RUNX-2* in hMSCs in OM, on CaP+Mn and on CaP+Cu at day 7 (Fig. 2A). *BMP-2* was upregulated in hMSCs on all coatings at day 7 and on CaP+Mn at day 21 (Fig. 2B). ALP activity was decreased in hMSCs on all coatings at day 7, except in CaP+Zn where no difference was detected. At day 21, ALP activity was upregulated in hMSCs in OM and a decrease was observed in hMSCs on CaP+Cu (Fig. 2C).

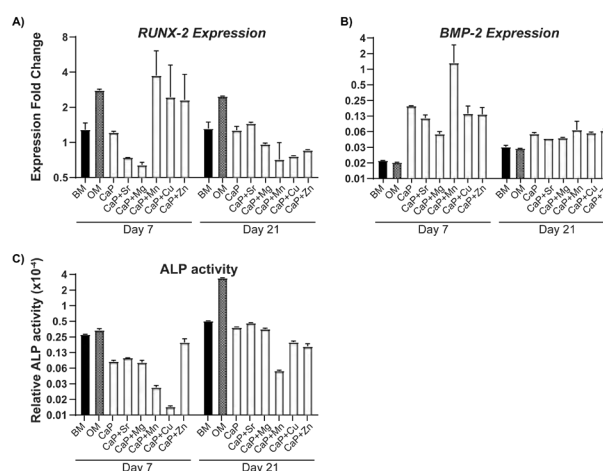


Figure 2. Gene expression analysis of osteogenic markers *RUNX-2* (A) and *BMP-2* (B) represented as fold change relative to day 0. N=2. C) ALP activity assay. N=2.

Conclusion and outlook: Here, we presented our efforts on screening osteogenic, angiogenic and immunomodulatory properties of CaP-based biomaterials with inorganic additives using a protein multiplex-based tool. The protein multiplex assay generated a substantial amount of biological data and differences in protein profiles of CaP biomaterials were detected. This data is currently being validated using conventional analyses.

References:

1. Jeong J et al. Biomaterials Research 23(1), 1-11, 2019;
2. Habraken W et al. Materials Today, 19(2), 69-87, 2016;
3. Schamel M et al. Materials Science and Engineering C(73), 99-110, 2017;
4. Habibovic P et al. Journal of the American Ceramic Society 85(3), 517-522, 2002;

Acknowledgements: This research has been made possible with the support of the Netherlands Organisation for Scientific Research Vidi grant (15604), the Dutch Province of Limburg (LINK project) and the Interreg Vlaanderen/ Nederland project 'BIOMAT-on-microfluidic-chip'. PH gratefully acknowledges the Gravitation Program 'Materials-Driven Regeneration', funded by the Netherlands Organization for Scientific Research (NWO) (024.003.013). ZTB gratefully acknowledges the NWO grant for women in STEM (Project 'Biotetris').

Oral Presentation
Session 8

Keynote session 8

Nanomachines with Controlled Shape and Motility for Delivery Applications

Prof. dr. Daniela Wilson
Institute for Molecules and Materials Nijmegen,
Radboud University Nijmegen



Abstract:

Cellular structures, the basic building blocks of life, are one of the most well studied complex systems. Their intricate architectures have inspired the design of synthetic analogues that can mimic both their structure and function. One of the great challenges of complex life-like molecular systems is to understand and design autonomous systems that not only can move directionally by harvesting different sources of energy but also can sense, communicate, interact and respond to clues from their environment and adapt to its changes. Here I will show how spontaneous self-assembly of smart polymeric building blocks can lead to autonomous and locomotive systems with controlled shape, motion and directionality. Autonomous nano and microscale life-like motile systems that can communicate and exert specific tasks on demand have the potential to become the next generation biomedical devices. The response and collective work of such systems in the presence of different stimuli will lead to more accurate, precise and selective treatments, while at the same time allowing for a better understanding of the communication mechanisms already existing in nature. These biomimetic motile systems are ultimately able to control their motion, directionality, speed and behavior in response to clues from their complex biological environment. Such properties could be potentially a game changer in the biomedical field, which at the moment rely only on passive high dose drug delivery systems. New designs of motilic systems that harness different sources of energy and their molecular assembly will be presented.

Biography:

Prof. Dr. Daniela A. Wilson received her Ph.D. degree in 2007 with “summa cum laude” distinction from “Gh. Asachi” Technical University of Iasi, Romania in the field of liquid crystalline materials. During her PhD research, she obtained two fellowships to continue her studies abroad in Japan at the Hyogo University in Himeji and in UK at the University of Hull. She then moved to the US at University of Pennsylvania, Philadelphia in the group of prof. V. Percec for her postdoctoral studies where she worked on several topics in the field of supramolecular chemistry (dendrimers, Janus dendrimers, dendrons and dendronized polymers), polymer chemistry and catalysis. In Philadelphia she contributed to the discovery of dendrimersomes, self-assembling vesicles formed from amphiphilic dendrimers. In 2012 she was awarded the prestigious ERC StG to start her independent academic career on self-assembled nanomachines. She is the recipient of the NWO Vidi grant and the Athena and Aspasia award. She is currently full professor holding the chair of Systems Chemistry Department at the Institute for Molecules and Materials, Nijmegen the Netherlands and theme leader of Nanomedicine in the Radboud Institute for Life Science (RIMLS) Nijmegen, The Netherlands, a university-wide role spanning from chemistry through translation research into the hospital. Her research interests focus on the design of intelligent, self-propelled, and self-guided supramolecular assemblies and their communication and interaction as next generation nanoengineered delivery systems.

Innervation In Bone Tissue Engineering Using Chemically Modified RNA

C.S.J. Polain¹, C. Plank², E. Bonvin³, F. Poulhes³, R. De la Vega Amador^{1,4}, C. Evans⁴, M. van Griensven^{1,4}, E.R. Balmayor^{4,5}

¹cBITE Department, MERLN Institute, Maastricht University, Maastricht, the Netherlands

²Ethris GmbH, Planegg, Germany

³OZ Biosciences SAS, Marseille, France

⁴Rehabilitation Medicine Research Center, Mayo Clinic, Rochester, MN, USA

⁵IBE Department, MERLN Institute, Maastricht University, Maastricht, The Netherlands

Introduction

Bone tissue engineering aims to regenerate bone using the intrinsic healing capacity of the body. Bone regeneration often includes the use of growth factors, that stimulate cellular proliferation and differentiation. In order to engineer viable bone tissue, osteogenesis, vascularization, and innervation are of paramount importance. To stimulate these cellular processes, known growth factors such as bone morphogenetic protein 2 (BMP-2) and vascular endothelial growth factor (VEGF) have been widely used. Recently, nerve growth factor (NGF) and Semaphorin-3A (SEMA-3A) have been investigated to support the innervation process in bone formation and regeneration. Importantly, the use of growth factors has several limitations, including adverse side effects given by the unavoidable use of supraphysiological amounts along with high cost. Gene- and transcript-therapies are proposed as an alternative. Transcript therapy is based on the application of protein coding mRNA to induce *in situ* protein production by the cells. As native mRNA is unstable and immunogenic, chemical modifications to mRNA (cmRNA) increase its stability and biocompatibility.

In this study, innervation for bone tissue engineering has been researched. On the one hand, we investigated the usability of NGF cmRNA in inducing NGF expression in human mesenchymal stem cells (hMSCs). On the other hand, expression of SEMA-3A in rat BMP2 cmRNA-engineered bone was evaluated. To obtain such cmRNA-engineered bone tissue, a critical sized-defect in rat femurs were treated with a collagen sponge containing BMP-2 cmRNA. Explants were harvested 4 and 8 weeks post implantation.

Materials and Methods

Transfection of hMSCs with NGF cmRNA

Transfection of hMSCs with NGF cmRNA (Ethris GmbH, Germany) was done using several experimental lipid vectors (RmesFect, NL51, NL37, and 3DFect from OzBiosciences, France, as well as Lipofectamine MessengerMax from Invitrogen, USA). Previously optimized conditions of cmRNA concentration and cmRNA:lipid ratio were used for transfection. Briefly, 15.6 pg cmRNA per cell was used to transfect hMSCs. Furthermore, the cmRNA:lipid w/v concentrations employed were 1:4 for RmesFect, 1:4 for NL51, 1:4 and 1:5 for NL37, 1:4 and 1:5 for 3DFect, and 1:1 for Lipofectamine MessengerMax. Expression of NGF was measured in cell supernatants at 1, 2, 3, and 5 days after transfection using a sandwich ELISA for NGF (R&D Systems, USA). To monitor cell viability, an MTS assay (Abcam, UK) was performed at 1, 3, and 7 days after transfection.

SEMA-3A expression in BMP2 cmRNA-engineered rat bone

In rats, 5 mm femoral defects were treated with collagen sponges containing 5 µg, 10 µg, 25 µg, and 50 µg BMP-2 cmRNA. As a comparison, 11 µg of the current clinical gold standard rhBMP-2 was used. Bone tissue was harvested at 4 and 8 weeks after implantation. Explants were fixated, decalcified, and embedded in paraffin. Samples were sectioned and mounted, and an immunohistochemical staining was performed using DAPI and an anti-SEMA-3A antibody (Abcam, UK). Samples were imaged using a Slide Scanner microscope (Nikon, Japan) for fluorescence microscopy.

Results and discussion

Transfection of hMSCs with NGF cmRNA

High levels of NGF were produced by hMSCs for up to 3 days post cmRNA transfection. Levels of NGF were higher at 24 hours post cmRNA transfection. Thereafter, a slow decrease in protein expression was observed. Interestingly, the use of NL37 lipid to form the cmRNA lipoplexes resulted in the highest NGF protein production. In terms of protein expression, the best lipid:cmRNA ratios were 1:4 and 1:5 for NL37. Adequate cell viability, ranging from 90-100%, was observed for all cmRNA transfection conditions evaluated.

SEMA-3A expression in cmRNA-engineered rat bone

Healing doses of BMP-2 cmRNA, that is 25 µg, and 50 µg showed the highest expression of SEMA-3A. SEMA-3A expression was particularly observed in callus tissue and *de novo* formed bone. This expression was observed as early as 4 weeks after cmRNA treatment and persisted up to 8 weeks. Interestingly, a similar pattern was observed when using the rhBMP-2 counterpart. Conversely, untreated defects showed little to no SEMA-3A expression.

Overall, our results highlight the potentialities of NGF cmRNA to be used as innervation stimulus for bone engineering. Additionally, we demonstrated the expression of the nerve factor SEMA-3A during cmRNA-bone healing *in vivo*.

Acknowledgements

Part of this work has been performed under the scope of the cmRNAbone project and has received funding from the European Union's Horizon 2020 research and innovation programme under the Grant Agreement No 874790. The *in vivo* experiments presented in this work were supported by the National Institutes of Health, NIH (Grant No R01 AR074395 from National Institute of Arthritis and Musculoskeletal and Skin Diseases, NIAMS).

Dual-functional Porous Polymethylmethacrylate Cement Loaded with Cisplatin for Reconstruction of Segmental Bone Defect Kills Bone Tumor Cells

Z Wang¹, LP Nogueira, HJ Haugen², ICM Van Der Geest², PC de A Rodrigues³, D Janssen³, T Bitter³, JJP van den Beucken¹, SCG Leeuwenburgh¹

Dentistry - Regenerative Biomaterials, Radboudumc, Philips van Leydenlaan 25, Nijmegen, The Netherlands
 Department of Biomaterials, Faculty of Dentistry, University of Oslo, Geitmyrsveien 69, Oslo, Norway
 Department of Orthopedics, Radboudumc, Geert Grooteplein Zuid 10, Nijmegen, the Netherlands

Introduction: Malignant bone tumors are usually treated by resection of tumor tissue followed by filling of the bone defect with bone graft substitutes.

Polymethylmethacrylate (PMMA) cement is the most commonly used bone substitute in clinical orthopedics in view of its reliability. However, the dense nature of PMMA renders this biomaterial unsuitable for local delivery of chemotherapeutic drugs to limit the recurrence of bone tumors. Here, we introduce porosity into PMMA cement by adding carboxymethylcellulose (CMC) to facilitate such local delivery of chemotherapeutic drugs, while retaining sufficient mechanical properties for bone reconstruction at load-bearing sites.

Materials and Methods: CMC powders were dissolved in the stock solution of cisplatin (2.0 mg/mL) to prepare the CMC hydrogel. Then, porous PMMA cements were prepared by adding different amounts of CMC hydrogel (1-8%) into Simplex[®] PMMA bone cements. The thermal, handling and mechanical properties of the porous PMMA cements were characterized.

Additionally, an *ex vivo* model was developed to assess the biomechanical and reconstructive properties. After that, scanning electron microscopy (SEM) was used for morphology analysis. The interconnective porosities of porous PMMA cements were determined and analyzed by micro-CT. For the drug release profile, ICP-MS was used to analyze the release of platinum. The anti-cancer efficacy of the releasates against osteosarcoma cells (MG-63) was evaluated by Cell Counting Kit-8 (CCK-8) assay.

Results and Discussion: With the increase of CMC incorporation, the compressive yield strength (σ_y), elastic modulus (E) and fracture toughness gradually decreased (Figure 1). Results showed a significant decrease between PMMA+2%CMC and PMMA+3%CMC, while no further changes in mechanical properties were observed for PMMA with 4%-8% CMC. An apparent increase in porosity was observed with increasing CMC content. Using 3D reconstructions, large numbers of small secluded pores were identified upon incorporation of 1-2% CMC, while 3-4% CMC incorporation showed large and interconnected pores (Figure 2). In addition, the release profile of cisplatin showed that PMMA-based cements containing 3% and 4% CMC released substantial amounts of cisplatin (12.1% and 16.6%), in contrast to cements containing lower amounts of CMC which hardly release any cisplatin (1.2%, 3.13% and 4.38%). This release of cisplatin efficiently killed osteosarcoma cells *in vitro*, which confirms the chemotherapeutic activity of these cisplatin- and CMC-loaded PMMA cements towards MG-63 cells.

Conclusions: PMMA cements can be rendered therapeutically active by introducing porosity using CMC to allow for release of cisplatin without compromising mechanical properties beyond critical levels. As such, our data suggest that our dual-functional PMMA-based cements represent a viable treatment option for filling bone defects after bone tumor resection.

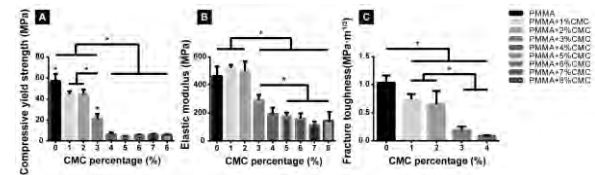


Figure 1 Mechanical properties of PMMA-based cements containing different amounts of CMC. (A) compressive yield strength, (B) elastic modulus and (C) fracture toughness.

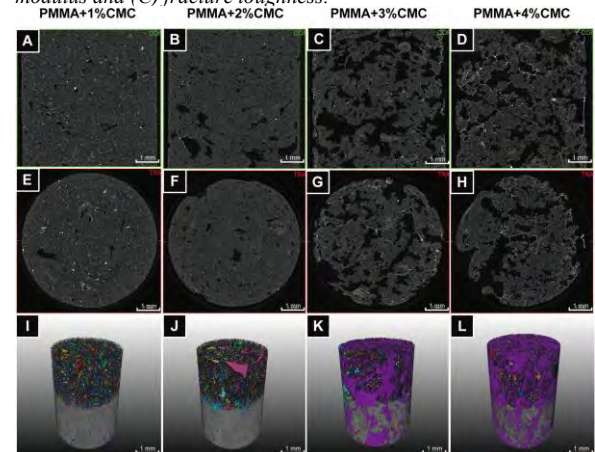


Figure 2 Representative micro-CT images and reconstructions of PMMA-based cements containing different amounts of CMC. (A-D) longitudinal sections, (E-H) transversal cross-sections and (I-L) 3D reconstructions of PMMA-based cements with different CMC content.

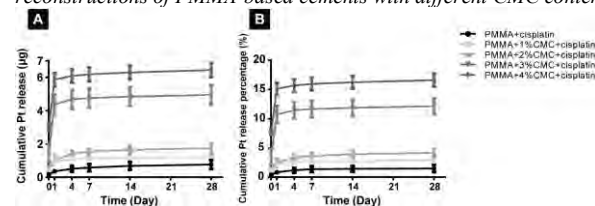


Figure 3 Release profile of cisplatin from porous PMMA assessed by ICP-MS. (A) cumulative Pt release and (B) cumulative Pt release percentage from CMC- and cisplatin-loaded PMMA cements.

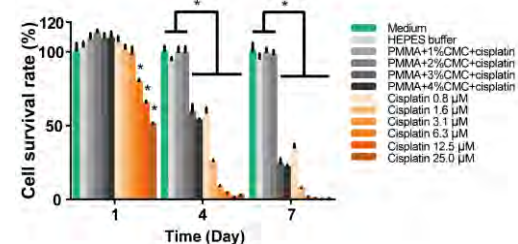


Figure 4 Effects of Pt release from PMMA-based cements with different CMC content (1-4%) on cultured MG-63 osteosarcoma cells at different time points. The 100% medium and 25% HEPES buffer were used as control groups.

Delivery of Bone Morphogenetic Protein 2 and Platelet-Derived Growth Factor to improve the osteogenic properties of a collagen/Magnesium-hydroxyapatite osteochondral scaffold

J. Xu¹, Shorouk Fahmy Garcia^{1,2}, Tim Wesdorp¹, Nicole Kops¹, Lucia Forte³, Giuseppe Filardo⁴, Pieter A.J. Brama⁵, Claudio De Luca³, Joachim Nickel⁶, Eric Farrell², Gerjo J.V.M. van Osch^{1,7,8}

1. Department of Orthopedics and Sports Medicine, Erasmus MC, University Medical Center, Rotterdam, Netherlands.
2. Department of Oral and Maxillofacial Surgery, Erasmus MC, University Medical Center Rotterdam, Netherlands
3. Fin-Ceramica Faenza, Faenza, Italy.
4. Applied and Translational Research Center, Rizzoli Orthopaedic Institute, Bologna, Italy.
5. Section of Veterinary Clinical Sciences, School of Veterinary Medicine, University College Dublin, Dublin, Ireland.
6. Department Tissue Engineering and Regenerative Medicine, University Hospital Würzburg, Würzburg, Germany.
7. Department of Biomechanical Engineering, Delft University of Technology, Delft, The Netherlands.
8. Department of Otorhinolaryngology, Erasmus MC University Medical Center, Rotterdam, The Netherlands.

Purpose: An osteochondral scaffold with a superficial collagen cartilage replacement layer and a collagen/Magnesium-hydroxyapatite (Mg-HA) bone replacement layer has demonstrated good clinical results in osteochondral defects [1]. However, subchondral bone repair remained suboptimal. In this study, we aimed to improve the osteogenic properties of this scaffold by incorporating Bone Morphogenetic Protein 2 (BMP-2) or Platelet-Derived Growth Factor-BB (PDGF-BB).

Materials & Methods

To evaluate the release kinetics of BMP-2 and PDGF-BB from different layers of the scaffold, the different layers were soaked in 35 μ l 28.5 μ g/ml BMP-2 or PDGF-BB solutions and the release over time was analysed by ELISA. Osteochondral defects (4 mm diameter, 4 mm height) were created in bovine osteochondral biopsies harvested from metacarpal-phalangeal joints. Osteochondral explants were implanted subcutaneously in 12-week-old athymic mice for 4-8 weeks. The percentage of the defect filled with cartilage or bone like tissue was quantified on histology. Immunohistochemistry was performed to investigate the inflammation in the early phase of repair.

Results

In vitro release assay showed that BMP-2 was released in a sustained-manner from both layers up to day 14 (8.2% from the 100% collagen layer and 9.2% from collagen/Mg-HA layer), while a rapid release of PDGF-BB in 6 hours (98.1% from the 100% collagen layer and 66.0% from the collagen/Mg-HA layer) was observed. The *in vivo* study indicated that formation of tissue repair was delayed in the defects filled with the scaffold (0.0% \pm 0.0%) compared with empty defects (8.1% \pm 4.8%) after 4 weeks ($p=0.043$), but not after 8 weeks (82.8 \pm 31.9% vs 68.8% \pm 36.2%, $p=0.503$). To further investigate the effect at the different layers, osteochondral defects were fully loaded either with a scaffold consisting of 100% collagen layer or a scaffold consisting of collagen/Mg-HA layer. More neutrophils, macrophages and tissue regeneration were observed in the defect filled with a collagen/Mg-HA layer (11.7% \pm 10.5%) than a 100% collagen layer (3.4% \pm 4.1%) after 4 weeks (Figure 1). To improve the bone forming capacity of the layered collagen/Mg-HA scaffold, 4 μ g BMP-2 or 100 ng or 2 μ g PDGF-BB was loaded into the scaffold. Histology indicated that slightly less neutrophils and M1 macrophages, and more tissue repair was observed in the scaffold loaded with

either 4 μ g BMP-2 (9.7% \pm 11.2%) or 2 μ g PDGF-BB (6.0% \pm 11.2%) than scaffold only (0.0% \pm 0.0%) after 4 weeks (Figure 2).

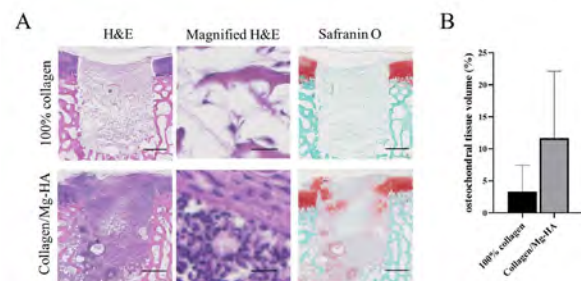


Figure 1. More cells and tissue regeneration were observed in the defects filled with a collagen/Mg-HA layer. (A) Representative images of the 4-week repair constructs stained with H&E and safranin-O. (B) the percentage of the defect filled with osteochondral tissue (%) in the osteochondral defects. Scale bars indicate 1 mm and 20 μ m (for the magnified images).

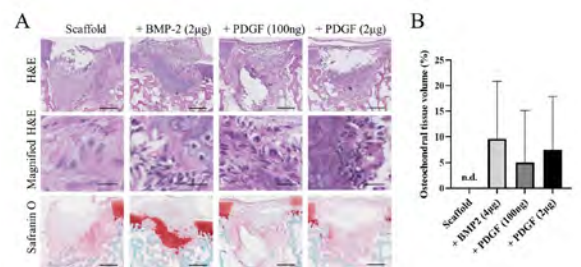


Figure 2. Absorption of BMP-2 or PDGF-BB might improve the osteochondral regeneration. (A) Representative images of the 4-week repair constructs stained with H&E and safranin-O. (B) the percentage of the defect covered with osteochondral tissue (%) in the osteochondral defects. Scale bars indicate 1 mm and 20 μ m (for the magnified images). n.d.: not detectable.

Conclusion

This study indicates that the collagen/Mg-HA layer evoked a stronger inflammatory response, which might be favourable for bone repair. Loading BMP-2 or PDGF-BB into the collagen/Mg-HA scaffold seems to be a promising approach to improve the osteogenic capacity of such scaffold.

Acknowledgements: This work is funded by EuroNanoMed3 program.

Reference:

[1] Di Martino, A. et al., Cell-Free Biomimetic Osteochondral Scaffold for the Treatment of Knee Lesions: Clinical and Imaging Results at 10-Year Follow-up, *Am J Sports Med*, 49(10):2645-2650, 2021.

Cellular Uptake and Activity of cmRNA and pDNA Lipid Complexes – Prospects for Gene Therapy and Tissue Engineering

C.B. Del Toro Runzer¹, S. Anand², C. Plank³, M. van Griensven^{1,4*}, E.R. Balmayor^{4,5*}

¹Dept. cBITE, MERLN Institute for Technology-Inspired Regenerative Medicine, Maastricht University, the Netherlands. ²Dept. of CTR, MERLN Institute for Technology-Inspired Regenerative Medicine, Maastricht University, the Netherlands. ³Ethris GmbH, Planegg, Germany. ⁴Mayo Clinic, Rochester, MN, USA. ⁵Dept. IBE, MERLN Institute for Technology-Inspired Regenerative Medicine, Maastricht University, the Netherlands

Introduction: Nowadays, the field of regenerative medicine is based on the joint effort of multiple disciplines. One example is the integration of tissue engineering with gene therapy in order to create biological substitutes that would transfer genetic material to restore or improve tissue function. When these fields merge, it is necessary to give a closer look and understand the undergoing processes at their interface. For instance, it is fundamental to investigate the mechanisms that reign the cellular access of genetic material and the underlying transfection and translation efficiencies. To look into these processes, this study focused on investigating three main variables: (1) the nucleic acid coding for the therapeutic protein (plasmid DNA, pDNA or chemically modified RNA, cmRNA); (2) the delivery vector to introduce the genetic material into the cells (Lipofectamine 3000 or 3DFect); and (3) the cell type that is expected to receive the genetic information and produce the desired protein. For the latter, we selected three human primary cell models that represent promising resources of cells for regenerative medicine in a wide range of pathological conditions, human mesenchymal stromal cells (hMSCs), human dermal fibroblasts (hDFs), and human osteoblasts (hOBs). In addition, to study the transfection efficiency and subsequent protein production in a three-dimensional environment, Electrospun (ES) scaffolds were used.

Materials and Methods: Complexes were always freshly prepared using non-supplemented Opti-MEM (Life Technologies, USA) by mixing selected vectors (Lipofectamine3000 (Invitrogen, USA) or 3DFect (OzBiosciences, France)) with respective nucleic acids (pDNA or cmRNA). The nucleic acids encoded Metridia Luciferase (MetLuc). The nucleic acid-to vector ratio used was 1:2. The nucleic acid-vector mixtures were incubated for 20 minutes at room temperature for complex formation. To investigate mechanism of cellular uptake MetLuc nucleic acids were fluorescently labelled with Label IT MFP488 Labeling Kit (Mirus Bio, WI). Subsequently, cells were incubated for 1 hour with endocytic inhibitors (i.e., chlorpromazine, wortmannin, and genistein (Sigma-Aldrich, USA)) and accumulation of labelled vectors within the cell was measured by flow cytometry. Correlative light and electron microscopy (CLEM) was used to visualize the cellular uptake of fluorescently-labelled complexes. For quantification of MetLuc expression, supernatants at different timepoints post transfection were collected, then 50 μ l of coelenterazin (Synchem UG & Co., Germany) were added to 50 μ l of the supernatant, and bioluminescence was measured instantly at $\lambda=480$ nm (BMG CLARIOSTAR, Germany).

Results and Discussion: While lipoplexes (Fig. 1A) utilized several entry pathways in hMSCs, hDFs, and hOBs, uptake from lipid rafts in caveolae serve mainly as the productive route for gene delivery by the lipid delivery vehicles (Fig. 1B, C). When comparing expression levels between cmRNA and pDNA (Fig. 1E), we observed that for fast dividing cells such as hDFs, pDNA yielded higher expression levels. On the other hand, for slow dividing cells such as hOBs, pDNA barely generated protein expression, while cmRNA was responsible for high MetLuc protein production. In the case of the hMSCs, which presented an intermediate doubling time, the combination vector/nucleic acid seemed more relevant than the nucleic acid *per se*. In all cases, protein expression was higher when the cells were seeded on ES scaffolds (Fig. 1D).

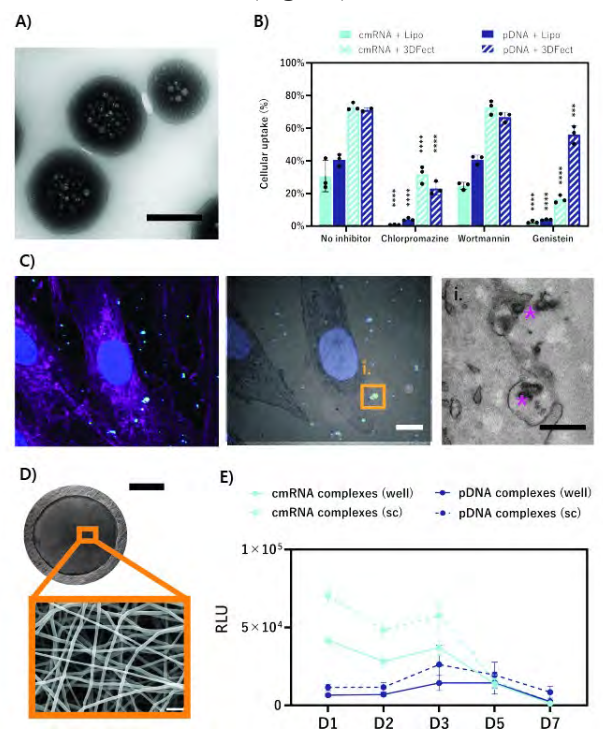


Figure 1. (A) Electron photomicrograph showing MetLuc cmRNA + 3DFect complexes. (B) Percentages of intracellular uptake of MFP488-labeled MetLuc complexes in hMSCs. (C) CLEM photomicrographs after transfection. Nuclear staining in blue, actin filaments in magenta, and lipoplexes are in green. (D) Magnified SEM photomicrograph of the nanofibers that compose the PEOT/PBT ES scaffold. (E) Kinetics comparison of MetLuc protein expression.

Acknowledgement:

This work has been performed as part of the cmRNAbone project and has received funding from the European Union's Horizon 2020 research and innovation programme under the Grant Agreement No 874790.

Oral Presentation
Session 9

Keynote session 9

Pathogenesis of Staphylococcal Biomaterial-Associated Infection

dr. Martijn Riool
Department of Medical Microbiology and Infection Prevention, Amsterdam UMC



Abstract:

Introduction

Infection of inserted or implanted medical devices (“biomaterials”) can have disastrous consequences, including removal of the device. Implantation of a biomaterial provokes an inflammatory response known as the “foreign body response”. *Staphylococcus epidermidis* and *Staphylococcus aureus* are the major causes of biomaterial associated infection (BAI), where *S. epidermidis* in absence of a foreign body hardly ever cause infection. Formation of biofilms on the biomaterial surface is generally considered the main reason for these persistent infections, but *S. epidermidis* has been shown to survive inside macrophages around biomaterials implanted in mice, and was retrieved from peri-catheter tissue in humans. Infections may arise early, from contamination during the implantation or insertion procedure by bacteria from the skin of the patients or from the surgical environment, or late by bacteria reaching the implant from other sites of the body by haematogenous spreading. Bacteria entering during surgery may adhere to the material to form a biofilm, and may enter the surrounding tissue and become internalized within host cells. Thus, the tissue surrounding a foreign body must be considered a niche for bacteria that cause BAI. In order to design strategies to prevent BAI, it is vital to understand the in vivo course of bacterial infection. The aim of the present study therefore was to compare the pathogenesis of early (i.e. infection during surgery) and delayed *S. aureus* experimental BAI (i.e. infection 2 days after implantation). Moreover, in order to understand the high infection-susceptibility of tissue around biomaterials, we aimed to unravel the molecular basis of the foreign body reaction and of biomaterial-associated infection. We assessed the gene expression underlying the foreign body response to titanium over time and the influence of *S. epidermidis* on this response.

Materials and Methods

For the early versus late infection study, titanium implants were placed subcutaneously in the back of mice and an inoculum of 10⁶ CFU of *S. aureus* was injected either along the implant immediately after implantation (i.e. early infection), or 2 days later (i.e. delayed infection). Mice were sacrificed at 1 or 4 days after implantation, and biopsies were collected to assess the bacterial colonization of both the biomaterial and the surrounding tissue. Multiple Spectral Imaging (MSI) was performed to stain macrophages, neutrophils and bacteria in one single section.

For the gene expression study, 4 experimental groups were compared in the same biomaterial-associated infection mouse model: a) sham surgery (no implantation of a biomaterial), b) implantation of a titanium biomaterial, c) sham surgery with an *S. epidermidis* infection, and d) implantation of a titanium biomaterial combined with an *S. epidermidis* infection (4 mice per experimental group). At 1 and 6 hours and 2, 4, 9, 14 and 21 days, bacterial colonization, histology (MSI) and gene expression were analysed. Gene expression was recorded using Affimetrix Mouse Gene-ST microarrays.

Results and Discussion

After 1 and 4 days, significantly more bacteria were cultured from tissue of mice with an early infection, than of mice with a delayed infection. All tissue biopsies of mice with early or delayed infection were culture positive after 1 day. The delayed group appeared to be less susceptible to infection, since after 4 days, the number of culture positive tissue samples (39%) was significantly lower than in the early infection group (83%). Moreover, after 1 day the implants had significantly lower levels of bacterial

colonization in the delayed infection group, both in numbers of bacteria and the numbers of culture positive implants. After 4 days, numbers of bacteria and infected implants were very low in both groups, with no difference between the early and delayed infection groups.

In the gene expression study, the histology and gene expression patterns showed distinct differences between sham (i.e. only surgery) and biomaterial groups possibly related to the foreign body response, and between biomaterial without and with infection. The analysis of the expressed gene sets is presently ongoing.

Conclusions

Mice were more susceptible to early than to delayed *S. aureus* infection. In delayed infection, less bacteria colonized the implant surface. However, even in delayed infection bacteria were cultured from the tissue, implying that in order to protect against early as well as delayed infection, antibacterial strategies should be directed against bacteria both in biofilms and in peri-implant tissue.

Moreover, the gene expression results are a powerful start towards understanding the molecular basis of the foreign body response and biomaterial-associated infection.

Biography:

Dr. Martijn Riool is postdoctoral researcher in the group of Dr. S.A.J. Zaat at the Department of Medical Microbiology and Infection Prevention at the Amsterdam UMC (location AMC), which focuses on biomaterial-associated infection and novel antimicrobial strategies. In 2010, he started his PhD project within the BMM NANTICO project, aimed at development of Non-adherent antimicrobial coatings. From 2014 to 2016, he worked as a research associate within the BALI consortium, developing novel tools to control biofilms by targeting both the prevention and treatment of biomaterial-associated infections, using the unique combination of Synthetic Antimicrobial Antibiofilm Peptides (SAAPs) and a controlled release system. Currently, his work is focused on customized treatment strategies for cranioplasty (CRANIOSAFE), and at developing a multi-functional supramolecular polymeric biomaterial with cell-adhesive and antimicrobial activity (SUPERACTIVE). Moreover, he is involved in the PRINT-AID, DARTBAC, NACQAC and STIMULUS projects, and he is work package leader in the EU Twinning project CEMBO on multispecies biofilms. Since November 2014, he was active member and management committee substitute for the Netherlands of the COST Action iPROMEDAI. In 2015 and 2018, he coordinated the iPROMEDAI Summer School on 'Antimicrobial Medical Devices', and he organized the iPROMEDAI Young Scientist Forum in 2017 in Thessaloniki, Greece. Moreover, he is management committee member of the COST Action ENIUS (European network of multidisciplinary research to improve the urinary stents). Lastly, he was vice chair of the European network AMiCI "Anti-Microbial Coating Innovations to prevent infectious diseases".

A Close Examination of the Bone Formation and Immune Response from a Devitalized Callus Mimetic

L. de Silva^{1,2}, F. Staubli^{1,2}, A. J. W. P. Rosenberg¹, A. Longoni^{1,2,3}, D. Gawlitta^{1,2}

¹Dept. of Oral and Maxillofacial Surgery & Special Dental Care, ²Regenerative Medicine Utrecht, Utrecht, the Netherlands. ³Dept. of Orthopaedic Surgery and Musculoskeletal Medicine, Centre for Bioengineering & Nanomedicine, University of Otago, New Zealand.

Introduction

Autologous bone grafting is currently the main treatment for bone defects. While several factors have led to its current practice as the gold standard treatment, it is still associated with multiple drawbacks such as limited availability and donor site morbidity. Over the years, various approaches have been explored to overcome this, particularly in the field of tissue engineering where stem cells are combined with biomaterial scaffolds. In recent years, endochondral bone regeneration (EBR) has been gaining more traction, where bone is remodeled from a cartilaginous, callus-mimicking construct following implantation *in vivo*. The current trend in the field is focused on moving this approach towards an off-the-shelf variant for clinical application. From this perspective the use of donor-derived (allogeneic) cells, as well as devitalizing the eventual tissues is an attractive approach.

We have previously shown that these callus mimetics derived from allogeneic mesenchymal stem cells (MSCs), once devitalized, enable full bridging of a femoral defect when implanted into immunocompetent rats [1]. However, there is still a need to fully elucidate the interplay between the immune response and new bone formation. In our previous study, we found that the activation of the immune system by non-autologous cartilage tissue can hamper EBR [2]. To further explore this, the immune response of vital and devitalized callus mimetics derived from syngeneic and allogeneic cells were compared in this study using a subcutaneous model in rats.

Materials and Methods

Rat MSCs (rMSCs) were isolated from the bone marrow of Brown Norway (BN; syngeneic) and Dark Agouti (DA; allogeneic) rats. rMSCs were encapsulated within collagen type I gel droplets and chondrogenically differentiated for 28 days, prior to devitalization [1]. Two chondrogenic spheroids per group were implanted into subcutaneous pockets in BN rats (n=7) for 3, 7, 14, 28 or 84 days. Mineralization of the explants was assessed via a microCT imaging system (Quantum FX) and quantified using ImageJ. New bone formation was analyzed via histological analysis and histomorphometry. Immune response was evaluated via immunohistological staining.

Results and Discussion

Hematoxylin and eosin (H&E) staining of the explanted samples revealed that the vital syngenic and devitalized spheroids were converted into bone including marrow cavities within 4 weeks (Fig. 1). Safranin-O/fast green staining indicated that there was more non-remodeled cartilage in the allogeneic groups than in the syngenic groups at 4 weeks. However, the presence of hypertrophic cartilage at the outer region of the spheroids could be an indication that active remodeling is still taking place. After 12 weeks, 5 of the 7 samples from the

vital syngenic group could not be retrieved due to resorption. Histomorphometry results after 3 months revealed no significant differences in terms of bone formation or cartilage presence between the groups except for the vital syngenic.

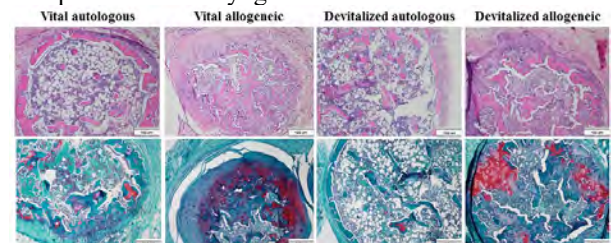


Figure 1. (Top) Subcutaneous endochondral bone formation after 4 weeks as demonstrated by H&E. (Bottom) Safranin-O/fast green staining showing the cartilage (red) that has not been remodeled.

Our initial analysis revealed no significant differences between groups in terms of CD68+ macrophages in the tissue surrounding the implants for up to 14 days. As the presence of macrophages can influence EBR through the secretion of pro- and anti-inflammatory cytokines, further analysis into the macrophage polarization is currently on-going. To determine neutrophil and T lymphocyte reaction, MPO and CD3+ immunohistochemical stainings are also planned.

Conclusion

No difference in bone formation was found after three months, although 70% of the samples from the syngenic group was resorbed. Overall, the allogeneic implants displayed slower bone formation, with the vital allogeneic group showing the slowest start. Therefore to further elucidate the relationship between bone formation and the immune response, it would be interesting to find out if the presence of M1 (pro-inflammatory) or M2 (anti-inflammatory) immune cells at early time points could be related to the differences in bone formation observed between the groups. In addition, the devitalized state of the implants also appears to affect the bone regenerative outcome. This could be related to a reported decreased immunogenicity of devitalized construct [3].

References

- Gawlitta, D., A. Longoni, L. Utomo, and A. Rosenberg, Engineered devitalized cartilaginous tissue for bone regeneration, European Patent Office, EP20195800.6, 11/9/2020.
- Longoni, A. et al (2020). Endochondral Bone Regeneration by Non-autologous Mesenchymal Stem Cells. *Front Bioeng Biotechnol.* 9;8:651.
- Muratov, R. et. Al (2010). New approach to reduce allograft tissue immunogenicity. *Experimental data. Interact Cardiovasc Thorac Surg.* 10(3):408-12.

Electrophoretic Deposition of Cu-doped Mesoporous Bioactive Glass/Chitosan Composite Coatings for Improved Soft Tissue Integration of Oral Implants

J. Han, N.H. Besheli, B.A.J.A van Oirschot, S.C.G. Leeuwenburgh, F. Yang

Radboud University Medical Center, Radboud Institute for Molecular Life Sciences, Department of Dentistry - Regenerative Biomaterials, Radboudumc, Nijmegen, The Netherlands

Introduction: Nowadays, dental implants are increasingly used in clinic to replace missing teeth aiming at restoration of oral aesthetics and function of patients. Histologically, peri-implant soft tissues adhering to implant surfaces create a protective barrier during the healing phase following implantation, which prevents oral pathogens from further invasion. However, the soft tissue around implants are typically poorly vascularized and cellularized compared with soft tissues surrounding natural teeth, which compromises soft tissue seal and increases the risk for bacterial invasion. Therefore, it is critical to improve peri-implant soft tissue integration during wound healing process by improving angiogenesis via implant coatings [1]. Copper as a trace element has been reported to improve angiogenesis by regulating vascular endothelial growth factor (VEGF) expression of endothelial cells [2]. Since limited studies have focused on dental peri-implant soft tissue integration especially its angiogenesis, the aim of this study is to develop an implant coating containing copper and evaluate its effect on angiogenesis. To this end, we firstly doped copper to mesoporous bioactive glass (MBG) nanoparticles, a promising inorganic carrier in the field of tissue engineering. Thereafter, we combined these Cu-MBG with chitosan through electrophoretic deposition (EPD) to obtain composite coatings. Subsequently, we performed a series of physicochemical as well as biological characterizations to evaluate the functional coating performance in vitro.

Materials and methods: Cu-MBG or MBG nanoparticles or their mixtures at 1:1 weight ratio were dispersed in chitosan solution and deposited on commercial pure Ti (cpTi) disks by means of electrophoretic deposition (EPD). The coating morphology was observed under scanning electron microscopy (SEM). Ion release from the coatings was measured by inductively coupled plasma atomic emission spectrometry (ICP-AES). Thereafter, human gingival fibroblasts (HGFs) were seeded on the disks and cultured for 1, 3 and 7 days for cytocompatibility test using Cell Counting Kit (CCK-8) assay. Human umbilical vein endothelial cells (HUVECs) were exposed to the extracts of the coatings to evaluate their angiogenicity. More specifically, HUVECs treated for 24 h were used in a transwell migration assay, and those treated for 12 h were counted for nodes and circles for tube formation assay.

Results and discussion: Under optimized coating conditions, homogeneous coatings could be formed on cpTi disks regardless of Cu-MBG:MBG ratio (Fig 1). Ion release profiles demonstrated the released amount of Cu^{2+} correlated to the content of Cu-MBG, whereas the released amounts of Si^{4+} and Ca^{2+} were similar for all groups. The concentration of released Cu^{2+} in Cu-MBG-MBG group was $8.2 \pm 1.3 \text{ ppm}$, which could reach the therapeutic concentration according to previous study

[3]. CCK-8 showed the HGFs proliferation in coating groups was somewhat reduced compared to groups without coating, but cells grew continuously up to 7 days. The result of the transwell migration assay indicated that the number of migrated cells in Cu-MBG:MBG = 1:1 group was significantly higher than other groups. In addition, both the numbers of formed nodes and circles in Cu-MBG:MBG = 1:1 group were the highest, with values that were almost two times than the control group.

Conclusions: A series of copper-doped MBG/chitosan composite coatings were successfully prepared via EPD technique with homogenous surface. The composite coatings were cytocompatible, and an optimal concentration of copper in the coating was observed with respect to their angiogenic efficacy.

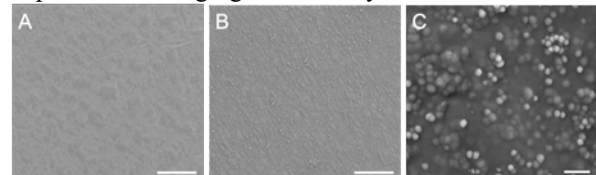


Fig 1. SEM images of (A) cpTi disk and (B,C) composite coating with Cu-MBG:MBG=1:1 at different magnifications. Scale bar = 100 μm in A and B; 500 nm in C.

References: [1] Abdallah MN, Badran Z, Ciobanu O, Hamdan N, Tamimi F. Strategies for Optimizing the Soft Tissue Seal around Osseointegrated Implants. *Adv Healthc Mater.* 2017;6(20):10.1002/adhm.201700549. [2] Zhou Y, Han S, Xiao L, et al. Accelerated host angiogenesis and immune responses by ion release from mesoporous bioactive glass. *J Mater Chem B.* 2018;6(20):3274-3284. [3] Li K, Xia C, Qiao Y, Liu X. Dose-response relationships between copper and its biocompatibility/antibacterial activities. *J Trace Elem Med Biol.* 2019;55:127-135.

Effect of immune response on endochondral bone regeneration using partially mismatched allogeneic MSCs

F. Staubli^{1,2}, A. Longoni^{1,2,3}, L. de Silva^{1,2}, N. Cristini^{1,2}, A. J. W. P. Rosenberg¹, D. Gawlitta^{1,2}

¹Dept. of Oral and Maxillofacial Surgery & Special Dental Care, ²Regenerative Medicine Utrecht, Utrecht, the Netherlands. ³Dept. of Orthopaedic Surgery and Musculoskeletal Medicine, Centre for Bioengineering & Nanomedicine, University of Otago, New Zealand.

In endochondral bone regeneration (EBR), a cartilaginous construct is implanted into a defect to trigger endochondral ossification, leading to bone defect repair¹. Typically, autologous or syngeneic multipotent mesenchymal stromal cells (MSCs) are exploited to generate cartilage implants *in vitro*. However, the use of patient-own cells is associated with significant drawbacks which hinder clinical translation, such as donor-site morbidity, no off-the-shelf solutions and donor-to-donor variability with respect to chondrogenic differentiation potential. The use of non-autologous MSCs presents a promising alternative to overcome these obstacles by donor screening and cell banking, bringing EBR one step closer towards clinical translation². However, a major drawback of non-autologous cells is their potential immunogenicity. So far, heterogenous neo-bone formation has been achieved when using donors and hosts with a complete immunological mismatch². Therefore, the goal of this study was to characterize the immune response triggered by allogeneic MSC-derived cartilaginous constructs with partial immunological mismatch between donor and host (partial MHC class I or MHC class II mismatches) and its effect on neo-bone formation.

To achieve this, MSCs were harvested from DA I rats and differentiated towards the chondrogenic lineage *in vitro*, using rat tail collagen I as a biomaterial carrier. The generated chondrogenic spheroids were implanted in a critical size femur defect in Dark Agouti (DA, MHC class I mismatch) or Brown Norway (BN, MHC class II mismatch) rats. Cell-free collagen carriers were included as negative controls. Formation of new bone tissue was assessed by microCT scans 0, 4, 8 and 12 weeks after implantation and by histological analysis (H&E, TRAP and Safranin-O/Fast green) of femora retrieved 12 weeks post-surgery. The systemic immune response was assessed by quantitatively analyzing anti-human IgG immunoglobulin and α 1-acid glycoprotein (AGP) in blood collected from the animals 0, 1, 2, 4, 8 and 12 weeks post-surgery. The local immune response was assessed by quantification of immune cell infiltration into the defect, done by immunohistochemical staining (CD3, CD68, iNOS, CD206, CD163, MPO) on femora retrieved 1 and 12 weeks post-surgery.

Twelve weeks after implantation, a larger amount of neo-bone formation was detected in both experimental groups compared to the control groups. However, no full bridging of the defect was achieved in any group. A bridging of $\geq 50\%$ was found in 4/7 animals receiving MHC class I mismatch grafts, as compared to 2/8 animals receiving MHC class II mismatch grafts (Figure 1). Neo-bone formation assessed by histomorphometry confirmed the results obtained by microCT scanning. Both mismatch grafts were invaded by pro-inflammatory macrophages and T-lymphocytes (1 and 12 weeks post-surgery). At these timepoints, less CD163+ anti-

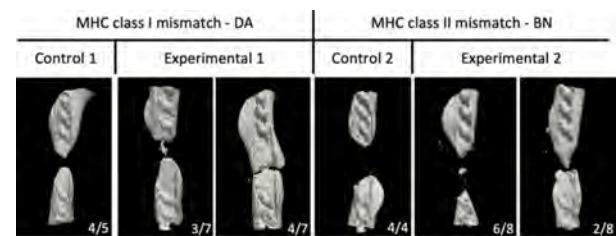


Figure 1: Results of the micro-CT analysis performed to quantify the mineralization volume. The 3D reconstructions display a representative sample for the control and the experimental groups 12 weeks post-surgery.

inflammatory macrophages and more CD3+ T-lymphocytes were found in mismatch class I animals and more CD68+ macrophages were found in mismatch class II animals compared to their respective collagen controls. Plasma concentrations of IgG increased over time in both groups, but only in mismatch class II animals the concentration increased to significantly higher levels over 12 weeks (compared to collagen control). No difference in AGP levels was found among experimental and control groups.

Our results demonstrate the feasibility of using partially mismatched allogeneic MSC-derived chondrocytes to elicit endochondral bone regeneration *in vivo*. Despite an increased immune response compared to the control groups, marked by infiltration of pro-inflammatory macrophages and T-lymphocytes (class I mismatch) or production of IgG (class II mismatch), bone formation occurred. However, the elicited immune response might have affected bone formation and hindered full defect bridging. Furthermore, differences in timing and quantity of certain immune players were distinguished between partial class I and class II mismatch animals compared to the controls. However, a clear correlation between the type and extent of the elicited immune response and the regenerative potential of the grafts cannot be made based on these results. Further studies need to be carried out in order to identify the interaction between activated immune players depending on the mismatch type and their effect on neo-bone formation.

References:

- ¹ Longoni et al. The impact of immune response on endochondral bone regeneration. NPJ Regen Med. 2018 Nov 29;3:22
- ² Longoni et al. Endochondral Bone Regeneration by Non-autologous Mesenchymal Stem Cells. Front Bioeng Biotechnol. 2020 Jul 9;8:651

Profiling the microRNA fingerprint of the human fracture hematoma

R. Groven^{1,2}, E.R. Balmayor¹, C. Peniche Silva¹, B. van der Horst^{1,2}, M. Poeze², T. Blokhuis², M. van Griensven¹
 1 Department of Cell Biology-Inspired Tissue Engineering, MERLN Institute for Technology-Inspired Regenerative Medicine, Maastricht University, Maastricht, The Netherlands
 2 Division of Trauma Surgery, Department of Surgery, Maastricht University Medical Center+, Maastricht, The Netherlands

Introduction Immediately after a fracture occurs, a fracture hematoma (fxH) is formed. fxH plays an important role in fracture healing and, under normal circumstances, aids in generating an environment in which a wide variety of cells orchestrate processes involved in fracture healing. MicroRNAs (miRNAs) may influence these processes. The aim of this study was therefore to determine the miRNA expression signature of human fxH in normal fracture healing and examine the potential influence of clinical parameters on these expression levels.

Methods fxH was harvested during fracture surgery. miRNAs were isolated, transcribed and pooled for qPCR array analysis and validation in the study population. Qiagen fibrosis- and inflammation qPCR arrays were used based on an extensive literature study related to fracture healing and osteogenesis. Additionally, miRNA targets were determined by means of Qiagen Ingenuity Pathway Analysis.

Results In total, fxH were harvested from 61 patients (*mean age 52 ± 9; 32 ♀*). From the array data, a selection of the twenty most regulated miRNAs, 10 up- and 10 down-regulated, was validated in the study population. The expression levels of seven out of these 20 miRNAs were correlated to several clinical parameters (fig. 1). The time interval between trauma and surgery showed to influence the expression of three miRNAs, other three miRNAs were expressed in a patient age dependent manner and one based on the severity of trauma.

Discussion This study portrayed the regulatory role and importance of miRNAs in human fxH, linked to key processes in fracture healing. The expression levels of seven validated miRNAs were correlated with several clinical parameters and showed to be involved in multiple processes that are important in the fracture healing cascade, such as, angiogenesis, mineralization and cellular differentiation. In silico target analysis revealed 260 mRNA targets for 14 out of the 20 validated miRNAs. These data broaden our view on potential therapeutic implications of miRNAs in fracture healing.

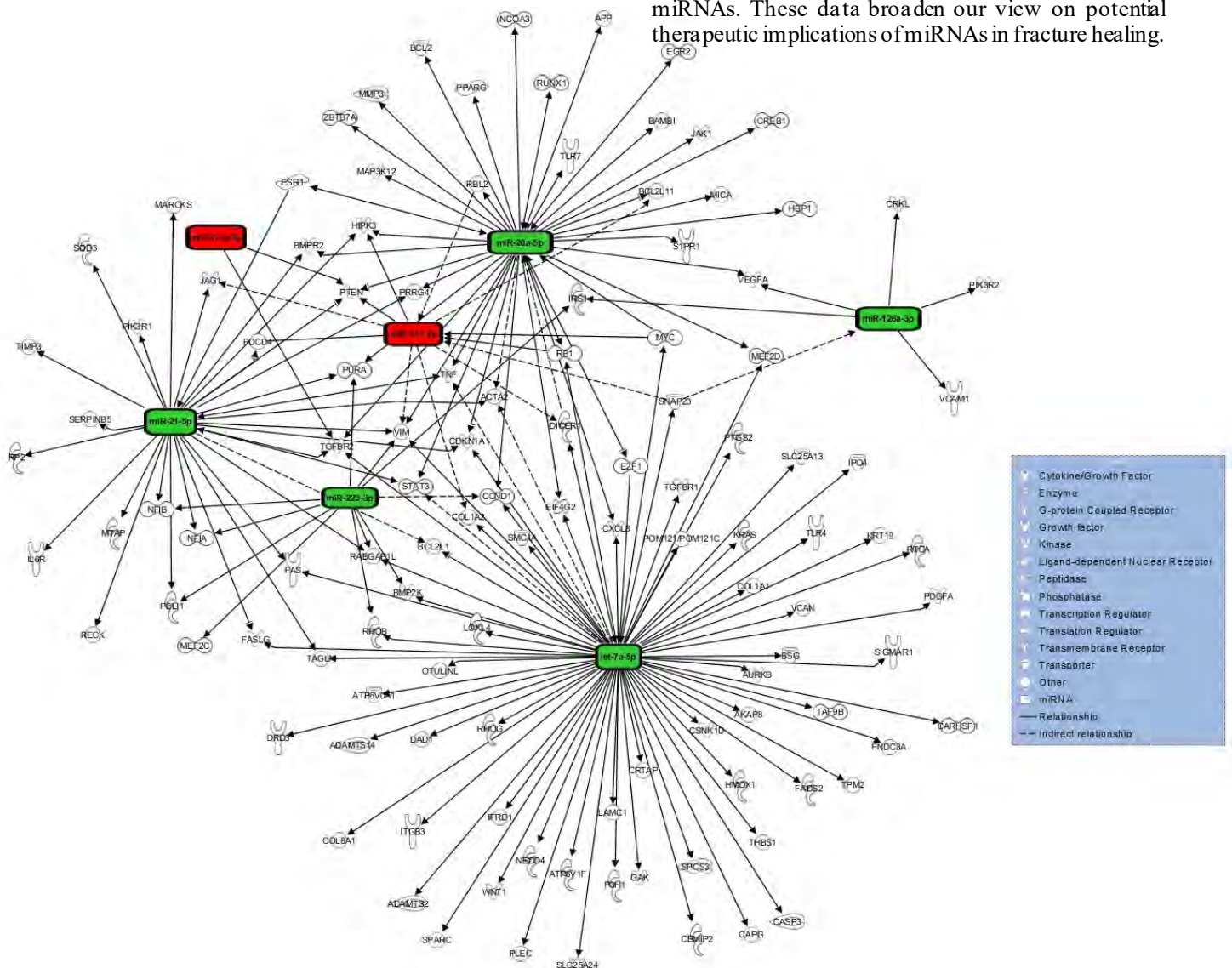


Figure 1: In silico target analysis, performed with Qiagen Ingenuity Pathway Analysis (IPA) software, of 7 miRNAs whose expression was dependent on the time interval between trauma and surgery, patient age, or severity of trauma. Green colour represents upregulated miRNA expression, red colour represents downregulated miRNA expression.

A universal nanogel-based coating approach for medical implants

D. Keskin¹, D. Ghosh¹, R. Bron¹, C. Rosman¹, C. Siebenmorgen¹, G. Zu¹, T. van Kooten¹, A.M. Forson¹, H. van der Mei¹, J. Sjollemma¹, M. Witjes², and P. van Rijn¹

¹University of Groningen, University Medical Center Groningen, Department of Biomedical Engineering, Groningen, The Netherlands

²University of Groningen, University Medical Center Groningen, Department of Oral and Maxillofacial Surgery, Groningen, The Netherlands

Introduction

The use of implants have increased the quality of life, for patients. However, secondary complications in the host body can lead to implant failure. Coatings have been regarded as an excellent possibility to induce desired responses or to prevent complications, as the bulk implant material does not need to be altered. However to apply a coating, a diverse range of chemical approaches have to be implemented owing to the distinct physiochemical and structural properties of the different classes of implant materials. The aim of the study is to develop a universal nanogel (nGel) coating approach that can be applied to most implant materials, ranging from bioglass, polymers, metals and rubbers and furthermore, investigate the stability of the coating in vitro and in vivo conditions.

Materials and methods

N-Isopropylacrylamide-*co*-*N*-(3-Aminopropyl)methacrylamide dihydrochloride p(NIPAM-*co*-APMA) core shell nGel particles were synthesized by free-radical precipitation polymerization reaction.^[1] The particles were characterized by zeta potential, while the coating was visualized by atomic force microscopy (AFM). The positively charged particles were spray coated and bound on the plasma oxidized, negatively charged implant surface by electrostatic interactions. The stability of the coating was determined in vitro by exposing nGel coated Teflon surfaces to physiological conditions in a shaker incubator for 21 days and in vivo by implanting methacryloyl ethyl thiocarbonyl Rhodamine B (MRB) labeled nGel coated (polyvinylidene fluoride) PVDF hernia mesh in mouse model for 13 days.

Results and Discussion

The positive zeta potential, 15.83 ± 0.11 mV at 24°C was attributed to the presence of V50 along with the protonated primary amine groups,^[2] introduced by APMA. On plasma oxidation, the surface of the material acquired negative charge. The positively charged nGel particles were deposited on the surface by spray coating technique and the particles were bound to the activated surface via electrostatic interactions^[3] (Figure 1). The homogenous uniform coating was characterized by AFM. In vitro data analyzed by AFM showed that the nGel coatings on teflon were stable after 21 days (data not shown), while the in vivo data demonstrated that the coatings on PVDF mesh were stable enough up to 13 days, after which the fluorescent signal was decreasing (Figure 2b). The short term in vivo test is considered as an initial proof for the stability of the nGel coating.

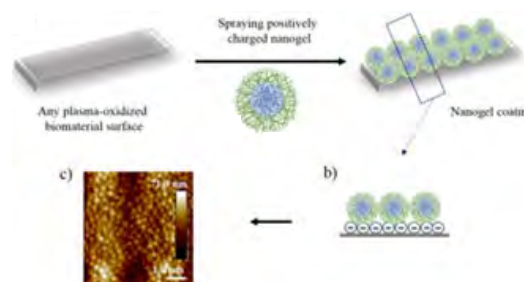


Figure 1: Schematic illustration of the universal nGel-based coating approach on implant surface.

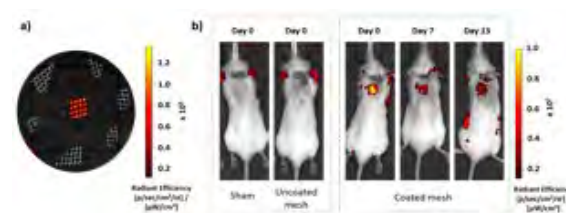


Figure 2: a) Representative fluorescence images of nGel coated mesh (labeled with MRB dye, in the middle) and uncoated meshes (grey) taken by IVIS before the implantation in the mice. b) Representative fluorescence images of mouse taken without and with the uncoated PVDF mesh and nGel-coated PVDF meshes at different time points.

Summary

The coating approach successfully formed a homogenous uniform coating on most implant surfaces, belonging to different classes of materials. The coating showed high stability in both in vitro and in vivo conditions.

References:

- [1] W. H. Blackburn, L. A. Lyon, *Colloid Polym. Sci.* **2008**, 286, 563.
- [2] L. Sigolaeva, D. Pergushov, M. Oelmann, S. Schwarz, M. Brugnoli, I. Kurochkin, F. Plamper, A. Fery, W. Richtering, *Polymers (Basel)*. **2018**, 10, 791.
- [3] D. Keskin, O. Mergel, H. C. van der Mei, H. J. Busscher, P. van Rijn, *Biomacromolecules* **2019**, 20, 243.

Oral Presentation
Session 10

Keynote session 10

Microelectromechanical organ-on-chip devices and platforms

Dr. Massimo Mastrangeli
Department of Microelectronics
Delft University of Technology



Abstract:

Stemming from the convergence of tissue engineering, microfluidics and microfabrication, organ-on-chip (OoC) technology can reproduce in vivo-like dynamic microphysiological environments for tissues in vitro. The possibility of realistic recapitulation of tissue and organ (patho)physiology in OoC devices may hold the key to bridge the current translational gap in drug development, and possibly foster personalized medicine. In this talk I will underline the biotechnological convergence at the root of OoC technology, and outline research tracks under development in our group at TU Delft along two main directions: fabrication of innovative microelectromechanical OoC devices, integrating stimulation and sensing of tissue activity, and their embedding within advanced platforms for pre-clinical research. I will conclude with remarks on the role of open technology platforms for the broader establishment of OoC technology in pre-clinical research and drug development.

Biography:

Massimo Mastrangeli is tenured Assistant Professor at TU Delft's Electronic Components, Technology and Materials laboratory, where he is developing innovative silicon/polymer-based organ-on-chip devices and advanced chip interconnect and packaging technology. Prior to joining TU Delft, Dr. Mastrangeli held research appointments at the Max Planck Institute for Intelligent Systems (Stuttgart, Germany) for soft small-scale robotics and self-assembly of granular matter, at Université Libre de Bruxelles (ULB, Belgium) for micromechanics and capillary micromanipulation, at École Polytechnique Fédérale de Lausanne (EPFL, Switzerland) for micro/nanofabrication and distributed robotics, and at imec Belgium (Leuven, Belgium) for fluidic microsystems integration and microelectronic packaging. Dr. Mastrangeli holds a B.Sc. and M.Sc. degree (both cum laude) in Electronic Engineering from University of Pisa (Italy) and a Ph.D. degree in Materials Engineering from University of Leuven (Belgium).

Culture of stem cell-derived kidney organoids in physiological oxygen enhances amount and patterning of the endothelial network

A. Schumacher¹, N. Roumans¹, V. Joris¹, T. Rademakers¹, M. van Griensven¹ and V. LaPointe¹

¹Department of Cell Biology–Inspired Tissue Engineering, MERLN Institute for Technology-Inspired Regenerative Medicine, Maastricht University, Universiteitsingel 40, 6229 ET Maastricht, The Netherlands

Introduction

Organoids are gaining significant interest in the field of regenerative medicine. Their ability to self-organize from pluripotent stem cells into functional organ-like structures makes them candidates for organ replacement or repair. We aim to produce functional kidney organoids from induced pluripotent stem cells (iPSCs) to build an implantable kidney graft to reduce or replace dialysis for patients with end-stage kidney disease. For this, we differentiate iPSCs and subsequently form organoids by aggregation. After 18 days of culture, these are several millimeters in size and comprise small nephron-like structures, with tubular segments and an immature endothelium. We see, however, that prolonged culture results in diminishing endothelial cells and deteriorating nephrons. Notably, the organoids grow in a transwell setup at an air-liquid interface, and are therefore directly exposed to a hyperoxic (21%) culture environment. This culture method has been used to culture kidney explants since the 1950s, however, there is little understanding of its effects. Knowing that kidneys develop *in vivo* in a hypoxic environment, we aimed to replicate this and gather more insight into the effect of oxygen in organoid vascularization.

Methods

For this, we cultured our organoids in a hypoxic environment, similar to the physiological range of oxygen in developing kidneys, for up to 20 days. We investigated the activation of the HIF1/2 pathways by immunofluorescence and the transcription of HIF responsive genes by gene analysis. Whole mount imaging facilitated by tissue clearing and subsequent 3D segmentation and analysis was performed to visualize and quantify the endothelial network.

Results

We found an increase in nuclear HIF1 α in podocytes in hypoxia and nuclear expression of HIF2 α in all cells, confirming HIF pathway activation. Gene expression analysis showed differential expression of VEGFA variants. Particularly, the *VEGF189* variant was significantly upregulated in hypoxia, which is associated with microvasculature formation. Whole mount imaging of the endothelial network revealed an increased amount of micro vessel-like network with homogenous morphology and enhanced interconnectivity (Figure 1). 3D quantification confirmed an increase of the total volume fraction of endothelial cells in hypoxia.

Conclusion

To conclude, kidney organoid culture at an air-liquid interface is hyperoxic and eventually leads to organoid deterioration. We hypothesized that culturing the organoids at physiological hypoxia could mimic *in vivo* nephrogenesis and vascularization. We found that indeed hypoxia promotes the formation of a homogenous and interconnected endothelial network.

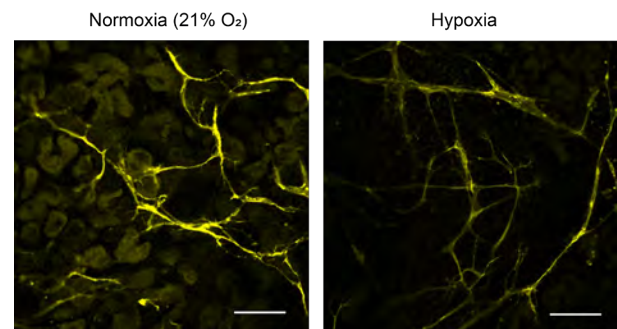


Figure 1: Whole mount immunofluorescence imaging reveals increased interconnected endothelial network (CD31, yellow) in kidney organoids cultured in physiological hypoxia compared to cell culture normoxia (21% O₂). Scale bar = 50 μ m.

Contact details:

Anika Schumacher

Anika.schumacher@maastrichtuniversity.nl

Ultra-High Throughput Production of Embryoid Bodies and Human Cardiac Organoids using In-Air Microfluidic generated Hollow Core-Shell Microcapsules

Bas van Loo¹, Nuno Araújo-Gomes¹, Simone ten Den², Vincent de Jong¹, Robert Passier², Tom Kamperman¹, Jeroen Leijten¹

¹ University of Twente, Developmental BioEngineering, Enschede, Netherlands

² University of Twente, Applied Stem Cell Technology, Enschede, Netherlands

s.r.vanloo@utwente.nl, jeroen.leijten@utwente.nl

Introduction:

Pluripotent stem cell-derived organoids hold great potential for tissue engineering and drug testing purposes. However, organoid production is characterized by batch-process techniques that associate with artisan, labor-intensive, and low throughput production processes.¹⁻³ Microfluidic technology offers solutions for improved production of cellular aggregates in terms of quality and production rate, which can be achieved via microfluidic encapsulation of cells in hollow core-shell microcapsules.⁴ We therefore hypothesized that microfluidic droplet generation could also be leveraged to realize high throughput production of pluripotent stem cell-derived organoids. Advantageously, we recently invented In-Air microfluidics, which allows the ultra-high throughput microfluidic production of micromaterials in an off-chip manner without the use of oils and surfactants.⁵ We here report that hollow core-shell microcapsules generated with In-Air microfluidics allowed for the production of embryoid bodies, which autonomously transformed in cavitated organoids that committed subsequently to the mesodermal and myocardial lineage.

Methods:

We developed a novel In-Air microfluidics setup for the production of hollow core-shell microcapsules, which consisted of a three nozzle design (Figure 1A). The first microjet contained a solution of 10% dextran and 0.05 M CaCl₂ and was actuated with a piezoelectric actuator (5 V_{pp}, 5 kHz). The second microjet contained a solution of 0.2% alginate and 10% (v/v) ethanol (EtOH) which encapsulated the droplets of the first microjet. The third microjet contained a solution of 0.2 M CaCl₂ and 55% (v/v) EtOH which encapsulated the droplet containing the solutions of the first and second microjet. The resulting layered droplets were captured in a 0.1 M CaCl₂ collection bath. This process allowed for inside-out and outside-in crosslinking of the alginate shell, resulting in monodisperse production of shape-stable hollow core-shell microcapsules with ~200 μm diameter at flow rates of over 4 ml/min. Human embryonic stem cells genetically modified with a dual-fluorescent reporter (i.e., MESP1/NKX2.5 and NKX2.5/ α-Actinin) were encapsulated at 0.5-10*10⁶ cells/ml (Figure 2b). Cell-laden microcapsules were collected in a surplus of collection medium, which guaranteed that the EtOH concentration within the core consistently remained <1%. Embryoid body formation cells was achieved by culturing in E8 stem cell medium, and functional myocardial organoid formation was achieved using BPEL differentiation medium.

Results and discussion:

Using different nozzle sizes (50/100/150 μm), monodisperse hollow core-shell microcapsules of various sizes (i.e., 80-300 μm in diameter) could be produced. In-air microfluidic encapsulation of human

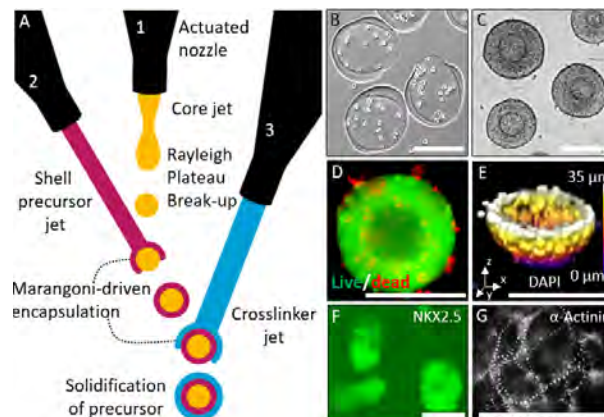


Figure 1: (A) Schematic of In-Air microfluidic set up for (B) embryonic stem cell encapsulation in hollow core-shell microcapsules, which results in (C) Embryoid bodies (D) with high cell viability (E) and cavitation. (F) Myocardial differentiation resulted in functional cardiac organoids which are positive for NKX2.5 and (G) α-actinin. Scale bar is 200 μm.

embryonic stem cells (Figure 1B) associated with the formation of embryoid bodies within 24 hours (Figure 1C) and cell viabilities of >95% immediately upon encapsulation (Figure 1D). Formed embryoid bodies, which continued to be metabolically active and proliferate for at least 28 days of culture. Remarkably, the microencapsulated embryoid bodies cavitated and formed organoids in a fully self-instructed and autonomous manner (Figure 1E) while remaining positive for Sox2 and Oct3/4. Upon differentiation, human embryoid bodies initially underwent mesoderm transition within four days of culture and committed to the myocardial lineage. After 7 days of culture, cardiomyocytes were positive for myocardial marker NKX2.5 (Figure 1F), and were positive for α-actinin after 14 days (Figure 1G), resulting in functional cardiac organoids that displayed self-induced synchronized cardiac contractions.

Conclusion:

Hollow core-shell microcapsules generated with In-Air microfluidics allowed for the production of human embryoid bodies that autonomously transformed in cavitated organoids, which could be triggered to become functional cardiac organoids. We anticipate that the facile, high-throughput, and clean nature of our platform can facilitate upscaled investigations for developmental studies, cell therapies, and drug screens.

Acknowledgements:

The authors acknowledge funding from Dutch Arthritis Foundation (#17-1-405) and European Research Council (ERC, Starting Grant, #759425).

Bibliography:

1. Brassard, J. A. et al. Cell Stem Cell 24, 860–876 (2019) 2. Lancaster, M. A. et al. Science 345, 1247125 (2014) 3. Dutta, D. et al. Trends Mol. Med. 23, 393–410 (2017) 4. van Loo, B. et al. Mater. Today Bio 6, 100047 (2020) 5. Visser, C. W. et al. Sci. Adv. 4, (2018)

Towards bone-remodeling-on-a-chip

M.A.M. Vis, E.S.R. Bodelier, K. Ito, S. Hofmann

Orthopaedic Biomechanics, Department of Biomedical Engineering and Institute for Complex Molecular Systems, Eindhoven University of Technology, P.O. Box 513, 5600 MB Eindhoven, the Netherlands

Introduction: Bone remodeling is the process of bone resorption by osteoclasts and bone formation by osteoblasts. It is the most fundamental physiological process that defines living bone. An imbalance in this process can cause metabolic bone diseases such as osteoporosis. Currently, no complete *in vitro* bone remodeling model is available. Such models could have the potential to increase our knowledge on the physiological and pathological processes underlying bone remodeling and could potentially improve drug development processes. Bone-on-a-chip technology has the great potential to advance bone research, allowing for the study of low cell numbers in high temporal and/or spatial resolution. In this study, microfluidic chip technology is used to create a bone remodeling model that contains the interaction between osteoblasts and osteoclasts.

Materials and Methods: A bone-on-a-chip microfluidic device that facilitates three-dimensional (3D) *in vitro* bone-like tissue formation was developed. A polydimethylsiloxane (PDMS) microfluidic device was fabricated by means of photo- and soft-lithography (Figure 1A). The device contained rectangular-shaped cell culture channels that were coated with fibronectin and seeded with human bone marrow derived mesenchymal stromal cells (MSCs) (Figure 1A). The MSCs were dynamically cultured for a period of 21 days by applying medium flow, resulting in shear stresses acting on the cells. Osteogenic medium was used to differentiate the MSCs towards the osteogenic lineage. The formed structures were analyzed with time-lapse brightfield imaging and confocal imaging using

immunohistochemical staining for the formation of collagen and the expression of the markers RUNX-2 and osteopontin. Alizarin Red and Picrosirius Red staining were used to visualize the deposition of calcium and collagen in the extracellular matrix respectively.

Results: Time-lapse imaging revealed self-assembly into 3D constructs within the channel, resembling bone trabeculae. At the end of the three-week culture period, brightfield imaging visualized a clear deposition of calcium (Alizarin Red staining) and collagen (Picrosirius Red staining) in the extracellular matrix produced by the cells. Confocal microscopy revealed the formation of 3D bone-like struts (Figure 1B). Immunohistochemical staining confirmed the formation of collagen type 1 and revealed the expression of the markers RUNX-2 and osteopontin, confirming the differentiation of the MSCs into the osteogenic lineage.

Conclusion: Overall, the results revealed mineralized bone-like struts that match the size and shape of human bone trabeculae. With this, the developed bone-on-a-chip microfluidic device showed the first step towards a 3D *in vitro* bone remodeling model, exhibiting bone-like tissue formation. In future research, osteoclasts will be added to create the co-culture microenvironment that is necessary for bone remodeling.

Acknowledgements: This work is part of the research program TTW with project number TTW 016.Vidi.188.021, which is (partly) financed by the Netherlands Organisation for Scientific Research (NWO).

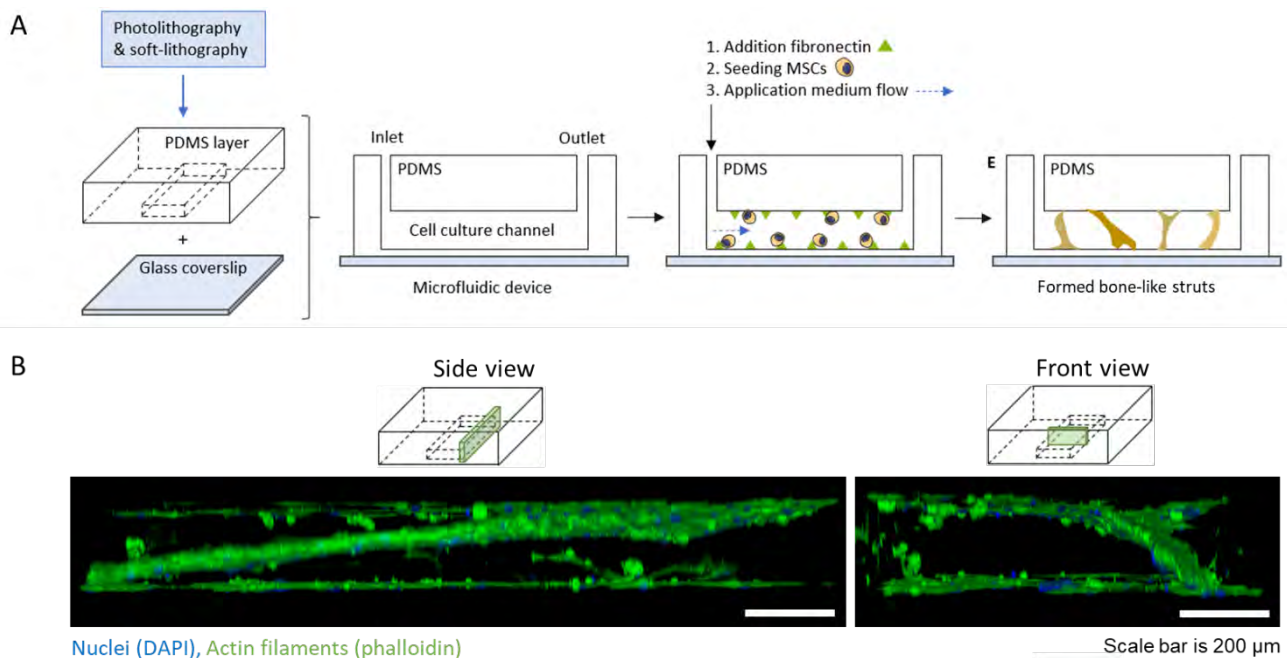


Figure 1 A. Photolithography and soft-lithography are used to fabricate a PDMS microfluidic cell culture chip. The chip exists of rectangular channels, coated with fibronectin and seeded with MSCs. In three weeks, the MSCs differentiate towards the osteogenic lineage and form bone-like struts in the channels. B. 3D confocal microscopy image of the formed bone-like struts in the channels after 3 weeks of cell culture.

Integration of Organoid- and Cell-filled Chondral Implants in Human Osteochondral Explants

M.W.A. Kleuskens¹, C.C. van Donkelaar¹, M.C. van der Steen², R.P.A. Janssen^{1,2,3} and K. Ito¹

¹Orthopaedic Biomechanics, Department of Biomedical Engineering, Eindhoven University of Technology, The Netherlands, ²Dept. of Orthopaedic Surgery and Trauma, Máxima Medical Center Eindhoven-Veldhoven, The Netherlands

³Dept. of Paramedical Sciences, Fontys University of Applied Sciences, Eindhoven, The Netherlands

Introduction: In the field of cartilage repair, integration of cartilage-resurfacing implants with the surrounding cartilage has shown to be a major challenge. Currently, this is only assessed pre-clinically at the last stage in animal studies. However, these are expensive and time consuming. Besides, they have a low throughput, and results obtained are often not directly translatable to humans. To reduce animal experimentation and overcome translational issues, and at the same time speed up implant development and increase throughput when proceeding from animal models to humans, an ex vivo human tissue-based approach was developed in which viability and biochemical content of human osteochondral explants could be maintained in culture for 28 days.¹ To evaluate whether this culture platform might be used to evaluate short-term implant integration in an early stage of implant development, we examined the integration of an autologous chondrocyte implantation (ACI)-like fibrin implant with the surrounding native cartilage.

Methods: Fresh chondrocytes were isolated from smooth human articular cartilage (n=5) of patients undergoing total knee replacement (TKR) surgery at the Máxima Medical Centre under IRB approval. Chondrocytes were cultured for 12 days in traditional 2D culture flasks (10⁶ cells in a T175 flask) and in spinner flasks (50000 cells/ml), supplemented with (spinner flasks) or without (2D culture flasks) porcine derived notochordal cell matrix (NCM) to induce cartilage organoid formation.^{2,3} Osteochondral explants with a smooth cartilage surface (Ø 10mm, 4mm bone length, 5 per donor) were isolated from tissue of six different TKR subjects and a Ø 6mm full-depth chondral defect was created in the center of each explant. Organoids and 2D cultured chondrocytes were implanted into the defects (10⁶ cells/80µl) using diluted Tisseel fibrin sealant (figure 1). The constructs were cultured for 28 days in a double-chamber culture platform, in which cartilage and bone compartments are separated to allow for supplementation of tissue-specific medium.^{1,4} After 1 and 28 days of culture, implants were evaluated for sulfated glycosaminoglycan (sGAG), hydroxyproline (HYP), and DNA content. Moreover, osteochondral sections were stained for analysis of integration and distribution of proteoglycans (PG) and collagen type II. Data were statistically analyzed using Kruskal-Wallis tests (statistical significance was set to p<0.05) and if appropriate, a Dunn's multiple comparison post-hoc test to compare between groups.

Results and discussion: After 28 days, the organoids in the bottom and on the sides of the defect remodeled and merged, and cells migrated through the fibrin glue and deposited matrix bridging the space between the organoids and between the organoids and the native cartilage. Newly formed tissue rich in PG was present in the organoid-filled and cell-filled defects, especially on the edges and in the corners (figure 2). In these PG rich

areas, the newly formed tissue integrated and interacted with the surrounding native cartilage and round cells resided in lacunae, assumed to be newly formed. It is hypothesized that the integration observed is indicative for in vivo integration. Towards the center of the implants a fading PG gradient was observed, and the cells present in this area had a less-rounded morphology. Immunohistochemical analysis shows presence of collagen type II in the corner areas of both the organoid and the cell containing implants after 28 days, indicating limited dedifferentiation of the chondrocytes. Even though biochemical analysis did not reveal significant differences between groups, a trend was observed towards increasing sGAG and HYP content over time, and a higher sGAG and HYP content in the organoid-filled defects compared to the cell-filled defects for both timepoints analyzed (figure 3). This higher sGAG and HYP content might be beneficial in terms of short-term load bearing. This human culture model can be used to test and identify promising implant strategies through ex vivo evaluation of integration and matrix production, leading to a decrease in animal experimentation. Expanding the ex vivo model by adding mechanical loading, co-culturing different cell types or adding cytokines might add more complexity to the ex vivo model, allowing for a more complete evaluation in an earlier stage of development, and therefore a further decrease in the number of animal studies and/or entering clinical trials with more detailed knowledge of potential implant behavior.

Acknowledgements: This work is supported by the partners of RegMed XB. Powered by Health~Holland, Top Sector Life Sciences & Health.

References: ¹Kleuskens MWA et al., *J. Orthop. Res.* 2020, ²Crispin JF et al., *Acta Biomater.* 2021, ³de Vries SAH et al., *Sci. Rep.* 2018, ⁴Schwab A et al., *Altex* 2017

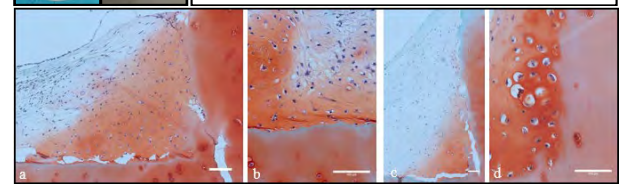
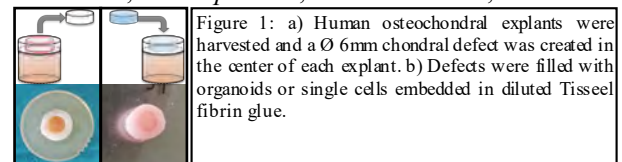


Figure 2: Representative images of sections stained with Safranin-O/fast green showing proteoglycan-rich tissue and cell morphology in the corners and edges of the defects filled with fibrin + organoids (a,b) or fibrin + cells (c,d). Scalebar = 100 µm.

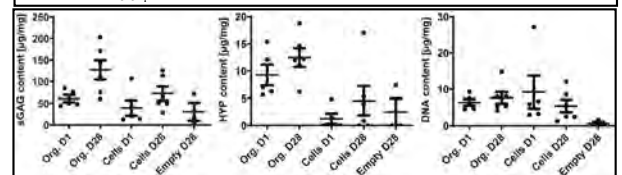


Figure 3: sGAG, HYP, and DNA content of the fibrin implants after 1 and 28 days of culture. Org. = organoids

Biochemical and Biophysical Tunable Smart Microbuilding Blocks to Instruct Engineered Living Tissues

N.G.A. Willemen*, T. Kamperman*, C.L. Kelder, M. Koerselman, M. Becker, M. Karperien, and J. Leijten

Department of Developmental BioEngineering, Faculty of Science and Technology, Technical Medical Centre, University Twente, Drienerlolaan 5, 7522NB Enschede, The Netherlands. Contact: n.g.a.willemen@utwente.nl

Introduction:

Modular tissue engineering exploits the 3D self-assembly of cells and building blocks into larger tissue constructs with higher complexity and resolution.^[1] However, current modular tissue engineering strategies have near-exclusively relied on static, non-responsive, micromaterials,^[2] whereas functionality of native tissues is dictated by their inherently dynamic nature.^[3] Here, we report on smart, dynamically tunable, microbuilding blocks of which the biochemical and biophysical properties can be altered via well-controlled secondary crosslinking strategies. The mechanical properties of the building blocks were modified post-synthesis by exploiting visible-light-induced secondary crosslinking of the free tyramines using ruthenium (Ru) and sodium persulfate (SPS) as initiators. The free biotins could be stepwise functionalized with biotinylated molecules of interest using competitive supramolecular complexation of avidin and biotin analogs.^[4] The spatiotemporal control over mechanical and chemical properties of smart building blocks within living modular tissues provided a highly tunable, well-defined, and dynamic cellular microenvironment, which allowed for the *in situ* modification of (stem) cell behaviour and fate.

Materials and Methods:

Microgel production: Hydrogel precursor droplets composed of 5% (w/v) Dextran-Tyramine-Biotin (DexTAB; ~1 mM biotin) and 22 U/mL horseradish peroxidase in phosphate buffered saline (PBS) were emulsified in 2% (w/w) Pico-Surf 1 containing Novec 7500 Engineered Fluid in the droplet generator.^[5]

Microgel functionalization and seeding: DexTAB microgels were consecutively incubated with 1 μ M neutravidin, washed, incubated with 1 μ M biotinylated or desthiobiotinylated molecule-of-interest, and washed again. Microgels were homogeneously co-seeded with cells into non-adherent 3% (w/v) agarose microwell chips at a density of 50 units per microwell.

In situ stiffening: Building blocks within modular tissues were *in situ* stiffened by incubating them with 2.5 mM of SPS and 1 mM of Ru. Free radical crosslinking was induced using 60 seconds of visible light irradiation. Differentiation was analyzed by histochemical staining.

Results:

Microgel precursor droplets were formed in a microfluidic droplet generator and crosslinked by controlled supplementation with H₂O₂ (Figure 2a). This resulted in formation of monodisperse DexTAB microbuilding blocks. The building block's stiffness predictably correlated with H₂O₂ supplementation (Figure 2d).

Next, the biotins in the microgel's shell were functionalized with c(RGDfK), which enabled autonomous self-assembly of microgels with cells owing to cell-microgel interactions (Figure 2f).

In situ chemical control was shown by sequentially endowing smart building blocks with (desthio)biotinylated fluorophores (Figure 2d).

Moreover, photo-induced crosslinking allowed for on-demand control of building block stiffness. Stem cell fate toward osteogenic and adipogenic lineages was temporally steered by *in situ* tuning the building block stiffness within modular tissues (Figure 2E).

Conclusion:

In conclusion, we developed the first biochemically, biophysically, and spatiotemporally controlled smart building blocks for modular tissue engineering. This allowed for the creation of highly tunable and defined cellular microenvironments, which more accurately resembled the dynamic microenvironment of cells in native tissues.

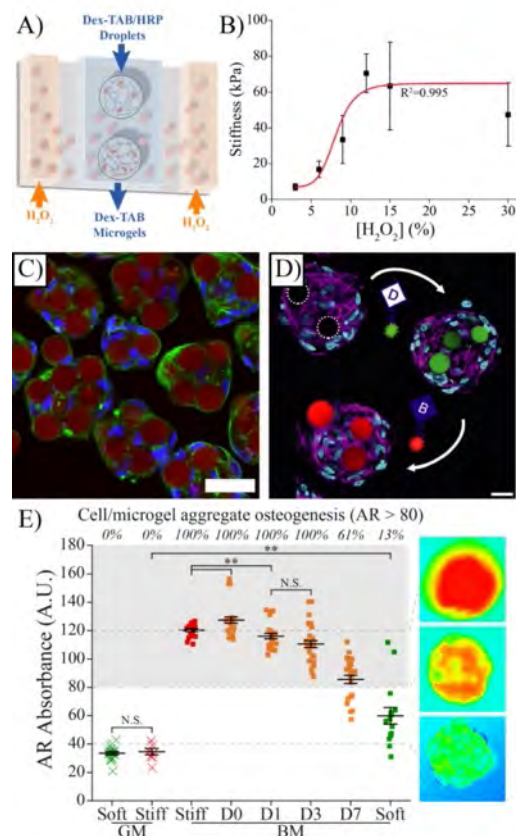


Figure 1: A,B) Stiffness of the building blocks was controlled by H₂O₂ supplementation. C) Cells and building blocks self-assembled into modular tissues. D) Demonstration of smart tissue engineered building blocks with *in situ* modification of modular tissue constructs. E) Osteogenic differentiation was temporally steered by *in situ* stiffening soft DexTAB microbuilding blocks.

References:

- [1] S. M. Oliveira *et al*, *Biotechnology Advances*, 33 (6), 2015.
- [2] A. Leferink *et al.*, *Adv. Mater.*, 26 (16), 2014.
- [3] W. P. Daley *et al*, *Journal of Cell Science*, 121, 255-264, 2008.
- [4] T. Kamperman *et al.*, *Nat. Commun.*, 10, 4347, 2019.
- [5] T. Kamperman *et al*, *Small*, 13 (22), 2017.

Poster abstracts

P1	Gabriele Addario, Maastricht University <i>Tubulointerstitium kidney model for future disease screening</i>
P2	Madison Ainsworth, University Medical Center Utrecht <i>Covalent protein immobilization on 3D-printed microfiber scaffolds for guided cartilage regeneration</i>
P3	Ane Albillos Sanchez, Maastricht University <i>A hyaluronic acid based bioink for osteochondral tissue engineering</i>
P4	Els Alsema, Eindhoven University of Technology <i>Covering blind spots in implant safety: an in vitro testing strategy for medical implant safety assessment</i>
P5	Sana Ansari, Eindhoven University of Technology <i>Development of a serum substitute medium for 3D in vitro bone models</i>
P6	Nuno Araújo-Gomes, University of Twente <i>Enzymatically crosslinked polyethylene glycol microgels for immunoprotection of non-autologous β-cell spheroids</i>
P7	Gizem Babuccu, University of Amsterdam <i>In vitro and ex vivo evaluation of diagnostic and antimicrobial capacity of triggered release devices in STIMULUS</i>
P8	Payal Balraadsing, University of Amsterdam <i>The effect of electrospun fiber diameter on Staphylococcus aureus and immune cell infiltration</i>
P9	Malin Becker, University of Twente <i>Mechanically tunable biomaterial for EMB3D printing of tubular structures with spatial biochemical control</i>
P10	Tristan Bodet, Maastricht University <i>Endothelium formation, challenge and optimisation</i>
P11	Torben van der Boon, University of Groningen/ University Medical Center Groningen <i>High-throughput screening to elucidate biomaterial-induced fibrosis</i>
P12	Maaïke Bril, Eindhoven University of Technology <i>A photoresponsive hydrogel to subject cells on-Demand to dynamically changing topographies</i>
P13	Hannah Brouwer, Eindhoven University of Technology <i>Developing strategies to study and analyze endothelial cell response to curvature</i>
P14	Amit Chandrakar, Maastricht University <i>Auger driven system for Melt Electrowriting Technique</i>
P15	Wen Chen, Radboud University <i>Combining mechanical tuneability with function Biomimetic fibrous hydrogels with nanoparticle crosslinkers</i>
P16	Wen Chen, Radboud University <i>Functional biomimetic hydrogel composite</i>
P17	Simone de Jong, Eindhoven University of Technology <i>Towards a synthetic ECM for kidney organoids</i>
P18	Bregje de Wildt, Utrecht University <i>Towards an in vitro platform to evaluate material-driven human bone regeneration</i>
P19	Mirko D'Urso, Eindhoven University of Technology <i>Tuning fibroblast-to-myofibroblast phenotype transition through mechanosensing</i>

P20	Francisca Luisa Fernandes Gomes, University of Twente <i>Lipid nanocoating effect on the hemocompatibility of polycaprolactone microparticles</i>
P21	Sammy Florczak, Utrecht University <i>Real-time monitoring of volumetrically bioprinted constructs</i>
P22	Clara Guarch Pérez, University of Amsterdam <i>3D printed Poly-ϵ-caprolactone composites as an antimicrobial carrier for fracture fixation applications</i>
P23	Esra Güben Kaçmaz, Maastricht University <i>Geometrically defined collagen microparticles for biomaterial-driven bottom-up bone tissue Engineering</i>
P24	Melvin Gurian, University of Twente <i>A microfluidic gradient generator to investigate the effects of metabolite concentration on stem cells</i>
P25	Negar Hassani Besheli, Radboud university medical center <i>Cellular uptake of antimicrobial mesoporous bioactive glass nanoparticles for treatment of bone infection</i>
P26	Věra Hedvičáková, Institute of Experimental Medicine of the Czech Academy of Sciences <i>The effect of blood derivatives compared to commercial FBS on AT-MSCs seeded on PCL scaffolds</i>
P27	Lei He, Maastricht University <i>Establishment of Selenium-incorporated Mesoporous Silica Nanoparticles (MSNs) for Osteosarcoma Therapy</i>
P28	Veronika Hefka Blahnová, Institute of Experimental Medicine of the Czech Academy of Sciences <i>In Vitro Intestine Model for Testing Cytotoxicity of Ag, Ti and Zn Nanoparticles</i>
P29	Carolin Hermanns, Maastricht University <i>Bioprinting a functional beta cell replacement device</i>
P30	Johanna Husch, Radboud university medical center <i>Adipose tissue-derived stromal vascular fraction shows superior osteogenic differentiation compared to donor-matched mesenchymal stromal cells</i>
P31	Dina Ibrahim, Eindhoven University of Technology <i>VEGF immobilization on supramolecular surfaces for enhanced endothelialization of implanted cardiovascular devices</i>
P32	Minye Jin, University of Twente <i>Luciferin-Bioinspired Hydrogel Scaffolds with Tunable Properties for 3D Cell Encapsulation</i>
P33	Castro Johnbosco, University of Twente <i>Mechanical confinement of single cells regulates the phenotype of stem cells</i>
P34	Klaudia Jurczak, University Medical Center Groningen <i>High-throughput screening to mimic tunica media smooth muscle cells alignment in porous blood vessel scaffold</i>
P35	Tom Kamperman, University of Twente <i>Tethering cells via oxidative crosslinking enables mechanotransduction in non-cell-adhesive materials</i>
P36	Zeynep Karagöz, Maastricht University <i>Win, lose or tie: a computational model of competition at the Cell-ECM interface</i>

P37	Paree Khokhani, University Medical Center Utrecht <i>Mimicking S. aureus response with combinational synthetic TLR-agonists for MSC osteogenesis in vitro</i>
P38	Mohammad Khoonkari & Marta Oggioni, University Medical Center Groningen /University of Groningen, <i>Complex coacervates as next generation bioinks</i>
P39	Lei Li, University of Groningen/ University Medical Center Groningen <i>Mg-Al layered double hydroxides nanoparticles coating with PEG prevents particles aggregation and degradation</i>
P40	Marieke Meteling, University of Twente <i>Extracellular protein identification cytometry (EPIC) single cell analysis</i>
P41	Rob Meuwese, Radboud university medical center <i>An expandable medical device to close surgically induced fetal membrane defects</i>
P42	Ahmed Mostafa, University of Twente <i>Engineered peptide-functionalized polymeric nanocarrier system to target pancreatic tumor Stroma</i>
P43	Dylan Mostert, Eindhoven University of Technology <i>3D Mechanical Constraint Model to Understand Remodeling in Beating Cardiac Microtissues</i>
P44	Roberto Narcisi, Erasmus University Medical Center <i>Cellular senescence impairs chondrogenic differentiation of MSCs</i>
P45	Nazia Noor, University of Twente <i>Mixed matrix membrane for urea removal in a wearable artificial kidney</i>
P46	Nada Rahmani, University Medical Center Utrecht <i>Application of microbe-derived agents for osteogenesis in a ceramics-based bone graft</i>
P47	Deeksha Rajkumar, University of Amsterdam <i>DARTBAC, preventing antibiotic resistance through novel medical device technology</i>
P48	Rajiv S. Raktue, Association of Dutch Burn Centres <i>Burn wound healing using full skin equivalents</i>
P49	Deepti Rana, University of Twente <i>Dynamically controlled VEGF presentation within biomaterial guides vascular network formation</i>
P50	Maritza Rovers, Eindhoven University of Technology <i>Biomedical engineered materials towards plant protoplast regeneration</i>
P51	Judith Schaart, Radboud university medical center <i>Developing a bone-on-a-chip to study bone formation pathways</i>
P52	Maik Schot, University of Twente <i>Bottom-up engineering of modular tissues with inherent capillary networks</i>
P53	Rienk Schuiringa, Eindhoven University of Technology <i>Construct of hyaluronic acid and chondroitin sulfate (meth)acrylate hydrogel and polyamide 6 spacer fabric mimics native cartilage mechanical properties</i>
P54	Eva Šebová, Institute of Experimental Medicine of the Czech Academy of Sciences <i>The effect of a Cathepsin K inhibitor on a bone model in vitro</i>
P55	Viktorie. Sedláčková, Institute of Experimental Medicine of the Czech Academy of Sciences <i>Co-culture as a model of intestinal tissue in vitro for early toxicological screening</i>
P56	Adrián Seijas-Gamardo, Maastricht University <i>A cell-adherent polymer template to create multiscale channel structures and cell patterns with a 3D hydrogel</i>

P57	Clio Siebenmorgen, University of Groningen/ University Medical Center Groningen <i>Dynamic covalent crosslinked hydrogel matrix using Pickering emulsion</i>
P58	Janne Spierings, Eindhoven University of Technology <i>A novel concept in ACL reconstruction surgery: an off-the-shelf decellularized and sterilized bone-ACL-bone allograft</i>
P59	Sangita Swapnasrita, Maastricht University <i>Sex-specific differences in kidney function of (non-)diabetic patients</i>
P60	Filipa Teixeira, Maastricht University <i>Biofabrication of pre-vascularised microtissues for bone tissue engineering</i>
P61	Vasileios Trikalitis, University of Twente <i>3D printed Tissue Self Assembly via Embedded Printing of Newtonian Fluid Suspension Bioinks</i>
P62	Marta Valverde, Utrecht University <i>Co-axial bioprinting of a convoluted proximal tubule for kidney disease modeling</i>
P63	Melissa van Velthoven, Radboud University <i>bFGF-Functionalized Polyisocyanopeptide Hydrogel for Tissue Regeneration of the Pelvic Floor</i>
P64	Arianne van Velthoven, Maastricht University <i>Labelling limbal stem cells with custom nanoparticles to track corneal regeneration</i>
P65	Cas van der Putten, Eindhoven University of Technology <i>Alignment of keratocytes and deposited matrices in concave micropatterned environments</i>
P66	Marloes van Mourik, Eindhoven University of Technology <i>Cell population characterization of enzymatically isolated articular chondrocytes and chondrons</i>
P67	Nikitha Vavilthota, University of Amsterdam <i>Efficacy of diagnostic and antimicrobial capacity of smart triggered release systems for medical devices in-vivo</i>
P68	Kest Verstappen, Radboud university medical center <i>Manipulation of astrocyte behavior on graphene-based biomaterials</i>
P69	Gerli Viilup, Maastricht University <i>Nanoparticle-based tracking and quantification of Col I and II in microtissues</i>
P70	Martina Viola, Utrecht University <i>Silk-based inks: from molecules to well-organized fibrous scaffolds</i>
P71	Annika Vrehan, Eindhoven University of Technology <i>Design of a 3D corneal stromal construct using supramolecular hydrogels functionalized with bioactive additives for encapsulation and recruitment of corneal keratocytes</i>
P72	Alexis Wolfel, University of Twente <i>A bioinspired strategy for controlled bio-functionalization of polyacrylamide hydrogels with bioligands</i>
P73	Xingzhen Zhang, Maastricht University <i>DNA modified MSN films as versatile biointerfaces to study stem cell adhesion processes</i>

Tubulointerstitium kidney model for future disease screening

G. Addario^{a,1}, S. Djudjaj^{b,1}, S. Fare^c, P. Boor^{b,d,e}, L. Moroni^a, C. Mota^a

^a Maastricht University, MERLN Institute for Technology-Inspired Regenerative Medicine, Complex Tissue Regeneration Department, 6229 ER, Maastricht, the Netherlands

^b Institute of Pathology, RWTH University of Aachen, Aachen, Germany

^c Dipartimento di Chimica, Materiali e Ingegneria Chimica, Politecnico di Milano, Milano, Italy

^d Division of Nephrology, RWTH University of Aachen, Aachen, Germany

^e Electron Microscopy Facility, RWTH University of Aachen, Aachen, Germany

E-mail addresses: g.addario@maastrichtuniversity.nl (G. Addario), sdjudjaj@ukaachen.de (S. Djudjaj), silvia.fare@polimi.it (S. Fare'), pboor@ukaachen.de (P. Boor), l.moroni@maastrichtuniversity.nl (L. Moroni), c.mota@maastrichtuniversity.nl (C. Mota).

Introduction: More than 10% of the worldwide population suffers from chronic kidney disease (CKD) with a rising tendency. [1] Patients with CKD have limited treatment options, with fibrosis being the pathological endpoint of CKD, where a remodeling of the ECM takes place. [2, 3] Therefore, novel therapies that could halt or even reverse the progression of CKD are urgently needed. [1] Bioprinting is considered one of the most promising approaches to generate novel 3D *in vitro* models and organ-like constructs [4], which can offer viable alternatives to investigate underlying pathomechanisms and progression of kidney diseases. [5, 6, 7] In this work, we aim to establish a robust protocol for the isolation of primary kidney cells from a transgenic reporter mouse, showing keratin 8 conjugated with a yellow fluorescent protein (K8-YFP), and to test their suitability for bioprinting.

Materials and Methods: Primary murine tubular epithelial cells (pmTECs), endothelial, fibroblast (pmFibroblasts) and primary endothelial cells were isolated. These cells were used in a new bioprinting platform laying the foundation for the development of a 3D renal tubulointerstitium model for *in vitro* studies. Polysaccharide biomaterial inks were characterized in terms of viscosity and printability. Endothelial cell line (HUVECs) and pmTECs were combined with polysaccharide biomaterial ink (alginate and pectin) and processed with a microfluidic 3D bioprinter. Cell viability and metabolic activity were evaluated for co-culture conditions. The production of core-shell bioprinted constructs was investigated by including HUVECs in the shell and pmTECs in a sacrificial core, producing a hollow tube.

Results and discussion: As tubular epithelial cells are the major cell type in the kidney, we primarily isolated these cells. The established method allowed a successful isolation of pmTECs, fibroblast and endothelial cells, but further culturing was only successful for pmTECs and pmFibroblasts. pmTECs and pmFibroblasts were positive for cell-specific markers, although their co-culture needs to be optimized. Immunohistochemistry of keratin expression showed increased expression in fibrotic tissue, as well as a different cell morphology in diseased tissue. The processing parameters to bioprint polysaccharide based biomaterial inks were optimized. We tested bioinks containing pmTECs and HUVECs, investigating cell survival and metabolic activity of the bioprinted constructs, leading to cell viability above 90%

after one week in culture. Finally, bioinks were processed in a core-shell arrangement to mimic the tubulointerstitium, where the peritubular capillaries wrap the renal tubule, showing high accuracy in cell deposition, dimension of the bioprinted constructs and capability to produce hollow filaments.

Conclusion: Microfluidic bioprinting strategy was used to build a novel 3D kidney *in vitro* model presenting primary murine tubular epithelial cells bioprinted for the first time. This model will facilitate the investigation of the interstitial fibrosis, whose underlying mechanisms are currently not completely understood. [8] This study lays the basis for an alternative 3D *in vitro* model for the investigation of mechanisms, potential therapies and the development of renal fibrosis.

References:

- [1] K. Jansen et al. *Current Pharmaceutical Design* 2017, 23.
- [2] E.M. Buhl et al. *EMBO Mol. Med.* 12 (3) (2020), e11021.
- [3] J. Majo et al. *Curr. Opin. Pharmacol.* 49 (2019) 82–89.
- [4] C. Mota et al. *Chemical Reviews* 2020.
- [5] T. M. Desrochers et al. *Adv Drug Deliv Rev* 2014, 69-70, 67.
- [6] N. Y. C. Lin et al. *Proc Natl Acad Sci U S A* 2019, 116, 5399.
- [7] M.J.F et al. *Essays in Biochemistry* (2021) EBC20200158.
- [8] S. Djudjaj, P. Boor, *Mol Aspects Med* 2019, 65, 16.

Covalent protein immobilization on 3D-printed microfiber scaffolds for guided cartilage regeneration

M.J. Ainsworth¹, O. Lotz^{2,4}, A. Gilmour^{2,4,5}, A. Zhang², D.R. McKenzie⁴, M.M.M. Bilek^{2,6}, J. Malda^{1,7}, B. Akhavan^{2,4,6}, M. Castillo^{1,8}

¹ Department of Orthopedics, University Medical Center Utrecht, Utrecht, the Netherlands

² School of Biomedical Engineering, University of Sydney, NSW, Australia

³ School of Aerospace, Mechanical & Mechatronic Engineering, The University of Sydney, NSW, Australia.

⁴ School of Physics, University of Sydney, NSW, Australia

⁵ Charles Perkins Centre, University of Sydney, NSW, Australia

⁶ Sydney Nano Institute, University of Sydney, NSW, Australia

⁷ Department of Clinical Sciences, Faculty of Veterinary Medicine, Utrecht University, Utrecht, the Netherlands

⁸ Department of Biomedical Engineering, Technical University of Eindhoven, Eindhoven, the Netherlands

Introduction: Current treatment strategies for articular cartilage defects have failed to produce mechanically competent, biologically functional treatment for the end-stage cartilage degeneration they cause. In this study, we hypothesize that the fabrication of well-organized microfiber reinforcing scaffolds [1] with covalently immobilized growth factors could support and guide the formation of new cartilaginous tissue. The presence of biomolecular cues, particularly transforming growth factor beta 1 (TGF β 1), is an important stimulus of the differentiation and maintenance of cartilage tissue [2]. We hypothesize that the presence of TGF β 1 can drive cartilage tissue formation in TE constructs and that this effect can be enhanced when TGF β 1 is immobilized. To achieve this, melt electrowriting (MEW) and atmospheric-pressure plasma jet (APPJ) treatment were integrated to produce well-organized microfiber scaffolds with covalently-immobilized TGF β 1.

Methods: Poly- ϵ -caprolactone melt electrowritten scaffolds were fabricated using a 3D-Discovery printer (regenHU), then functionalized using a computer-controlled APPJ device (4.5 kV discharge voltage, 1.9 L/min feed gas flow, 60 mm/s, 5 mm spaced-parallel line trajectory) [3], generating a controlled functionalization pattern (Figure 1i). TGF β 1 was then immobilized onto the MEW scaffolds using submersion in solution (1 μ g/mL TGF β 1 in PBS, 24 hrs, 4°C). Detergent (Tween20/sodium dodecyl sulfate (SDS)) washing steps were undertaken to remove non-covalently bound protein molecules. Characterization of protein immobilization was performed using enzyme-linked immunosorbent assay (ELISA) and immunofluorescence detection. *In vitro* experiments were performed by seeding equine mesenchymal stromal cells (MSCs) (~16x10⁶ cells/mL) into the MEW scaffolds and were cultured for 28 days (Figure 1i). The culture groups consisted of (i) plasma-treated-scaffolds w/ immobilized TGF β 1, (ii) plasma-treated-scaffolds w/o TGF β 1, (iii) untreated-scaffolds w/ TGF β 1 in the culture medium, and (iv) untreated-scaffolds in basal medium. Neo-cartilage formation was quantified with dimethyl methylene blue/picogreen assays for glycosaminoglycan (GAG) production and confirmed with histological analysis.

Results: Covalent immobilization of TGF β 1 was achieved using the APPJ-functionalization approach [3]. ELISA results following intensive 5% SDS washing confirmed TGF β 1 immobilization and immunofluorescently-labelled TGF β 1 was detected in microfiber scaffolds (following 0.1% Tween20 washing). The APPJ treatment also resulted in increased hydrophilicity of the MEW scaffolds, causing more

efficient cellular infiltration. *In vitro* analysis demonstrated that GAG production (DNA-normalized) was significantly enhanced in both the immobilized TGF β 1 (i) and TGF β 1 in medium groups (iii), compared to the control groups (ii & iv). This finding was further validated by the increased production of GAGs and collagen type II, observed in histological sections (Figure 1ii).

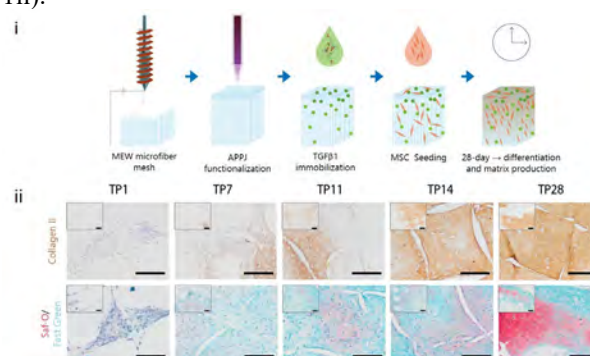


Figure 1: i) Schematic of methodology. The microfiber mesh is first produced using MEW and then functionalized using APPJ. TGF β 1 is then immobilized and MSCs are seeded and cultured for 28 days. ii) Immunohistochemistry collagen type II and safranin-O stained paraffin sections from time points (TP) 1, 7, 11, 14 and 28. Scale bars = 200 μ m.

Conclusions: We have demonstrated that APPJ-facilitated covalent immobilization of TGF β 1 retains the growth factor's bioactivity and stimulates the differentiation of MSCs into the chondrogenic lineage. Our results also demonstrate that the new constructs with immobilized TGF β 1 support *in vitro* neo-cartilage formation. Furthermore, integrating MEW and APPJ surface activation within a single printing platform will allow for biofunctionalization during the MEW of microfiber scaffolds for gradient and patterned protein guidance for neo-cartilage formation.

Acknowledgements: This research was funded by the Netherlands Organization for Scientific Research (024.003.013), the EU's H2020 Marie Skłodowska-Curie RESCUE co-fund (#801540), and an Office of Global Engagement Partnership Collaboration Award between the University of Sydney, Utrecht University, and the Australian Research Council.

References:

- [1] Castillo et al. 2019. Acta Biomaterialia.
- [2] Wang et al. 2014. Birth Defects Res C Embryo Today.
- [3] Alavi et al. 2020. ACS Applied Materials & Interfaces.

A hyaluronic acid based bioink for spheroid-based osteochondral tissue engineering

A. Albillos Sanchez¹, I. Beren¹, M. Baker¹, L. Moroni¹, C. Mota¹

¹Maastricht University, MERLN Institute for Technology-Inspired Regenerative Medicine, Complex Tissue Regeneration Department, 6229 ER, Maastricht, The Netherlands.

Introduction: Osteoarthritis (OA) is a degenerative joint disease that affects 1 in 3 people over 65 years old (1). The prevalence of OA is growing due to the increase of OA risk factors, such as obesity, sedentarism and joint injury. OA established treatments include microfracture, autologous chondrocyte implantation, and total joint arthroplasty in end-stage cases. These treatments often lead to complications and fail to deliver long-lasting satisfactory results. Therefore, tissue-engineering approaches aim to obtain *de novo* tissues to aid in the treatment of this disease (2). 3D bioprinting holds great promise in the generation of osteochondral constructs because it allows to deposit living cells combined with biomaterials in a layer-by-layer fashion (3). When combined with spheroids in a bottom-up approach, this technology has the potential to produce joint implants with the inbuilt biological information to produce osteochondral tissue in a process that mimics the endochondral ossification route. In our work, we investigated hyaluronic acid as a biomaterial ink to form a spheroid-based bioink for bioprinting of osteochondral constructs.

Materials and Methods: Hyaluronic acid was methacrylated (HAMA) and combined with Lithium phenyl-2,4,6-trimethyl-benzoylphosphinate (LAP) as a biomaterial ink. Hydrogels and bioprinted scaffolds were photocrosslinked with UV. Human mesenchymal stromal cell (hMSC) spheroids were encapsulated and bioprinted in the synthesized biomaterial ink. Cell viability and distribution were assessed after one and seven days in culture. hMSC spheroids were differentiated towards bone and encapsulated in the biomaterial ink at different stages of differentiation. Microtissue-to-microtissue fusion capacity within the biomaterial was accessed.

Results and Discussion: Cell viability and distribution were assessed after one and seven days in culture, showing good cell viability and spheroid-to-spheroid fusion capacity within the biomaterial. Biomaterial inks were used to produce bioprinted scaffolds, and processing parameters were optimized to achieve a high microtissue density. hMSC spheroid differentiation was addressed with specific stainings and gene expression analysis via quantitative polymerase chain reaction (qPCR).

Conclusions/Summary: HAMA is a suitable biomaterial to form a spheroid-based bioink that allows microtissue migration. Ongoing and future experiments include osteochondrogenic differentiation analysis of encapsulated and bioprinted constructs. Furthermore, the optimization of the bioink formulation will take into

account bioprintability, spheroid fusion and degradation behavior.

Acknowledgements: This research was funded by the European Union's Horizon 2020 framework program, call SC1-BHC-07-2019 - Regenerative medicine: from new insights to new applications, JointPromise - Precision manufacturing of microengineered complex joint implants, under grant agreement 874837. Project website: <http://www.jointpromise.eu/>.

References:

1. Hawker GA. Osteoarthritis is a serious disease. *Clin Exp Rheumatol.* 2019;37(S3-S6).
2. Daly AC, Freeman FE, Gonzalez-Fernandez T, Critchley SE, Nulty J, Kelly DJ. 3D Bioprinting for Cartilage and Osteochondral Tissue Engineering. *Adv Healthc Mater.* 2017;6(22).
3. Mota C, Camarero-Espinosa S, Baker MB, Wieringa P, Moroni L. Bioprinting: From Tissue and Organ Development to in Vitro Models. *Chem Rev.* 2020;120(19):10547-607.

Covering Blind Spots in Implant Safety: an *In Vitro* Testing Strategy for Medical Implant Safety Assessment

E.C. Alsema^{1,2}, H.M. Braakhuis¹, J. de Boer^{2,3}, N.R.M. Beijer¹

¹Centre for Health Protection, National Institute for Public Health and the Environment (RIVM), Bilthoven, The Netherlands.

²Department of Biomedical Engineering, Eindhoven University of Technology, Eindhoven, The Netherlands.

³Institute for Complex Molecular Systems, Eindhoven University of Technology, Eindhoven, The Netherlands.

Introduction

A large variety of medical implants are currently available on the market and used in patients around the world, such as vascular stents, hip replacements or surgical meshes. Although the vast majority of patients benefit from these implants, some can develop health complaints in response to the implanted material. The immune response to the material can play a major role in this, leading to complications such as excessive fibrosis and pain. Prior to market allowance, medical devices are assessed for adverse effects through a range of preclinical *in vivo* and *in vitro* toxicity tests, such as those described in the ISO-10993 series. However, these tests mostly evaluate the effect of chemicals leaching out of the material. We identify two aspects as blind spots in the safety assessment of implants: a lack of focus on the effect of physical stimuli, as well as on the immunogenicity of materials.

Aim and Approach

In this study we are developing a human-relevant, *in vitro* testing strategy to improve the assessment of the immune response to implant materials. To inform the design of the testing strategy we are adopting an approach from the field of toxicology, constructing what is known as an Adverse Outcome Pathway or AOP. AOPs serve as a framework to describe a series of causally-linked key events that lead to the development of an adverse effect (Fig. 1). By combining insights obtained from implants that have been surgically removed from patients with current knowledge from the literature, we are building an AOP for surgical mesh implants.

This AOP can then be used as a guide to design mechanistic assays to measure the key events *in vitro*. Our *in vitro* model is based on direct interaction of cells with implant materials in their final form, thus exposing them to both chemical and physical stimuli. As a case study, we are using a commercially available monofilament polypropylene (PP) surgical mesh, coated with fibronectin to improve cell attachment. L929 fibroblasts or THP-1-derived macrophages are seeded on top of the coated mesh (Fig. 2). At 24 and 48h cytokine production, cell morphology and cytotoxicity will be assessed.

Results

Cell attachment of both L929 fibroblasts and THP-1-derived macrophages to PP mesh was improved upon coating with fibronectin, compared to uncoated mesh. Preliminary results also showed that IL-8 and TNF- α production was increased in THP-1-derived macrophages cultured on PP mesh compared to tissue culture-treated polystyrene.

Outlook

Future experiments will focus on the comparison of our *in vitro* model to the *in vitro* methods currently described in the ISO-10993 standards. Based on the findings from the AOP, we will also expand our analysis to measure the defined key events in our *in vitro* model. In this way, we aim to develop a more comprehensive testing strategy and improve the safety of medical implants.

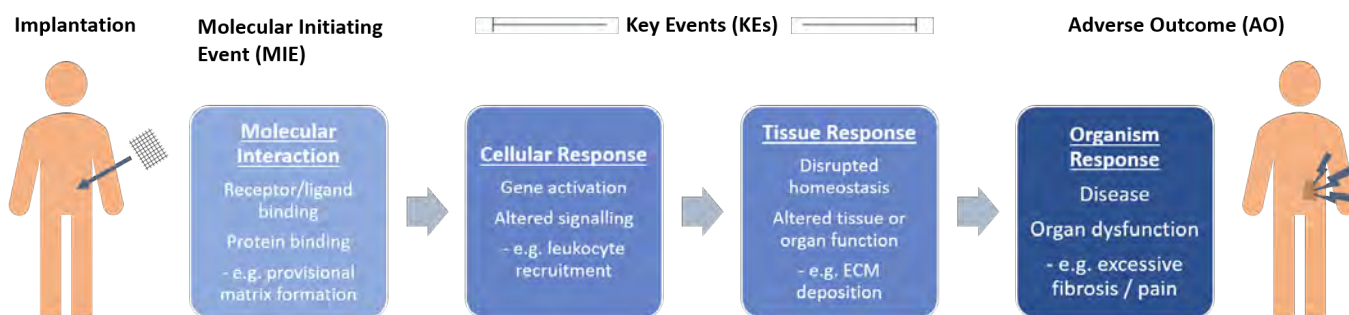


Figure 1: the Adverse Outcome Pathway framework, used to organise information on the pathways leading to an adverse outcome into a series of key events.

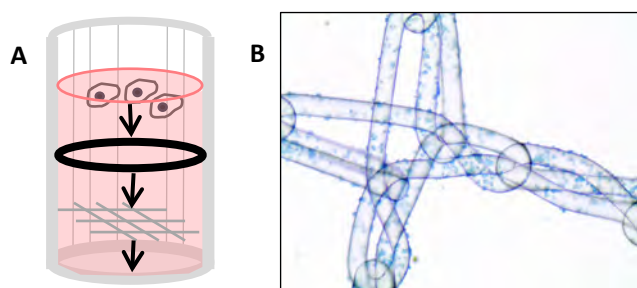


Figure 2: (A) *in vitro* exposure method, cells are seeded on top of a fibronectin-coated polypropylene mesh anchored to the bottom of a 48-well plate with a rubber O-ring, (B) methylene blue staining of THP-1-derived macrophages on a fibronectin-coated mesh.

Development of a serum substitute medium for 3D *in vitro* bone models

Sana Ansari, Keita Ito, Sandra Hofmann

Orthopaedic Biomechanics, Department of Biomedical Engineering and Institute for Complex Molecular Systems, Eindhoven University of Technology, P.O. Box 513, 5600 MB Eindhoven, the Netherlands; s.ansari@tue.nl

Introduction

Fetal bovine serum (FBS) is a widely used supplement in cell culture media which provides cells with vital factors including growth factors, hormones and vitamins essential for cell survival, growth and division [1]. However, the use of FBS in *in vitro* cell culture is controversial. FBS is a variable and undefined medium supplement with unknown and complex composition. It may contain unpredictable factors that have an influence on cell responses which can even change results between batches. FBS-containing medium should be avoided wherever possible. Lately, the use of human *in vitro* bone models using bone tissue engineering techniques with the potential to be used as an alternative to *in vivo* models has increased [2]. To create such models, the influence of unknown and complex composition of FBS should be avoided by formulating a defined and more controlled medium supplement. The aim of this project was to develop a 3D human *in vitro* bone model in a defined serum substitute medium. Such medium formulation should not only diminish the influence of unknown factors of FBS but should also enable the investigation on the effect of different soluble factors on cell behaviour and *in vitro* bone tissue formation.

Materials and Methods

A defined serum substitute medium was prepared by adding essential components for cell survival, growth and differentiation to Dulbecco's Modified Eagle Medium (DMEM) as basal medium. 1×10^6 human bone marrow-derived MSCs (hBMSC, passage 4) were seeded on silk fibroin scaffolds and differentiated towards the osteogenic lineage in either serum substitute medium (SSM) (Table 1) or FBS-containing medium (FBS) for three weeks. Osteogenic differentiation was induced by adding dexamethasone (100 nM), ascorbic acid (50 μ g/ml) and β -glycerophosphate (10 mM) to the media. The cells grown in the two medium compositions were compared in the following parameters: cell viability, cell adhesion to scaffold, osteoblast differentiation, collagen production and mineral deposition.

Table 1 serum substitute medium components

Component
Bovine serum albumin
Gluta max
Antibiotic Antimycotic
Insulin-Transferrin-selenium
Basic fibroblast growth factor
Chemical defined lipid concentrate
Gluta thione

Results and Discussion

We have shown before that the formation of functional 3D self-organizing co-culture of osteoblasts and osteocytes is possible in our system [3]. However, to

omit the unpredicted influences of FBS, a specialized serum substitute medium to create 3D human *in vitro* bone models needs to be formulated. In the serum substitute medium, cells were able to survive (Figure A and B), attach to silk fibroin scaffolds (Figure C), differentiate towards the osteogenic lineage (Figure D, E and F), and secreted collagen (Figure G and H) and deposited minerals (Figure I, J and K) over 3 weeks of culture.

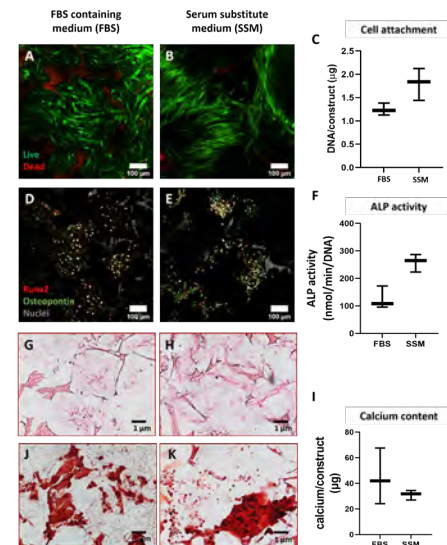


Figure 1 cellular behavior under serum substitute medium. The cellular viability (A, B), the DNA content of scaffolds (C), differentiation of hBMSCs towards osteoblasts (D, E, F), collagen production (G, H) and mineral deposition (J, K, I).

Summary

Considering the disadvantages of using FBS in culture medium, developing a medium with a serum substitute for cell culture with known and defined components is highly recommended. In this project, a specified serum substitute medium was formulated to develop 3D *in vitro* bone models. This medium will provide an opportunity to do basic research on the physiology of the cells and investigate the cellular behaviour by varying concentrations of single soluble parameters.

Acknowledgement

We gratefully acknowledge the financial support by the Dutch Ministry of Education, Culture and Science (Gra vitation Program 024.003.013).

Reference

- [1] J. van der Valk *et al.*, "Optimization of chemically defined cell culture media - Replacing fetal bovine serum in mammalian *in vitro* methods," *Toxicol. Vitr.*, 2010, 24, 1053–1063.
- [2] B. de Wildt *et al.*, "From bone regeneration to three-dimensional *in vitro* models: tissue engineering of organized bone extracellular matrix", *Current Opinion in Biomedical Engineering*, 2019, 10, 107-115
- [3] A. Akiva *et al.*, "An organoid for woven bone", *Advanced Functional Materials*, 2021, 17, 2101524

Enzymatically crosslinked Polyethylene Glycol microgels for immunoprotection of non-autologous β -cell spheroids

N. Araújo-Gomes^{1*}, B.M. Liszka-Zoetebier^{1*}, S.R. van Loo¹, S. Nijhuis¹, T. Kamperman¹, P. de Vos², A.M. Smink², B. de Haan², M. Karperien¹ and J. Leijten¹

¹Leijten Lab, Department of Developmental BioEngineering, TechMed Centre, University of Twente, The Netherlands
²Section of Immunoendocrinology, Department of Pathology and Medical Biology, University Medical Center Groningen, University of Groningen, Groningen, The Netherlands.

Introduction: Transplantation of non-autologous β -cells is currently regarded as a promising therapy for the treatment of type 1 diabetes, which is caused by massive β -cell destruction and resulting insulin shortage. To counteract host immune responses, new materials are being developed to encapsulate implanted β -cells, capable of inhibiting the diffusion of large immune molecules (i.e. IgG) whilst enabling diffusion of small molecules (i.e. Insulin and glucose), in a semi-permeable fashion¹. Clinical translation of these materials has remained elusive not only due to their immunogenic character, but also due to their low-throughput production on current microfluidic platforms. In this study, we describe high-throughput fabrication of non-immunogenic, immunoprotective, and enzymatically crosslinked polyethylene glycol-tyramine (PEG-TA) microgels to facilitate β -cell delivery.

Materials and Methods:

Enzymatically crosslinked hollow 20 kDa PEG-TA microgels were produced using a delayed outside-in crosslinking strategy² in the presence of horseradish peroxidase and non-cytotoxic concentrations of hydrogen peroxide. The polymer was prepared following a two-step synthesis protocol (ester activation and amidation). Three distinct formulations of the polymer were tested (2,5%, 5%, and 10%) and characterized in terms of permeability, size, and stiffness. Hollow microgels containing MIN6 pancreatic cells were extensively characterized *in vitro* based on variables such as cytocompatibility, cyto-immunity, permselectivity, glucose responsiveness. Finally, an *in vivo* implantation study using diabetic STZ-mice was performed to investigate immunoprotectiveness and confirm reestablishment of normoglycemia.

Results and Discussion:

Monodisperse β -cell laden microgels with $\sim 120 \mu\text{m}$ and shell thickness of $20 \mu\text{m}$ were produced in a consistent fashion. FITC-IgG ($>150 \text{ kDa}$) diffusion experiments confirmed *in vitro* the immunoprotectiveness of the microgels even after 30 days of spheroid growth within the microgels. Moreover, incubation of BSA-FITC ($>66,5 \text{ kDa}$) with hollow microgels have confirmed the diffusion of smaller molecules like BSA, ensuring transport of nutrients, hormones, waste products, and growth factors through the microcapsule's shell. When laden with MIN6, these remained glucose responsive, capable of releasing insulin without cell death or loss-of-function (Fig.1).

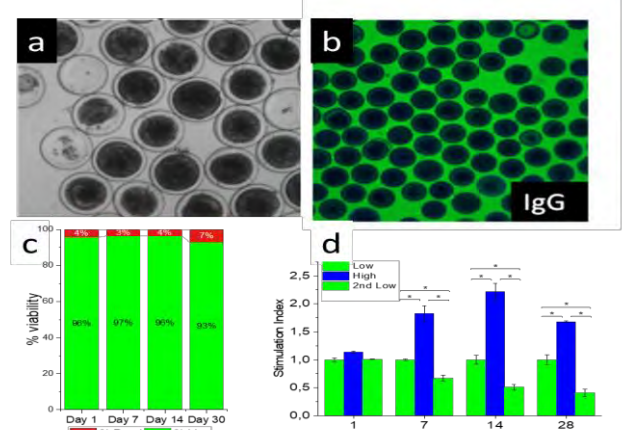


Fig.1 *In vitro* characterization of β -cell laden PEG-TA microgels

Immunological assessment of the microgels showed no macrophage activation nor surface attachment of macrophages. Additionally, multiplexed ELISA analysis on live blood immune reactivity was performed, which demonstrated an inverse polymer concentration-dependent response, which was confirmed by qPCR. Intraperitoneal implantation of β -cell laden microgels in diabetic mice showed restoration of normal glucose values and good tissue integration overall, with histology revealing alive aggregates at the time of sacrifice (14 days) (Fig.2).

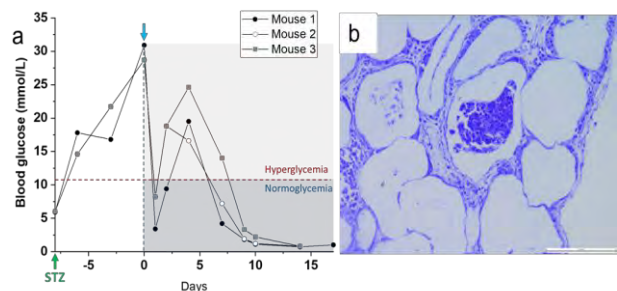


Fig.2 Reestablishment of normoglycemia in diabetic mice after implantation of β -cell laden PEG-TA microgels.

Conclusions:

Consistent high throughput microfluidic production of immunoprotective PEG-TA microgels was achieved. The produced microgels revealed good suitability for shielding and delivering non-autologous beta-cells within a living host.

Acknowledgements:

Financial support was received from the European Research Council (ERC, Starting Grant, #759425) and JDRF award 2-SRA-2018-684-S-B.

Bibliography:

- Lewińska D, Biomaterials Science, 8, 1536-1574, 2020
- van Loo SR *et al.*, Materials Today Bio, 6:100047,2020

In vitro and ex vivo evaluation of diagnostic and antimicrobial capacity of triggered release devices in STIMULUS

Gizem Babuccu¹, Nikitha Vavilthota¹, Martijn Riool¹, Sebastian A.J. Zaat^{*,1}

¹ Dept. of Medical Microbiology and Infection Prevention, Amsterdam institute for Infection and Immunity, Amsterdam UMC, University of Amsterdam, Meibergdreef 15, 1105 AZ Amsterdam, The Netherlands
g.babuccu@amsterdamumc.nl

Healthcare-associated infections (HAIs) include bloodstream infections, wound infections, urinary tract infections, and pneumonia. These infections can be acquired in any health care facility, including hospitals and surgical centers. Specifically, the wound infections may be obtained in surgery or trauma and induce systemic infection and sepsis with the contribution of planktonic and biofilm mode of growth of microorganisms. According to the World Health Organization (WHO)'s declaration, increasing morbidity, prolonged hospital stay, and increased treatment costs are the consequences of HAIs. Thus, there is a critical need for novel antimicrobial strategies and products to reduce the emerging antibiotic resistance and search for cutting-edge detection systems.

Therefore, the European Marie Skłodowska training network STIMULUS⁴ “Stimuli Responsive Materials for the Rapid Detection and Treatment of Healthcare Associated Infections” aims at 1) creating medical devices that signal when an infection is present and thereby reduces the unnecessary prescription of antibiotics and hence the spread of antibiotic resistance, and 2) releasing potent antimicrobials triggered by an external or wound-related stimulus to treat the infection.

This project aims at assessing the antimicrobial and antibiofilm efficacy of novel cationic antimicrobial peptides (CAMPs¹) and particularly a group of such CAMPs designated as Synthetic Antimicrobial and Antibiofilm Peptides (SAAPs²) against relevant bacterial species for wound infection and urinary tract infection, such as *Pseudomonas aeruginosa*, *Escherichia coli*, *Acinetobacter baumannii*, *Proteus mirabilis*, *Staphylococcus aureus*, *Staphylococcus epidermidis* and *Streptococcus pyogenes*. Moreover, this project also includes testing potential synergy of these peptides with conventional antibiotics using checkerboard analysis³ besides designing in vitro and ex vivo models to assess the microbicidal capacity of triggered release devices developed within the STIMULUS consortium against these bacterial strains.

In conclusion, we aim to create rapid screening systems for theranostic antimicrobial devices and to analyse the effectiveness of novel antimicrobial peptides that can be used in wound dressing therapies.

The STIMULUS project has received funding from the European Union's Horizon 2020 research and innovation program under the Marie Skłodowska-Curie grant agreement No. 955664.

1. Thapa, R. K., Diep, D. B., & Tønnesen, H. H. (2020). Topical antimicrobial peptide formulations for wound healing: Current developments and future prospects. *Acta Biomaterialia*, 103, 52-67.
2. de Breij, A., Riool, M., Cordfunke, R. A., Malanovic, N., de Boer, L., Koning, R. I., ... & Nibbering, P. H. (2018). The antimicrobial peptide SAAP-148 combats drug-resistant bacteria and biofilms. *Science Translational Medicine*, 10(423).
3. Koppen, B. C., Mulder, P. P., de Boer, L., Riool, M., Drijfhout, J. W., & Zaat, S. A. (2019). Synergistic microbicidal effect of cationic antimicrobial peptides and teicoplanin against planktonic and biofilm-encased *Staphylococcus aureus*. *International Journal of Antimicrobial Agents*, 53(2), 143-151
4. www.stimulus-etn.eu

The effect of electrospun fiber diameter on *Staphylococcus aureus* and immune cell infiltration

Payal P.S. Balraadjsing¹, Marieke C.F. de Graaf¹, Anna de Breij², Peter H. Nibbering², Sebastian A.J. Zaat¹

1. Department of Medical Microbiology & Infection Prevention, Amsterdam institute for Infection and Immunity, Amsterdam UMC, University of Amsterdam, Meibergdreef 9, 1105 AZ Amsterdam, The Netherlands.
2. Department of Infectious Diseases, Leiden University Medical Center, Albinusdreef 2
2333 ZA Leiden, The Netherlands

p.balraadjsing@amsterdamumc.nl

Electrospun micro- and nanofibrous matrices are promising biomaterials for *in situ* tissue engineering applications (e.g. heart valve replacement). Despite the many advantages in the use of these matrices, their properties such as fiber diameter and pore size might predispose for bacterial infection due to limited immune cell infiltration. To assess the susceptibility to infection of poly(ϵ -caprolactone) (PCL) electrospun matrices with different fiber diameters, *Staphylococcus aureus* and immune cell infiltration was studied. The infiltration depth of *S. aureus* increased with increasing fiber diameter. In the PCL matrix with small fiber diameters (<1 μm), large aggregates of *S. aureus* bacteria accumulated within the top layer, whereas within the

PCL matrices with medium (3 μm) and large (6 μm) fiber diameters small clumps and single bacterial cells were observed. Infiltration of macrophages was similarly fiber diameter dependent. The macrophages present within the different matrices all internalized *S. aureus*. The migration of primary immune cells (monocytes, granulocytes) through electrospun matrices with small fiber diameters towards the chemoattractant fMLP was significantly reduced, but not completely abolished. This suggests that these immune cells may in principle reach *Staphylococcus* bacteria even in the deeper parts of our PCL matrices with fibers of <1 μm in diameter, provided that a potent chemoattractant is present.

Mechanically tunable biomaterial for EMB3D printing of tubular structures with spatial biochemical control

M.L. Becker¹, M.R. Schot¹, J. Leijten¹

¹ Leijten Lab, Dept. of Developmental BioEngineering, TechMed Centre, University of Twente, Drienerlolaan 5, 7522 NB Enschede, The Netherlands

Introduction:

Embedded 3D (EMB3D) printing has been reported as a promising tool to engineer complex tissues^{1,2}. When used in context of FRESH (freeform reversible embedding of suspended hydrogels) 3D printing the bath acts commonly solely as a support bath and is sacrificed post printing¹. Further, the utilization of sacrificial inks in an embedding bath that is crosslinked after printing has been reported². As the bath embodies the bulk of the solidified construct, these structures often lack mechanical and chemical gradients, as well as on-demand tunability. Here, we report on a novel material that serves as an embedding bath during printing and allows for the implementation of mechanical gradients and spatially organized chemical functionalization.

Methods:

Dextran as a backbone was functionalized with tyramine and biotin moieties, resulting in a dually crosslinkable polymer named Dex-TAB³. Protein/ligand interaction between biotin and avidin resulted in a physically crosslinked bath. A sacrificial gelatin ink was extruded into the bath using an Inkredible+ 3D printer. Covalent crosslinking was achieved via two routes, namely enzymatic inside-out crosslinking and photo-induced crosslinking. Post-printing the tissue's biotin moieties allowed for on-demand local chemical functionalization.

Results and Discussion:

Rheological characterization of the physically crosslinked bath revealed shear thinning and self-healing properties (Fig 1), highly suitable for EMB3D printing.

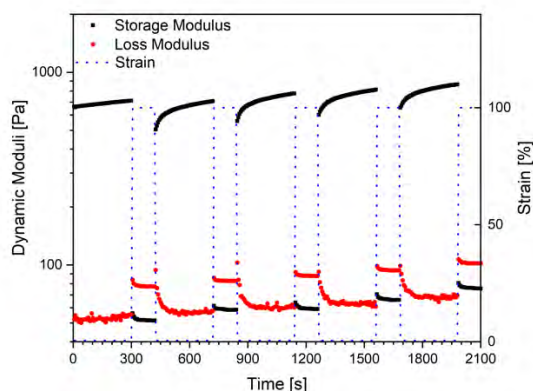


Figure 1: Dynamic moduli of physically crosslinked gels in dependence on applied strain showing self-healing behaviour.

Covalent photo crosslinking induced a 3-fold increase of the storage modulus, stabilizing embedded structures. Tubular structures could be printed and separated from the residual bath (Fig 2). Enzymatic inside-out

crosslinking enabled the formation of stable stiffness gradients within printed structures. Similarly, the channel surface could be functionalized with micrometer-thin coatings of bioinstructive moieties (Fig 2).

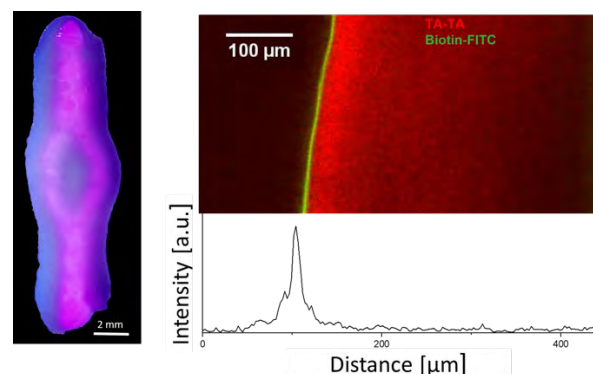


Figure 2: Left, printed bifurcating structure with fluorescent dye in channels (pink) and crosslinked Dex-TAB (blue). Right, confocal image of a channel wall with the hydrogel (red) and local surface functionalization (green) with an intensity profile over the image indicating the local presence of FITC at the channel wall.

Conclusion:

We report on a novel and dually crosslinkable hydrogel suitable for EMB3D printing in combination with an inside-out crosslinking approach resulting in tubular structures. Due to the diffusion based inside-out crosslink mechanical gradients are implemented. The presence of the biotin allows for local on-demand functionalization with bioinstructive moieties.

Acknowledgements:

Financial support was received from the European Research Council (ERC, Starting Grant, #759425) and the Dutch Research Council (NWO, Vidi Grant, #17522).

References:

1. Lee, A. *et al.* 3D bioprinting of collagen to rebuild components of the human heart. *Science* (80-.). **365**, 482–487 (2019).
2. Wu, W., Deconinck, A. & Lewis, J. A. Omnidirectional printing of 3D microvascular networks. *Adv. Mater.* (2011). doi:10.1002/adma.201004625
3. Kamperman, T. *et al.* Spatiotemporal material functionalization via competitive supramolecular complexation of avidin and biotin analogs. *Nat. Commun.* **10**, 1–11 (2019).

Contact: Malin Becker, m.l.becker@utwente.nl

Endothelium formation: Challenges and optimization

T. Bodet¹, P. Wieringa¹, C. Mota¹, L. Moroni¹

¹Maastricht University, Complex Tissue Regeneration department, MERLN Institute for Technology-Inspired Regenerative Medicine, Maastricht, the Netherlands

Introduction:

The vascular endothelium is a cellular monolayer at the interface of the bloodstream and tissues. Despite the complexity and diversity of blood vessels, an inherent characteristic of those is the presence of a single layer of endothelial cells on the luminal side. Endothelial cells provide a selectively permeable barrier and control the vessels' contraction and relaxation, but also release enzymes, which control blood clotting, immune function, and platelet adhesion. Here, we aim at developing a model that contributes to the formation of a complete and functional endothelium, including the possibility of direct imaging.

Material and Methods:

A PDMS device was fabricated casting a Petri dish perforated with a 25G (0.5.25 mm) needle and punched in the center to form a 4x9 mm empty cavity. The needle was removed and replaced by 2 individual 25G needles at each extremity of the PDMS device. An optical fiber of 325µm diameter was inserted through both needles and a human fibrin hydrogel was poured into the cavity and clotted at 37° for 25 min. Once the hydrogel was formed, the optical fiber was carefully removed to form an empty single channel of ~300µm diameter. The macro-vessel was seeded with HUVECs (PromoCell) cell suspension at 20 or 30x10⁶ cells/mL and maintained in a static condition for 2h, 3h, or 4h for cell adhesion. After sufficient anchoring, the macro-vessel was perfused, using a peristaltic pump, with endothelial growth media (EGM2, PromoCell) at 0, 10, or 100 µL/min.

The endothelium integrity was analyzed via immunofluorescence markers - Hoechst (nuclei), VE-cadherin (adherens junction), ZO-1 (tight junction), e-NOS (nitric oxide synthase) - under confocal and epifluorescent microscopes.

Results and discussion:

Multiple parameters have been evaluated in order to form a complete endothelium. Here, we considered the wall shear stress (0; 0.5; 5.03 dynes/cm², respectively adjusting the flow rate at 0; 10; 100µL/min), the cell seeding density (20; 30 x10⁶ cells/mL), and cell adhesion time (2h; 3h; 4h).

High flow rate (100µL/min) and low adhesion time (2h) led to cell detachment during active perfusion from day 1. In static condition (0 µL/min) and high cell adhesion time (4h), the cells seemed to lack nutrients and showed a limited proliferation rate with an incomplete endothelium obtained at day 14. Regarding the cell seeding density, increasing the amount of cells in the channel often led to cell cluster formation, which detached under the active flow that resulted in clogging the channel outlet from day 0 to day 1. In the case of a flow rate at 10 µL/min, a cell seeding density of 20 x 10⁶ cells/mL, and an adhesion time of 3h, a confluent endothelium can be observed after 7 days presenting tight cell-cell junctions.

We can interpret that the absence of flow rate or a long adhesion time lead to cell death due to a lack of nutrient, while a high flow rate (100 µL/min) and a short adhesion time (2h) result in an insufficient cell anchoring, so an incomplete endothelium formation. In addition, a homogeneous cell distribution in the channel seems more crucial for the endothelium formation than injecting an excess of cells. Hence, the key for a functional endothelium is the balance between flow, adhesion, and cell distribution within the channel.

Conclusion:

We developed a model that allows the formation of a complete endothelium as well as to evaluate the endothelium barrier function in vitro of a macro-vessel of ~300µm in diameter in a human fibrin hydrogel through dynamic perfusion. Our approach has the potential to create a human vascularized model that could be used for pathophysiological studies and to test new treatments for the repair or regeneration of functional tissues.

Contact:

tristan.bodet@maastrichtuniversity.nl

High-throughput Screening to Elucidate Biomaterial-induced Fibrosis

Torben (T.A.B.) van der Boon, Liangliang Yang, Lu Ge, dr. Qihui Zhou, and dr. Patrick van Rijn

W.J. Kolff Institute for Biomedical Engineering and Materials Science, University of Groningen/ University Medical Center Groningen (UMCG), Ant. Deusinglaan 1, Groningen, The Netherlands

Introduction: Nowadays, it is becoming common knowledge that the human body, its tissues and cells react to biophysical and biochemical cues located on biomaterial surfaces.^[1,2] Identifying how these parameters influence cellular behavior is of crucial importance and will aid us in the further development of medical implant technology. Unfortunately, in many studies attempting to identify these physicochemical properties' influence on cell behavior, investigation of individual properties is the conventional method, leaving out a significant number of other variables which are encountered *in vivo*, which is where cells always interact with multiple cues simultaneously.^[3,4] We have developed an orthogonal double gradient platform which allows us to investigate just such complex situations in a high-throughput screening (HTS) fashion. The platform grants us the power to screen the cell response towards thousands of these combined parameters in single cell experiments, which will result in the optimization of material properties to enhance biomaterial and implant function. Currently, we are in the final platform optimization stage, after which we will screen silicone rubber's susceptibility to fibrosis and scar tissue formation.

Method: PDMS double orthogonal gradients (DOGs) are prepared by sequential imprinting – and shielded air plasma oxidation treatments in accordance with previously published methodology.^[4–7] Primary human dermal fibroblasts will be cultured on the DOGs for 7 days and stained for early fibrosis biomarkers (Collagen-II and α -SMA).

Results and Discussion: Every imaginable position on the orthogonal double gradient surfaces has a unique combination of three surface parameters, possessing 'real', clinically relevant values. This allows us to investigate a virtually unlimited amount of different parameter combinations, within their respective ranges, on single substrates. Wavy topography gradients range from $\lambda = 1,5 \mu\text{m} - 10 \mu\text{m}$ and $A = 50\text{nm} - 1,5 \mu\text{m}$, the smallest wavelengths corresponding with the smallest amplitudes going from small to big, in a coupled fashion. Stiffness gradients range in Young's Modulus from $\sim 50 - 500 \text{MPa}$, and 'wettability' gradients from $5 - 90^\circ$ in water contact angle (WCA). As a 'proof of concept', we cultured hBM-MSCs on the platforms for 24 h, imaged the cells via automated fluorescence microscopy and identified the cell response with respect to cell density, cell spreading, and nucleus area. We have found that the synergistic effect of

abovementioned parameter combinations all influence cell behavior in a different manner with regard to these relatively 'simple' assessable characteristics. Our current work involves the translation of 'hotspots' or regions of interest (ROI) to homogeneous parameter substrates, as a last verification step in the optimization process, as well as the screening of biomaterial susceptibility to fibrosis and scar tissue formation.

Conclusion: The highly efficient cell screening tool we have created with our DOG platform allows us to screen cell response to combined physical parameter influence in a high-throughput fashion, investigating thousands of different parameter combinations in single cell experiments. It will serve its purpose to facilitate enhanced biomaterial development.

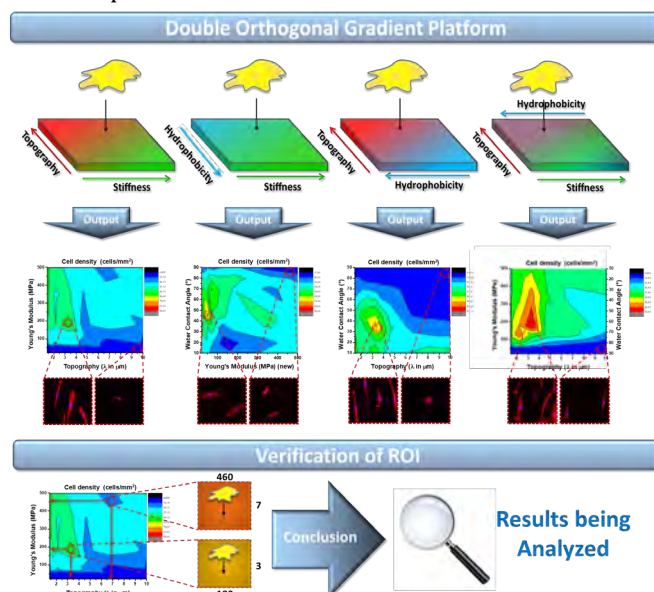


Figure 1. HTS approach. Different physicochemical biomaterial properties influence cell behavior in a complex manner. The screening platforms consists of four different parameter combinations within a gradient-like range. The influence on, in this example 'Cell density', is identified in single cell studies via fluorescence immune-staining and automated imaging and analysis. Hits, or ROI's, are translated to homogeneous substrates to verify the screening outcome.

References:

- [1] G. Huang, F. Li, X. Zhao, Y. Ma, Y. Li, M. Lin, G. Jin, T. J. Lu, G. M. Genin, F. Xu, *Chem. Rev.* **2017**, Oct 25; 117(20):12764-12850.
- [2] W. L. Murphy, T. C. McDevitt, A. J. Engler, *Nat. Mater.* **2014**, Jun; 13(6):547-57.
- [3] A. M. Schaap-Oziemlak, P. T. Kühn, T. G. van Kooten, P. van Rijn, *RSC Adv.* **2014**, 4, 53307.
- [4] P. T. Kühn, Q. Zhou, T. A. B. van Der Boon, A. M. Schaap-Oziemlak, T. G. van Kooten, P. van Rijn, *ChemNanoMat* **2016**, 2, 407 - 413
- [5] Q. Zhou, P. T. Kühn, T. Huisman, E. Nieboer, C. van Zwol, T. G. van Kooten, P. van Rijn, *Sci. Rep.* **2015**, 5, 16240.
- [6] Q. Zhou, L. Ge, C. F. Guimarães, P. T. Kühn, L. Yang, P. van Rijn, *Adv. Mater. Interfaces* **2018**, 5(18)
- [7] L. Yang, L. Ge, and P. Van Rijn, *ACS Appl. Mater. Interfaces* **2020**, 12, 25591-25603
- [8] T.A.B. van der Boon, L. Yang, L. Li, D. E. Córdova Galván, Q. Zhou, J. de Boer, P. van Rijn, *Adv. Biosyst.* **2020**, 4, 1900218.

A Photoresponsive Hydrogel to Subject Cells On-Demand to Dynamically Changing Topographies

M.J. Bril^{1,2}, A.P.H.J. Schenning^{2,3}, C.V.C. Bouten^{1,2}, N.A. Kurniawan^{1,2}

¹ Department of Biomedical Engineering, Eindhoven University of Technology, PO Box 513 5600 MB Eindhoven, The Netherlands

² Institute for Complex Molecular Systems, Eindhoven University of Technology, PO Box 513 5600 MB Eindhoven, The Netherlands

³ Department of Chemical Engineering & Chemistry, Eindhoven University of Technology, PO Box 513 5600 MB Eindhoven, The Netherlands

Introduction: *In vivo*, cells continually engage in a complex and highly dynamic interplay with their extracellular microenvironment. Both in healthy and diseased conditions, the cellular microenvironment undergoes structural changes, resulting in e.g., changes in surface topographies^{1,2}. However, to date, the majority of cell studies are performed under static conditions, i.e., a constant topographical signal is presented to the cells, which is a poor recapitulation of the native cellular microenvironment. To bridge this gap, we come up with a new approach to subject cells to on-demand dynamic changes in topographies.

Materials & Methods: A light-responsive poly(N-isopropylacrylamide) (pNIPAM) hydrogel is used that changes topography upon masked illumination with blue light³. Local illumination converts the light-responsive hydrophilic merocyanine (MCH⁺) to the hydrophobic spiropyran (Sp) moiety, which results in local hydrogel shrinking. Removal of the light returns the hydrogel towards its original flat state. Subsequently, normal human dermal fibroblasts (nhDF) are seeded on top, and nuclei and actin cytoskeleton morphology are investigated using fluorescence staining and confocal imaging.

Results: UV-vis data confirm that the hydrogel is photoresponsive under cell culture conditions after three rounds of illumination. Profilometry measurements reveal that a variety of topographies can be controllably induced in 15 min by using photomasks with different designs, and that these gels can switch topography without altering hydrogel stiffness ($E = \sim 500$ kPa).

Additionally, nhDFs can adhere to the hydrogel and survive illumination with blue light. Nuclei and actin cytoskeleton staining show that cells are able to respond to the induced topographies.

Conclusion: We developed a cell compatible, photoresponsive SBS-coated Sp-containing pNIPAM hydrogel that changes topography on-demand and in a reversible fashion. This study demonstrates that cells are able to respond to the induced topography, and future work will reveal the rate of actin cytoskeleton remodeling events by using live cell imaging.

Altogether, this approach will allow us to gain a more fundamental understanding about how cells can sense and respond to dynamic topographical changes in their microenvironment. Ultimately, this knowledge can boost the development of better tissue engineering constructs and/or steer tissue regeneration.

References:

1. Miller, C. J. & Davidson, L. A. The interplay between cell signalling and mechanics in developmental processes. *Nature Reviews Genetics* vol. 14 733–744 (2013).
2. Kim, S., Uroz, M., Bays, J. L. & Chen, C. S. Harnessing Mechanobiology for Tissue Engineering. *Developmental Cell* vol. 56 180–191 (2021).
3. Stumpel, J. E. *et al.* Photoswitchable ratchet surface topographies based on self-protonating spiropyran-NIPAAM hydrogels. *ACS Appl. Mater. Interfaces* **6**, 7268–7274 (2014).

Developing Strategies to Study and Analyze Endothelial Cell Response to Curvature

H.F.M. Brouwer^{1,2}, C. van der Putten^{1,2}, C. Tang^{1,2}, M. Dias-Castilho^{3,4}, N.A. Kurniawan^{1,2}, C.V.C. Bouten^{1,2}.

1. Soft Tissue Engineering and Mechanobiology, Department of Biomedical Engineering, Eindhoven University of Technology, PO Box 513, 5600 MB Eindhoven, The Netherlands

2. ICMS, Eindhoven University of Technology, 5600 MB Eindhoven, The Netherlands

3. Department of Orthopedics, University Medical Center Utrecht, Utrecht University, 3508 GA Utrecht, The Netherlands

4. Department of Biomedical Engineering, Eindhoven University of Technology, 5612 AZ Eindhoven, The Netherlands

Introduction: The extracellular environment presents a variety of three-dimensional (3D) structural cues that play an important role in controlling endothelial cell (EC) behavior, with curvature (e.g. of vasculature or matrix fibers) being a cue that is present *in vivo* across different length scales.¹ A better understanding of the processes involved in the interaction between ECs and curved geometries will improve the micro and macro structural design of scaffolds for (micro) vascular tissue regeneration. The actin cytoskeleton is known to play a key role in EC responses to structural cues, yet knowledge regarding EC responses to curved substrates is lacking. Therefore, the aim of this study was to develop an *in vitro* experimental setup to investigate the cell morphological response, and the corresponding actin cytoskeletal architecture, of human umbilical vein endothelial cells (HUVECs) to curved substrates.

Methods: We developed three approaches that allowed quantification of *in vitro* cell and actin organization and orientation: a homogeneously coated two-and-a-half dimensional (2.5D) cell culture chip, a protein patterned 2.5D cell culture chip, and a 3D fiber mesh approach. The 2.5D chip contained half cylindrical structures of 3 different convex curvatures: $\kappa = 1/500, 1/250, 1/125 \mu\text{m}^{-1}$, whereas the 3D scaffolds contained melt-electrowritten PCL fibers with a curvature of $\kappa = 1/5 \mu\text{m}^{-1}$. The 2.5D chip was either homogeneously coated to create a single-cue environment, or protein-patterned (20 μm wide lines and gaps, applied perpendicular to the cylinder long axes) to introduce contact guidance cues orthogonal to the cylindrical axis and thereby create a multi-cue environment. HUVECs were cultured on all three platforms for 24 to 72 hours. After fixation F-actin was stained using Phalloidin-Atto (65906, Sigma-Aldrich) and nuclei were stained using Hoechst 33342 (R37605, Invitrogen). Cells were imaged with a confocal microscope and images were analyzed using a custom-made MATLAB script. A distinction was made between apical and basal actin, and the influence of curvature on cell and nucleus morphology was analyzed.

Results and Discussion: The three different approaches were successfully developed and showed the possibility to analyze single cell morphometrics and intracellular actin stress fiber orientation in 2.5D/3D, distinguishing between basal and apical actin. The results indicate that, on the homogeneously coated curvatures, HUVECs and their stress fibers tended to align in the direction of the cylindrical long axis while nucleus area increased with increasing curvature. Interestingly, this is different from previous findings describing wrapping of HUVECs around smaller micron-scale curved geometries.^{2,3}

Additional protein-patterning did not affect cell and nucleus orientation, suggesting a dominant effect of the curvature. In a proof of principle experiment on 3D fibers, single HUVECs showed alignment along the long axis of single fibers as well.

Conclusion: 2.5D and 3D experimental set-ups and corresponding analyses were successfully developed and evaluated for HUVEC morphometric responses. These approaches create novel opportunities to investigate the interaction between cells and curved substrates *in vitro* in a highly controlled and detailed way.

[1] Assoian, R. K., Bade, N. D., Cameron, C. v. & Stebe, K. J. Cellular sensing of micron-scale curvature: a frontier in understanding the microenvironment. *Open Biology* **9**, 190155 (2019).

[2] Jones, D. *et al.* Actin grips: Circular actin-rich cytoskeletal structures that mediate the wrapping of polymeric microfibers by endothelial cells. *Biomaterials* **52**, 395–406 (2015).

[3] Fioretta, E. S., Simonet, M., Smits, A. I. P. M., Baaijens, F. P. T. & Bouten, C. V. C. Differential response of endothelial and endothelial colony forming cells on electrospun scaffolds with distinct microfiber diameters. *Biomacromolecules* **15**, 821–829 (2014).

Contact details presenting author: h.f.m.brouwer@tue.nl

Auger driven system for Melt Electrowriting Technique

A. Chandrakar, L. Moroni & P. Wieringa

Maastricht University, MERLN Institute for Technology-Inspired Regenerative Medicine, Complex Tissue Regeneration Department, Universiteitssingel 40, 6229, ER, Maastricht, the Netherlands

MEW is a manufacturing technique of producing ultra-fine fibre using electrical instabilities from polymer melts contrary to electrospinning (ESP) process that uses polymer solution. In MEW, the polymer melt delivery to the nozzle outlet is typically provided by a pressure-driven system; this gives the system good control over the flow rate of the polymer melt through a nozzle and improved startup time, compared to a piston-driven piston. However, with trying to process high molecular weight polymers, the resulting increase in polymer melt viscosity requires unachievable extrusion pressure on the order of MPa. It is also challenging to extrude polymer melts through a small nozzle and maintain a consistent small flow rate. To ensure a consistent polymer flow raw material is typically preheated overnight to ensure polymer melt homogeneity and to remove any pockets of air, thus ensuring an uninterrupted supply of polymer can be maintained. However, for a thermally sensitive polymer, preheating for a prolonged time can degrade the polymer and drastically change its viscoelastic properties and the mechanical and molecular properties of the resulting polymer scaffold. Due to the above drawbacks of the current pressure-driven system, we designed a new auger-driven system for MEW.

Auger is designed to achieve a minimum and consistent flow rate. Auger modelling and simulation is performed with the help of COMSOL. Here, the manufacturing capability of the auger screw is also taken into account. Simulation results are verified by experiments for polycaprolactone of Mw: 45kDa polymer. The polymer's flow rate coming out of the nozzle at different speeds and temperatures is recorded and compared to simulation results. A good correlation between simulation and experimental results are obtained. Auger-driven MEW system is then characterized and compared with pressure-driven MEW system at different flow rates while keeping all other MEW parameters constant. We saw no significant variation on the measured fibre diameters for all flow rates between pressure and auger-driven systems and displays excellent reproducible results.

In MEW, the diameter of the fabricated scaffold depends both on flow rate and initial jet thickness. With a lower flow rate and small jet thickness, one can expect a lower filament diameter. With this new auger-driven system, we could extrude and control the molten polymer via a small nozzle, resulting in nanofiber production and making a hybrid scaffold consisting of nano and micro scaffold using a single run and single melt head for the first time. We also observed that the new system was also effective at removing air and vapour pockets within the molten polymer via compression and upward pressure due to centrifugal force during extrusion and spinning. This was noticeable for the PLLATMC polymer, which has a hydroscopic nature that leads to vapour bubbles

within the polymer melt and cannot be maintained at a high temperature without significant polymer degradation, precluding an overnight preheating step. When this polymer is extruded via the pressure-driven system, we observed a regularly interrupted jet spinning and with noticeable air pockets within fibres. In contrast, our auger-driven system generated smooth uniform fibre. This confirmed our ability to supply the MEW process with an uninterrupted polymer supply and use raw materials without preheating. Our computational modelling determined that our system was theoretically capable of generating consistent polymer melt flow rates that were invariant to melt viscosity. We were able to extrude highly viscous material of viscosity greater than 25,000 Pa.s via an auger driven system that is currently not possible with any other driven system used for MEW. However, due to the polymer's rapid solidification, the diameter obtained was much larger, i.e. in the order of 50 to 60 μm .

New designed auger driven MEW system provides several advantages compared to the pressure-driven system while maintaining the same fiber consistency as the pressure-driven system. Auger driven system can significantly increase the complexity of the scaffold fabricated by MEW. Future work will focus on tuning the auger rotation motion to the fabricated scaffold by varying fibre diameter in a single run.

Combining mechanical tuneability with function: Biomimetic fibrous hydrogels with nanoparticle crosslinkers

W. Chen, P. H. J. Kouwer

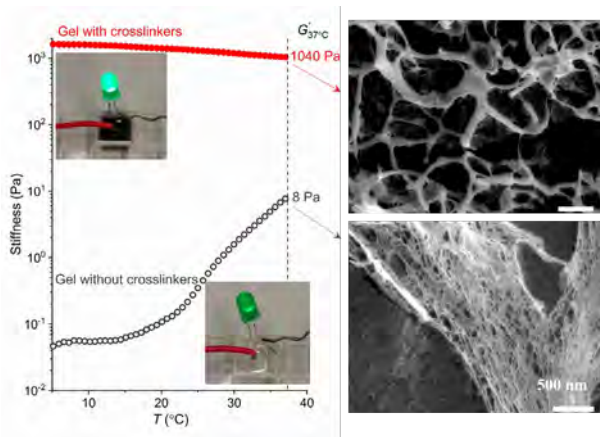
Institute for Molecules and Materials, Radboud University, Heyendaalseweg 135, 6525 AJ Nijmegen, The Netherlands

Fibrous networks of biopolymers possess unique properties: mechanical stability at low concentrations, an extremely porous architecture and strong stiffening at small deformations. An outstanding challenge is to find methods that allow us to tailor the mechanical properties of these bio networks or their synthetic equivalents without changing the polymer concentration, which simultaneously changes all other hydrogel properties. Here, we prepare networks of dilute (0.1 wt-%) fibrous hydrogels and crosslink them with functional rod-shaped nanoparticles. We observe that the crosslinking induces an architectural change that strongly affects the mechanical properties of the hydrogels with a 40-fold

increase in stiffness. The effect is strongest at the lowest polymer and particle concentrations (99.8 % water) and is tailorable through tuning the crosslink density.

Moreover, the nanoparticle components in the composite offer the opportunity to introduce an additional function; we report gels with magnetic and conductive properties.

However, through the generic crosslinking approach of a fibrous network with decorated nanoparticle crosslinkers as presented in this work, virtually any functionality may be introduced in highly responsive hydrogels, providing a guide to design next generations of multi-functional soft materials.



Functional biomimetic hydrogel composite

W. Chen, P. H. J. Kouwer

Institute for Molecules and Materials, Radboud University, Heyendaalseweg 135, 6525 AJ Nijmegen, The Netherlands

Nanocomposite hydrogels have attracted increasing interests in biological and industrial field, since nanomaterials have excellent physical, chemical, electrical, and biological characteristics. As an external magnetic field (EMF) is remotely controllable and biocompatible, we develop magnetic-responsive functionalized nanocomposite hydrogels. Firstly, we describes a novel, highly adaptive nanocomposite hydrogel composed of magnetically sensitive magnetite nanorods and a stress-responsive synthetic matrix. Nanorod rearrangement after application of (small) magnetic fields induces strain in the network, which results in a strong (over tenfold) stiffening even at minimal (2.5 wt-%) nanorod concentrations. Moreover, the stiffening mechanism yields a fast and fully reversible response. We demonstrate the value of magnetic stiffening in a 3D MCF10A epithelial cell experiment, where simply culturing on top of a permanent magnet gives rise to changes in the cell morphology. Secondly, to tailor the mechanical properties without changing the component, we prepare networks of dilute (0.1 wt-%) fibrous hydrogels and crosslink them with functional rod-shaped nanoparticles. We observe that the crosslinking induces an architectural change that strongly affects the mechanical properties of the hydrogels with a 40-fold increase in stiffness. The

effect is strongest at the lowest polymer and particle concentrations (99.8% water) and is tailorable through tuning the crosslink density. The nanoparticle components in the composite offer the opportunity to introduce additional function; we report gels with magnetic and conductive properties. Natural biomaterials exhibit anisotropic microstructures and mechanical properties simultaneously, which are still challenging to develop such anisotropic behaviors synthetically. Thirdly, a facile one-step approach for fabricating hydrogels with a hierarchically anisotropic architecture and direction-dependent mechanical properties is proposed. A fibrous hydrogels (0.1 wt%) crosslinked with magnetic functionalized-nanoparticle fillers are prepared to form a continuous polymer-particle network with improved mechanical properties. In the presence of low magnetic field (mT), the anisotropic hydrogels are readily developed with less than 0.1 wt% of shape-different nanoparticles during gelation. Moreover, the electrostatic repulsion by the negatively charged nanoparticles induces the resistance of compressive forces applied orthogonally. Such stimuli-responsive hydrogels with architectural control are providing a guide for designing new biomaterials in tissue engineering.

Towards a Synthetic ECM for Kidney Organoids: the Development of 2D and 2.5D Supramolecular Matrices for iPSC Cultures

S.M.J. de Jong, P.Y.W. Dankers^{1,2,3}

¹Institute for Complex Molecular Systems, Eindhoven University of Technology, ²Department of Biomedical Engineering, Eindhoven University of Technology, ³Laboratory for Cell and Tissue Engineering, Eindhoven University of Technology, P.O. Box 513, 5600 MB Eindhoven, The Netherlands

Introduction:

Human induced pluripotent stem cells (hiPSCs) are mostly cultured on flat, stiff, polystyrene surfaces coated with ECM proteins for the differentiation towards kidney organoids. In the natural ECM, however, stem cells experience a different environment in terms of biochemical composition and mechanical properties. It has been shown that surface stiffness influences the differentiation and eventually kidney organoid formation. Supramolecular biomaterials can be used to exactly control the bioactivity and stiffness of a material, offering an interesting platform for the culture and differentiation of iPSCs towards kidney organoids. Here we present two studies. First, the culture of iPSCs on supramolecular ureido-pyrimidinone (UPy) modified polyethylene glycol (PEG) based hydrogels was investigated. In addition, in the natural situation the cells grow in a 3D matrix, relying more on cell-cell and cell-matrix interactions. Culturing iPSCs in 3D, however, also brings a long difficulties in culture. 2.5D matrices, i.e. diluted matrices placed on top of monolayers of cells, might therefore be a solution as cells have shown to behave as if they are cultured in 3D, while simplifying culturing. Therefore, secondly, hiPSCs were cultured in 2.5D matrices and the interaction with the matrix was examined. As a first step, natural proteins were used, i.e. Matrigel and laminin, and later diluted UPy-hydrogels will be used as 2.5D matrices.

Materials and methods:

In the first project, bifunctional UPy- and monofunctional UPy-polymers were dissolved separately in PBS or under basic conditions and heated to 70°C. After cooling down the solutions were sterilized with UV, neutralized and mixed. The solutions were pipetted in a well plate and incubated at 37°C to gelate. After 1 hour hiPSCs were seeded in Essential 8 (E8) medium. The cells were followed for 3 days and medium was changed daily. In the second project hiPSCs were seeded on Matrigel-coated plates. The next day the medium was replaced with E8 medium supplemented with 240 µg/ml Matrigel or 150 µg/ml Laminin Cultrex. The next day the medium was replaced with either the same ECM-matrix supplemented medium, or the medium was changed back to E8 medium.

Results and discussion:

In the first study, hiPSCs seeded on pristine UPy-hydrogels did not survive. The addition of UPy-cRGD, however, improved the survival and adhesion. A coating of vitronectin or Matrigel on top of these gels allowed proper adhesion and proliferation of the hiPSCs. Next, a library of hydrogels varying in mechanical properties will be created and hiPSCs maintenance will be investigated, as well as their differentiation towards renal progenitor cells.

In the second study 2.5D matrices were created on top of a layer of hiPSCs (Figure 1). Diluted layers of Matrigel on top of the hiPSCs resulted in the formation of hollow spheroids, as opposed to monolayer formation in the control condition. In laminin 2.5D matrices the hiPSCs started to grow upwards and began to form spheroids, although the effect is less strong than in Matrigel 2.5D matrices. Next, synthetic 2.5D matrices will be created with UPy-based fibers, studying the interaction of hiPSCs with these matrices, as well as their differentiation towards renal progenitor cells.

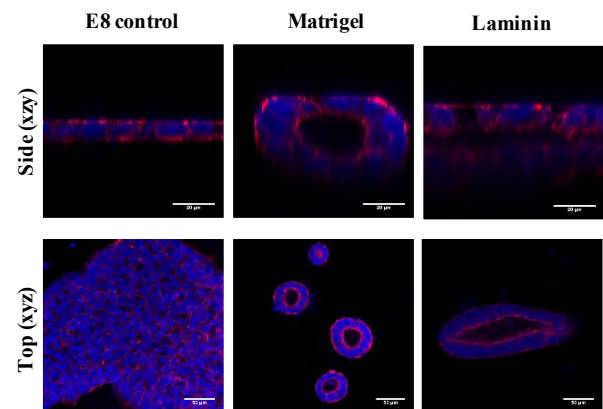


Figure 1: Immunofluorescent pictures of hiPSCs cultured in 2.5D matrices for 2 days. Pictures were taken from the top (xyz) and from the side (xzy). Blue: DAPI, red: actin.

Conclusion:

Here the use of synthetic matrices for hiPSC cultures was investigated, and the first steps were made for both 2D and 2.5D cultures. With the UPy-hydrogel a suitable material seems to have been found for hiPSC culture for further steps. In addition, it was shown that 3D hiPSC structures can be formed by diluting Matrigel and laminin in the medium, showing an interesting new approach for creating kidney organoids from hiPSCs. Next, supramolecular 2.5D matrices will be created as well.

Towards an *in vitro* platform to evaluate material-driven human bone regeneration

B.W.M de Wildt¹, E.E.A. Cramer¹, L.S. de Silva², K. Ito¹, D. Gawlitta² and S. Hofmann¹

1. Orthopedic Biomechanics, Department of Biomedical Engineering and Institute for Complex Molecular Systems (ICMS), Eindhoven University of Technology, Eindhoven, The Netherlands. 2. Department of Oral and Maxillofacial Surgery & Special Dental Care, University Medical Center Utrecht, Utrecht University, Utrecht, The Netherlands.

Introduction: Bone tissue is mostly capable of healing without any scar formation. Nevertheless, in 2 - 5% of the fractures, bone fails to bridge the defect resulting in a non-union [1,2]. *In situ* tissue engineering is a potential treatment approach, where implanted smart materials make use of the bone's innate capacity to regenerate upon implantation. After *in vitro* assessment, such materials are routinely studied in animal models. However, current models represent human physiology insufficiently which is likely one of the reasons that less than 10% of preclinically developed treatments are approved for regular clinical use [3,4]. To enable the investigation of human bone regeneration upon biomaterial implantation and address the principal of reduction, refinement and replacement of animal experiments [5], we aimed at developing a 3D *in vitro* human bone defect model using a tissue engineering approach. Such models will allow studying a material's potential to induce cell migration and vascularization, which are critical processes in the early stages of bone regeneration.

Materials and Methods: Silk fibroin scaffolds were produced with two 3 mm diameter defects per scaffold, representing the bone model. Scaffolds (N = 4) were seeded with human mesenchymal stromal cells (MSCs) and GFP transfected human umbilical vein endothelial cells (HUVECs) in a 1:1 ratio. Scaffolds were cultured for a period of 2 weeks supplemented with endothelial growth medium to support vascularization, followed by a period of 2 weeks supplemented with osteogenic medium to support osteogenesis. After 3 weeks, a fibrin clot (control), a blood clot mimic (ELAREM™ Matrix, PL Bioscience, Aachen, Germany), and a soft callus mimic (cartilages spheres) were implanted as regenerative materials, aiming at mimicking physiological bone regeneration of the scaffold defects for an additional 2 weeks. Vascularization, bone-like matrix formation in the scaffold, and regeneration were followed with weekly confocal microscopy using the GFP expressed by the HUVECs and viable dyes for the cell nucleus, collagen, and minerals.

Results: After 2 weeks, vascular-like structures were visible throughout the scaffold (Figure 1A). Vascular-like structures maintained present for 4 weeks and scaffold pores were filled with collagen and minerals indicating bone-like tissue formation (Figure 1B). Two weeks after material implantation, MSCs had migrated into the fibrin clot (Figure 1C). The blood clot mimic was found to stimulate the migration of the HUVECs into the clot (Figure 1D). The soft callus mimic induced the migration of both MSCs and HUVECs into the clot surrounding the spheres (Figure 1E). HUVECs appeared to be attached to the soft callus mimic, indicating the potential of the soft callus mimic to attract vascularization.

Discussion and Conclusion: To enable the investigation of material-driven human bone regeneration *in vitro* with the aim to reduce, refine, and replace animal experiments, we developed a 3D *in vitro* human bone defect model that allows the evaluation of a material's potential to induce cell migration and vascularization. To validate this model, physiologically relevant materials were used. Our initial results show that the soft callus mimic induced both MSC and HUVEC migration and even seemed to induce soft callus vascularization.

References:

1. Zura, R. et al. *JAMA Surg.* 2016
2. Mills, L.A. et al. *Acta Orthop.* 2017.
3. Montagutelli, X. *Futur. Sci. OA* 2015.
4. Thomas, D.W. et al. *Clinical Development Success Rates 2006-2015*; 2016.
5. Holmes, A. et al. *Regen. Med.* 2009.

Acknowledgements: This work is part of the research program TTW with project number TTW 016.Vidi.188.021, which is (partly) financed by the Netherlands Organization for Scientific Research (NWO) and has been financially supported by the Ministry of Education, Culture and Science (Gravitation Program 024.003.013) and the Marie Skłodowska-Curie Actions (Grant agreement RESCUE #801540).

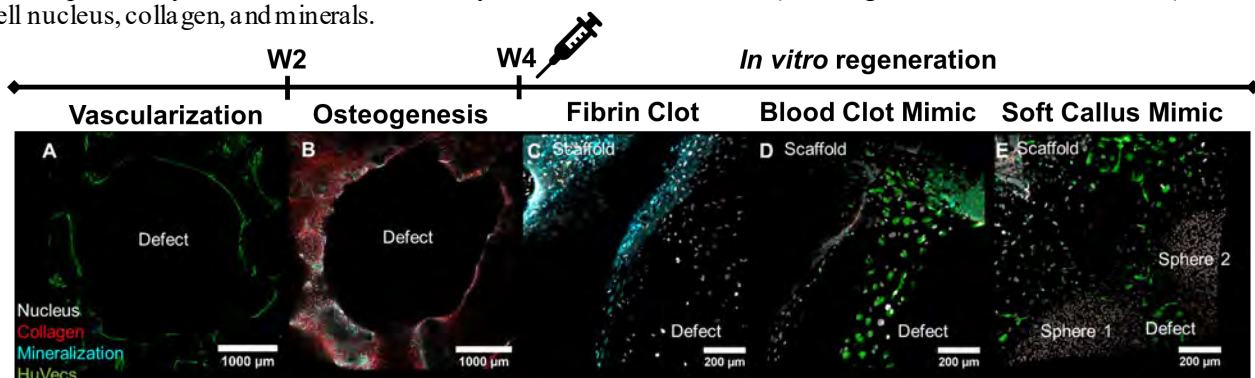


Figure 1. Confocal microscopy results indicating vascular-like structures at week 2 (A), bone-like tissue formation at week 4 (B), and migration of HUVECs (green) and MSCs (white) 2 weeks after implantation of the materials (C-E).

Tuning fibroblast-to-myofibroblast phenotype transition through mechanosensing

M. D'Urso^{1,2} and N. A. Kurniawan^{1,2}

¹ Department of Biomedical Engineering, Eindhoven University of Technology, Eindhoven, The Netherlands

² Institute for Complex Molecular Systems, Eindhoven University of Technology, Eindhoven, The Netherlands

Fibroblasts are a ubiquitous cell type that can be found throughout the human organism and that plays a critical role in maintaining tissue homeostasis¹. They can be activated by the cooperation between the biochemical response^{2,3} and mechanosensing, which allows cells to perceive mechanical signal from the environment⁴. Such cues have a dynamic role affecting several important cellular behaviors, including the fibroblast-to-myofibroblast transition (FMT)⁵, which takes place at the onset of injuries, leading, if not correctly regulated, to loss of function and to stiffening of the tissue.

At the single-cell level, sensing of different environmental cues, such as substrate stiffness and ligand distribution, leads to adhesion events that transduce the information through rearrangements of the cytoskeleton, leading to different cell phenotypes, characterized by different cellular morphometric parameters values such as eccentricity. However, the transduction of the signals from environmental cues to cellular responses is still poorly understood.

In this project, we aimed to understand, and thereby tune, fibroblast phenotype by high-precision manipulation of the physical and mechanical environments of the cells. We combined spatial control of adhesion contact regions using maskless protein micropatterning and substrates with tunable stiffness in order to decouple and characterize the interplay of two of main indexes that change during the transition between healthy and pathological states. Further, we developed quantitative automatized morphometric analysis of cell images on these micropatterned substrates and evaluated the effects of different combination of stiffness and patterns features on fibroblast phenotype.

This approach is envisioned to provide a deeper knowledge on how spatial distribution of FAs and stiffness are correlated during different phases of FMT and paves the way for a deeper knowledge on the physical and mechanical regulation of fibroblast-to-myofibroblast phenotype transition.

References:

1. Kanekar, S., Hirozanne, T., Terracio, L. & Borg, T. K. Cardiac fibroblasts: Form and function. in *Cardiovascular Pathology* vol. 7 127–133 (1998).
2. Wynn, T. A. & Ramalingam, T. R. *Mechanisms of fibrosis: Therapeutic translation for fibrotic disease. Nature Medicine* vol. 18 (Nature Publishing Group, 2012).
3. Luo, F. *et al.* Arsenic trioxide inhibits transforming growth factor- β 1-induced fibroblast to myofibroblast differentiation in vitro and bleomycin induced lung fibrosis in vivo. *Respir. Res.* **15**, 51 (2014).
4. van Putten, S. *et al.* Mechanical control of cardiac myofibroblasts. *J. Mol. Cell. Cardiol.* **93**, 133–142 (2016).
5. D'Urso, M. & Kurniawan, N. A. Mechanical and Physical Regulation of Fibroblast–Myofibroblast Transition: From Cellular Mechanoresponse to Tissue Pathology. *Front. Bioeng. Biotechnol.* **8**, (2020).
6. van der Putten, C. *et al.* Protein Micropatterning in 2.5D: An Approach to Investigate Cellular Responses in Multi-Cue Environments. *ACS Appl. Mater. Interfaces* **13**, 25589–25598 (2021).

Lipid Nanocoating Effect on the Hemocompatibility of Polycaprolactone Microparticles

F.L. Fernandes Gomes¹, D. Wasserberg², J. van Weerd², P. Jonkheijm³, J. Leijten¹

¹Leijten Lab, Department of Developmental BioEngineering, Faculty of Science and Technology, Technical Medical Centre, University of Twente, Drienerlolaan 5, 7522 NB Enschede, The Netherlands

²LipoCoat BV, Hengelosestraat 535, 7521 AG Enschede, The Netherlands

³Department of Molecules and Materials, Laboratory of Biointerface Chemistry, Faculty of Science and Technology, MESA+ Institute for Nanotechnology, University of Twente, Drienerlolaan 5, 7522 NB Enschede, The Netherlands

Introduction

Compounds with poor water solubility constitute more than 40% of active pharmaceutical ingredients¹ and are inherently linked to lower absorption rates and bioavailability, thereby requiring extensive formulation adjustments during development.

Bioprotective carriers are one example of such adjustments, and are commonly made of inorganic materials, amphiphilic materials, or hydrophobic-hydrophilic core-shell structures. Silica nanoparticles, whether mesoporous or nonporous, have been extensively used in nanomedicine due to their easily tunable properties, but both are known for their hemolytic profiles.² Polycaprolactone (PCL), a biodegradable hydrophobic polyester, has also been used in drug delivery systems³, but its hydrophobicity and tendency for plasma protein adsorption may potentially trigger severe inflammation, platelet activation, and thrombus formation.⁴ A promising approach to improve the hemocompatibility of these materials is to endow these surfaces with a bioinert coating, particularly one that mimics the natural hemocompatibility of cell membranes.

In this work, PCL microparticles were coated with two proprietary lipid formulations as potential hemocompatibility-enhancing coatings.⁵ This effect was first investigated in terms of hemolysis rate and clotting time. Silica microspheres were used as a hemolytic control. To the best of our knowledge, this constitutes the first hemocompatibility testing of the application and effect of synthetic lipid formulations on pristine PCL microparticles.

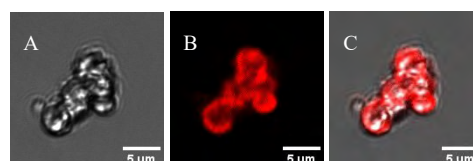
Methodology

PCL microparticles (MPs) were produced via a water-in-oil-in-water emulsion with solvent evaporation technique. The organic phase consisted of 3% w/v PCL (M_n 10kDa) in CH_2Cl_2 , while first and second aqueous phases consisted of ultrapure water and 0.3% w/v Mowiol® 40-88, respectively. Silica microspheres ($0.10 \pm 0.03 \mu\text{m}$) were purchased from Polysciences, Inc. (Warrington, PA, USA). The particles were then coated with two fluorescent lipid formulations - A and B. Coated and uncoated PCL MPs were characterized in terms of hydrodynamic size and zeta potential, and using confocal laser scanning microscopy (CLSM) and scanning electron microscopy. Hemolysis and clotting time assays were conducted on PCL and silica at 37°C using isolated human red blood cells and platelet-poor plasma, respectively.

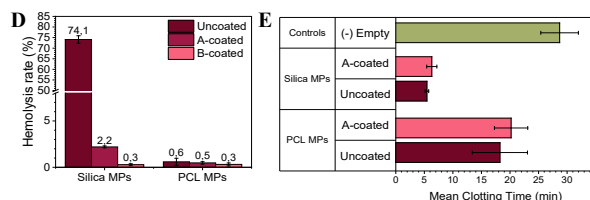
Results

PCL MPs (uncoated and A-coated) exhibited high polydispersity, with a single particle size range of 0.2-5 μm as determined by DLS and CLSM. Zeta potential

(mean \pm SD) values were $-3.1 \pm 0.52 \text{ mV}$ and $-3.1 \pm 0.21 \text{ mV}$, respectively. Fluorescent halos of variable thickness were detected in the A-coated PCL MPs, likely corresponding to a multilayered lipid coating (Figs. A-C). Further coating characterization will be conducted.



Hemolysis rates of PCL were lower than 2% on all conditions, thus confirming its non-hemolytic nature. Most interestingly, the hemolysis rate of silica particles (74.1%) was reduced to 2.2% and 0.3% with coatings A and B, respectively (Fig. D). Clotting times of silica and PCL particles were slightly delayed upon application of coating A, although not significantly (Fig. E). Future tests with coating B will provide further clarification.



Conclusion

Hydrophobic PCL MPs were produced and successfully coated with a synthetic lipid layer. PCL spheres proved to be naturally non-hemolytic and not pro-coagulating while both lipid coatings showed an improvement of the hemolysis rates on both materials. Further studies will focus on protein adsorption and complement activation.

Acknowledgements

F.L. Fernandes Gomes acknowledges the TechMed Donor Service of the University of Twente and all its collaborators and donors. Authors acknowledge financial support from Health~Holland (Project LSHM19074).

References

- Fahr, A. & Liu, X. *Expert Opinion on Drug Delivery* **4**, 403-416, doi:10.1517/17425247.4.4.403 (2007).
- Croissant, J. G., Fatieiev, Y., Alma lik, A. & Kha shab, N. M. *Advanced Healthcare Materials* **7**, 1700831, doi:<https://doi.org/10.1002/adhm.201700831> (2018).
- Malikmammadov, E., Tanir, T. E., Kiziltay, A., Hasirci, V. & Hasirci, N. *Journal of Biomaterials Science, Polymer Edition* **29**, 863-893, doi:10.1080/09205063.2017.1394711 (2018).
- Kostina, N. Y. *et al. Macromolecular Bioscience* **16**, 83-94, doi:<https://doi.org/10.1002/mabi.201500252> (2016).
- van Weerd, J. US2020405641A1 (2020).

Real-Time Monitoring of Volumetrically Bioprinted Constructs

S. Florczak, D. Ribezzi, Prof. J. Malda, Dr R. Levato

Department of Orthopaedics, University Medical Center Utrecht, Utrecht University, 3584CX,
Utrecht, The Netherlands.

Introduction: Volumetric printing (VP) holds much promise for future endeavors in the field of Biofabrication. This high-speed, light-based approach to additive manufacturing solves many issues that have plagued more traditional techniques such as bioprinting via extrusion-based or stereolithographic techniques; in particular regarding scalability, speed, and cytocompatibility. VP enables for the fabrication of clinically sized structures within tens of seconds, and it does so using photocurable resins without the need for any extrusion or layer-by-layer deposition. There are however new challenges yet to be tackled with this technique. Most notably, the capacity to monitor and quantify the progress of a structure during the printing process. This is difficult due to the nature of the approach, which relies on a precisely calculated 3-dimensional light dosage to be delivered within a volume of resin. During printing, this, empirically, does not produce much change, and so the result of the delivered dosage and consequent degree of cure is only fully realised once the fabricated structure is removed from its resin and washed. Here we propose a technique that takes advantage of Schlieren imaging to visibly monitor minute changes in the refractive index of the resin during crosslinking. Furthermore, we used Entropy-based image processing to quantify – in real time – the progress of the print. This allowed us to infer and predict the point at which dosage of light was sufficient such as to produce a structure with an optimal geometry. This method of analysis was also demonstrated for both cell-laden, and geometrically non-isotropic (perpendicular to the tomographic axis) structures. Finally, the approach was used to automatically stop the printing process once the theoretical optimal dosage conditions were achieved, thus resulting in an automated printing regime.

Methods: A home-built volumetric printer was used to sequentially fabricate pairs of cylindrical structures comprising of gelatin methacryloyl (GelMA) with a visible-light photoinitiator (lithium phenyl-2,4,6-trimethylbenzoyl -phosphinate). First, one cylindrical structure was used for physical measurement to verify diametrical accuracy. The printing of the second cylinder was imaged under a classical optical Schlieren method, by which a collimated pinhole light source was used to illuminate the samples during printing. This was then captured by a CCD sensor and recorded. The statistical entropy of these images was measured within the region of interest over time. The data used from the analyses was used to generate both a curve of statistical entropy over time, and a point in time corresponding to optimal geometrical accuracy. This was then repeated for GelMA structures laden with immortalized Mesenchymal Stromal Cells (MSCs) at concentrations of 0.5, 2.5 and 5 million/mL. More complex conical structures were also printed in order to demonstrate the applicability of the technique for use with geometries that were non-isotropic perpendicular to the tomographic axis. To do

so, it was first necessary to homogenize the print time across the entire structure irrespective of the model's cross-sectional geometry. This was implemented by first determining the gelation threshold of the GelMA bio-resin through a sol-fraction analysis at the boundary between its crosslinked and un-crosslinked states. This data was then fed into a simplified resin-kinetics model which adjusted the relative intensity of each layer to ensure simultaneous curing across an entire model. The geometric accuracy of the conical structures were then verified through microCT scanning.

Results and Discussion: Through a combination of Schlieren imaging and entropy-based analysis, a relationship was established between the entropy curves of the printed structures over time, and the point of optimal cure. In particular we observed that the cylindrical GelMA structures reached a point of optimal cure (and hence optimal diametric accuracy) just prior to reaching the global maxima of statistical entropy. For cell-laden structures, a high degree of optical scatter arising from a refractive index mismatch between the cell components and the bio-resin was seen with increasing concentration. The dimensional accuracy of the conical structures was verified under microCT, and shows similar features in their entropy profile over time during printing. Using feature extraction and signal processing it was possible to implement an automatic printing regime whereby the illumination time was controlled through feedback from the entropy signal.

Conclusions: This study demonstrated that through the use of Schlieren imaging and entropy measurements, a simple quantitative approach can be taken to determining the progress of a print in real time. This can then be used to predict when sufficient light dosage has been delivered to the resin. By adjusting the relative intensities between the layers, this technique can be applied to most arbitrary geometries, and shows potential for cell-laden structures.

3D printed Poly-ε-caprolactone composites as an antimicrobial carrier for fracture fixation applications

C.M. Guarch Pérez¹, B. Shaqour^{2,3}, M. Riool¹, P. Cos², S.A.J. Zaat¹

¹Department of Medical Microbiology and Infection Prevention, Amsterdam institute for Infection and Immunity, Amsterdam UMC, University of Amsterdam, 1105 AZ Amsterdam, The Netherlands, ²Laboratory for Microbiology, Parasitology and Hygiene (LMPH), Faculty of Pharmaceutical, Biomedical and Veterinary Sciences, University of Antwerp, Universiteitsplein 1 S.7, 2610 Antwerp, Belgium, ³Mechanical and Mechatronics Engineering Department, Faculty of Engineering & Information Technology, An-Najah National University, P.O. Box 7, Nablus, Palestine

INTRODUCTION: Bacterial infections are still a serious healthcare complication in orthopedic and trauma surgery worldwide. The biofilm forming species *Staphylococcus aureus* and *Staphylococcus epidermidis* are the most common pathogens associated to orthopedic infections. Fractures have infection rates ranging from 5 to 10 % for closed fractures and even higher rates (up to 30 %) for open fractures^{1,2}. These infections are not easy to diagnose and extremely difficult to treat due to the ability of bacteria in biofilm to survive the immune response and antibiotic treatment.

Clinically, implant infections are principally prevented by the application of skin antiseptics and systemic antibiotic prophylaxis. Despite the reduction of infection rates, systemic antibiotic prophylaxis cannot provide sufficient protection in the surgical wound because the antibiotic concentration in the bone is limited.

Compared to systemic administration, local antibiotic prophylaxis has been shown to provide a higher antibiotic dose and bioavailability at the wound bone site with minimum toxic effects³. However, there are still not enough biomaterials and antibiotics combinations available for patients neither personalized implant sizes.

AIM: Therefore, bone fixation plates made of a composite of polycaprolactone, hydroxyapatite and halloysite nanotubes (PCL-HA-HNT) loaded with gentamicin sulphate (GS) were fabricated by fused filament fabrication (FFF) 3D printing technology. GS was chosen for its broad-spectrum activity and thermostability required in the printing process. PCL is a commonly used biomaterial for its low inflammatory response induction, slow resorption rate and hydrophobic character. HA and HNT were used to increase the mechanical strength of the devices. Since HA is considered osteoconductive and osteoinductive, its addition may improve the implant biocompatibility. Additionally, HA increases the osteoconductive properties, causes no inflammatory response, and has very low toxicity in humans⁴.

METHODS: PCL was loaded with 20 % HA and 2.5 % HNT (w/w). GS was added at 2 % and 5 % (w/w). The neat PCL and the non-loaded and GS loaded composites were hot melt extruded using a mini extruder to produce a filament with a diameter of around 1.75 mm. Subsequently, filaments were analyzed for their thermal properties using a differential scanning calorimeter (DSC) and for their mechanical properties using tensile and bending testing. Subsequently, filaments were used to 3D print samples at temperatures of 120°C, 130°C and 150°C for PCL, non-loaded and GS loaded composites,

respectively. The GS release of the PCL-HA-HNT fixation plates was measured *in vitro* with the o-phthalaldehyde reagent at 1, 6 and 24 h, and 2, 3, 4, 6, 8, 11 and 14 days. The 2 and 5% GS loaded and non-loaded PCL-HA-HNT fixation plates were challenged with 2.5 µL of 10³ CFU of *S. aureus* JAR 06.01.31 in an *ex vivo* model with mouse femurs.

RESULTS: Filaments were successfully extruded with the required diameter for 3D printing. The thermal properties for the produced filament showed a decrease in crystallinity of PCL due to the presence of filler particles which occupied the space needed for crystal growth. The tensile and flexural elastic modules were significantly improved after adding the filler materials. The release kinetics showed a burst release of GS for the 2 and 5 % GS loaded plates during the first 24 h that was followed by a sustained release for the next 2 weeks. The murine femur *ex vivo* model showed a complete killing of *S. aureus* in the bone as well as on the fixation plates of the composites loaded with 5 % of GS and a significant reduction in the number of CFUs in the composites loaded with 2 % of GS compared to the constructs of non-loaded composite.

CONCLUSIONS: In conclusion, the produced composite shows promising antibacterial properties. Additionally, the ability of using FFF 3D printing to produce patient specific implants may provide wider range of solutions for patients. Our next step will be to study the antimicrobial efficacy of the constructs against *S. aureus* in an *in vivo* bone defect infection mouse model.

REFERENCES:

- ¹ ter Boo, G. J. A., Grijpma, D. W., Moriarty, T. F., Richards, R. G., & Eglin, D. (2015). Antimicrobial delivery systems for local infection prophylaxis in orthopedic and trauma surgery. *Biomaterials*, 52, 113-125.
- ² Morgenstern, M., Vallejo, A., McNally, M. A., Moriarty, T. F., Ferguson, J. Y., Nijs, S., & Metsmakers, W. J. (2018). The effect of local antibiotic prophylaxis when treating open limb fractures: a systematic review and meta-analysis. *Bone & joint research*, 7(7), 447-456.
- ³ Turgut, H., Sacar, S., Kaleli, I., Sacar, M., Goksin, I., Toprak, S., ... & Baltalarli, A. (2005). Systemic and local antibiotic prophylaxis in the prevention of *Staphylococcus epidermidis* graft infection. *BMC infectious diseases*, 5(1), 91.
- ⁴ Torres, E., Fombuena, V., Vallés-Lluch, A., & Ellingham, T. (2017). Improvement of mechanical and biological properties of polycaprolactone loaded with hydroxyapatite and halloysite nanotubes. *Materials Science and Engineering: C*, 75, 418-424.

Geometrically Defined Collagen Microparticles for Biomaterial-Driven Bottom-Up Bone Tissue Engineering

E. Güben Kaçmaz, Z. Tahmasebi Birgani, P. Habibović, R. Truckenmüller

Department of Instructive Biomaterials Engineering, MERLN Institute for Technology-Inspired Regenerative Medicine, Maastricht University, Universiteitssingel 40, 6229 ER Maastricht, The Netherlands

Introduction: Bone, a multicellular, vascularized and innervated tissue with complex hierarchical structure, has the ability to restore itself after injuries. However, in critical-sized defects, the regenerative capacity of bone is not sufficient. The gold standard treatment for such defects, i.e., autograft, is limited with availability and other complications. Therefore, there is a growing interest in effective bone tissue engineering (BTE) therapies to restore defected bone [1, 2].

The most common BTE approach is the top-down approach, which aims to construct a biocompatible meso-scale scaffold, to be implanted in the defect alone or combined with relevant cells. Using a monolithic scaffold in top-down TE is often associated with non-uniform distribution of cells throughout the single-piece biomaterial and limited control over the spatial resolution of the components of the resulting three-dimensional (3D) construct [3, 4].

The more recent and alternative bottom-up TE approach involves creating modular 3D constructs through (self-) assembly of cellular and materials-based micro- or nano-sized building blocks. In order to increase tissues' structural complexity, modulate cell-cell and cell-material interactions at different length scales to orchestrate cellular differentiation, and better control the cell distribution. This approach offers design freedom and tuning of the materials-based building blocks in diverse ways and in terms of number, size, outer shapes, stiffness and surface chemistry and topography [4-6].

Previous research often focused on developing soft microgel particles, in many cases with cells encapsulated in the gels, as biomaterial building blocks for bottom-up TE [5], which may not translate into the most suitable biomaterials for mimicking the mineralized bone matrix in BTE. Here, we propose a bottom-up approach for BTE in which engineered (bio)mineralized collagen microparticles (COL-MPs) with well-defined geometries, prepared using an adopted particle replication in a non-wetting template (PRINT) [7], play the role of bone matrix-mimicking building blocks. This abstract presents the first steps towards development of COL-MPs.

Materials and methods: A collagen solution of 3.7 mg/ml was prepared in 0.1 M NaOH and 10X phosphate-buffered saline (PBS), and casted onto a polydimethylsiloxane (PDMS) template, prepared with a standard soft lithography technique, featuring particles micromolds. The COL-MPs formed in the PDMS mold were incubated at 37 °C for 72 hours, cross-linked with 50 mM 1-ethyl-3-(3-dimethylaminopropyl)carbodiimide (EDC) and 25 mM N-hydroxysulfosuccinimide sodium (NHS) overnight at room temperature, quenched with 0.1 M Na₂HPO₄ and 2 M NaCl for 2 hours at room temperature, and finally washed with PBS. In order to release the COL-MPs, a 4% w/v poly (vinyl alcohol) (PVA) solution was poured onto the mold and dried. The formed PVA film was peeled off, removing the COL-

MPs from the PDMS mold, and dissolved in water, resulting in released free-standing COL-MPs.

Results and discussion: The collagen fabrication protocol introduced here was previously used to generate mesoscale fibrillar collagen scaffolds [8]. Our preliminary results showed successful preparation of COL-MPs with this protocol in a particle replication technique. We showed that the COL-MPs maintained their shape and integrity in the micromolds during incubation and crosslinking. However, shrinkage of COL-MPs was observed during PVA film formation (Figure 1).

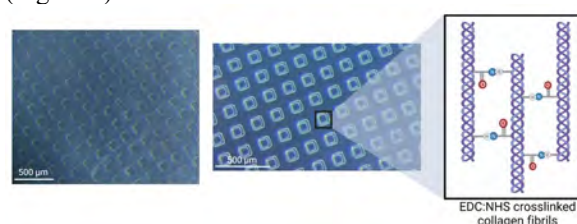


Figure 1. Bright-field images of COL-MPs after casting onto the PDMS mold (left) and after crosslinking with EDC-NHS (right); scale bars: 500 μ m.

Conclusion and perspective: Here, we have shown the first step towards development of collagen-based MPs to be used for bottom-up BTE. Further steps include optimizing the fabrication process and characterizing the properties of the MPs. In addition, we aim to (bio)mineralize the COL-MPs in order to mimic the native matrix of bone tissue. Subsequently, the (bio)mineralized COL-MPs will take part in generating hybrid three-dimensional bone-like assemblies, with human stem cells and MPs as matrix-mimicking and cellular building blocks, respectively.

References:

- [1] A. Oryan et al., 2014, Journal of Orthopaedic Surgery and Research 9(1), 1-27.
- [2] L.E. Miller & J.E. Block, 2011, Orthopedic Research and Reviews 3, 31-37.
- [3] J.W. Nichol & A. Khademhosseini, 2009, Soft Matter 5, 1312-1319.
- [4] A. Leferink et al., 2014, Advanced Materials 26, 2592-2599.
- [5] A. Salerno et al., 2019, Journal of Clinical Medicine, 8(11), 1816.
- [6] V.M. Gasper et al., 2020, Advanced Materials 32, 1903975.
- [7] J. Xu et al., 2013, Angewandte Chemistry International Edition England 52, 6580-6589.
- [8] D. de Melo Pereira et al., 2020, Frontiers in Bioengineering and Biotechnology 8, 554565.

Acknowledgements:

The study is conducted with the support of the Study Abroad Program of the Ministry of National Education of the Republic of Turkey. This research has been in part made possible by the Dutch Province of Limburg (program "Limburg INvesteert in haar Kenniseconomie/LINK"; grant nos. SAS-2014-00837 and SAS-2018-02477), the Gravitation Program of the Netherlands Organisation for Scientific Research (NWO) (project "Materials-Driven Regeneration"; grant no. 024.003.013) and the NWO Incentive Grant for Women in STEM (Project "Biotetris"; grant no. 18748).

A microfluidic gradient generator to investigate the effects of metabolite concentration on stem cells

M. Gurian¹, Y.W.E. Schreurs¹, L.S. Moreira Teixeira², and J. Leijten¹

¹Leijten Laboratory, Department of Developmental BioEngineering, University of Twente, The Netherlands.

²Teixeira Laboratory, Department of Developmental BioEngineering, University of Twente, The Netherlands.

Introduction

Metabolites are essential for the survival, function, and fate of cells.(1, 2). Indeed, nutrient deprivation contributes to the rapid loss of implanted cells and prevascular tissues. Knowledge on the minimal levels of nutrients that are required to maintain cell viability could aid predictable survival of living implants. However, current knowledge is typically based on static culture systems in which cells are exposed to an initially chemically controlled medium, that rapidly decreases in its nutrient content over time(3). Consequently, this has limited our understanding of the critical metabolite concentrations for cell survival and function.

We here report on the development and use of a dynamic microfluidic-based cell culture platform for the determination of minimal metabolic requirements for the survival and function of mesenchymal stem cells.

Method

Soft-lithography and replica molding was used to create microfluidic devices that were composed of a gradient generator followed by parallel cell culture chambers (figure 1). These are then bound to PDMS coated glass slides by plasma activating the surfaces, while a polydopamine coating was used to ensure cell attachment on the hydrophobic chamber surfaces.

Fluorescein dye was used as model metabolite to validate the generation of distinct concentrations in a controlled manner with the microfluidic device.

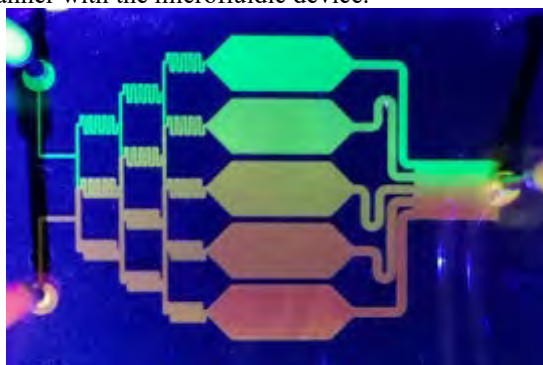


Figure 1: Color gradient generated with the microfluidic device

Results

The analysis of the generated fluorescein concentrations conformed that the gradient generators offered a long-term stable and linear control over the concentrations in each cell culture chamber (figure 2). Subsequently, chemically defined media with quantified nutrient composition were flown through the microfluidic device at a refresh rate of once per minute to confirm neglectable amount of nutrient loss e.g. due to absorption to the microfluidic channels. Cells were seeded at 10000 cells/cm² and exposed to a range of metabolite concentrations. We conformed that the dynamic media flow was sufficiently fast to maintain constant metabolite concentrations within each chamber, while keeping the hydrodynamic shear sufficiently low

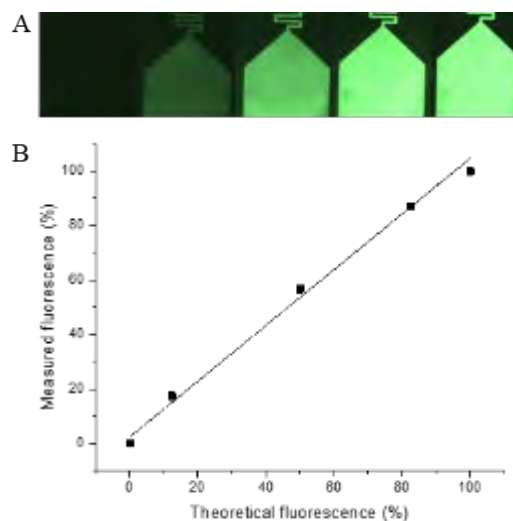


Figure 2: Concentration gradient validation with fluorescein sodium salt. A) Representative pictures of the cell culture chambers, showcasing the intensity range created with the device. B) Relative measured fluorescence intensity value over the expected theoretical value.

(<0.3 dyn/cm² (4)) to avoid causing effects on cell behavior. Cells were then cultured over a maximal period of seven days to quantitatively determine the minimal concentrations to sustain cell survival as well as function for a panel of relevant metabolites in a time-resolved manner.

Conclusion

This approach allowed the determination of the relative importance of individual metabolites on the survival of mesenchymal stem cells, which offers novel fundamental insights what is required to avoid starvation-induced cell loss of implanted cells and prevascular tissues.

Acknowledgements: Financial support was received from the European Research Council (ERC, Starting Grant, #759425).

References:

1. C. M. Metallo, M. G. Vander Heiden, Understanding Metabolic Regulation and Its Influence on Cell Physiology. *Mol. Cell.* **49**, 388–398 (2013).
2. Y. P. Wang, Q. Y. Lei, Metabolite sensing and signaling in cell metabolism. *Signal Transduct. Target. Ther.* **3**, 1–9 (2018).
3. K. De la Luz-Hdez, Metabolomics and Mammalian Cell Culture. *Metabolomics* (2012), doi:10.5772/30979.
4. S. D. Stone, B. C. Hollins, Modeling shear stress in microfluidic channels for cellular applications. *Proc. - 29th South. Biomed. Eng. Conf. SBEC 2013*, 117–118 (2013).

Contact: m.gurian@utwente.nl

Cellular Uptake of Antimicrobial Mesoporous Bioactive Glass Nanoparticles for Treatment of Bone Infection

Negar Hassani Besheli, Juul Verbakel, Dongmei Deng, Fang Yang, Alessandra Cambi, Sander Leeuwenburgh

Radboud University Medical Center, Radboud Institute for Molecular Life Sciences, Department of Dentistry - Regenerative Biomaterials, Philips van Leydenlaan 25, Nijmegen, The Netherlands

Introduction: Successful treatment of bone infection has become a major clinical challenge due to the emergence of antibiotic-resistant bacteria. These hard-to-treat pathogens can induce severe bone infection and even intracellular persistence of these pathogens upon their invasion into host cells such as macrophages and osteoblasts. Besides the limited therapeutic efficacy of currently available antibiotics against resistant bacteria, their low penetration into host cell plasma membranes increases the chance of recurrence of infection, which imposes an ever-increasing challenge for various surgical application areas. Therefore, advanced biomaterials possessing inherent antimicrobial properties along with internalization ability are urgently required to combat resistant bacteria.

Mesoporous bioactive glass (MBG) nanoparticles have received increasing attention in bone-related applications due to their excellent functional properties including cytocompatibility, apatite-inducing capacity, and antimicrobial properties. The intrinsic antimicrobial properties of MBG nanoparticles can be improved through the incorporation of trace amounts of therapeutic ions like copper, zinc, or silver, being highly beneficial in combating resistant bacteria. In this study, we synthesized antibiotic-free antimicrobial MBG nanoparticles enriched with copper ions. We further investigated their antibacterial properties and cellular uptake to assess their potential for treating bone infection.

Method: Copper-containing MBG nanoparticles were synthesized through the microemulsion assisted sol-gel method. The antibacterial efficacy of synthesized nanoparticles was investigated against Methicillin-resistant *Staphylococcus aureus* (MRSA) bacteria by monitoring bacterial growth kinetics and performing resazurin reduction assay. To facilitate nanoparticle internalization, amino silanization process was done to introduce amine groups into the particle structure. UV-Vis spectroscopy and confocal microscopy were used to quantify and visualize the internalization process of nanoparticles into preosteoblasts and macrophages, respectively. To further detect the subcellular localization of nanoparticles, a colocalization assay of MBG nanoparticles with LysoTracker® Red was performed. Finally, the ionic release profile of Cu, Si, and Ca was studied in artificial lysosomal fluid (ALF) using Inductively coupled plasma (ICP) analysis.

Results: Synthesized copper-containing nanoparticles (~ 100 nm) exhibited remarkable antibacterial performance against MRSA as evidenced by complete eradication of bacteria at concentrations higher than 0.5 mg/ml (figure 1-a). Surface amination of MBG nanoparticles resulted in a shift from a negative zeta potential of -19 ± 0.4 mV to a positive zeta potential of

26 ± 3 mV. Quantitative results showed an uptake efficiency of nanoparticles of about 30% for both cell types. Confocal microscopy also confirmed that nanoparticles were efficiently internalized by cells and were present in the cell cytoplasm after 24 h of incubation in both cell types (figure 1-b). Subsequently, a colocalization study indicated stable encapsulation of nanoparticles in lysosomal vesicles localized in the perinuclear region (figure 1-b). In addition, the release study confirmed the degradability of particles in ALF medium by sustained release profiles of Si and Ca ions over 7 days.

Conclusion: In conclusion, the synthesized antibiotic-free copper-containing MBG nanoparticles exhibited favorable antibacterial properties against resistant bacteria. Particle surface properties in terms of size and surface charge facilitated their internalization into preosteoblast and macrophages. Therefore, these nanoparticles can be considered as a potential candidate in developing effective antibiotic-free antimicrobial biomaterials (as components of e.g., hydrogels, coatings, and nanocomposites) to treat infected bone defects.

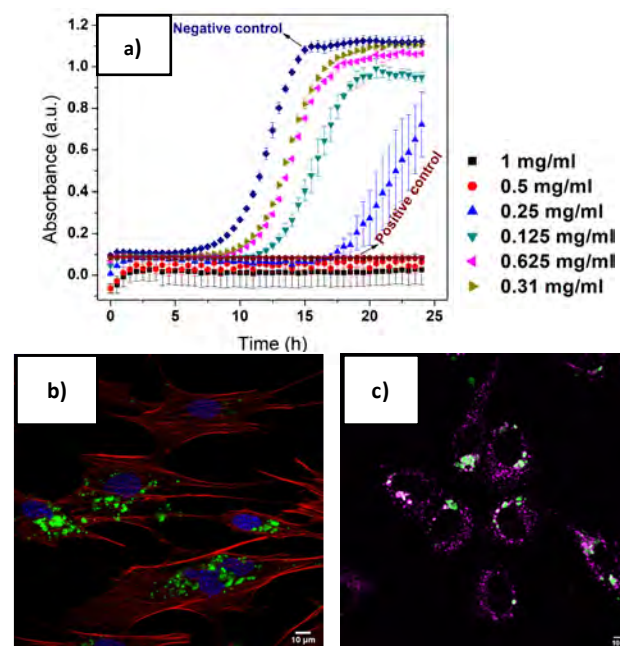


Figure 1- a) Bacterial growth curve exposed to MBG nanoparticles with increasing serial dilution of particles for 24h. b) Intracellular uptake of labelled MBG nanoparticles by pre-osteoblast cells (Red = F-actin filaments, blue = nucleus, and green = FITC-labelled MBG nanoparticles), and c) Colocalization of labelled nanoparticles with lysosomes in which lysosomes labelled by LysoTracker® Red present as magenta. Labelled nanoparticles and nanoparticle which colocalized with lysosomes indicated as green and white, respectively.

The effect of blood derivatives compared to commercial FBS on AT-MSCs seeded on PCL scaffolds

Věra Hedvičáková¹, Veronika Hefka Blahnová¹, Věra Sovková¹, Olga Kuten², Aiva Simaite³, Lacza Zsombor^{2, 4}, Eva Filová¹

¹Institute of Experimental Medicine of the Czech Academy of Sciences, Videnska 1083, Prague 4, 14220, Czech Republic

²OrthoSera GmbH, 3500 Krems, Austria

³InoCure, Politických vězňů 935/13, 11000, Prague 1, Czech Republic

⁴Institute of Sport and Health Sciences, University of Physical Education, Budapest, Hungary

The aim of tissue engineering (TE) is to develop a suitable temporary bone substitute to support the bone healing cascade. One approach is the electrospinning method to produce fibrous scaffolds. By electrospinning, the fibers with diameter from tens of nanometers to hundreds of micrometers are produced. Such scaffold, if produced from biocompatible polymer, offers numerous contact points for cell adhesion and therefore are suitable as bone scaffolds. Moreover, to promote the adhesion of cells from the surrounding area to the defect site, it is advisable to modify the scaffold with bioactive compounds. Blood derivatives are suitable candidates for use in TE as they are naturally occurring substances in the bone healing cascade and can be used as autologous bioactive compounds.

In the present study, poly-ε-caprolactone (PCL) was used to produce fibrous scaffolds by electrospinning method. On these scaffolds, adipose tissue derived mesenchymal stem cells (AT-MSCs) were seeded in diverse culture conditions: growth media supplemented with fetal bovine serum (FBS), growth media supplemented with hyperacute serum (hypACT), growth media supplemented with platelet lysate (PL), osteogenic media with FBS, osteogenic media with hypACT or osteogenic media with PL. AT-MSCs were cultured on PCL scaffold for 35 days. During the

experiment, metabolic activity, DNA quantification and alkaline phosphatase (ALP) activity were detected.

The measurement of metabolic activity of the AT-MSCs, performed using the MTS assay, showed increased activity of the AT-MSCs when cultured in osteogenic media supplemented with either FBS or PL. Higher cell proliferation was detected when hypACT or PL were added to the media. The most prominent differences were visible when ALP activity was measured. Clearly addition of hypACT or PL into the osteogenic media induced higher ALP activity, an early marker of osteogenic differentiation.

Positive effect on osteogenic differentiation of AT-MSCs cultured in osteogenic media supplemented with either hypACT or PL was demonstrated by fostered ALP activity. Platelets contain alpha granules that are filled with growth factors (GFs). These GFs are involved in the successful physiological healing of bones. Positive effect of these compounds was demonstrated *in vitro* compared to FBS, that is standardly used as *in vitro* media supplement but can not be used for human medicine. Therefore, blood derivatives, such as tested PL and hypACT, are potential compounds that are suitable for the functionalization of scaffolds for bone TE.

Acknowledgement: This study has been supported by Research and Innovation Staff Exchange program project IP Osteo “Induced pluripotent stem cell for bone and cartilage defects” under grant agreement 824007.

Establishment of Selenium-incorporated Mesoporous Silica Nanoparticles (MSNs) for Osteosarcoma Therapy

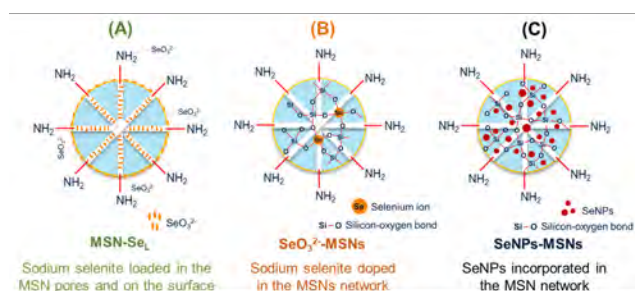
L. He, Pamela Habibovic *, Sabine van Rijt *

Department of Instructive Biomaterials Engineering (IBE), MERLN Institute for Technology-Inspired Regenerative Medicine, Maastricht University, the Netherlands.

Introduction:

Common treatments for osteosarcoma (OS), one of the most common malignant bone tumors, involve surgical resection combined with adjuvant chemo/radiotherapy. However, anti-OS treatment efficacy has gradually decreased on either shrinking tumor size pre-surgically or clean residual tumor cells post-surgically due to side effects such as drug resistance [1]. Inorganic ions and compounds such as selenium (Se) have received attention as promising alternative therapeutic option for OS therapy. Therapeutic ions have advantages in their use including their biocompatibility, stability, easy preparation, low cost of development, and dose-dependent selectively. Se, an essential micronutrient in biological tissue, can maintain metabolism and repair DNA as an anti-oxidant in low doses while at high dose Se is oxidative and can induce apoptosis by generating ROS [2–3]. ROS, a double-edge sword, enable to boost metabolism in low concentration while to induce apoptosis in higher amount above threshold [3]. ROS have already been verified as promising probes for selectively inhibit OS since common cancer cells contain higher level of ROS compared to normal cells [3]. Thus, Se can be a great ionic candidate for selectively inhibiting OS cells. Se obtains various oxidation states (i.e. 0, +4, and +6), which show different options for Se delivery. However, direct Se delivery also confronts some challenges such as less targeted efficiency and uncontrollable accumulation. Thus, nanoparticle (NP) can be introduced in Se delivery to synthesize different anti-OS nanoscale particles, which are able to possibly achieve tissue targeting, controllable release and efficient cellular internalization. MSNs have been widely used as nanoparticle delivery system due to their good biocompatibility, tunable size and surface that can be modified easily. On account of its mesoporous structure, MSNs can incorporate Se ions in several ways [4]. In this study, we incorporated Se into MSNs in 3 different ways, namely: loaded in the mesopores and on the surface (MSN-Se_L), incorporated in the silica matrix (SeO₃²⁻-MSNs), and incorporates as Se nanoparticles (SeNP-MSNs) (scheme 1). The aim of this study was to compare Se incorporation methods on its biological activity. [5–6].

Experimental design and methods:



All groups of synthesized Se-MSNs was first characterized by DLS, TEM and FTIR. Then ICP-MS was used to detect the total Se content in every groups of Se-MSNs to prove if Se was incorporated into MSNs. In vitro, MTS assay was used for cytotoxicity tests for all groups of Se-MSNs in both OS cell (Saos-2) and osteoblast (hFOB 1.19). The MTS was finally detected by microplate reader.

Results and discussions:

The three groups of Se-MSNs were successfully synthesized with good homogeneity and similar size around 80-100 nm as was confirmed with DLS and TEM. ICP-MS results showed that MSN-Se_L and SeO₃²⁻-MSNs, around 5 and 6% of selenite ions were incorporated. In SeNP-MSNs, results showed only around 2% of silicon existed and contain more than 95% of Se. Next, cell cytotoxicity assays were performed in OS cells and in osteoblast healthy cells (OB). In OS cells, all groups showed dose-dependent trends on inhibiting OS activities with IC₅₀ values in 72, 42 and 56 μg/ml respectively. The IC₅₀ values also showed that last two groups of Se-MSNs displayed more promising anti-OS effects. In OB, all groups showed significant decreased cytotoxicity towards OS and OB cells, proving our MSN-Se can selectively inhibit OS activity with limited effect on healthy cells. SeO₃²⁻-MSNs group showed the best selectivity among the three groups.

Conclusion:

In this work, three new different Se-incorporated MSNs have been developed. Specific Se amount in every groups and variables have also been detected, proving different forms of Se can be incorporated in MSNs. In vitro, selectivity of Se on anti-OS have also been verified. Thus, it can be concluded Se-MSNs can be a great candidate as novel anti-OS in OS therapy.

Reference:

- [1] Meltzer, Paul S., and Lee J. Helman. *New England Journal of Medicine* 385.22 (2021): 2066-2076.
- [2] Wang, Yifan, et al. *ACS nano* 10.11 (2016): 9927-9937.
- [3] Yang, Haotian, et al. *Journal of Experimental & Clinical Cancer Research* 37.1 (2018): 266.
- [4] Palanikumar, L., et al. *ACS Biomaterials Science & Engineering* 4.5 (2018): 1716-1722.
- [5] Chen, Jingjing, et al. *Colloids and Surfaces B: Biointerfaces* 190 (2020): 110910.
- [6] Zengin, A., et al. *Nanoscale* 13.2 (2021): 1144-1154.

In Vitro Intestine Model for Testing Cytotoxicity of Ag, Ti and Zn Nanoparticles

V. Hefka Blahnová¹, V. Sedláčková¹, K. Vocetková¹, E. Šebová¹, A. Simaite², A. Novotná², R. Divín², T. Červená¹, E. Filová¹

¹Institute of Experimental Medicine of the Czech Academy of Sciences, Vídeňská 1083, Prague 4, 14220, Czech Republic

²InoCure, Politických vězňů 935/13, 11000, Prague 1, Czech Republic

Ingestion is one of the main ways how nanoparticles (NPs) enter the body, a question regarding their effect on disrupting of gastro-intestinal barrier integrity and cell viability arises. To clarify whether and if the NPs influence the barrier, there is need for a model to be established which would ideally meet also a current effort in scientific community to reduce the number of animal studies. Therefore, one of the aims of tissue engineering is also to develop an *in vitro* intestine model for testing the nanoparticles cytotoxicity. Firstly, we used metabolic activity test to determine cytotoxic concentrations of Ag (Silver nanopowder) and ZnO NPs for each of HT29 and Caco2 cell type separately. HT29 is a cell line isolated from colorectal adenocarcinoma exhibiting similarity do enterocytes. Caco2 is a mucus producing cell line isolated from colorectal carcinoma, too. Subsequently, we created and characterized an *in vitro* intestine model by seeding a co-culture of HT29 an Caco2 cells. The co-cultures were seeded in insert made of nanofibrous scaffolds prepared from blended poly-ε-caprolactone with cellulose acetate. Both types of NPs were added into basal culture media. On the days 1, 2 and 3 we performed MTS assay, LDH metabolic assay, Luciferase permeability assay and qPCR analysis.

From NPs concentrations ranging from 12.5 to 500 µg/mL we identified those which were clearly toxic for each cell type separately. Decrease in metabolic activity was observed after addition of 25 µg/mL and higher of ZnO and 250 µg/mL and higher of Ag NPs. In following experiments, we used a tolerated NPs concentration, toxic NPs concentration and lethal NPs concentration. For ZnO it was 12.5, 25 and 50 µg/mL and for Ag 125, 250 and 500 µg/mL. The presented work confirmed that individual cell types in co-culture influence each other during response to cytotoxic agent exposure. Which explains the fact that our data does not copy results from monoculture experiments.

Thus, it is obvious that the effort to develop tissue models is reasonable even though the complexity of experimental system is much lower than in animal model. This limitation can be partially overcome by constructing a dynamic system that engages more tissues models, e.g. intestine and liver. Therefore, the future perspective of this project is to develop bioreactor enabling such culture conditions.

Acknowledgement: This work was supported by Ministry of Industry and Trade of the Czech Republic, project number FV40437.

Bioprinting a functional beta cell replacement device

C. Hermans, R.H.W. de Vries, T. Rademakers, A.A. van Apeldoorn

MERLN Institute for Technology-Inspired Regenerative Medicine - Cell Biology-Inspired Tissue Engineering (cBITE),
Universiteitsingel 40 6229ER Maastricht, The Netherlands

Introduction:

Type 1 diabetes is an autoimmune disorder where the insulin producing cells are destroyed. Under normal circumstance, daily insulin injections are enough to control blood glucose in these patients, but for some patients it isn't. In clinical islet transplantation (CIT) donor islets are delivered into the portal vein of the patient. Although CIT is a promising treatment, limitations remain. The main limitation is the limited cell survival because the liver is a suboptimal implantation site. 3D bioprinting is used to microencapsulate islets of Langerhans within a macro-structured device. By selecting the appropriate hydrogel and printing method, beta cells can be immunoprotected while displaying proper function in the 3D delivery device. Here we report on a customized Ultimaker 2+ system™ adapted for 3D printing of an alginate based beta cell replacement device for primary rat and human islets. We showed that primary rat and human islets have good viability and show proper glucose responsiveness comparable to controls using 1.5% ultrapure alginate.

Materials and Method:

Diffusion properties of different alginate based hydrogels were tested using fluorescent recovery after photobleaching (FRAP). Based on the FRAP results primary rat and human islets were mixed with a 1.5% w/v ultrapure alginate prior to printing. All samples were printed with a customized Ultimaker 2+ system and the same settings into a 10mm diameter disc. Alginate was crosslinked using 20 mM BaCl₂ with 119 mM NaCl and 10 mM MOPS. After crosslinking the samples were washed in 9% NaCl and PBS containing MgCl₂/CaCl₂ and placed in culture medium. At Day 1 and 7 of cell culture, beta cell function and viability was determined via GSIS and a live/ dead assay respectively.

Results and Discussion:

FRAP showed that 1.5% ultrapure alginate had the best diffusion properties, which is important for cell function and survival. Both human islets (figure 1) and rat islets were viable and functional after 7 days in culture.

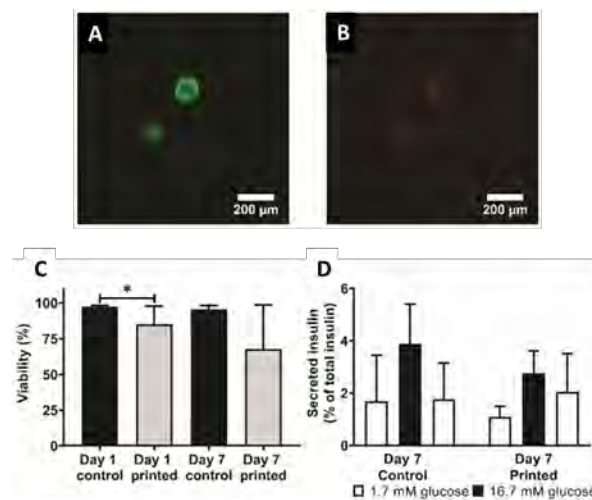


Figure 1: live (green) and dead (red) staining of printed human islets (A, B), quantification of viability of control and printed islets on Day 1 and Day 7 (C), Secreted insulin during a static glucose-stimulated insulin-secretion (GSIS) test by culturing alternatively in low and high glucose solutions (D)

Conclusion and Outlook:

We report islets and beta cells are not negatively affected by 3D bioprinting. Careful selection of the printing conditions and bioink supports endocrine function. In addition, we showed that 1.5% ultrapure alginate has the most optimal mass transport of the tested hydrogels and is printable using the right conditions. The next step would be an *in vivo* study in small animals.

Acknowledgement:

This work is supported by DON.



Adipose Tissue-Derived Stromal Vascular Fraction Shows Superior Osteogenic Differentiation Compared To Donor-Matched Mesenchymal Stromal Cells

JFA Husch, C Woud, J Vossen & JJJP van den Beucken

Dentistry – Regenerative Biomaterials, Radboud Institute of Molecular Life Sciences, Radboudumc, Philips van Leydenlaan 25, 6525 EX Nijmegen, The Netherlands

Introduction

Stromal vascular fraction (SVF) is the primary isolate obtained after enzymatic digestion of adipose tissue that contains various cell types¹. Its successful application for cell-based construct preparation in an intra-operative setting for clinical bone augmentation² and regeneration³ has previously been reported. However, the performance of SVF-based constructs compared to traditional *ex vivo* expanded adipose tissue-derived MSCs (ATMSCs) remains unclear and direct comparative analyses are scarce⁴. Consequently, we here aimed to compare the osteogenic differentiation capacity of donor-matched SVF and ATMSCs.

Materials and Methods

Human adipose tissue from 5 different donors was used to isolate SVF, which was further purified using adherent cell culture to obtain donor-matched ATMSCs. The cell populations were characterized for MSC, endothelial and hematopoietic markers by flow cytometry before, and by immunocytochemistry after osteogenic culture for 3 donor-matched SVF and ATMSCs populations. For normalized seeding densities of donor-matched cell populations, the plastic adherent fraction within SVF and ATMSCs was determined after an incubation of 24 h for 4 donors. Thereafter, SVF and ATMSCs from the same donors were seeded and cultured in osteogenic differentiation medium for 28 days. Proliferation and mineralization were analyzed during the culture period.

Results and Discussion

Flow cytometric analysis revealed the homogenous nature of ATMSCs, while SVF consisted of different cell lineages (Figure 1A). Plastic adherence was significantly lower for SVF compared to donor-matched ATMSCs for all donors evaluated (Figure 1B). Remarkably, all donor-matched comparisons showed either accelerated or more robust mineralization for SVF (Figure 1C). This could relate to endothelial cells found present within SVF during early osteogenic culture for all 3 donors analyzed (Figure 1D).

Conclusion

Our data demonstrate superior osteogenic differentiation capacity of SVF over donor-matched ATMSCs. Further preclinical studies will explore whether this effect also extends to osteoinductive capacity of SVF in an ectopic implantation model.

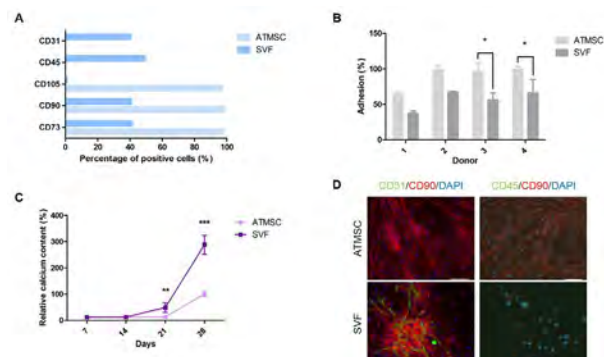


Figure 1: Representative flow cytometric analysis for endothelial (CD31), hematopoietic (CD45), and MSC (CD105, CD90, CD73) marker expression of SVF and donor-matched ATMSCs for one donor ($n=1$) (A). Plastic adherent fraction determined for SVF and donor-matched ATMSCs for 4 donors after 24 h ($n=2-3$) (B). Representative relative calcium content of SVF and donor-matched ATMSCs after 28 days of osteogenic differentiation culture for one donor ($n=3-4$) (C). Data is presented relative to the ATMSC control on day 28. Representative immunocytochemical staining for an endothelial (CD31) or hematopoietic (CD45) with a MSC (CD90) marker of SVF and donor-matched ATMSCs after 7 days of osteogenic differentiation for one donor ($n=3-4$) (D). Scale bar indicates 100 μm . * $p<0.05$, ** $p<0.01$, *** $p<0.001$ vs. donor-matched ATMSCs.

Acknowledgement

This study received financial support from the Dutch ZonMw GameChanger Project “ioCOMPONENTS” (Grant No. 40-41400-98-16032).

References

- Helder MN, Knippenberg M, Klein-Nulend J, Wuisman PIJM. Stem Cells from Adipose Tissue Allow Challenging New Concepts for Regenerative Medicine. *Tissue Eng* 13(8), 1799-1808, 2007
- Prins HJ, Schulten EA, Ten Bruggenkate CM, Klein-Nulend J, Helder MN. Bone Regeneration Using the Freshly Isolated Autologous Stromal Vascular Fraction of Adipose Tissue in Combination with Calcium Phosphate Ceramics. *Stem Cells Transl Med* 5(10), 1362-1374, 2016
- Saxer F, Scherberich A, Todorov A, Studer P, Miot S, Schreiner S, Güven S, Tchang LA, Haug M, Heberer M, Schaefer DJ, Rikli D, Martin I, Jakob M. Implantation of Stromal Vascular Fraction Progenitors at Bone Fracture Sites: From a Rat Model to a First-in-Man Study. *Stem Cells* 34(12), 2956-2966, 2016
- Zhang Y, Grosfeld EC, Camargo WA, Tang H, Magri AMP, van den Beucken JJJP. Efficacy of intraoperatively prepared cell-based constructs for bone regeneration. *Stem Cell Res Ther* 9, 283, 2018

VEGF Immobilization on Supramolecular Surfaces for Enhanced Endothelialization of Implanted Cardiovascular Devices.

D.M. Ibrahim, M.G.J. Schmitz, P.A.A. Bartels, S. A. E. Twisk, A.I.P.M. Smits,

P.Y.W. Dankers, C.V.C. Bouten

Department of Biomedical Engineering and Institute for Complex Molecular Systems,
Eindhoven University of Technology, Eindhoven, the Netherlands

The lack of a hemocompatible blood-material interface represents a major challenge for implanted synthetic biomaterials that are in direct contact with blood. Such synthetic biomaterials are extensively used in utilizing tissue-engineered cardiovascular devices. The optimal way to meet such a pivotal hemocompatibility requirement is to create an endothelial lining at the implanted blood-material interface. This is mimicking the natural anti-thrombotic surface lining the cardiovascular system. Regenerating the endothelium can be ideally achieved through *in situ* endothelialization. This requires i) implanting a biomaterial with specific characteristics to recruit and interact with circulating cells that can form a functional endothelium directly in the body, and ii) targeting the most favorable cell source for *in situ* endothelialization. The source of cells recruited in such process has been under investigation, with the main focus on circulating endothelial progenitor cells (EPCs). However, EPCs represent a very small fraction of the peripheral blood (0.002%-0.01%). Growing evidence suggests that the more abundantly present monocytes (CD14+) have a strong potential to differentiate into endothelial-like cells, thereby contributing to endothelium formation on implanted artificial surfaces.

In this work, we designed a biomaterial to recruit and differentiate circulating monocytes for enhanced endothelialization. To this end, a supramolecular biomaterial based on hydrogen bonding units is functionalized via a modular approach with a heparin-binding peptide, to subsequently bind heparin and vascular endothelial growth factor (VEGF) to the material. VEGF is known for being a strong mitogen for endothelial cells and recently by its ability to direct monocytes differentiation into endothelial-like cells. Moreover, since monocytes have a VEGF receptor on their surfaces, it is hypothesized that the presence of VEGF on the newly developed supramolecular surfaces will promote monocytes capturing underflow. Our results showed the VEGF can be immobilized on the supramolecular biomaterial in an active form through binding to heparin via two different strategies. This was confirmed by studying the biological activity on human umbilical vein endothelial cells (HUVECs) in strict starvation conditions to highlight the VEGF effect. In these conditions, HUVECs displayed a surface coverage on the VEGF functionalized surfaces with 6.2 and 13 folds as compared to the non-functionalized surfaces or the surfaces with heparin only, respectively. Also, the immobilization of the VEGF on the surfaces through binding to heparin maintained the biological activity of the VEGF as evident with a surface coverage that is 3.7 folds higher as compared to VEGF immobilization directly on the surface. In addition, HUVECs maintained a spread morphology with a well-developed actin cytoskeleton on the surfaces where VEGF is biologically active. These results confirmed the functionality of the newly developed system. As a next step, the system's ability to direct monocytes differentiation into endothelial cells was tested. Monocytes cultured on the VEGF functionalized surfaces displayed endothelial markers (CD144, CD31) after 14 days in culture. Currently, we are testing the capability of the VEGF functionalized system on capturing monocytes under flow conditions and direct their endothelial differentiation. These data suggest the potential of using this newly developed VEGF functionalized supramolecular surfaces for implanted cardiovascular devices including tissue-engineered grafts.

Luciferin-Bioinspired Hydrogel Scaffolds with Tunable Properties for 3D Cell Encapsulation

M. Jin^{1,2,3}, G. Kocer¹, J.I. Paez^{1,3}

¹INM – Leibniz Institute for New Materials, Campus D2-2, 66123, Saarbrücken, Germany

²Chemistry Department, Saarland University, 66123, Saarbrücken, Germany

³University of Twente, Drienerlolaan 5, 7522 NB, Enschede, The Netherlands

Introduction. Hydrogels are used as extracellular matrix mimics for diverse applications such as 3D cell culture, drug delivery and tissue engineering. There is a growing interest in covalent reactions for hydrogel crosslinking for cell encapsulation. In nature, fireflies synthesize luciferin through a condensation reaction between 2-cyanobenzothiazole (CBT) and cysteine (Cys). Luciferin is the substrate of the enzyme luciferase, giving rise to their bioluminescent reaction. Inspired by the biochemistry of fireflies, we apply the CBT-Cys condensation reaction as a strategy to develop polyethylene glycol (PEG) hydrogels with tunable properties for cell encapsulation. The hydrogels are fabricated under physiological conditions and present tunable gelation rate and mechanical strength, are homogeneous at the microscale, and present good cytocompatibility. Our findings expand the toolkit of click chemistries for fabrication of tunable biomaterials.

Materials and Methods. 4-arm, 20 kDa PEG macromers carrying either CBT or Cys functional groups were synthesized. Hydrogels were prepared under physiological conditions (37°C, 20 mM HEPES buffer, pH 7-8). Crosslinking process, biofunctionalization with enzymatically cleavable crosslinker peptide (VPM) and cell-adhesive peptide cyclo(RGDfK(C)), and encapsulation of human mesenchymal stem cells (hMSCs) took place one-pot. The resulting hydrogels were cultured for 1 and 3 days. Cell viability, cell behavior and cell-materials interactions were evaluated by live/dead assay, cytoskeletal and morphological characterization, respectively. Proliferation ability of cells was assessed by Ki67+ nuclei staining. Mechanical strength and gelation kinetics of the resulting hydrogels were characterized by shear rotational rheology.

Results and Discussion. PEG hydrogels crosslinked via CBT-Cys ligation were successfully prepared under physiological conditions (Fig. 1a) following established protocols [1]. Hydrogels at 5 wt% polymer concentration in HEPES buffer pH 8.0 showed a fast gelation time (< 30 s) and good mechanical strength ($G' \sim XX$ Pa after swelling), as revealed by rheology. The gelation rate could be tuned by pH modulation: the gelation time increased from seconds to a few minutes when adjusting the pH from 8 to 7. Importantly, this pH-tuning of gelation rate was achieved without changing the final mechanical strength of the gel (Fig. 1b). The optimal gelation times allowed proper mixing of precursors and cell suspension, leading to hydrogels with homogenous crosslinking degree and homogenous distribution of encapsulated cells across the material. In addition, by adjusting molar mass, multivalency and topology of PEG precursors, final mechanical strength after swelling ranged elasticity values of soft natural tissues ($G' = 60 - 2075$ Pa). CBT-Cys hydrogel featuring cell-adhesiveness and cell-degradability were

fabricated and tested for culture of hMSCs. A high cell viability (>90%) found at days 1 and 3 days post-encapsulation demonstrated the good cytocompatibility of the hydrogel. Cell spreading in all dimensions was observed, marked by high cell volume, the formation of F-actin stress fibers and filopodial protrusions in all dimensions (Fig. 1c). Cells were able to remodel their environments when biological cues were given, namely enzymatic degradability and cell-adhesiveness. Cells also maintained their proliferation capacity, which is important for future biomedical applications. All these features demonstrate that CBT-Cys hydrogels are non-cytotoxic and support the encapsulation and proliferation of hMSCs [2].

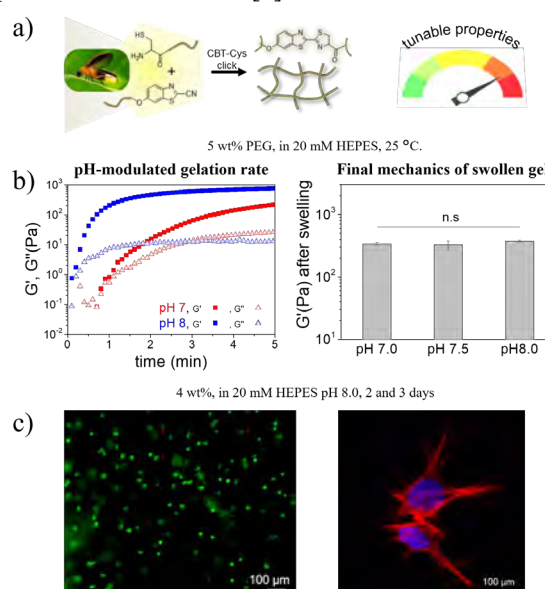


Figure 1. a) Hydrogel formation through CBT-Cys condensation. b) pH-regulation of gelation rate does not affect the final mechanical strength. c) High viability of encapsulated hMSCs and study of their F-actin organization in luciferin-inspired hydrogels with cell-adhesive and cell-degradable cues.

Conclusions. Luciferin-bioinspired hydrogels showcase fine-tunable properties for 3D cell encapsulation. This hydrogel platform presents fast and tailorable gelation rate, adjustable mechanical strength within physiological range, and is suitable for cell culture applications. Cell-encapsulating hydrogels based on CBT-Cys “click” ligation are being further developed as injectable and printable formulations for applications in tissue engineering and regenerative medicine.

References: [1] J. I. Paez*, A. de Miguel-Jiménez, R. Valbuena-Mendoza, A. Rathore, M. Jin, A. Gläser, S. Pearson, A. del Campo*. *Biomacromolecules* **2021**, 22, 7, 2874. [2] M. Jin, G. Kocer, J. I. Paez*, *ACS Appl. Mater. Interfaces* **2022**, in press, doi.org/10.1021/acsami.1c22186.

Mechanical confinement of single cells regulates the phenotype of stem cells

Castro Johnbosco, Malin Becker, Kannan Govindaraj, Tom Kamperman, and Jeroen Leijten

Leijten Lab, Department of Developmental BioEngineering, TechMed Centre, University of Twente, The Netherlands.

Introduction: The interplay between microenvironmental mechanics and cellular biology effectively guides cell function and fate. However, cellular heterogeneity in primary cell populations is widely known, yet single-cell resolution data on this heterogeneity in mechanobiology has remained scarce as current state of art systems are mostly geared towards multi-cellular cultures and population-level analyses. Moreover, mechanotransduction within three-dimensional environments occurs distinctly from the 2D environments on which most of our knowledge relies. Hence, a robust system to study mechanoregulation in 3D microenvironments at the single-cell level is required. We here propose a miniaturized system based on coating individual cells within an engineered pericellular matrix to scrutinize the mechanistic interaction of mechanotransduction on stem cell fate within 3D environments at single-cell resolution.

Methods: Dextran conjugated with tyramine moieties (Dex-TA, 15% DS) containing mesenchymal stromal cells (MSC's) was flown as the disperse phase in a flow-focusing microfluidic chip, which allowed for the creation of microdroplets containing a single cell. The emulsion was then flown into a connected crosslinking chip where the crosslinker solution (H_2O_2) was flown in the opposite direction thereby crosslinking the polymer networks through diffusion. Varied H_2O_2 concentrations induced different mechanical properties of the microgels. Cell-laden microgels of distinct stiffnesses (soft, medium, and stiff) were stimulated to commit to the chondrogenic lineage using a differentiation medium. The differentiation process was mapped at distinct time points using nanoindentation, immunohistochemistry, and gene expression analyses.

Results: Microfluidic chips were generated by casting PDMS on silicon wafers bearing the design produced by photolithography. In short, microchannels of height, 30 μm (droplet generation chip), and 100 μm (crosslinking chip) were obtained. Dex-TA (10 w/v%) HRP 44 units/ml, and Opti prep 8% constituted the aqueous phase along with MSCs at 10^7 cells/ml. The microgels obtained with different concentrations of H_2O_2 (2.5 wt%, 5 wt%, 10 wt%) showed varying stiffness and were categorized as soft (14 kPa), medium (40 kPa), hard (80 kPa). The cell-laden microgels were analyzed throughout differentiation (21 days) using nanoindentation to map the stiffness gradient during differentiation which increased linearly for medium and soft gels while the hard gels increased in stiffness at the onset and gradually retained their stiffness constant. Immunostainings were performed to check the differentiation markers such as COL2A, ACAN, COL6, and SOX9 for chondrogenesis. Medium stiffness gels are more prone towards differentiation showing the matrix formation more evidently than the soft and hard gels. Gene expression analysis was correlated with immunostaining analysis stating the medium gels act as a prominent candidate for

phenotypical change in MSC's towards chondrocytes using required mechanical stimulation.

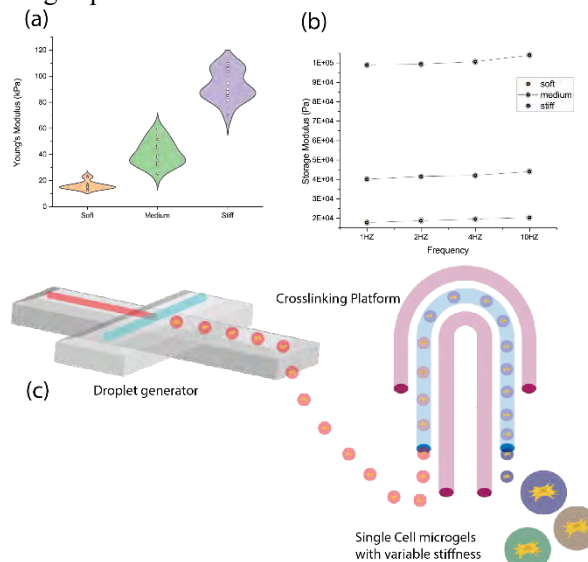


Figure 1: Young's modulus of microgels (a), DMA of microgels (b), Microgel production (c),

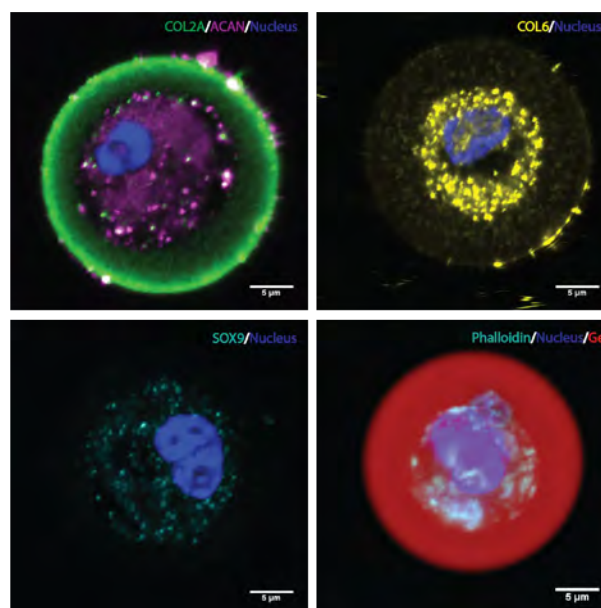


Figure 2: Confocal immunofluorescence images of single-cell chondrogenic differentiation markers

Conclusions: Single-cell chondrogenesis was obtained by varying the mechanical confinement around the cells. Thus mechanics at the immediate matrix interfaces influence the phenotype of stem cells.

Acknowledgments: Financial support was received from the Dutch Research Council (NWO, Vidi Grant, #17522).

References

1. Mao, A et.al *Nature Mater* **16**, 236–243 (2017)
2. Kamperman, T et.al *Adv. Materials*. 2021. 2102660.

Contact: Castro Johnbosco, c.johnbosco@utwente.nl

High-throughput Screening to Mimic Tunica Media Smooth Muscle Cells Alignment in Porous Blood Vessel Scaffold

K.M. Jurczak¹, R. Zhang¹, R. Schuurmann², H.G.D. Leuvenink³, J.L. Hillebrands⁴, R. Bank⁴, J.P.P. Mde Vries⁵, P. van Rijn¹

1. W.J. Kolff Institute for Biomedical Engineering and Materials Science, University Medical Center Groningen (UMCG), Ant. Deusinglaan 1, Groningen, The Netherlands
2. University of Groningen, Faculty of Medical Sciences, Groningen, University Medical Center Groningen (UMCG), Ant. Deusinglaan 1, Groningen, The Netherlands
3. University of Groningen, Department of Cardiology/ Thoracic Surgery, University Medical Center Groningen (UMCG), Ant. Deusinglaan 1, Groningen, The Netherlands
4. University of Groningen, Department of Pathology and Medical Biology, University Medical Center Groningen (UMCG), Ant. Deusinglaan 1, Groningen, The Netherlands
5. University of Groningen, Department of Surgery, University Medical Center Groningen (UMCG), Ant. Deusinglaan 1, Groningen, The Netherlands

Introduction:

With the movement towards the animal study reduction, the development of functional blood vessel model has become an urgent need for the pre-clinical testing of cardiovascular diseases and blood vessel disorders, such as aortic aneurysm. The ideal vascular scaffold should resemble the 3D geometry of native blood vessel and reconstitute its three layers including tunica intima, tunica media and tunica adventitia (1),(2). The secondary medial layer consists of circumferentially oriented smooth muscle cells (SMCs) which are particularly important for the contractile function of blood vessel (3). Reproducing the adequate cellular orientation and facilitating SMCs colonization to enable standardized studies in CVD research still remains a challenge. We are fabricating vascular scaffolds from poly(trimethylene carbonate) (PTMC), the material that is flexible, biodegradable and biocompatible (4). For directing smooth muscle orientation, we are investigating the biophysical factors such as anisotropic topography using in house high throughput screening platform (HTS). The technology enables to identify optimum material parameters in a single cell experiment at the same time evading adverse effects of cell-material interactions(5).

Methods:

Porous structures should facilitate cell proliferation and nutrient flow, therefore the porosity in PTMC is prepared by freeze extraction method using 1,4-dioxane as a polymer solvent and ethanol as non-solvent. To promote continuously varying surface parameter, PTMC is imprinted from stretched and plasma oxidized molds as described previously (6). The response of SMCs from porcine origin is further investigated.

Results and discussion:

The protocol for the creation of PTMC porosity had been established. Porosity of PTMC is evaluated by electron microscopy (SEM). As previously published the pore size in range of 50-100 μm should facilitate vascular permeability and support flow of oxygen and nutrients (7). PTMC anisotropic topography

gradients are characterized via atomic force microscopy (AFM). Measurements of created wrinkles are taken along the surface area covered by the prism mask during plasma oxidation process. The wrinkle size increases from the least exposed side (close side of the mask) to the most exposed side (open side of the mask).

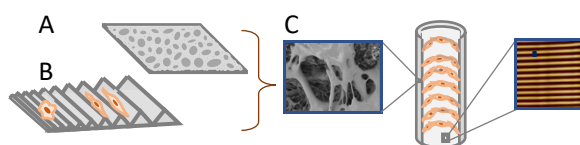


Fig1. Design of a tunica media scaffold (C) combining material's porosity (A) and topography (B) that facilitates nutrients flow and directs cells orientation inside the scaffold.

Conclusion:

Combination of porous PTMC material with highly efficient screening technology of topography gradients can be a crucial tool for organized cell alignment and controlled phenotype of SMCs in tunica media. Development of such tissue engineered vascular scaffolds can provide a real benefit in pre-clinical testing of aortic aneurysm patients, stent graft placements and other cardiovascular disorders.

References:

1. T. Wu, *et al. ACS Appl. Bio Mater.* **1**, 833–844 (2018).
2. C. Tomasina, *et al. Materials (Basel).* **12**, 2701 (2019).
3. T. Jungst, *et al. Vascular Grafts. Adv. Funct. Mater.* **29** (2019).
4. Z. Guo, *et al. Polym. Adv. Technol.* **28**, 1239–1244 (2017).
5. L. Yang, *et al. Adv. Healthc. Mater.* **2000117** (2020).
6. Q. Zhou, *et al. Sci. Rep.* **5**, 16240 (2015).
7. Y. Song, *et al. Acta Biomater.* **6**, 1269–1277 (2010).

Tethering Cells via Oxidative Crosslinking Enables Mechanotransduction in Non-cell-adhesive Materials

T. Kamperman^{1,2}, S. Henke¹, J.F. Crispim¹, N.G. Willemen¹, P.J. Dijkstra¹, W. Lee³, H.L. Offerhaus³, M. Neubauer⁴, A.M. Smink⁵, P. de Vos⁵, B. de Haan⁵, M. Karperien¹, S.R. Shin², J. Leijten¹

¹University of Twente, Dept. of Developmental BioEngineering, Enschede, NL | ²Brigham and Women's Hospital, Harvard Medical School, Division of Engineering in Medicine, Boston, USA | ³University of Twente, Optical Sciences, Enschede, NL | ⁴University of Bayreuth, Physical Chemistry II, Bayreuth, DE | ⁵University Medical Center Groningen, Pathology and Medical Biology, Groningen, NL. | Email: t.kamperman@utwente.nl

Introduction: Cell–matrix interactions govern cell behavior and tissue function by facilitating transduction of biomechanical cues.^[1] Engineered tissues often incorporate these interactions by employing cell-adhesive materials. However, using constitutively active cell-adhesive materials impedes control over cell fate and elicits inflammatory responses upon implantation.^[2] Here, an alternative cell–material interaction strategy that provides mechanotransductive properties via discrete inducible on-cell crosslinking (DOCKING) of materials, including those that are inherently non-cell-adhesive, is introduced. This method crosslinks tyramine-functionalized macromolecules to tyrosine residues that are naturally present in extracellular protein domains via an enzyme-mediated oxidative reaction.

Materials and Methods: To visualize DOCKING, mesenchymal stem cells (MSCs) and 3T3 cells were labeled with tyramide-AF647 by incubation with 3 U/ml horseradish peroxidase (HRP) and 0.3 mg/ml H₂O₂ in PBS. MSCs were individually tethered within 3D dextran-tyramine (Dex-TA) microniches using a previously reported microfluidic encapsulation system.^[3] Hydrogels' stiffness was determined by nano-indentation. Viability and metabolic activity of cells was analyzed using calcein AM/EthD-1 and MTT staining, respectively. Adipogenic and osteogenic differentiation were analyzed using Oil-Red-O and Alizarin Red S staining, respectively. For transcriptome analysis, MSCs from three different human bone marrow donors were tethered and cultured in bipotential differentiation medium, and subsequently lysed and sequenced. To identify cellular protein targets of DOCKING, biotin-tyramide was tethered to MSCs, isolated from cell lysates using a pull-down assay, and analyzed using liquid chromatography combined with mass spectrometry (LC-MS). To compare host response, Dex-TA and Dex-TA-RGD hydrogel disks were subcutaneously implanted in C57BL/6 mice.

Results and Discussion: Here, we report on the discrete inducible on-cell crosslinking (DOCKING), of non-cell-adhesive biomaterials onto cells via oxidative crosslinking of phenolic moieties. Specifically, we demonstrated that Dex-TA could be enzymatically crosslinked with tyrosine-rich extracellular fibronectin, thereby forming pericellularly tethered hydrogel microniches. The intrinsically bio-inert and non-cell-adhesive Dex-TA hydrogel elicited a reduced inflammatory response upon implantation in mice as compared to its RGD-modified cell-adhesive counterpart. Importantly, enzyme-mediated oxidative crosslinking enabled the controlled mechano-transduction from non-cell-adhesive Dex-TA hydrogel

to encapsulated cells via cell tethering. As a proof-of-concept, we leveraged an advanced microfluidic system to tether individual mesenchymal stem cells (MSCs) within micrometer-sized hydrogel matrices (i.e., microgels) using DOCKING to control MSC function and fate at single cell resolution (**Figure 1**). Through timed modulation of microgel stiffness, we could program the lineage commitment of microencapsulated stem cells, thereby indicating DOCKING-mediated mechanotransduction in a bioligand-free material. Proteome and transcriptome analyses revealed that DOCKING predominantly targets proteins associated with the cellular meta-adhesome, and that 3D on-cell-tethered biomaterial mechanics can induce early onset cell-fate-programming mechano-transduction pathways independent of cell size changes.

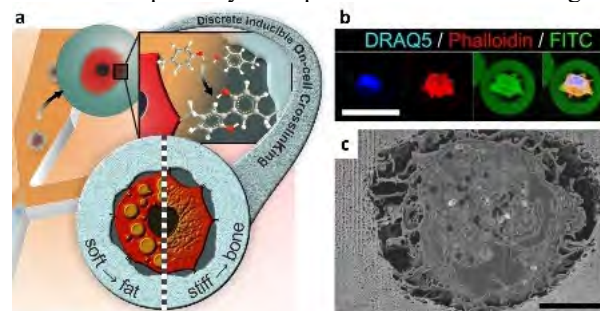


Figure 1. Tethering cells within non-cell-adherent 3D microniches via DOCKING. (a) Schematic representation of DOCKING in combination with droplet microfluidics to program the fate of 3D-tethered stem cells using tunable microniche mechanics. (b) Confocal microscopy and (c) scanning electron microscopy combined with focused ion beam sectioning revealed that cells are 3D-tethered to the intrinsically non-cell-adhesive Dex-TA hydrogel.

Conclusions: In short, DOCKING is a bio-inspired and cytocompatible cell-material tethering method that enables the formation of intrinsically non-cell-adhesive yet mechano-instructive biomaterials eliciting a minimal inflammatory response, which primes it as a promising new strategy to control interactions between cells and materials. This novel method opens up numerous opportunities in the biomedical field that, for example, benefit from mitigating the chronic inflammation associated with conventional bioligand-functionalized materials as well as providing novel strategies to mechanically program and study (stem) cells in a 3D, temporally controlled, and single-cell-resolution manner.

References: [1] Discher DE, et al., 2005, *Science*, 310(5751), 1139. [2] Lee TT et al, 2015, *Nature Materials*, 14(3), 352. [3] Kamperman T, et al, 2017, *Small*, 13(22), 1603711.

Win, Lose or Tie: a Computational Model of Competition at the Cell–ECM Interface

Z Karagöz¹, T Geuens¹, V LaPointe¹, Mv Griensven¹, A Carlier¹

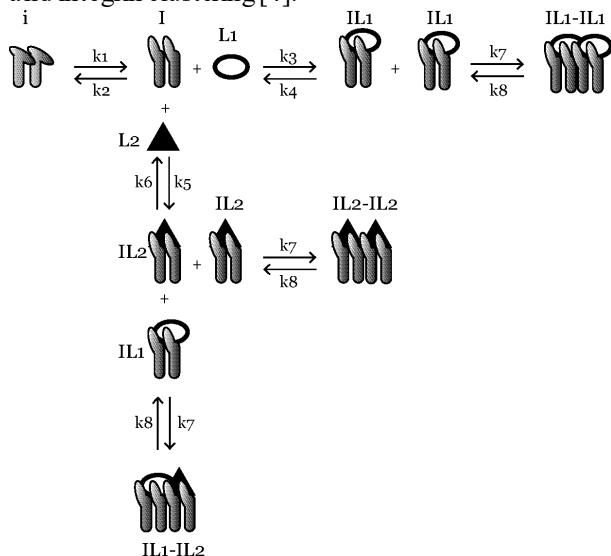
¹ Department of Cell Biology–Inspired Tissue Engineering, MERLN Institute, Maastricht University, Universiteitssingel 40 (UNS40), 6229 ER, Maastricht, the Netherlands

Introduction

The extracellular matrix (ECM) is a mesh of fibrous proteins that forms the basis of the tissue architecture and structurally supports the cells. Biophysical cues provided by the ECM are translated into biochemical signals by transmembrane integrin proteins. Understanding the interaction between the ECM and integrins is particularly important when designing instructive biomaterials and organoid culture systems. Previous studies suggest that fine-tuning the ECM composition and mechanical properties can improve organoid development [1]–[3]. Testing the effect of numerous different ECM ligands and mechanical properties of cell culture systems is experimentally complex but computationally achievable.

Methods

We developed an ordinary differential equation–based model that enabled us to simulate three main interactions, namely integrin activation, ligand binding and integrin clustering [4].



In contrast to previously published computational models, we account for the binding of more than one ligand to the same type of integrin. Binding rates of integrin $\alpha 5 \beta 3$ (*i* and **I**) and its two ligands, fibronectin (**L1**) and von Willebrand Factor A (**L2**), were obtained from the literature [5]. The binding rate constant for **L1** (k_3) was 10^4 times higher than the binding rate for **L2** (k_5). Initial conditions for ECM ligands were retrieved from proteomics analysis of kidney organoid ECM, performed in our department.

By simulating the model with different initial conditions for competing ligands and testing different sets of binding rates, we demonstrated that all the integrins are active and bound to a ligand at the steady state. The ligand with the higher binding rate (**L1**) occupies more integrins at the steady state than does the competing

ligand (**L2**), among single integrins as well as in clusters. Only when the binding rate constants for the competing ligands were set to be equal, the effect of initial concentration was pronounced. Local parameter sensitivity analysis was in accordance with these observations. The L2-bound integrin concentration (**IL2**) was most sensitive to the changes in binding and unbinding rates of the two competing ligands (k_3 , k_4 , k_5 , k_6). Furthermore, the **IL2** concentration is sensitive to the decrease in **L1** initial concentration but not to the changes in **L2** initial concentration.

In conclusion, the competition between the two ligands in the model system was driven by the integrin binding rate constants.

Discussion

The model is only a simplified representation of complex interactions at the cell–ECM interface. As it is, the model highlights the importance of correctly estimating the ligand–integrin binding rates in the design of advanced cell culture systems [4,6].

Future work will focus on extending the computational model with intracellular pathways, including developing data-driven approaches to identify and calibrate the pathways of interest. With cell type specific, quantitative input on integrin–ligand binding rates, this model can be used to develop instructive cell culture systems.

References

- [1] Geuens T, van Blitterswijk CA, LaPointe VLS., *Npj Regen Med* 2020;5:1–6.
- [2] Gjorevski N, Sachs N, Manfrin A, Giger S, Bragina ME, Ordóñez-Morán P, et al, *Nature* 2016;539:560–4.
- [3] Garreta E, Prado P, Tarantino C, Oria R, Fanlo L, Martí E, et al, *Nat Mater* 2019;18:397–405.
- [4] Karagöz Z, Geuens T, LaPointe VLS, van Griensven M, Carlier A., *Front Bioeng Biotechnol* 2021;9:340.
- [5] Hudson S V., Dolin CE, Poole LG, Massey VL, Wilkey D, Beier JI, et al., *Sci Rep* 2017;7:1–13.
- [6] Karagöz Z, Rijns L, Dankers PYW, van Griensven M, Carlier A., *Comput Struct Biotechnol J* 2021;19:303–14.

We gratefully acknowledge the Gravitation Program “Materials Driven Regeneration” funded by the Netherlands Organisation for Scientific Research. (024.003.013)

Mimicking *S. aureus* response with combinational synthetic TLR-agonists for MSC osteogenesis *in vitro*

P.K. Khokhani^{1,3}, J. Alblas^{1,3}, H. Weinans^{1,3}, M.C. Kruyt¹, D. Gawlitza^{2,3}

¹Department of Orthopaedics, University Medical Center Utrecht, Utrecht, The Netherlands

²Department Oral and Maxillofacial Surgery & Special Dental Care, University Medical Center Utrecht, Utrecht, The Netherlands

³Regenerative Medicine Center, Utrecht, The Netherlands

Introduction:

Strategies to enhance local bone formation, especially those synergizing with osteoinductive signals, are of great interest. Multiple studies indicate that pro-inflammatory mediators can act to stimulate bone formation.¹ Therefore we addressed the question whether pathogen-derived factors leading to a broad activation of the innate and consequently adaptive immune system, could enhance the efficacy of bone substitutes.

Bacterial infections generally lead to osteolysis and impaired bone healing, however, it was observed in a previous study that gamma irradiated (γ) *Staphylococcus aureus* led to excessive subperiosteal bone formation in a rabbit tibia model. This underscored that sterile inflammation from γ *S. aureus* could be harnessed for osteo-immunomodulation¹.

Upon infection, bacterial components are detected and processed predominantly by the host immune system via the toll-like receptors (TLRs) namely TLR2, TLR8, TLR9 and NOD-2². Activation of TLRs results in the release of pro-inflammatory cytokines that affect MSC differentiation³. Recent evidence from *in vitro* studies show that synthetic TLR-agonists possess immune-modulatory properties that may promote osteogenesis⁴.

In this study, we aim at recreating the immune-modulatory response exhibited by γ *S. aureus* by using a combination of various synthetic TLR-agonists (cocktails).

Methods:

The inflammatory effect of γ *S. aureus* and the cocktails on the immune cells isolated from human blood will be examined and osteogenic stimulation potential of the cocktails will be evaluated using multipotent mesenchymal stromal cells (MSCs).

Peripheral blood mononuclear cells (PBMCs) were isolated from blood collected from healthy human donors (n = 6) using the density gradient centrifugation method. After isolation, PBMCs were stimulated with γ *S. aureus* or different cocktails prepared by combining agonists for TLR2, TLR9, TLR8, and NOD-2. After 24 hours, the conditioned medium (CM) was collected and stored until further use. CM from unstimulated PBMCs was used as a control. MSCs stimulated with CM were used to measure metabolic activity (Alamar blue assay on day 3, 7 and 10) and cell proliferation (DNA content on day 10).

Furthermore, osteogenic capacity of the MSCs (n = 3) cultured with the conditioned media obtained from the unstimulated and/or stimulated PBMCs with γ *S. aureus* and/or cocktails-, was determined. Alkaline phosphatase activity, an early marker of osteogenic differentiation at 3,7,10, and 14 days and mineralization, a later marker of osteogenesis at day 28. Bone-specific

osteocalcin and osteonectin presence was measured by immunohistochemistry at day 14). The cytokine composition of the conditioned medium is characterized and signalling pathways active in MSCs.

Results and Discussion:

The conditioned medium from unstimulated PBMCs did not affect the metabolic activity or cell proliferation of the MSCs. Currently, experiments investigating the effect of the conditioned media obtained from γ *S. aureus* and/or different cocktails-stimulated PBMCs on osteogenic differentiation capacity on MSCs are ongoing.

In this study, we aim to demonstrate the feasibility of our *in vitro* model that takes into account the influence of the immune cells on MSC differentiation. This *in vitro* set up can provide insights into the mechanisms involving γ *S. aureus* recognition and also in identifying the combination of factors responsible for promoting bone formation. It is proven that γ *S. aureus* enhances bone formation *in vivo*. Therefore, we hypothesize that γ *S. aureus* enhances the osteogenic differentiation capacity of MSCs. Furthermore, we aim to mimic the cellular responses to γ *S. aureus* exposure by substituting it with a combination of synthetic TLR-agonists. In terms of safety and clinical translation, TLR-agonists as immune modulators are advantageous as they are already being used in clinical trials⁵. Thus, formulations with TLR-agonists used in this study can serve as clinically relevant immune-modulatory bone enhancing agents.

References:

1. Croes, M. *et al.* The role of bacterial stimuli in inflammation-driven bone formation. *Eur. Cell. Mater.* **37**, 402–419 (2019).
2. Askarian, F., Wagner, T., Johannessen, M. & Nizet, V. *Staphylococcus aureus* modulation of innate immune responses through Toll-like (TLR), (NOD)-like (NLR) and C-type lectin (CLR) receptors. *FEMS Microbiol. Rev.* **42**, 656–671 (2018).
3. Guihard, P. *et al.* Induction of osteogenesis in mesenchymal stem cells by activated monocytes/macrophages depends on oncostatin M signaling. *Stem Cells* **30**, 762–772 (2012).
4. Khokhani, P. *et al.* Use of Therapeutic Pathogen Recognition Receptor Ligands for Osteo-Immunomodulation. *Materials* **14**, 1119 (2021).
5. Luchner, M., Reinke, S. & Milicic, A. TLR Agonists as Vaccine Adjuvants Targeting Cancer and Infectious Diseases. *Pharmaceutics* **13**, 142 (2021).

Funding/acknowledgements

This work is funded by PPS allowance from Health-Holland LSH-TKI (grant number: LSHM18011) and EU's H2020 research and innovation programme under Marie S. Curie Cofund RESCUE (grant agreement No 801540).

Complex Coacervates as Next Generation Bioinks

M. Khoonkari^{1,2}, M. Oggioni¹, J. E. Sayed¹, M. K. Włodarczyk-Biegun¹, P. v. Rijn³, M. Kamperman¹

- 1- Polymer Science group, Zernike Institute for Advanced Materials, University of Groningen, Nijenborgh 4, 9747 AG Groningen, The Netherlands
- 2- Department of Medical Oncology, University of Groningen, University Medical Center Groningen, Hanzeplein 1, 9713 GZ, Groningen, Netherlands.
- 3- W.J. Kolff Institute for Biomedical Engineering and Materials Science-FB41, Groningen, University of Groningen, University Medical Center Groningen, A. Deusinglaan 1, 9713 AV Groningen, The Netherlands.

Abstract

Bioprinting is a tissue engineering technique that gained attention in recent years, with novel bioinks continuously being formulated to combine better printability and biocompatibility with minimal use of additional (chemical) treatments [1]. The key requirement of a bioink to enable printability is that it has to flow when subjected to the shear stress through the needle but behave as a free-standing solid without shape relaxation once printed [2]. Considering the aforementioned characteristics, complex coacervates systems are well-suited candidates as bioink. Complex coacervation is an associative liquid-liquid phase separation phenomenon driven by electrostatic attraction between oppositely charged macro-ions (e.g. polysaccharides, proteins etc.) and counterion release, resulting in a polymer rich aqueous phase in equilibrium with a polymer poor phase [3]. For a given polyelectrolyte couple, depending on the salt concentration of the medium, a complex coacervate either behaves as a free-flowing viscoelastic fluid or a rigid polyelectrolyte complex solid or anything in between [2, 4]. In our work, we made use of this versatility to develop a complex coacervate-based 3D printing bioink composed of hyaluronic and chitosan biopolymers (Figure 1). The printability of these complex coacervates (i.e. composed of hyaluronic (HA) acid and chitosan (CH)) was shown to depend on the average molar mass of the components, the pH and the ionic strength at which they are prepared.

By fine-tuning the previously mentioned physico-chemical parameters we were able to produce a set of bioinks that can be used in different environmental conditions. The developed bioinks can not only be dried and re-hydrated without loss of shape fidelity, but also be printed into a liquid medium (fresh-printing) without the need of any chemical modification or post-printing curing process. These promising results show the potential of coacervate-based bioinks to be used as 2D and 3D scaffolds in cell culture studies.

Keywords: complex coacervation, polyelectrolytes, 3D bioprinting.

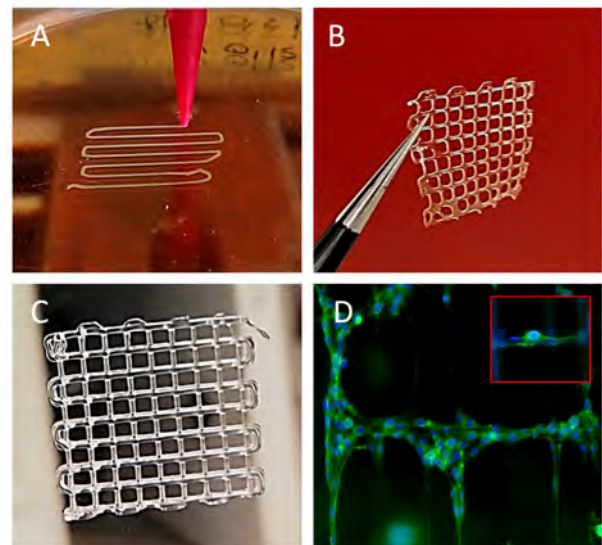


Figure 1. Hyaluronic acid-chitosan complex coacervate as an ink for 3D bioprinting. Fresh printing of coacervate within a water bath (A), dehydrated (dried) printed scaffold (B), rehydrated printed scaffold (C), immunofluorescent microscopy images of 3T3 cells cultured on the printed coacervate scaffold, Blue: Nuclei, Green: F-Actin (D).

References

- [1] N. Paxton et al, *Biofabrication*, 2017, 9, 044107
- [2] A. Schwab, R. Levato, M. D'Este, S. Piluso, D. Eglin, and J. Malda, *Chem. Rev.*, 2020, 120, 11028–11055
- [3] C. E. Sing, S. L. Perry, *Soft Matter*, 2020, 16, 2885–2914
- [4] Q. Wang, J. B. Schlenoff, *Macromolecules* 2014, 47, 3108–3116

Mg-Al layered double hydroxides nanoparticles coating with PEG prevents particles aggregation and degradation: mechanism and effect on the stability in physiological conditions

Lei Li, Eliza M. Warszawik, and dr. Patrick van Rijn

W.J. Kolff Institute for Biomedical Engineering and Materials Science, University of Groningen/ University Medical Center Groningen (UMCG), Ant. Deusinglaan 1, Groningen, The Netherlands

Introduction: Layered double hydroxides (LDHs), also known as hydrotalcite like compounds^[1] are considered as biocompatible nanocontainers^[2], and have been explored as drug delivery carriers^[3] since their discovery in 1842 by Swedish scientists^[4]. LDHs have versatile features suitable for drug delivery, which include high surface area, particle swelling property, memory effect, high anion exchange capacity and stable physicochemical properties^[5]. LDHs have a special layered structure and exchangeable ability of interlayer ions, and a series of functional new materials can be designed by exchange of anions between the layers of LDHs^[6]. Like many other nanoparticles, LDH particles tend to aggregate in the presence of physiological environment. The increased particle size after aggregation reduces the cellular uptake rate of LDHs, and increases inflammatory responses. Particle aggregation may also cause blood vessel clotting, leading to animal death. So it is necessary to use some methods, like conducting surface modification to increase the stability of the particles. Moreover, to our knowledge the colloidal stability of coated particles in physiological conditions has not been yet accessed.

In this study, we investigated various methods of de-aggregation of hydrotalcites and isolation of single HTC particles. Then, we modified the surface of hydrotalcites with carboxylic acid (COO-) terminated methoxy-PEG chains and studied the colloidal stability of coated particles in physiological conditions.

Method: We tried different physical ways (grinding, tip-sonication, bath-sonication) to de-aggregate the hydrotalcites particles, and then the de-aggregated particles were further coated with carboxylic acid terminated methoxy-PEG 5k.

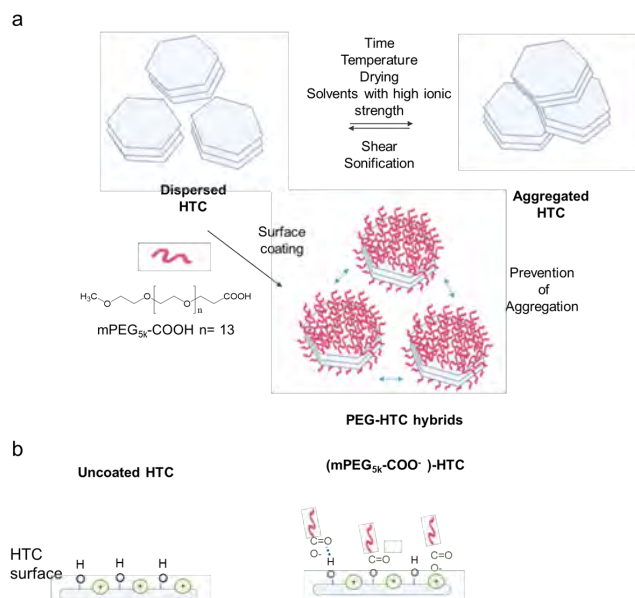
Then we investigated the stability of the de-aggregated particles and further surface modified particles in aqueous suspensions. The solution of the particles was diluted with water or 10 mM sodium buffered saline (PBS). Two different pH of the PBS buffers were selected: 7.4, 6.5 as they resemble the pH of the physiological fluids, the extracellular pH of more acidic extracellular pH of some of the cancer cells, respectively. After diluting suspension with PBS, we followed the particle size by DLS over time.

Results and Discussion: Particle drying or autoclaving (AU) which are often performed as a part of fabrication process of hydrotalcites lead to increased particles surface charge and formation of aggregates larger than 3000nm. It was able to

decrease the size of particles to around 1000nm by grinding. Then, If the grinded particles were further treated by bath sonication for 2 h or tip sonication for 5min, the size of the particles could be further reduced to around 300 nm, which is very close to the actual size of hydrotalcite under TEM.

The physical method can effectively de-aggregate hydrotalcite, but after a period of time, the particles would form aggregation again. The stability of the particles was obviously improved after modified with carboxylic acid (COO-) terminated methoxy-PEG chains. This is because the long chain of methoxy-PEG can provide steric hindrance to prevent agglomeration.

Conclusion: In this work we successfully de-aggregated hydrotalcites particles by grinding and sonication, and also further improved the stability of the particles by the modification with carboxylic acid terminated methoxy-PEG 5k.



Scheme 1. Schematic illustration of HTC particles aggregation and disaggregation mediated by different events/forces and the strategy to prevent particles aggregation by surface coating with PEG; a) functional groups on the surface and structural positive charge in uncoated HTC b) interactions between the surface of hydrotalcites and different PEG coatings

References:

- [1] Chimene, David, D. L. Alge, and A. K. Gaharwar. *Advanced Materials* 27.45(2016):7261-7284.
- [2] Li, Bei, et al. *Advanced Materials* (2017):1700373.
- [3] Choy, Jin Ho, et al. *Applied Clay Science* 36.1-3(2007):0-132.
- [4] G. Mishra, B. Dash, S. Pandey. *Applied Clay Science* 153 (2018): 172-186.
- [5] Vittoria, Vittoria, et al. *Recent Patents on Nanotechnology* 6.3(2012):-.
- [6] Trikeriotis, M, and D. Ghanotakis. *International Journal of Pharmaceutics* 332.1(2007):176-184.

Extracellular Protein Identification Cytometry (EPIC) single cell analysis

Marieke (M.A.W.) Meteling¹, Castro (C.) Johnbosco¹, Tom (T.) Kamperman¹, and Jeroen (J.C.H.) Leijten¹

¹Leijten Lab, Department of Developmental BioEngineering, TechMed Centre, University of Twente, The Netherlands

Introduction

One of the main methods to investigate cellular function, such as to study the degree of differentiation of stem cells, donor cell quality, and cellular response to drugs or inflammatory molecules, is to analyse the extracellular matrix (ECM) deposition of cells. Current methods such as Western blot, mass spectroscopy, or immunostaining, either require the removal of cells and processing of the ECM prior to analysis, or only allow for the analysis of the ECM of a few hundred cells or less. In the first case, the bulk ECM is analysed and cannot be attributed to a specific cell, while in the latter case too few cells are analysed to be able to draw conclusions regarding subpopulations within the entire cell population. Moreover, these techniques can only be employed to a limited extent to analyse ECM deposition in 3D cell culture. Hence, we propose Extracellular Protein Identification Cytometry (EPIC) single cell analysis as a novel method that allows quantifying specific pericellular matrix proteins of individual cells within a 3D microenvironment in a high-throughput manner.

Methods

Human mesenchymal stem cells (hMSCs) were cultured up to passage 4 and were used for encapsulation.

Dex-TA was synthesised as previously reported^{2,3}.

Microfluidic droplet generators for single cell encapsulation were produced using standard photolithography for the patterned wafers and replica moulding for the PDMS chips bonded to microscopy glass slides. Two different chip designs were used for droplet generation and delayed gelation, as has been previously described¹.

For cell encapsulation¹, detached hMSCs (10^7 cells/ml) were resuspended in 5% Dex-TA dissolved in sterile PBS mixed with 44 U/ml HRP and 8% OptiPrep. The flow rates were 6 μ l/min, 2 μ l/min and 30 μ l/min for the oil phase with 2% Pico-Surf, aqueous phase with cells, and H₂O₂ solution respectively.

The generated microgels were retrieved with Pico-Break treatment and washed with PBS¹. The remaining microgels were transferred to chondrogenic differentiation medium⁴ and cultured for three weeks.

For immunostaining the microgels were washed with PBS and fixed with 4% PVA. Permeation was performed with 0.25% TritonX-100 in PBS. The microgels were blocked with 1% BSA in PBS for 1 hour. For 24 h each the microgels were incubated with primary antibodies anti-collagen II (ab34712) and anti-aggrexin (ab232628) at 4°C, followed by washing with PBS. This was repeated for the secondary antibodies, Alexa Fluor 488 (COL2A) and 647 (ACAN) respectively. DAPI was added to visualise the nucleus. Imaging was performed with a confocal microscope.

For the sorting of cell-laden and cell-free microgels, the microgels were stained with 0.5% (v/v) Vybrant DiO and sorted with a FACS Aria II instrument.

Results and Discussion

Single cell microgels were generated as previously described¹. The encapsulated cells were cultured for three weeks in chondrogenic differentiation medium, to allow for pericellular matrix deposition. As a proof of concept, the microgels were fixed and immunostaining for chondrogenic differentiation markers COL2A and ACAN was performed. Confocal analysis showed that a pericellular matrix formed and could be visualised using indirect immunofluorescence (Fig. 1A).

To determine whether fluorescence signals within the hydrogel could be detected with FACS, microgels were stained with Vybrant DiO. Based on the microgel's fluorescent signal, it was possible to detect and sort empty from cell-laden gels (Fig. 1B).

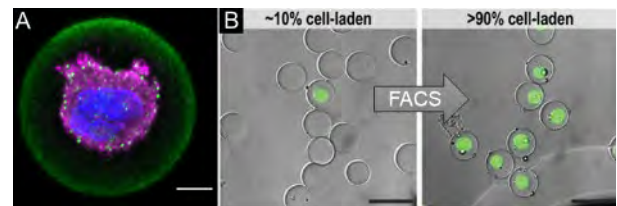


Figure 1: A) Confocal image of encapsulated hMSC stained for COL2A (green), ACAN (pink) and DAPI (blue) after chondrogenic differentiation. B) Fluorescent signal of cells in microgels is detectable with FACS⁵. Size bars: black 50 μ m, white 7 μ m

Conclusion & Outlook

Cells could be encapsulated and cultured for 3 weeks in the microgels. Antibody staining of specific ECM proteins was possible and visible under a confocal microscope. Also, it was shown that it is possible to detect, quantitate, and sort encapsulated cells using FACS based on their fluorescent signal.

As a next step, the encapsulated cells stained with antibodies will be analysed with FACS. Suitable antibodies will be investigated to allow for both quantitative multiplexed FACS analysis, as well as specific binding to ECM proteins of interest.

Acknowledgements

The authors acknowledge Niels Willemsen for technical support. Financial support was received from the European Research Council (ERC, Starting Grant, #759425) and the Dutch Research Council (NWO, Vidi Grant, #17522).

References

1. Kamperman T, et al. *Small*. 2017;13(22)
2. Wennink JWH, et al. *Macromol. Symp.* 2011;309, 213.
3. Jin R, et al. *Biomaterials*. 2007;28(18)
4. Zhong L, et al. *Stem Cells Dev.* 2016;25(23)
5. Kamperman T, et al. *Adv Healthc Mater.* 2017;6(3)

Contact

m.a.w.meteling@utwente.nl, jeroen.leijten@utwente.nl

An expandable medical device to close surgically induced fetal membrane defects

R.T.C. Meuwese^{1*}, E.M.M. Versteeg¹, J. van Drongelen², D. de Hoog¹, D. Bouwhuis¹, F.P.H.A. Vandembussche^{2,3}, T.H. van Kuppevelt¹, W.F. Daamen¹

1. Department of Biochemistry, Radboud Institute for Molecular Life Sciences, Radboud university medical center, PO Box 9101, 6500 HB, Nijmegen, The Netherlands
 2. Department of Obstetrics & Gynaecology, Radboud university medical center, PO Box 9101, 6500 HB, Nijmegen, The Netherlands
 3. Department of Obstetrics & Gynecology, Helios Klinikum Duisburg, An der Abtei 7, 47166 Duisburg, Germany
- *Corresponding author: Rob.Meuwese@radboudumc.nl

INTRODUCTION: Iatrogenic preterm premature rupture of membranes (iPPROM) after minimally invasive fetal surgery remains a strong trigger for premature birth. As fetal membrane defects do not heal spontaneously and amniotic fluid leakage and chorioamniotic membrane separation may occur, we developed a collagen plug with shape memory, that is biocompatible and can be fetoscopically applied. This plug expands upon employment to seal fetal membranes, hence minimizing amniotic fluid leakage and potentially iPPROM.

MATERIALS AND METHODS: Lyophilized type I collagen plugs were given shape memory and crimped to fit through a fetoscopic cannula (\varnothing 3 mm). Expansion of the plug was examined in phosphate-buffered saline (PBS). Its sealing capacity was studied *ex vivo* using human fetal membranes, and *in situ* using a porcine bladder model.

RESULTS: The crimped plug with shape memory expanded and tripled in diameter within one minute when placed into PBS (Fig. 1), while a crimped collagen plug without shape memory did not expand beyond 3 mm. In both human fetal membranes and porcine bladder, the plug expanded in the defect, secured itself in, and sealed the defect without membrane rupture.

CONCLUSION: In conclusion, a collagen plug with shape memory is a promising medical device to rapidly seal a fetoscopic defect in fetal membranes at the endoscopic entry point.

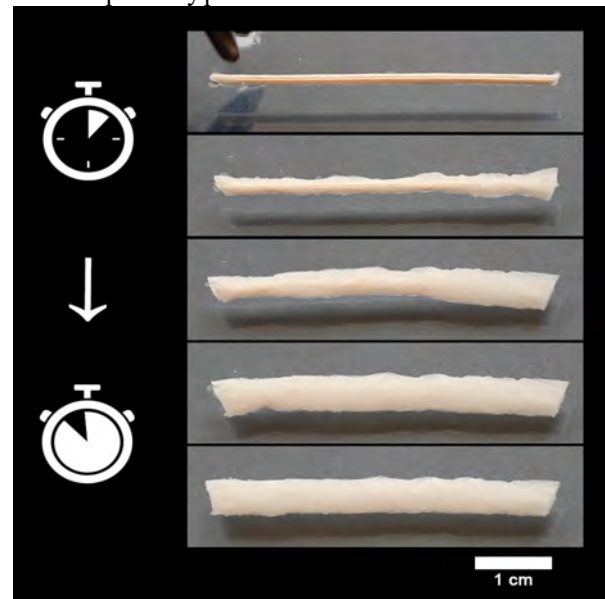


Figure 1. Collagen plug with shape memory expands upon wetting in PBS and tripled in diameter within one minute. Bar is 1 cm.

Engineered Peptide-functionalized Polymeric Nanocarrier System to Target Pancreatic Tumor Stroma

A.M.R.H. Mostafa, J. Schnittert, P. R. Kuninty, T. Satav, J. Prakash

Engineered Therapeutics, Department of Biomaterials, Science and Technology, Tech Med Center, University of Twente, 7500AE Enschede, The Netherlands.

Email: a.m.r.h.mostafa@utwente.nl

Introduction:

Pancreatic ductal adenocarcinoma (PDAC) is characterized by its highly desmoplastic and abundant stroma which accounts for up to 90% of total tumor mass. Cancer-associated fibroblasts (CAFs) is the major contributor cell-type in desmoplasia and the major source of CAFs is pancreatic stellate cells (PSCs) [1,2]. Due to its highly secretory function, CAFs produce the majority of extracellular matrix (ECM) proteins and cytokines [2]. CAFs are responsible for the promotion of various tumorigenic properties of PDAC, including angiogenesis, proliferation, immune suppression and chemoresistance [3]. This highlights CAFs as a promising therapeutic target in the tumor treatment. In this study, we have identified the transmembrane receptor integrin alpha 11 (ITGA11) as a highly upregulated receptor on CAFs selectively, while no overexpression was observed in normal human pancreatic tissue and other normal human organs including liver, lungs, kidneys, spleen, breast, hence, a potential drug targeting receptor [4]. In order to selectively target CAFs, we developed an ITGA11-binding novel peptide (namely AXI). In this study, we aim to establish an AXI-based polymeric nanoparticles as a suitable targeted drug delivery system capable of selective delivery of inhibitory cargo to CAFs in order to attenuate pancreatic cancer.

Methods:

The 12 amino acid-long AXI peptide sequence against ITGA11 was selected using phage display method. Microscale thermophoresis was implemented to test the peptide affinity towards ITGA11. *In vitro* binding assay was carried out to test its selectivity to activated PSC. To demonstrate the capability of this peptide to enhance the selective targeting of drug delivery systems to CAFs, we functionalized the surface of PLGA/PCL polymeric nanoparticle with either AXI as a targeting ligand or the scrambled version (sAXI) as a control. *In vitro* uptake study was performed to investigate the specific uptake of this nanoparticle system (Dil-labelled) by activated PSCs. Immunocompetent, subcutaneous syngeneic KPC pancreatic cancer murine model which is known for its abundant desmoplastic tumor stroma was utilized to evaluate the biodistribution of our nanoparticle system. Mice were intravenously injected with either AXI- or sAXI-conjugated nanoparticles, labeled with both rhodamine (for tissue accumulation studies) and near-infrared dye cy7 (for biodistribution live imaging studies).

Results and Discussion:

We showed selective binding of our novel AXI peptide to the ITGA11 receptor, as determined with microscale thermophoresis. Corresponding to elevated levels of ITGA11 in TGF- β -activated PSCs, we showed higher accumulation of AXI in the activated cells compared to quiescent ones. In contrary, we demonstrated a

significant reduction of AXI binding potential to PSCs after ITGA11 receptor knockdown. Importantly, upon nanoparticle-surface functionalization with our peptide, AXI-conjugated nanoparticles showed higher accumulation in PSCs in *in vitro* uptake studies, compared to both sAXI-conjugated nanoparticles and the unconjugated ones (Fig. 1A). *In vivo* biodistribution animal study demonstrated higher accumulation of AXI-nanoparticles into animal tumors compared to the sAXI-nanoparticles (Fig. 1B, C). After tumor harvesting, intratumoral histological analysis demonstrated higher colocalization of rhodamine-labelled AXI-NPs with ITGA11-expressing CAFs and higher tumor tissue penetration compared to sAXI counterparts.

Conclusion:

Our study reveals a novel peptide engineered polymeric nanocarrier system which is in potential to target the tumor stroma in pancreatic tumor. Using *in vivo* imaging data, we demonstrate that our novel nano-targeting platform might be able to target CAFs and reprogramme them in the tumor stroma to enhance therapeutic efficacy of anticancer drugs.

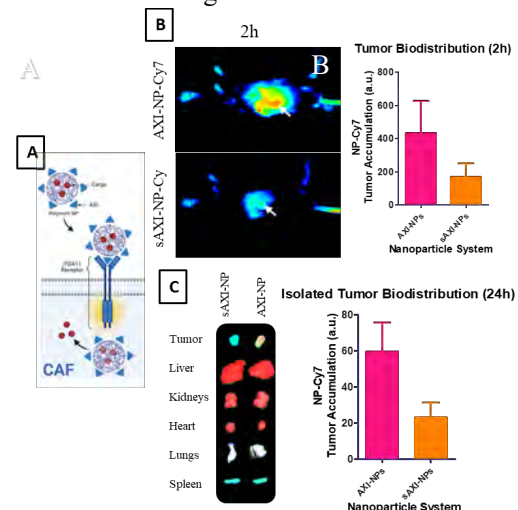


Figure 1. A) Schematic representation of uptake affinity of AXI-NPs towards ITGA11-expressing CAFs. B) Biodistribution and quantification of cy7-labelled AXI and sAXI nanoparticles in KPC animal tumor model 2 hours after NPs intravenous injection. Arrows are indicative of tumors. C) Accumulation of AXI/sAXI-NPs in tumor and organs 24h after intravenous injection.

References:

1. Schnittert, J., Bansal, R., Storm, G. and Prakash, J. (2018). Integrins in wound healing, fibrosis and tumor stroma: High potential targets for therapeutics and drug delivery. *Advanced Drug Delivery Reviews*, 129, pp.37-53.
2. Kuninty, P. R., Bansal, R., S., D. G., Mardhian, D. F., Schnittert, J., van Baarlen, J., Storm, G., Bijlsma, M., van Laarhoven, Metselaar, J. M., Kuppen, P. J. K., Vahrmeijer, A., Ostman, A., Sier, C. F. M., Prakash, J. (2019) ITGA5 inhibition in pancreatic stellate cells attenuates desmoplasia and potentiates efficacy of chemotherapy in pancreatic cancer. *Science Advances* Sep 4;5(9):eaax2770.
3. Schnittert, J., Bansal, R. and Prakash, J. (2019). Targeting Pancreatic Stellate Cells in Cancer. *Trends in Cancer*, 5(2), pp.128-142.
4. Schnittert, J., Bansal, R., Mardhian, D., Van Baarlen, J., Ostman, A. and Prakash, J. (2019). Integrin α 11 in pancreatic stellate cells regulates tumor stroma interaction in pancreatic cancer. *The FASEB Journal*, 33(5), pp.6609-6621.

3D Mechanical Constraint Model to Understand Remodeling in Beating Cardiac Microtissues

D. Mostert^{1,2}, I. Jorba^{1,2}, N.A. Kurniawan^{1,2}, C.V.C. Bouten^{1,2}

1 Eindhoven University of Technology, Department of Biomedical Engineering, PO Box 513, 5600 MB Eindhoven, The Netherlands. Tel: +31 (0)402472279

2 Institute for Complex Molecular Systems (ICMS), PO Box 513, 5600 MB Eindhoven, The Netherlands. Tel: +31 (0)402473532

Corresponding email: d.mostert@tue.nl

Introduction: In the beating and mechanically active human myocardium, cardiomyocytes (CMs) and quiescent cardiac fibroblasts (cFBs) are linearly arranged as dense cellular aggregations surrounded by an anisotropic collagen matrix to enable electromechanical coupling between cells and aid in their coordinated contraction¹. Upon cardiac injury, ischemia results in a massive loss of CMs and initiates adverse remodeling of the anisotropic structure, typically found in healthy myocardium, into disorganized fibrotic tissue. Disruption of the highly organized structure does not only result in impaired coordinated contraction but also in compromised differentiation, matrix remodeling and mechanotransduction of resident and newly injected or recruited cardiac cells². Understanding the remodeling processes in beating cardiac tissues is therefore crucial to provide new insights to (re)engineer structural organization in living cardiac tissues *in vivo* and *in vitro*. The desire to regain the structural anisotropy of tissues after injury is not specific for the myocardium and poses a challenge in many biological tissues³. To date, several mechanical constraint models have been proposed to study the organization of both cells and collagen in response to changes in the mechanical microenvironment. De Jonge et al. showed that releasing constraints in one direction resulted in anisotropic cell and tissue reorganization in fibroblast populated hydrogels⁴. Moreover, van Spreeuwel et al. demonstrated that imposing either uniaxial or biaxial constraints onto cardiac microtissues, consisting of cFBs and CMs, resulted in anisotropic or isotropic organization, respectively⁵. However, it remains unclear whether changing mechanical constraints in cardiac microtissues, containing beating CMs, results in anisotropic cell and tissue reorganization.

Aim: We aim to investigate how cardiac beating influences the formation and remodeling of a aligned *in vitro* 3D engineered cardiac microtissues. Moreover, by exploring the relationship between structural tissue organization, tissue mechanics, and the expression of cardiac specific proteins, we aim to investigate if regaining structural anisotropy, found in healthy human myocardium, can restore coordinated contraction in the cardiac microtissues.

Materials and Methods: We generated microscale constructs of cFBs and hPSC-CMs within 3D matrices, inspired by micro tissue gauges (μ TUGs)⁶, called cardiac microtissues. Micropillars of polydimethylsiloxane (PDMS) were used to constrain the remodeling of collagenous 3D matrices while simultaneously reporting tissue forces during this process. After two days of biaxial tissue formation, constraints were removed in one direction in microtissues consisting of either cFBs,

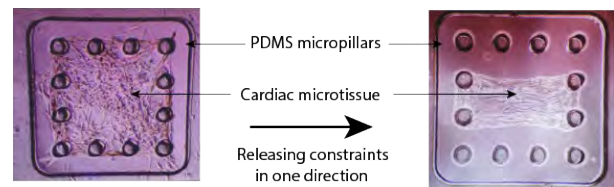


Figure 1: Cardiomyocytes and cardiac fibroblasts are seeded in a collagen/Matrigel mixture between PDMS micropillars, forming an isotropic microtissue. After two days, remodeling is induced by constraint release in one direction. Tissue contractility, as well as collagen and cell organization, is analyzed up to five days after post release.

or cFBs in co-culture with hPSC-CMs (Figure 1). By concurrent usage of a viable collagen probe (CNA-35 OG) and fluorescently labeled hPSC-CMs, both cell and matrix organization can be followed over time in the same sample. Moreover, tissue contraction forces can be quantified using finite element modeling of micropillar deflections and cardiac marker expression can be analyzed using confocal microscopy.

Results and Discussion: We demonstrated that removal of mechanical constraints in one direction enabled the remodeling from disorganized towards a aligned cardiac microtissues. Orientation analysis of both cells and the collagen network demonstrated the highest oriented cell and fiber fraction in the direction of the constraints after five days of culture whereas no preferred orientation was observed in biaxially constrained constructs. Collectively, releasing constraints in biaxially constrained cardiac microtissues resulted in remodeling towards anisotropic tissue organization.

Conclusion and Outlook: Collectively, this study aims to highlight the dynamic relationship between structural organization, cellular forces, and cellular phenotype and presents an approach to study this relationship within cardiac microtissues. After demonstrating the ability of our approach to induce anisotropy in cardiac microtissues, next steps are to systematically compare remodeling regimes in cardiac microtissues of 1) cFBs alone, 2) cFBs in co-culture with beating hPSC-CMs, and 3) cFBs in co-culture with non-beating hPSC-CMs to assess the effect of CM contraction on regaining anisotropy and investigate whether this increases the coordinated contraction of these microtissues.

Acknowledgements: This project is funded by the Materials Driven Regeneration (MDR) Gravitation Program.

References:

- ¹ Parker et al., *Phil Trans Roy Soc B*, 2007;
- ² Gabriel Costa et al., *Pathophysiology*, 2018;
- ³ Isenberg et al., *Materials Today*, 2006;
- ⁴ De Jonge et al., *Ann Biom Eng*, 2013;
- ⁵ v. Spreeuwel et al., *Int Biol*, 2014;
- ⁶ Legant et al., *Int Biol*, 2012

Cellular senescence impairs chondrogenic differentiation of MSCs via TGF β signaling interference

C Voskamp¹, WJLM Koevoet², GJVM van Osch^{1,2}, R Narcisi¹

¹ Department of Orthopaedics and Sports Medicine, Erasmus MC, University Medical Center Rotterdam, 3015 CN Rotterdam, the Netherlands; ² Department of Otorhinolaryngology, Erasmus MC, University Medical Center Rotterdam, 3015 CN Rotterdam, the Netherlands. GJVM van Osch and R Narcisi contributed equally

Introduction and objective: Mesenchymal stem/stromal cells (MSCs) are often studied for their possible tissue engineering applications. During *in vitro* expansion, however, MSCs enter a state of permanent growth arrest while remaining metabolically active, known as cellular senescence. Senescence can negatively affect tissue homeostasis and an increased amount of senescence cells can be found in pathological tissues, such as osteoarthritic cartilage. Moreover, It has been shown that cellular senescence may alter the differentiation capacity of MSCs towards the osteogenic and adipogenic lineage, while little is known on how cellular senescence affect the chondrogenesis. Therefore, the aim of this study was to determine the effect of senescence on chondrogenic differentiation capacity of MSCs.

Materials and Methods: Cellular senescence was induced in MSCs in monolayer prior chondrogenic differentiation, or at different time points during chondrogenic pellet culture (day-7 or day-14) using a validated gamma irradiation protocol based on a 20 Gy stimulation. The typical senescence markers *P16*, *P21* and *IL16*, and the β -galactosidase staining were used to confirm irradiation-induced senescence.

Chondrogenic differentiation capacity was induced by a standard protocol for 21 days using a 3D pellet culture system (200,000 MSCs per each pellet), and evaluated by (immuno)histochemistry, DMB (dimethylmethylene blue) assay for glycosaminoglycan quantification and RT-PCR for the chondrogenic markers *SOX9*, *COL2A1* and *AGCN*. To investigate the paracrine effect of senescent cells on recipient cells, we treated chondrogenic pellets using 2-day conditioned media from senescent cells and treat chondrogenic pellets for 24h, which were then analyzed for the expression of chondrogenic (*SOX9*, *COL2A1* and *AGCN*) and catabolic (*MMP-1*, *MMP-3*, *MMP-13* and *ADAMTS4*) markers at mRNA level. Western blot analysis on phosphorylated SMAD2 (P-Smad2 monoclonal antibody) was performed to identify TGF β signaling activation. Non senescent cells or conditioned media from non-senescent cells was used as control.

Results: When cellular senescence was induced prior differentiation, it abolished the chondrogenic capacity of MSCs (Figure 1) with more than 95% reduction of GAG and Collagen type-2 deposition, as well as for all the chondrogenic markers measured by RT-PCR, in all the donor tested. A similar trend but with a less significant reduction was observed when senescence was induced at day-7 of differentiation. Interestingly, no effect on chondrogenic differentiation was detected when irradiation-induced senescent was applied at day-14 of differentiation.

Moreover, medium conditioned by pellets cultures made of senescent cells had no significant effect on the

expression of catabolic and anabolic markers measured by RT-PCR in recipient chondrogenic pellets. This suggests the negligible paracrine effect of senescent cells in our model.

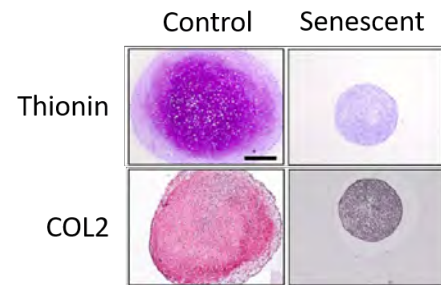


Figure 1: Representative images ($N=9$) of the (immune)histological evaluation of pellet cultures after 21 days of chondrogenic induction in the indicated conditions. Thionin stains Glycosaminoglycans, COL2 = immunostaining for Collagen type-2. Bar = 150 μ m.

In order to better understand whether or not senescence was able to interfere with the chondrogenic differentiation process at molecular level, we analyzed the ability of senescent MSCs to respond to TGF β , the main pro-chondrogenic factor for MSCs. Upon stimulation with TGF β 1, phosphorylated SMAD2 levels (one of the main intracellular TGF β effectors) were strongly reduced in senescent MSCs compared to control (Figure 2).

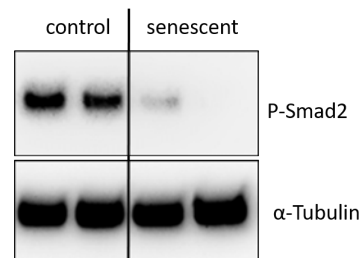


Figure 2: Representative images of Western Blot analysis ($N=6$) performed on monolayer MSCs stimulated with TGF β 1 for 30 minutes in the indicated conditions. α -Tubulin was used as reference protein.

Conclusions: In this study we showed that cellular senescence reduced the chondrogenic differentiation capacity of MSC, but only when senescence occurs early during differentiation, and likely by negatively impacting the ability of the cells to respond to the pro-chondrogenic factor TGF β 1. This is a step forward in the understanding of the molecular mechanisms governing cellular senescence in MSC, and towards better optimizing the use of MSC for tissue engineering applications.

Mixed Matrix Membrane for Urea Removal in a Wearable Artificial Kidney

N. Noor¹, P. Driest², G.P. Claassen¹, I. Geremia¹, J.A.W. Jong², B. Lentferink³, C.F. van Nostrum², W.E. Hennink², K.G.F. Gerritsen³, D. Stamatialis¹

¹(Bio) Artificial Organs, Biomaterials Science and Technology, TechMed Centre, Faculty of Science and Technology, University of Twente, P. O. Box 217, 7500 AE, Enschede, The Netherlands

²Department of Pharmaceutics, Utrecht Institute for Pharmaceutical Sciences (UIPS), Utrecht University, Universiteitsweg 99, 3584 CG Utrecht, The Netherlands

³Department of Nephrology and Hypertension, University Medical Centre Utrecht, 3584 CX Utrecht, The Netherlands

Abstract: A wearable artificial kidney would provide end-stage kidney disease (ESKD) patients a continuous therapy for better health and quality of life. The concept is based on continuous regeneration of a small volume of dialysate so that it can be reused in a closed loop. Urea removal from dialysate is one of the major challenges. Here we propose application of mixed-matrix membranes (MMMs) that contain novel sorbents for urea removal. Hollow fiber (HF) MMMs were prepared using polyethersulfone polymer dope containing ninhydrin or phenylglyoxaldehyde (PGA) functionalized polystyrene sorbent particles. Urea removal tests were done both in static and dynamic mode. Dynamic urea removal by the MMM with ninhydrin sorbents at 70 °C was much higher than that under static conditions (3.4 ± 0.3 vs 1.3 ± 0.1 mmol/g sorbent particles in 4 hours).

Urea removal capacity of the ninhydrin sorbent particles in the HF-MMM in dynamic setup was higher than that of the suspended particles alone which was attributed to an additional physisorption effect. HF-MMMs containing PGA sorbent particles were analyzed as well. A correlation among the membrane morphology, transport property, and urea adsorption capacity is drawn for the two different particles incorporated HF-MMMs. In short, incorporation of urea sorbents in HF-MMM arrangement promises lower amount of material usage for the removal of daily produced urea by a ESKD patient.

E-mail:

N. Noor: n.noor@utwente.nl

P. Driest: p.j.driest@uu.nl

G.P. Claassen: g.p.claassen@student.utwente.nl

I. Geremia: ilar.geremia@gmail.com

J.A.W. Jong: j.jong@nextkidney.com

B. Lentferink: B.H.Lentferink@umcutrecht.nl

C.F. van Nostrum: C.F.vannostrum@uu.nl

W.E. Hennink: W.E.Hennink@uu.nl

K.G.F. Gerritsen: K.G.F.Gerritsen@umcutrecht.nl

D. Stamatialis: d.stamatialis@utwente.nl

Application of Microbe-derived Agents for Osteogenesis in a Ceramics-based Bone Graft

N.R. Rahmani¹, A. Duits¹, M. Croes¹, P. Khokhani¹, J. Alblas¹, D. Gawlitta², H. Weinans¹, M.C. Kruyt¹

¹Department of Orthopaedics, University Medical Center Utrecht, Utrecht, The Netherlands

²Department Oral and Maxillofacial Surgery and Special Dental Care, University Medical Center Utrecht, Utrecht, The Netherlands

Introduction

Bone grafting is among the most frequent form of transplantation, utilized to manage a variety of maxillofacial and orthopedic cases such as fracture repair, reconstruction surgery, spinal fusion. Synthetic grafts mimicking properties of human bones are continuously developed as an alternative to autologous bone grafts. The host's inflammatory reaction towards synthetic grafts is a critical factor that determines the long-term fate of an implanted material. The terms 'advanced' or 'smart' biomaterials are often correlated with materials showing immune-interacting properties that benefit regeneration.

Recent evidence suggests that inflammation towards certain bacterial, fungal, and viral components can have a positive effect towards osteogenesis¹⁻³. Presumably, the mechanism involves the activation of the innate immune cells, that recognize these components as Pathogen Associated Molecular Patterns (PAMPs). The inflammatory milieu generated then provides the cues that propagate repair and regeneration of new bone tissue. On the other hand, excessive and prolonged inflammation will activate bone-resorbing cells. Due to their immune-modulating properties, PAMPs show the potential to be applied as a biological agent to advance synthetic bone grafts.

This study tests a broad range of PAMPs on their potential to enhance osteogenesis in a biphasic calcium phosphate (BCP) graft. BCP grafts loaded with PAMPs are implanted ectopically in subcutaneous pockets of rabbits. Bone morphogenetic protein-2 (BMP-2) is loaded onto constructs to trigger osteogenesis outside the bone niche.

Materials and Methods

Implant preparation

The PAMPs investigated in this study include inactivated *Staphylococcus Aureus*, inactivated *Candida Albicans*, Bacillus Calmette-Guérin (BCG), peptidoglycan, lipopolysaccharide, lipoteichoic acid, Poly (I:C) high molecular weight, CpG oligodeoxynucleotide type c, Pam3CSK4, and curdlan.

The scaffolds used were biphasic calcium phosphate discs (d=9mm, h=6mm) comprising of 65% to 75% Tri-Calcium Phosphate (TCP—Ca₃(PO₄)₂) and 25% to 35% Hydroxyapatite (HA—Ca₁₀(PO₄)₆(OH)₂), with a porosity of ±75% (MagnetOs; Kuros Biosciences).

PAMPs were diluted in PBS and a suboptimal dose of BMP-2 was pipetted onto BCP discs, then air-dried overnight. The release profile of loaded PAMPs were measured at different time points.

Animal Study

A total of 24 New Zealand White Rabbits (female, 5 months old, 4.5-5 kg) were included in the study

according to approved protocols from the Committee for Animal Experimentation. Prior to surgical intervention, peripheral blood was collected and stimulated with varying concentrations of PAMPs, subsequently measured for IL-6 and IL-1β to determine the immune response. Surgical procedure was conducted to implant BCP constructs in separate subcutaneous pockets, with a total of 10 pockets per animal. On week 2 and 3, fluorochrome labels using Calcein Green and Xylenol Orange were administered. To monitor the systemic response, rabbit's body weight, temperature, and serum acute phase proteins were measured weekly. The constructs were implanted for 5 weeks and then harvested for histomorphometry analysis.

Results

PAMPs stimulated a dose-dependent response in rabbit blood with increased levels of both IL-6 and IL-1β. Surgical procedure was tolerated by the animals and no significant changes in body weight or temperature were observed during the study. One rabbit reached humane end point, due to pain behaviour, and excluded from the study. Preliminary results of histomorphometry analysis showed high donor variation in the control group. Less than half (43%) responded to suboptimal dose of BMP-2. In implants in which bone formed ectopically, the mean percentage of bone tissue was 11.5% ± 8.3. Further analysis is ongoing to quantify bone tissue in BCPs loaded with PAMPs.

Discussion

This study aims to address the possible application of PAMP-based immunomodulators for bone regenerative strategies. Preliminary results suggests that host's blood recognized the investigated PAMPs and elicited an inflammatory response dependent on dose. High donor variation may impose a challenge for further analysis of the histomorphometry results. The variation we observed is in line with previous studies reporting higher variation in subcutaneous region compared to intramuscular locations in rabbits.

References

- ¹Croes, M et al. (2017). *Tissue Eng. Part C: Method* **11**: 673-683.
- ²Shi, Y et al. (2018) *Adv. Functional Materials* **46**:1804483.
- ³Croes, M et al. (2019) *European cells & materials* **37**:402-419.

Funding/acknowledgements

This work is funded by PPS allowance from Health-Holland LSH-TKI (grant number: LSHM18011) and EU's H2020 research and innovation programme under Marie S. Curie Cofund RESCUE (grant agreement No 801540)

DARTBAC, Preventing Antibiotic Resistance Through Novel Medical Device Technology

Deeksha Rajkumar¹, Payal P.S. Ba Ira adjsing¹, Martijn Riool¹, Sebastian A.J. Zaat¹

1. Department of Medical Microbiology & Infection Prevention, Amsterdam Institute for Infection and Immunity, Amsterdam UMC, University of Amsterdam, Meibergdreef 9, 1105 AZ Amsterdam, The Netherlands.

deeksharajkumar8@gmail.com

Medical device (biomaterial)-associated infection is a major risk in the use of biomaterials. These infections are most frequently caused by staphylococci. Generally, these infections are difficult to treat due to tolerance or resistance to antibiotics. Biofilm formation on the implant surface contributes to phenotypic tolerance, and possibly to antimicrobial resistance (AMR) and persistent infection. The bacteria can also survive intracellularly in peri-implant tissue, increasing their resistance to antibiotic treatment. As many antibiotics are incapable of eliminating bacteria in biofilms on the implant surface and in peri-implant tissue, it is imperative to develop and validate alternative antimicrobial technologies. These technologies should additionally enhance the efficacy of current antibiotics allowing combination therapy. The objective of this project, within DARTBAC*, is to foster the development of novel *in vitro* models for biofilm formation, bacteria-host cell interactions and intracellular persistence, and to apply these test methods to evaluate novel technologies

that do not induce resistance to antibiotics. These technologies will include Synthetic Antimicrobial and Antibiofilm Peptides (SAAPs), novel bioactive glass S53P4 formulations, anti-staphylococcal antibodies, and novel antimicrobial polymers. This study will thus offer novel antimicrobial strategies as well as sustainable methods for evaluating antimicrobial activity and cell cytotoxicity, and insight in synergistic activity with conventional antibiotics. This way, the project aims to contribute to safer medical devices and lower risks of antibiotic resistance.

*DARTBAC, Dutch Antimicrobial Resistance Technology development and Biofilm Assessment Consortium focusses on the development and assessment of efficacy and safety of novel antimicrobial technologies for combating infections associated with medical devices.

Burn Wound Healing Using Full Skin Equivalents

Rajiv S. Raktoc^{1#}, Patrick P. G. Mulder^{1,2#}, Marcel Vlig¹, Anouk Elgersma¹, Magda M. W. Ulrich^{1,3}, Esther Middelkoop^{1,3}, Bouke K. H. L. Boekema¹

¹Preclinical Research, Association of Dutch Burn Centres (ADBC), Beverwijk, The Netherlands

²Laboratory of Medical Immunology, Department of Laboratory Medicine, Radboud University Medical Center, Nijmegen, The Netherlands

³Department of Plastic, Reconstructive & Hand Surgery, Amsterdam University Medical Centre, Amsterdam, The Netherlands

#These authors contributed equally to this work

Introduction: The healing of deep burn injury is a complex process that often leads to severe scar formation, leaving patients with both aesthetic and functional problems. Standard treatment of deep burn wounds includes the use of split-thickness skin autografts. Although skin graft surgery is often successful, this method harbors unwanted side-effects such as scar development, reduced elasticity and impaired joint movement caused by contractions. Furthermore, in case of extensive burn injury, the skin donor site availability is limited. In an attempt to overcome these limitations and optimize wound healing, dermal substitutes are being used to cover large wound areas and several clinical trials have already shown success. The generation of full skin equivalents (FSEs) from such scaffolds enables the *in vitro* study of skin development and wound healing in a standardized setting. A better understanding of tissue restoration in dermal scaffolds could improve burn care and limit scar formation.

Materials and Methods: FSEs were established using two types of clinically approved, collagen-elastin-based dermal scaffolds: Matriderm and Mucomaix. Human skin-derived keratinocytes and fibroblasts were cultured in the dermal scaffolds for 21 days to establish FSEs. Subsequently, a contact burn injury (80°C, 20 seconds) was applied and the models were monitored for 2 weeks. FSE using de-epidermalized dermis and human *ex vivo* skin were used for comparison.

Results and Discussion: Immunohistochemical staining of unburned FSEs revealed the presence of pan-cytokeratin, early differentiation marker cytokeratin-10, late differentiation marker involucrin, and proliferating basal keratinocytes, indicating that the FSEs harbor proper epidermal morphogenesis. Furthermore, basement membrane components collagen type 4 and laminin- α 5 could be detected in the FSEs, indicating development of a healthy dermis.

Burn injury could successfully be applied to the FSEs. The models remained viable for at least 2 weeks post burn and showed re-epithelization around the wound area. This finding suggests that the newly developed FSEs can be used as *in vitro* burn wound models.

Summary: Here, we show a novel *in vitro* burn wound model that allows investigation of skin development, wound healing and medicinal intervention for (burn) wound treatment. The next step in the development of the Matriderm- and Mucomaix-based skin models is to elucidate the effects of different cell types derived from scar, eschar and fetal tissue on wound healing. This could

further augment the understanding of skin repair and improve burn care management.

Mailing list:

RSR: rraktoc@burns.nl
PPGM: pmulder@burns.nl
MV: mvlig@burns.nl
AE: aelgersma@burns.nl
MMWU: mulrich@burns.nl
EM: emiddelkoop@burns.nl
BKHLB: bboekema@burns.nl

Dynamically Controlled VEGF Presentation within Biomaterial Guides Vascular Network Formation

D. Rana and J. Rouwkema

Department of Biomechanical Engineering, Technical Medical Centre,
University of Twente, 7522NB Enschede, The Netherlands
Presenting Author's Email: d.rana@utwente.nl

Introduction

Guiding and controlling self-organizing vascular network formation within engineered tissue is important for the successful regeneration or repair of the damaged tissue/organ. Among other factors, dynamically controlled presentation of biochemical cues such as, growth factors (GFs) & cytokines, have been identified to play vital role in guiding network formation *in vivo*. However, the conventional GF delivery systems lack the required dynamic control over GF bioavailability. Therefore, there is an urgent need for developing sophisticated GF delivering tools that can provide spatial and temporal control over GF presentation within 3D microenvironments. In our rational approach, we employ oligonucleotides based aptamers, that are affinity ligands designed to recognize proteins with high affinity and specificity.¹ The developed aptamer-functionalized biomaterials were systematically studied for their dynamically controlled GF presentation and its bioactivity for guiding vasculature.

Materials & Methods

The aptamer-functionalized hydrogels were prepared via photo-polymerization of gelatin methacryloyl (GelMA) and acrydite functionalized aptamers having DNA sequence specific for binding to vascular endothelial growth factor (VEGF₁₆₅). Visible light photoinitiator, tris(2,2'-bipyridyl)dichloro-ruthenium(II) hexahydrate with sodium persulfate was used. Biofabrication technique, such as photopatterning was used to identify the spatial resolution of the GF localization and guiding vascular network formation. The human umbilical vein endothelial cells (HUVECs) and mesenchymal stem cells (MSCs) were used. The samples were double photopatterned into lines with varying widths (300, 500 & 800µm) of aptamer-functionalized hydrogels next to plain GelMA lines (blue beads) (300µm-width), making an interface. Post fabrication, the samples were loaded with VEGF for 1hr. We speculate that the patterned aptamer regions would be able to sequester more VEGF from the culture medium, compared to GelMA lines during 1hr of loading. To study the on-demand, triggered VEGF release, the complementary sequences (CSs) to the aptamers were added at day4 of the culture and its effect on vascular network formation was studied.

Results & Discussion

The results obtained from physicochemical analysis of the photopatterned samples confirmed higher aptamer retention and fluorescently labelled CS hybridization within acrydite functionalized aptamer regions than the plain GelMA regions, for as long as 10 days at 37°C. The immunofluorescence anti-VEGF antibody staining confirmed high and localized VEGF retention within the aptamer functionalized regions than the GelMA regions. Furthermore, in co-culture experiments, the developed

patterned samples showed high cellular viability and ability to guide microvascular network formation (by HUVECs and MSCs) confined within GelMA patterned regions where VEGF loaded aptamer-functionalized regions acts as a VEGF source during 10 days of culture (Figure 1). However, differences in the microvascular organization was observed in the samples with triggered VEGF release on day5, compared to the samples without the VEGF release. These observations altogether confirmed the ability of patterned aptamer functionalized hydrogels in controlling self-organizing microvascular networks within 3D microenvironment.

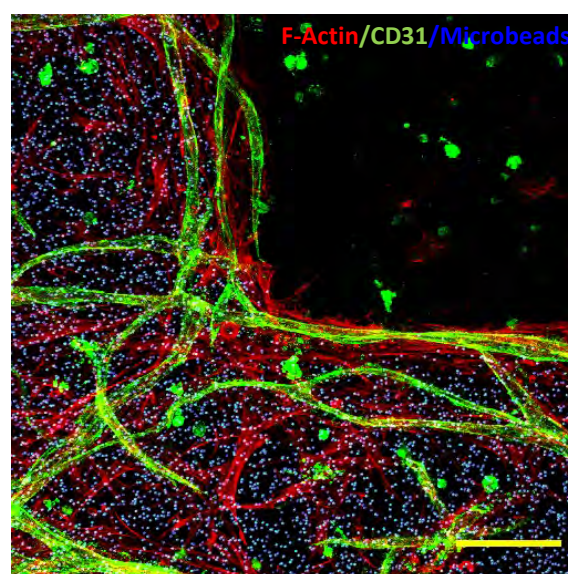


Figure 1: The guided vascular network formation confined within photo-patterned GelMA region whereas the VEGF loaded aptamer-functionalized regions acts as a source that ensures VEGF gradient required to guide the vasculature. Blue fluorescent microbeads indicates GelMA photo-patterned region. Scale bar is 100µm.

Conclusions

The present study confirms the potential of photopatterned aptamer-functionalized hydrogels in guiding self-organizing microvascular networks within 3D microenvironment, by spatiotemporally controlling VEGF bioavailability.

Acknowledgements:

This work is supported by an ERC Consolidator Grant under grant agreement no 724469.

References

1. D. Rana, A. Kandar, N. Salehi-Nik, I. Inci, B. Koopman, J. Rouwkema. *BioRxiv* (2020) doi: <https://doi.org/10.1101/2020.09.22.308619>.

Biomedical engineered materials towards plant protoplast regeneration

Maritza M. Rovers, Patricia Y.W. Dankers

Department of Biomedical Engineering and Institute for Complex Molecular Systems, Eindhoven University of Technology, P.O. Box 513, 5600 MB Eindhoven, The Netherlands

Introduction

In daily life, crops provide food, feed, fuel and other consumable resources for human life. Currently, the food system faces many challenges such as hidden hunger, changes in dietary habits, water efficiency and climate change. In addition, the world's population is predicted to reach 9.6 billion of people by the year 2050, which will put our food supplies under far greater stress.¹ This causes an urgent need for innovations in plant cell biology to increase the agricultural productivity.

This is being approached by the production of high value crops by crop breeding, which allows crops to be mutated in a controlled manner by genome editing.¹ The editing reagents required for genome editing are delivered into protoplasts, which are plant cells from which the cell wall has been removed.² A crucial part in the gene-editing of plants is the regeneration of protoplasts towards plants, which is a challenging and time-consuming process. While the influence of growth medium on protoplast development has been extensively researched, there is still little knowledge about the influence of the physical environment on the development of single protoplasts towards multicellular plant-structures.

In fact, the field of biomedical engineering has booked great progress on the principle of developing multicellular structures out of single cells by the use of biomaterials. These biomaterials mimic the physical environment of cells to stimulate regeneration and growth. Here, we hypothesize that the knowledge obtained in this field could be translated towards the field of plant cell biology to use biomedical engineered biomaterials as a synthetic cell wall to improve the process of protoplast regeneration.

Aim

For this purpose, we aim to encapsulate single *Tobacco Bright Yellow 2* (BY-2) protoplasts in microgels based on supramolecular ureido-pyrimidinone (UPy) molecules by water-in-oil droplet microfluidics. These supramolecular molecules can self-assemble by non-covalent interactions into dynamic fibrous aggregates and give rise to microgels when combined with droplet microfluidics.³ The encapsulation of single protoplasts in microgels over bulk hydrogel culture creates a platform to investigate individual cells in a physiological relevant synthetic 3D microenvironment. It provides the possibility to study environmental properties of the hydrogel (e.g. stiffness and bioactivity) on the protoplast, which could accelerate the discovery of new hydrogel formulations for protoplast regeneration. These protoplasts will be studied on their capability of regenerating their cell wall by assessing the deposition of cell wall components (e.g. pectin and cellulose) by the protoplasts.

Materials and Methods

BY-2 cells were cultured in MS-medium and protoplasts were enzymatically obtained by subculturing 10% PCV

in protoplast medium with 1% (w/v) cellulase Onozuka R-10 and 0.5% (w/v) macerozyme R-10.⁵ The fully synthetic microgels are composed of supramolecular UPy-based molecules that can form UPy-units by self-complementary quadruple hydrogen bond formation. The UPy-microgels were generated using a tip-loading approach in the microfluidic device, prepared according to a previously described method.⁴ Polymer pre-solutions of 0.25 wt% UPy₂-PEG_{10K} mixed with BY-2 protoplasts and 2.25 wt% UPy-glycinamide were prepared separately and loaded in the tips to generate cell encapsulated microgels at 1.25 wt%.³

Results and Discussion

The UPy-hydrogel system was designed as a synthetic environment to provide the protoplasts with physical support and thereby replacing the cell wall. Droplet microfluidics was used to generate monodisperse picolitre-sized supramolecular microgels at 1.25 wt% with encapsulated BY-2 protoplasts (Figure 1, blue arrow). However, also empty microgels (orange), microgels with multiple protoplasts (yellow) and non-encapsulated protoplasts (green) were generated (Figure 1). This might be caused by the stickiness of the protoplasts which sequentially initiates clogging of the microfluidic channel. Consequently, pressure builds behind the clogged cells, which causes the cells to be pushed through the channel at varied flow speeds.

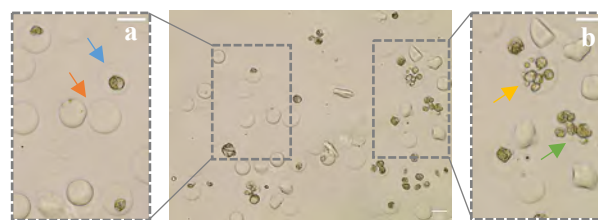


Figure 1: Tobacco BY-2 protoplasts encapsulated in 1.25 wt% UPy-microgels (blue arrow). Scale bar = 50 μ m.

Conclusion and Outlook

We demonstrated that using droplet microfluidics, supramolecular microgels can be used to encapsulate plant protoplasts and thereby serve as a synthetic micro-environment. Next, we intend to optimize the encapsulation and aim to identify the influence of different microgel compositions on the regeneration capacity of the protoplasts. Encapsulation will be improved by small adaptations in the chip design, such as removing the pillars to improve the flow of the protoplasts. Furthermore, different weight percentages of UPy₂-PEG_{10K} will be used to mix in the protoplasts. We hypothesize that the long PEG chains of the polymer can shield the protoplast in order to lower the stickiness.

References

1. Chen K., et al., *Annu. Rev. Plant Biol.* 70, 667–697 (2019)
2. Eeckhaut T., et al., *Planta* 238, 991–1003 (2013)
3. Diba M., et al., *Adv. Mater.* 33, 37 (2021)
4. Sinha N., et al., *J. Vis. Exp.* 144, e57848 (2019)
5. Lei R., et al., *MethodsX* 2, 24–32 (2015)

Developing a Bone-on-a-Chip to Study Bone Formation Pathways

J. Schaart¹, P. Jonkheijm², N. Zeijen², N. Sommerdijk^{1,3}, A. Akiva^{1,3}

1) Dept. of Biochemistry, Radboudumc, Radboud Institute for Molecular Life Sciences, Geert Grooteplein Zuid 28, 6525GA, Nijmegen, The Netherlands

2) Dept. of Molecules and Materials, University of Twente, Biointerface Chemistry, TechMed Centre MESA+ Institute for Nanotechnology, Enschede, The Netherlands

3) Electron Microscopy Center, Radboudumc, Radboud Institute for Molecular Life Sciences, Geert Grooteplein Zuid 28, 6525GA, Nijmegen, The Netherlands

Bone constitutes a major part of the vertebrate body and it fulfills multiple important functions, including supporting the stature and locomotion. Mature bone consists of a highly organized, mineralized collagen matrix in which the bone cells, osteoblasts, osteoclasts and osteocytes, are embedded.

During bone formation, the collagen matrix is deposited by osteoblasts. After this, the bone matrix is mineralized with hydroxyapatite, which gives bone its unique mechanical characteristics. However, currently it is unknown how mineral is transported and delivered to the matrix and which pathways are involved in this mineralization process.

To study the development of bone, *in vitro* culture models in which the bone development can be mimicked are needed. Recently, the first organoid for immature, young (woven) bone was developed in which mesenchymal stem cells were differentiated to a co-culture of osteoblasts and osteocytes and during this process a mineralized matrix resembling the bone matrix was deposited. [1]

Currently, we are developing a model system in which the collagen organization of mature bone can be captured. To do so, we aim to develop a bone-on-a-chip, creating a 3D culture in which bone formation can be

studied *in situ* using fluorescence and electron microscopy. In a large-scale 3D osteoblast culture we achieved the induction of alignment of the deposited collagen matrix by fixation of the culture on two sides. This culture system will now be minimized to a bone-on-a-chip, which will enable us to include a fluid flow for nutrition and biochemical stimulation combined with mechanical stimulation to mimic the physiological conditions in developing bone more closely. To do so, osteoblasts are cultured on PDMS chips which contain pillar arrays [2] as guidance cues for the collagen orientation. The culture allows for live fluorescence microscopy to monitor the matrix development and when an event of interest is observed, part of the culture will be punched and cryo-preserved after which high resolution fluorescence and electron microscopy will be performed to study the processes involved in bone matrix formation.

1. Akiva, A., et al., *An Organoid for Woven Bone*. *Advanced Functional Materials*, 2021. **31**(17).
2. Zeijen, N.J.L., *Directing cell differentiation in organ-on-chip devices through microarchitecture and supported lipid bilayers*. 2021, University of Twente: Enschede. ISBN:978-90-365-5190-8

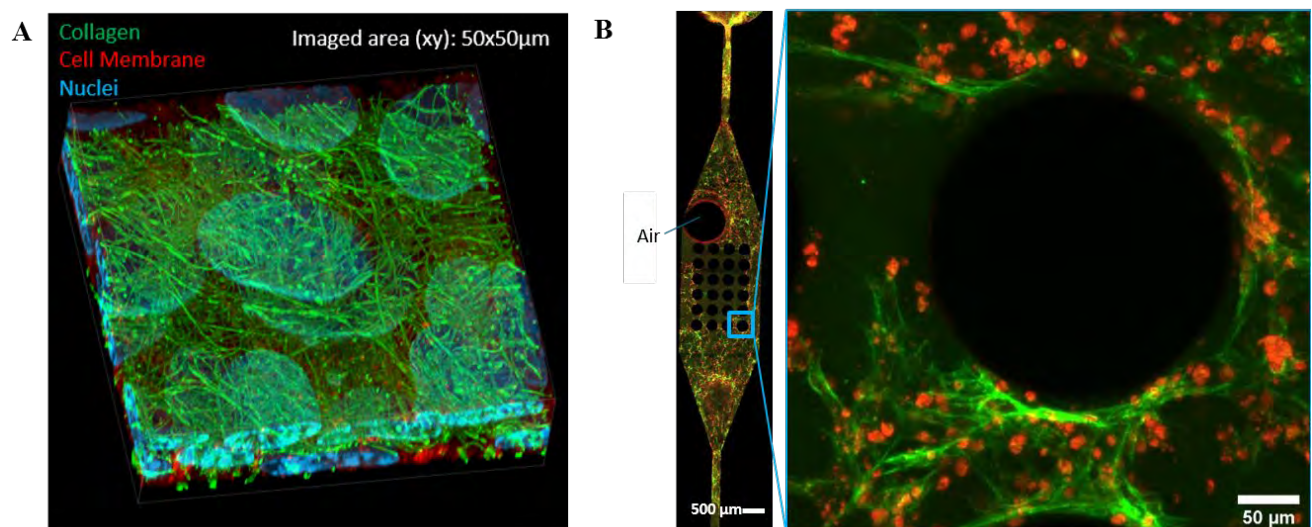


Figure 1 A) 3D representation of fluorescently stained collagen (green), cell membranes (red) and nuclei (blue) imaged with a iyscan microscopy. The collagen was produced by osteoblasts in a monolayer cell culture. B) Overview image (left, scalebar: 500 μm) and zoom in (right, scalebar: 50 μm) of collagen (green) produced by osteoblasts (red) in a PDMS chip with a pillar array.

Bottom-up Engineering of Modular Tissues With Inherent Capillary Networks

M.R. Schot¹, C.A. Paggi^{1,2}, M.L. Becker¹, J. Leijten¹

¹ Department of Developmental BioEngineering, TechMed Centre, University of Twente, The Netherlands

² Applied Microfluidics for BioEngineering Research Group, TechMed Centre, University of Twente, the Netherlands

Introduction: The vascular tree is essential for the function and survival of tissues. However, engineering vascular trees within 3D tissues has remained challenging. Current methods to produce channel-like structures in engineered tissues such as 3D printing are able to mimic large vessels, but struggle to produce highly dense capillary networks at high speeds, limiting their translation to clinically sized constructs.¹ Microporous annealed particles (MAP) offer an interesting alternative due to their microporous nature, essentially offering an inherent dense microporous network of channels without having to create it.² Here, we aim to use our recently developed in-air microfluidics (IAMF) technique to produce cell-laden microgels at ultra-high throughput production rates to create MAP tissues, allowing for the bottom up development of engineered tissues with inherent highly dense capillary sized pore networks.³

Materials and Methods: To generate dual-crosslinkable microgels, a piezo-actuated microjet composed of 0.5% (w/v) alginate-tyramine (ATA) was collided with a continuous microjet of 0.1mM calcium chloride (CaCl₂). Upon impact, the CaCl₂ wraps around the alginate drops via Marangoni flow, and microgels are formed via outside-in diffusion of CaCl₂ ions (see figure 1a for a schematic representation). Cell encapsulation was achieved by dissolving cells in ATA at concentrations ranging from 1x10⁶ cells/mL to 10x10⁶ cells/mL. Microgel size, sphericity, monodispersity and cell encapsulation were characterized using fluorescent and phase contrast microscopy. MAPs were created by packing microgels using suction-assisted filtration and subsequent crosslinking with ruthenium (Ru), sodium persulfate (SPS) and visible light. The interconnected network of pores inside of MAPs of varying sized building blocks was analyzed using confocal microscopy. MAP perfusability was further analyzed by a hydraulic conductivity assay and by perfusing MAPs on chip with 1 μm fluorescent particles.

Results and Discussion: Microgels of sizes ranging from 100 μm to 300 μm with a CV below 5% could be produced at flow rates ranging from 0.9 mL/min to 4.5 mL/min depending on nozzle size (figure 1b-c). Cells could be successfully encapsulated at varying concentrations and with >80% viability after 1 day for several cell types including hepatocytes, stellate cells and endothelial cells. MAP formation was successfully achieved using Ru/SPS and remained stable upon exposure to hydrodynamic stress. MAPs were imaged using MicroCT (figure 2a). Confocal microscopy revealed highly dense networks of capillary sized pores in MAPs engineered from a variety of building block sizes (figure 2b). Interestingly, the pore size distribution appears independent of microgel size, whereas the pore

density was strongly influenced by microgel size. Lastly, MAPs showed an increased perfusability and hydraulic conductivity as opposed to nanoporous ATA hydrogels.

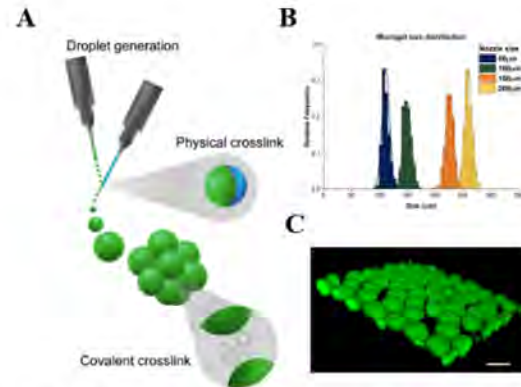


Figure 1: A) Schematic representation of microgel formation using in-air microfluidics and subsequent MAP formation from microgels. B) Microgel size distribution for each used nozzle size. C) Microgel morphology as imaged with confocal microscopy (scalebar: 100 μm).

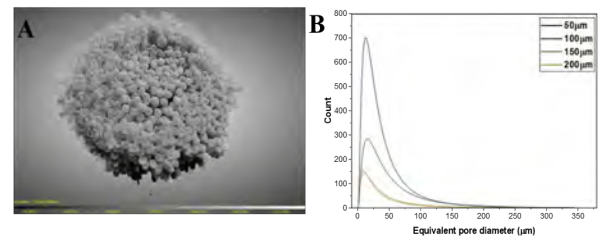


Figure 2: A) Micro-CT image of a MAP made of ~150 μm microgels. B) Pore size distribution of MAPs built using microgels generated with nozzles of varying sizes showing capillary sized pores independent of microgel building block size.

Conclusions:

By combining IAMF and ATA, we were able to produce microgels of controlled sizes in ultra-high throughput, which allowed for the production of voluminous MAPs using a second, visible light based crosslinking system. All MAPs contained interconnected porous networks, and associated with high viability of encapsulated cells. Currently, we are creating liver MAPs and analyzing their functionality in vitro.

Acknowledgements:

Financial support was received from the European Research Council (ERC, Starting Grant, #759425).

Bibliography:

- 1 Kolesky, D. B. *et al. PNAS*, 12, 3179-3184 (2016)
- 2 Annamalai, R. T. *et al. Ann. Biomed. Eng.* 47, 1223-1236 (2019)
- 3 Visser, C. W. *et al. Sci. Adv.* 4, 1-9 (2018)

Contact

M.R. Schot; +31-534-898-152; m.r.schot@utwente.nl

Construct of Hyaluronic Acid and Chondroitin Sulfate (meth)acrylate hydrogel and Polyamide 6 spacer fabric mimics native cartilage mechanical properties

Rienk (G.H.) Schuiringa¹, M. Mihajlovic^{1,2}, T. Vermonden², C.C. van Donkelaar¹, K. Ito¹.

¹Orthopaedic Biomechanics, Dept. Biomedical Engineering, Eindhoven University of Technology, PO 513, 5600 MB, The Netherlands.

² Department of Pharmaceutics, Utrecht Institute for Pharmaceutical Sciences (UIPS), Science for Life, Utrecht University, 3508 TB, Utrecht, the Netherlands

Introduction: Hydrogels are soft materials, made of hydrophilic polymer networks able to absorb and retain water. Such materials are particularly suitable for cartilage tissue engineering, however mimicking the load-bearing properties of cartilage is still a challenge¹. To design biomimetic hydrogels, chondroitin sulfate (CS) and hyaluronic acid (HA) are very attractive, as they are present in native cartilage. Both polymers attract water due to their hydrophilicity and high negative charge density. The latter is of importance, because in native cartilage there is a strong correlation between the load-bearing properties of articular cartilage and its total glycosaminoglycan (GAG) content². The attraction of water by GAGs induces swelling, which is restricted by the collagen fibers, resulting in an osmotic pressure³. To induce an osmotic pressure in a biomimetic hydrogel, fiber-reinforcement can be used to restrict the swelling. Schäfer, et al. previously showed that using warp-knitted spacer fabrics, consisting of a knitted top and bottom layer which are connected by pile yarns, injected with a non-swelling agarose hydrogel, the Young's Modulus was doubled or tripled compared to the hydrogel alone. Nevertheless, regarding the stiffness, native cartilage outperformed the constructs by 10 times⁴. The objective of this study was to determine the effect of restricted swelling by a warp-knitted spacer fabric of a biomimetic swelling hydrogel on the stiffness of the construct, so called HydroSpacer, compared to native cartilage.

Method: Polyamide 6 (PA6) warp knitted spacer fabrics (Karl Mayer Textilmaschinenfabrik GmbH) were used as the restricting scaffold. Methacrylation of HA and CS was performed following a previously reported method⁵. CSMA and HAMA hydrogel solution was prepared by dissolving the polymers in PBS at desired concentration (10 wt%, with CSMA:HAMA ratio 6.5:1). The resulting polymer solution was supplemented with lithium phenyl-2,4,6-trimethylbenzoylphosphinate (LAP) photoinitiator (0.3 w/v%), subsequently injected in the PA6 spacer fabrics (Ø8 x 3 mm) using a Teflon mold. Hydrogels were crosslinked using UV light for 15 minutes at a distance of 3 cm from the light source (UV lamp VL-4.LC, A. Hartenstein GmbH, wavelength 365 nm). After polymerization, the HydroSpacers were placed inside a circular cassette (Ø8 x 3.5 mm; R05 resin, Envisiontec) to prevent lateral swelling of the hydrogel and bathed in PBS at 37°C. Full thickness cartilage samples were obtained from bovine patellas using a razor blade and were cut to fit in the confined cassettes using a biopsy punch of 8 mm diameter prior to testing. To determine

the stiffness and viscoelastic properties of the constructs and cartilage, samples were tested in a semi-confined environment within the circular cassettes. Compression tests were performed using an indenter (Ø 5mm), with a strain of 15% and a strain rate of 15% strain/sec.

Results: No significant differences were found between the CSMA HAMA PA6 HydroSpacer and native bovine cartilage for both the initial modulus and equilibrium modulus (Fig 1A-B). Moreover, the HydroSpacer demonstrated similar time-dependent properties as native bovine cartilage (Fig 1C).

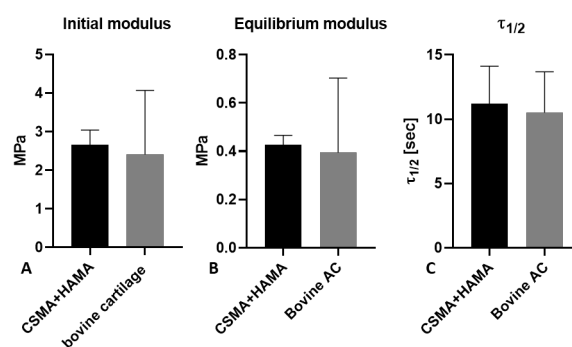


Figure 1 Initial modulus (A) equilibrium modulus (B) and viscoelastic properties (C) of CSMA HAMA PA6 HydroSpacers and bovine cartilage.

Discussion: CSMA HAMA PA6 HydroSpacers showed similar mechanical behavior compared to native bovine cartilage in a semi-confined testing environment. For a tissue engineering approach, CSMA/HAMA as a biomimetic hydrogel showed already beneficial effects on chondrocyte encapsulation⁶. Future steps will include testing biological cell performance inside these HydroSpacers.

Acknowledgements: This research was performed under the framework of Chemolot InSciTe, supported by the partners of Regenerative Medicine Crossing Borders (www.regmedxb.com) and powered by Health~Holland, Top Sector Life Sciences & Health.

References:

1. Cook RF, Oyen ML. *J Phys Mater.* 2021
2. Kempson GE, et al. *Biochim Biophys Acta - Mol Cell Res.* 1970
3. Korhonen RK, et al. *J Biomech.* 2003
4. Schäfer B, et al. *Materials (Basel).* 2020
5. Abbadessa A, et al. *Carbohydr Polym.* 2016
6. Levett PA, et al. *PLoS One.* 2014

The effect of a Cathepsin K inhibitor on a bone model *in vitro*

E. Šebová¹, V. Hedvičáková¹, V. Sovková¹, E. Filová¹

¹Institute of Experimental Medicine of the Czech Academy of Sciences, Videňská 1083, Prague 4, 14220, Czech Republic

Osteoporosis is a worldwide common disease with higher risk in postmenopausal women and older individuals. Cathepsin K (CTSK) inhibitor has been investigated as a potential anti-osteoporotic drug by inhibiting osteoclasts guided bone resorption. The main idea of the whole project is finding a new strategy for osteoporotic bone treatment. We focus on the local positive effect of nanoparticles with encapsulated CTSK inhibitor with gradual release. The encapsulated drug formulation will be incorporated into a scaffold to fill a bone defect or fracture. The aim of this study was to determine effective but safe concentration of this anti-osteoporotic drug. Three concentrations (low, medium, high) were tested *in vitro* in a bone model to examine the effect on both, osteoclasts and osteoblasts involved in bone remodeling. Osteoclasts have bone-resorbing activity carried out by their typical enzymes, tartrate-resistant acid phosphatase (TRAP) and CTSK. Inhibition of CTSK leads to reduced bone resorption and thus increases new bone formation by osteoblasts. Rat peripheral blood mononuclear cells were used as a first *in vitro* bone model in co-culture with rat primary osteoblasts. As a second bone model we used co-culture of THP-1 monocytic cell line and SaOS-2 osteosarcoma cell lines with the same drug dosing procedure. After osteoclasts formation, the CTSK inhibitor was added to the basal culture medium.

The MTS assay was used to measure cell metabolic activity. During the experiment, osteoblastic activity of SaOS-2 by alkaline phosphatase (ALP) and osteoclastic activity of osteoclasts by the activity of carbonic anhydrase II (CA II), TRAP and CTSK were measured. The addition of a CTSK inhibitor led to changes in the metabolic activity of both co-culture models compared to co-culture without drug supplementation. This anti-osteoporotic drug also affects all osteoclastic enzymes, not only CTSK activity. We also observed a weak effect on decreased ALP activity. However, changes were not the same in both bone models.

Our future perspective is to determine a proper concentration of CTSK inhibitor that will affect CTSK produced by osteoclasts, without any effect on other enzymes, and also to test the drug in a bone model with a higher resemblance to real bone. We would like to stimulate better bone physiology with dynamic culture conditions in bioreactors. Knowledge of both positive and negative effects would help in testing of nanoparticles with encapsulated drug as further part of the project. Avoiding negative side effects and finding the most suitable *in vitro* bone model, can help to prevent any complications in *in vivo* experimental application and protect animals from suffering. Acknowledgement: Work was supported by a grant from the Technology Agency of the Czech Republic – FW01010662.

Co-culture as a model of intestinal tissue *in vitro* for early toxicological screening

V. Sedláčková¹, V. Hefka Blahnová¹, A. Simaite², E. Filová¹

¹Institute of Experimental Medicine of the Czech Academy of Sciences, Vídeňská 1083, Prague 4, 14220, Czech Republic

²InoCure, Politických vězňů 935/13, 11000, Prague 1, Czech Republic

Live animal testing is an integral part of toxicological screening. Nevertheless, countless efforts have been made to “replace, reduce and refine” animal-based experiments to address their shortcomings. In our model we employed a co-culture of Caco2 and HT29 intestinal cell lines to reflect on the complexity of the intestinal tissue.

Monocultures of Caco2 and HT29 and Caco:HT29 co-cultures in five different ratios (9:1, 7:3, 5:5, 3:7 and 1:9) were cultured on tissue culture plastic (TCP). Alkaline phosphatase (ALP) activity was measured on day 7, 14, and 21. To verify the ability of mucin production in different mono- and co-cultures, the mucin was stained on day 21 by alcian blue. In the following step, Caco2 and HT29 monocultures and selected co-culture (Caco2:HT29 ratio of 7:3) were cultured in a 3D environment to mimic the *in vivo* intestinal architecture. The cell cultures were grown on nanofibrous scaffolds (mixture of poly- ϵ -caprolactone and cellulose acetate) for 21 days with ALP activity measured on days 3, 7, 14 and 21 post-seeding. The two cell types were distinguished by staining HT29 cell type with a Cell Tracker and visualized using confocal microscopy. Furthermore, to determine a suitable post-seeding time of the co-culture model for the purpose of toxicological testing, the β -actin staining using Phalloidin conjugated with Alexa Fluor 633 was performed and visualized using confocal microscopy. On TCP, the model maintained a suitable ratio of Caco2 and HT29 for 21 days as verified by quantification of ALP on days 3, 7, 14 and 21. On days 7, 14 and 21 the ALP activity was significantly higher in Caco2 monoculture and Caco2:HT29 co-cultures of 9:1 and 7:3 ratio compared to HT29 monoculture and Caco2:HT29 co-culture 1:9. Moreover, in contrast to Caco2 monoculture, Caco2:HT29 co-culture displayed the ability of producing mucin, a functional feature of the small intestine. The presence of both cell types in our co-culture model was confirmed by means of staining HT29 cells with Cell Tracker stain.

In the following step where the cells were cultivated in a 3D environment, Caco2 monoculture displayed significantly higher ALP activity on day 21 compared to HT29 monoculture and Caco2:HT29 co-culture, suggesting the co-culture ratio was preserved. The β -actin staining revealed different morphologies of Caco2, HT29 monocultures and Caco2:HT29 co-culture (all experimental days) and confirmed the confluency of all cultures on day 7.

We conclude that present co-culture of Caco2:HT29 7:3 cultivated in 3D environment can serve as an intestinal tissue model for early toxicological screening, maintaining a suitable ratio of the two cell types for 21 days. In future, improvements of the model in terms of complexity shall be investigated such as an employment

of additional cell types or an influence of dynamic culture conditions.

Acknowledgement: This work was supported by Ministry of Industry and Trade of the Czech Republic, project number FV40437.

A Cell-Adherent Polymer Template to create Multiscale Channel Structures and Cell Patterns with a 3D Hydrogel

A.Seijas-Gamardo¹, A.Chandrakar¹, T.Bodet¹, M.van der Spoel¹, S.Albargati¹, F.Barbugian¹, L.Moroni¹, R. Hoogenboom^{2,3}, V. de la Rosa³, P. Wieringa¹

¹MERLN Institute, Maastricht University, The Netherlands

²Ghent University, Belgium

³Avroxa BVBA, Belgium

Native tissues are characterized by its 3D organization and distribution of cells, with specific cell-cell and cell-extracellular matrix (ECM) interactions dictating tissue function. The spatial distribution of cells and ECM in tissues is not arbitrary, with interconnected lumen structures and specifically located cell populations creating a fundamental structure-function relationship that determines the role of specific tissues. Therefore, the capability to mimic this 3D environment is key for a correct *in vitro* modeling of tissues and for future tissue engineering applications. Here we present a templating strategy using a thermally responsive polymer and we show the fabrication, in one step, a network of interconnected channels within a hydrogel. While other polymers have been previously described for similar applications, including pNIPAM and PnPrOx, we uniquely show that our template can create a defined 3D polymer scaffold to which cells can adhere, leading to the subsequent formation of a channel network that directly incorporates cells.

This approach is based on a family of bespoke oxazoline polymers (OXA) that have been specifically designed to have a uniquely tunable range of lower critical solubility temperature (LCST), above which it remains insoluble and below which it is triggered to dissolve.

We characterized the LCST by monitoring polymer solubility via optical transmission. We characterized this by preparing films of each polymer formulation on coverslips via spin coating, and monitoring the water contact angle (WCA) when the polymer and water are maintained at temperatures ranging from 37°C to 5°C.

In addition, we characterized the polymers mechanical and melt rheological properties and based on this, optimized the production of polymer filaments via fused deposition modelling (FDM) and melt electrowriting (MEW). We were able to generate filament scaffolds ranging in diameter from the millimeter to micron scale. Using an in-house customized microscope stage with temperature control and time lapse stereomicroscopy, we directly monitored the dissolution dynamics of these polymer filaments while being held at 37°C and from 37°C to 5°C, mimicking the transition of the scaffold from a cell incubator to a standard lab refrigerator.

A 4 mg/ml collagen pre-gel solution was used to embed the filaments, crosslinked the gel at 37°C, and then trigger to dissolve. We show the formation of microchannels that were perfusable with gravity-driven fluid flow, visualized via fluorescence microscopy of a fluorescent nanobeads suspension.

To explore the use of OXA microfilaments, we focused on the biomimetic formation of Schwann cell-lined microchannels to guide axon growth. We created a customized support system to facilitate microfiber handling and confirmed that rat Schwann cells (rSCs)

could adhere to the polymer fibers. The seeded templates were embedded within collagen and cooled, with rSCs found to localize to the resulting microchannels. These channels were also able to support axon growth from iPSC-derived human sensory neurons. Additionally, we show how the complete fabrication of the device was compatible with cell culture. We embedded primary fibroblasts in the collagen hydrogel, exposing them to its crosslinking and to the dissolution of the microfilaments, triggered with low temperatures.

Here, we demonstrate the value of this novel templating technology to generate different *in vitro* models (Fig.1), allowing the culture of different cell types in specific locations and we establish its potential for other 3D *in vitro* model and tissue engineering applications.



Figure 1. 3D render of the finalized device (top view) used for *in vitro* modeling in tissue engineering, featuring different regions for cell culture, in this case 2 microwells interconnected between them by microchannels inside a collagen hydrogel.

Dynamic covalent crosslinked hydrogel matrix using Pickering Emulsion

Clio Siebenmorgen*, Guangyue Zu*, and Patrick van Rijn

W.J. Kolff Institute for Biomedical Engineering and Materials Science, University of Groningen/ University Medical Center Groningen (UMCG), Ant. Deusinglaan 1, Groningen, The Netherlands

* These authors contributed equally to this work

Keywords: NIPAM Microgel, Dynamic Matrix Formation, Pickering Emulsion

Introduction: Healing of wounds is a complex ensemble of cells, growth factor and extracellular matrix proteins. Hereby, mesenchymal stem cells (MSC), that are able to differentiate into other cell types, such as bone and cartilage cells, play an important role in the healing process. MSCs are involved in all wound healing phases, regulating immune and inflammatory response, and enhancing tissue regeneration.^[1] However, MSCs show beneficial properties, only limited amount can be isolated from patients, making this the biggest drawback for biomedical applications. Thus, it is very crucial to be able to culture these stem cells in vitro, without altering their cell behavior.

In vivo stem cell behavior is highly depending on the biochemical and biophysical signals in the cell niche.^[2] The key approach is to design a biomedical system which can mimic those niches and ultimately be able to isolate the replicated stem cells for tissue engineering applications. [3][4]

Encapsulating stem cells into synthesized hydrogels is a promising method since well-defined features of these particles can be achieved by tuning the physical and chemical properties, leading to multiplication of stem cells with retaining the cell stemness.

The aim of this project is the development of a hydrogel-based matrix using dynamic covalent chemistry. Making use of amine containing and ketone containing NIPAM hydrogels, spontaneous matrix formation is facilitated in a reversible manner with tunable hydrogels in terms of physicochemical properties. Ultimately, a hydrogel-based matrix can be used to encapsulate and expand stem cells, requiring a micro/macro-porosity, which was considered in the systems development.

Method: The matrix formation is based on an imine formation of ketone functionalized and amine functionalized NIPAM hydrogels. Hollow structures are being formed on the interface of two immiscible solvents based on a Pickering emulsion. Hereby, chloroform containing ketone hydrogel is tip sonicated with an amine hydrogel aqueous phase. The resulting matrix is separated for imaging and its pH responsiveness, and stability is being investigated.

Results and Discussion: Upon tip sonication of amine and ketone functionalized microgels, the matrix formation was investigated using fluorescence microscopy. Hereby, Nile Red labelled CHCl_3 containing ketone functionalized hydrogels and H_2O containing Nile Blue labelled amine

functionalized hydrogels were imaged. The corresponding matrix is depicted in Figure 1 showing an oil containing core, with capsules of several microns up to 100 μm in size.

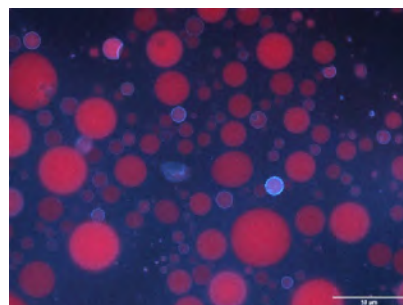


Figure 1: Merged fluorescence microscopy image of Nile Red labelled CHCl_3 and Nile Blue labelled amine hydrogels

Formation of a dynamic covalent crosslinked hydrogel matrix based on imine bonds, allows the incorporation of a pH responsive system, as imine bonds only remain stable under neutral conditions.^[5] We analyzed the stability of the matrix under pH 4, 7 and 10. Figure 2b displays the instability of the matrix in basic and acidic conditions after 20 h. Whereas, the matrix remained stable under neutral conditions, proofing the formation of imine bonds between amine and ketone functionalized hydrogels.

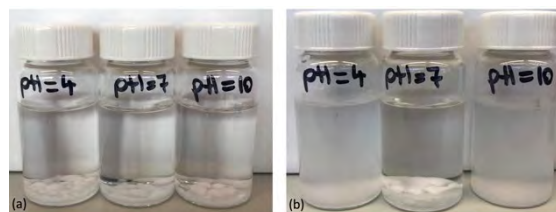


Figure 2: Hydrogel matrix at pH 4, 7 and 10; (a) $t = 0$; (b) $t = 20$ h

Conclusion: In this work we present the successful formation of an external stimuli responsive dynamic covalent crosslinked hydrogel matrix based on imine bonds. To successfully encapsulate and culture stem cells, further investigations on the physical properties, such as stability upon oil removal and stiffness of the matrix need to be investigated in order to mimic the desired cell niches for encapsulation.

References:

- [1] S. Maxon, E. A. Lopez, D. Yoo, A. Danilkovitch-Miagkova, M. E. LeRoux, *SCTM* **2012**, 1:142-149
- [2] S. Allazetta, M. P. Lutolf, *Current opinion in biotechnology* **2015**, 35, 86-93
- [3] M. Hashemi, K. Kalakinia, *Life Sciences* **2015**, 143, 139-146
- [4] S. Sart, T. Ma, Y. Li, *BioResearch open access* **2014**, 3, 137-149
- [5] E. Cordes, W. Jencks, *JACS* **1962**, 84, 832-837

A novel concept in ACL reconstruction surgery: an off-the-shelf decellularized and sterilized bone-ACL-bone allograft

Janne Spierings¹, Jorge Alfredo Uquillas¹, Antonio van der Lande¹, Aysegül Dede Eren¹, Manon Bertrand², Huipin Yuan³, Rob Janssen^{1,4}, Keita Ito¹, Jan de Boer¹, Jasper Foolen¹

¹Department of Biomedical Engineering, Eindhoven University of Technology, Eindhoven, The Netherlands, ²HCM Medical, Nijmegen, The Netherlands, ³Huipin Yuan's Lab, Sichuan, China, ⁴Maxima Medical Centre Eindhoven/Veldhoven, Eindhoven, The Netherlands

Introduction: Each year, 1% of active individuals rupture their anterior cruciate ligament (ACL) resulting in direct knee instability and altered posture and gait [1]. Tendon autografts are the current gold standard for ACL reconstruction (ACLR), despite lacking native compositional, structural, and mechanical properties. ACLR too often results in re-rupture, knee instability, and osteoarthritis [2,3]. This study aims to generate a decellularized and sterilized human bone-ACL-bone allograft (ultrAClean) that abrogates these graft discrepancies and mitigates post-operative problems.

Methods: Fresh-frozen human cadaveric knees (n=9) were obtained from the Radboud UMC, Nijmegen. ACLs with attached femoral and tibial bone blocks were excised and ACLs were assigned to the control (unprocessed) or ultrAClean group. Decellularization was conducted via freeze-thawing, incubation in Triton X-100, and enzymatic treatment using Benzonase. Sterilization was conducted using supercritical CO₂. Subsequently, DNA amount was quantified (Qubit dsDNA assay), cell nuclei were stained (Hematoxylin and Eosin), and DNA fragment length (gel electrophoreses) was evaluated to confirm decellularization. Next, mechanical, compositional, and structural properties were determined, and *in vitro* cell cytotoxicity and proliferation were assessed. For preliminary *in vivo* evaluation in a pig, ultrAClean was wrapped around a LARS ligament and inserted adjacent to a porcine ACL. After 6 months, the host ACL, LARS, and ultrAClean were evaluated using histology.

Results: In ultrAClean tissue, DNA content was significantly reduced to 44 ± 34 ng/mg dry weight

(p<0.0001), visible nuclei could not be detected (Fig. 1A-B), and only trace amounts of intact DNA (>12000 base pairs) were found (Fig. 1C). Mechanical properties (maximum failure load and Young's modulus) did not significantly change (Fig. 2A-B). Type-I collagen content also did not change significantly (Fig. 2C); however, glycosaminoglycan (GAG) content was significantly reduced by 60 percent in ultrAClean tissue (Fig. 2C). Control and ultrAClean tissue did not reveal noticeable cytotoxic effects to rat-derived tenocytes up to 7 days in culture (Fig. 3A), and cells were able to proliferate on native and ultrAClean tissues at a similar rate up to 5 days in culture (Fig 3B).

Discussion: Human bone-ACL-bone tissue was successfully decellularized according to previously set guidelines [4], without affecting mechanical properties and structure. Although GAGs were partly lost upon decellularization, no significant effect was found on the mechanical behavior of ultrAClean, and GAG levels in grafts can easily recuperate *in vivo* after implantation [5]. Altogether, our data strongly suggests the feasibility to generate a decellularized and sterilized human bone-ACL-bone allograft. Future studies will validate whether ultrAClean results in a milder ligamentization process compared to the current gold standard autografts and thereby reduces post-operative issues.

References: [1] Ruano JS, et al. J Athl Train. 2017, [2] Hadjicostas PT, et al. Knee Surg Sports Traumatol Arthrosc. 2008, [3] Handl M, et al. Knee Surg Sports Traumatol Arthrosc. 2007, [4] Faulk DM, et al. J Clin Exp Hepatol. 2015, [5] Dede Eren A, et al. J Immunol Regen Med. 2020.

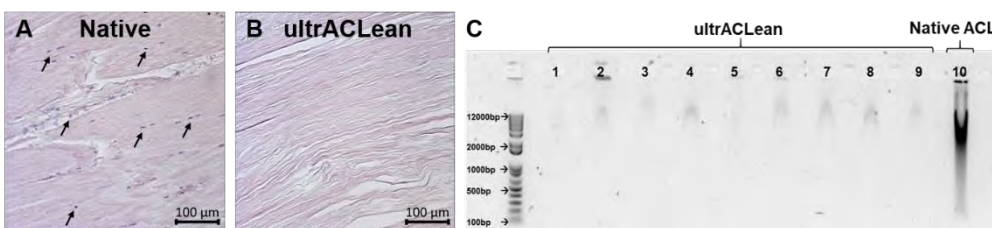


Figure 1. Decellularization efficiency of human ACL tissue.

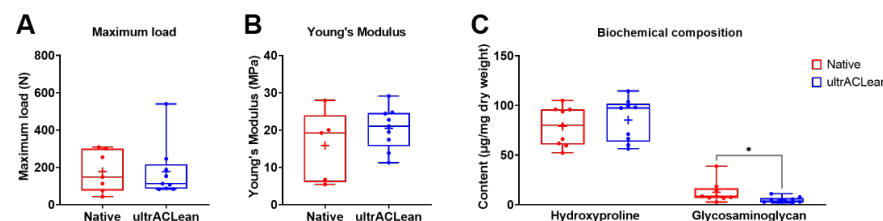


Figure 2. Mechanical properties and biochemical composition of human ACL tissue.

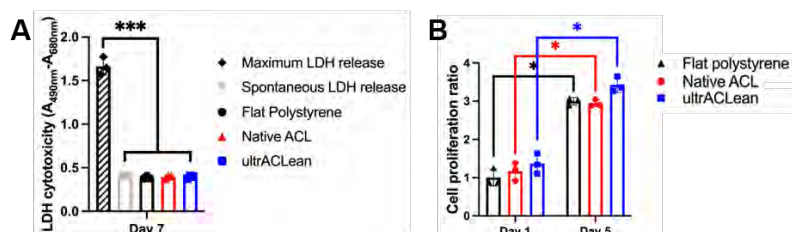


Figure 3. *In vitro* cell evaluation of human ACL tissue.

Sex-specific Differences in Kidney Function of (Non-) Diabetic Patients

S Swapnasrita¹, A Carlier¹ and A Layton²

¹Department of Cell-Biology Inspired Tissue Engineering, MERLN Institute for Technology-Inspired Regenerative Medicine, Maastricht University, Maastricht, the Netherlands

²Department of Applied Mathematics, Department of Biology, Cheriton School of Computer Science, and School of Pharmacology, University of Waterloo, Waterloo, Ontario, Canada, N2L 3G1

Introduction

Kidneys play an essential role in the regulation of pH, electrolytes and fluids. Diabetes, one of the most prevalent diseases in the 21st century is characterised by an enlargement of the glomerular and tubular size of the kidney, affecting the kidney filtration rate. Since renal transporters vary along the nephron segments of rodents [1], we hypothesise that the diabetes-induced changes in kidney may exhibit significant sex differences. The goals of this study are to computationally (i) analyse how kidney function is altered in male and female patients with moderate and severe diabetes, and (ii) assess the renal effects, in diabetic women and men, of an anti-hyperglycemic therapy that inhibits the sodium-glucose cotransporter 2 (SGLT2).

Materials and Methods

To accomplish these goals, we have developed computational models of kidney physiology, separate for male and female patients with diabetes[2]. The final segmental cell-based transport model is a composite model of one superficial nephron and five juxtamedullary nephrons to represent all classes of nephrons present in the kidney, all weighted by their population found in the kidney. The model predicts luminal and cytosolic solute concentrations of 15 typical solutes found in kidneys along with fluid flow rates and hydrostatic pressure. To adapt the nephrons to that of a diabetic patient, we have increased the effective surface area of the proximal convoluted tubules to address the hypertrophy seen in such patients. We increased the plasma glucose concentration from 5mM in a non-diabetic case by 72% and 300% in (i) moderately and (ii) severely diabetic cases respectively. The glomerular filtration rate (GFR) was increased by (i) 27% and (ii) 10%. To model SGLT2 inhibition, we lowered the GFR by 3%, reduced SGLT2 activity by 90% and maintained the healthy blood glucose levels.

Results and Discussion

1. Kidney function in diabetic patients *without* SGLT2 inhibition

Without drug intervention, glucose excretion was absent in moderately diabetic patients, similar to healthy patients but increased to 0.6 mol/day in severely diabetic patients (Fig. 1, left column). In the former, hypertrophy, often seen in diabetic patients was able to compensate for the increased glucose load. Na⁺ and Cl⁻ excretion was limited in either cases but urine K⁺ concentration increased in both sexes and both cases. Osmotic diuresis was also observed in both cases.

2. Kidney function in diabetic patients *with* SGLT2 inhibition

Under SGLT2 inhibition, the glucose and sodium reabsorption reduces by 80%. Thus, the glucose excretion increases up to 0.7 mol/day in moderately diabetic case and up to 2 mol/day in severely diabetic patients (Fig. 2, right column). Severe natriuresis is observed in men with sodium excretion increased by 228% but more limited in women, increasing by 68%. The thick ascending limbs in women with higher activity of NKCC2 is able to compensate for the lower absorption in the proximal tubules. Similar effects are seen for K⁺ and Cl⁻ excretion. Extreme diuresis is seen in all cases.



Figure 1: Solute concentration and urine volume compared to levels in healthy patients. MF/MM: moderately diabetic female/male, SF/SM: severely diabetic, SGLT2i: SGLT2 inhibition.

Conclusions/Summary

Model simulations suggest that SGLT2 inhibition, which constricts the afferent arteriole to attenuate glomerular hyperfiltration, can limit Na⁺-glucose transport, consequently raising luminal [Cl⁻] at the macula densa and finally restoring the tubuloglomerular feedback signal. By inducing osmotic diuresis in the proximal tubules, SGLT2 inhibition reduces paracellular transport, eventually leading to diuresis and natriuresis, albeit blunted in women, in part due to their higher distal transport capacity.

References

1. Veiras, L.C., et al., *Sexual dimorphic pattern of renal transporters and electrolyte homeostasis*. Journal of the American Society of Nephrology, 2017. **28**(12): p. 3504-3517.
2. Layton, A.T. and H.E. Layton, *A computational model of epithelial solute and water transport along a human nephron*. PLoS computational biology, 2019. **15**(2): p. e1006108.

Biofabrication of Pre-vascularised Microtissues for Bone Tissue Engineering

Filipa C. Teixeira¹, Lorenzo Moroni¹, Carlos Mota¹

¹Maastricht University, MERLN Institute for Technology-Inspired Regenerative Medicine, Complex Tissue Regeneration Department, Universiteitssingel 40, 6229 ER Maastricht, The Netherlands

Spheroids represent an attractive building block unit for tissue engineering (TE) applications, especially when pre-vascularized. These biological building blocks allow to better recapitulate and mimic the *in vivo* 3D microenvironment, mainly the cell-to-cell and cell-to-extracellular matrix (ECM) interactions. Furthermore, the capacity of spheroids to fuse with each other makes them a promising building block for bottom-up TE approaches. In addition to bottom-up approaches, spheroids are being investigated also in bioprinting to form 3D complex-shaped constructs for tissue and organ regeneration [1]-[4]. The ability to promote adequate vascular morphogenesis in spheroids is a complex process, which is still not completely understood.

In this study, we aim to use vascularized spheroids for bone TE, and evaluate the potential of endothelial cells and their role in osteogenic differentiation. First, we investigated the optimal culture conditions to generate vascularized spheroids using human mesenchymal stromal/stem cells (hMSCs) and human umbilical vein endothelial cells (HUVECs). Spheroid fusion and endothelial sprouting post encapsulation were investigated to access the assembly into a larger tissue intermediate to form 3D complex vascularized macro-tissues.

Results showed that the hMSCs/HUVEC ratio strongly influenced the stability, compactness and sprouting of microtissues. Furthermore, cell viability was largely influenced by the ratio and size of the microtissues. Future studies will aim at inducing differentiation to these microtissues and their bioprintability for the creation of vascularized bone implants.

Acknowledgement:

This research was funded by the European Union's Horizon 2020 framework program, call SC1-BHC-07-2019 - Regenerative medicine: from new insights to new applications, JointPromise - Precision manufacturing of microengineered complex joint implants, under grant agreement 874837. Project website: <http://www.jointpromise.eu/>.

References:

- [1] B. Ayan et al., *Sci. Adv.*, vol. 6, no. 10, p. eaa5111, Mar. 2020.
- [2] D. N. Heo et al., *Biofabrication*, Oct. 2020.
- [3] V. Mironov, R. P. Visconti, V. Kasyanov, G. Forgacs, C. J. Drake, and R. R. Markwald, *Biomaterials*, vol. 30, no. 12, pp. 2164–2174, Apr. 2009.
- [4] C. Norotte, F. S. Marga, L. E. Niklason, and G. Forgacs, *Biomaterials*, vol. 30, no. 30, pp. 5910–5917, Oct. 2009.

3D printed Tissue Self Assembly via Embedded Printing of Newtonian Fluid Suspension Bioinks

V.D. Trikalitis¹, N.J.J. Kroese², M.Kaya^{3,4}, V.Schwach², I.S.M. Khalil³, S.Misra^{3,4}, R.Passier² and Jeroen Rouwkema¹

¹ Vascularization Lab, Department of Biomechanical Engineering, University of Twente, The Netherlands

² Advanced Stem Cell Technologies, TNW, University of Twente, The Netherlands

³ Surgical Robotics Laboratory, Department of Biomechanical Engineering, University of Twente, The Netherlands

⁴ Surgical Robotics Laboratory, Department of Biomedical Engineering and University Medical Centre Groningen, University of Groningen, The Netherlands

Introduction

In extrusion printing, it is crucial that the ink is shear-thinning, so that it can flow through a nozzle. It should also rapidly recover upon deposition in order to maintain its shape post-deposition. This shear-thinning and rapid recovery behavior limits significantly the materials that can be used in 3D printing, and in combination with the biocompatibility requirements, the available materials that can be used for 3D bioprinting are quite limited. Recently, embedded 3D printing has been developed based on granular and yield stress hydrogel support baths where materials can be added within the bath via extrusion, after which the support bath self-heals and supports the added material. This enables the 3D printing of materials that normally do not recover to a solid-state quickly enough after deposition, however the same prerequisites of shear thinning and shear recovery still apply. Newtonian fluids can readily flow through an orifice since they exhibit constant viscosity, and homogenous suspensions of particles with a volume fraction (ϕ) of $\phi < 0.1$ in a liquid, behave predominantly as Newtonian fluids. However if the ϕ of the particle suspension drastically increases after deposition, especially at $\phi > 0.64$, the suspension transitions into a solid, that can maintain its shape. Diffusion can be utilized as a method to reduce the liquid content of a suspension. Utilizing the synergy of these phenomena, we report the successful embedded 3D printing of Newtonian fluids and dilute solid suspensions such as microgels, cell spheroids, and cellular particle suspensions within yield stress fluid self-healing embedding baths. Tissue structures were 3D printed and extracted by diluting the support baths after 7 days of cell culture.

Materials and Methods

For the yield stress fluid embedding bath, 1.5% w/v Xanthan gum (G1253, Sigma-Aldrich, USA) powder was dissolved in mili-Q water, or a cell proliferation medium for the tissue fabrication experiments. For the suspension bioinks, 0.25% Alginate microspheres (IamFluidics B.V.) coated with PLL-FITC, polystyrene particles stained with coumarin-6, RFP-SMC spheroids and purified cardiomyocytes, were tested for the printing demonstrations and tissue fabrication. Blunt tip straight and 90° bent nozzles with ID ranging from 200 μ m to 600 μ m were used in the 3D printer (ROKIT INVIVO). Multicolor fluorescence microscopy imaging was performed in a custom built imaging setup, that allows real-time visualization of embedded injection on a moving stage. For the visualization, a 0.1% w/v Rhodamine in Mili-Q solution including polystyrene particles stained with coumarin-6, at a $\phi = 0.1$ was used to image the suspension ink.

Results

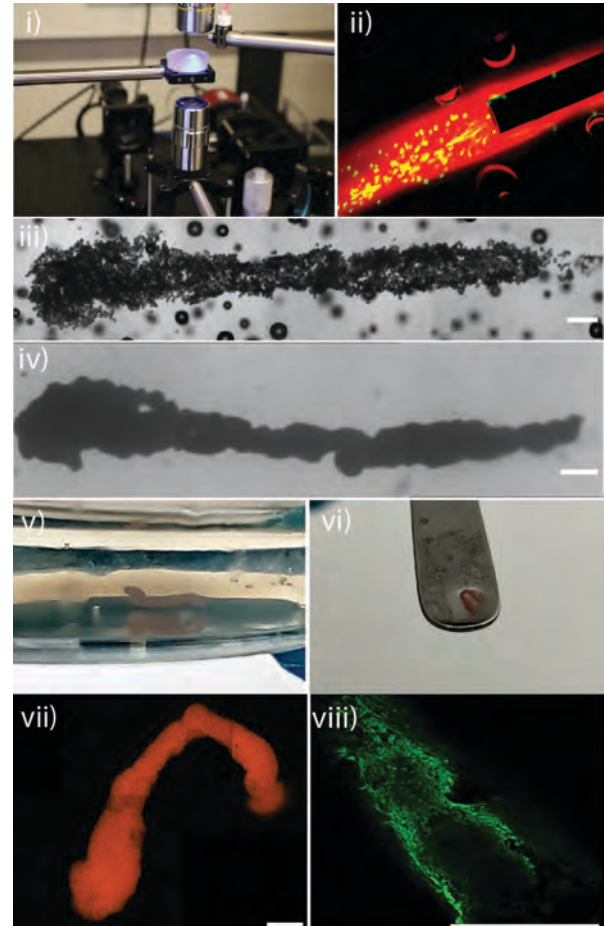


Figure 1: i) Custom imaging setup for real-time visualization of embedded injection. ii) Image frame of printing a suspension of polystyrene particles (green) in a rhodamine liquid phase (red) within a xanthan gum embedding bath. iii) 3D printed line of SMC spheroids in Xanthan Gum bath immediately after printing. iv) Compacted SMC tissue fiber at Day 4 of cell culture. v) Macroscopic image of tissue fiber at Day 7. vi) SMC fiber extracted with a spatula from the xanthan bath. vii) Confocal imaging of SMC fiber after extraction at Day 10. viii) Confocal imaging of SMC fiber with Actin staining showing cellular alignment and no spheroid pattern indicating successful fusion. Scale bar indicates 500 μ m in all images.

Summary

We demonstrate a method for 3D printing Newtonian liquid inks within a yield stress fluid embedding bath. In our work, we challenge the notion that bioinks should have shear-thinning and shear recovery properties. Instead we use dilute suspensions as inks, which is the most common state of matter during cell culture protocols. By utilizing the diffusive properties of liquids within hydrogel matrices, the dilute suspensions become *in-situ* jammed particle constructs. When cells are included, we observed dense tissue self-assembly that can be extracted after maturation.

Co-axial Bioprinting of a Convoluted Proximal Tubule for Kidney Disease Modeling

Marta (M.) G. Valverde^{1*}, A.M. van Genderen^{1,2*}, P.E. Capendale^{1,2}, E. Sendino Garvi¹, C.C.L. Schuurmans^{2,3}, M. Ruelas², J.T. Soeiro², G. Tang², J. Jansen⁴, M.J. Janssen¹, S. Mihaila¹, T. Vermond³, R. Masereeuw¹, Y.S. Zhang²

¹Div. Pharmacology, Utrecht Institute for Pharmaceutical Sciences, Utrecht University, Universiteitsweg 99, 3584 CG Utrecht, The Netherlands.

²Division of Engineering in Medicine, Department of Medicine, Brigham and Women's Hospital, Harvard Medical School, 65 Landsdowne Street, Cambridge, MA 02139, USA

³Div. Pharmaceutics, Utrecht Institute for Pharmaceutical Sciences, Utrecht University, Universiteitsweg 99, 3584 CG Utrecht, The Netherlands.

⁴Department of Pathology and Pediatric Nephrology, Radboud University Medical Center, Nijmegen, The Netherlands

*These authors contributed equally to this work.

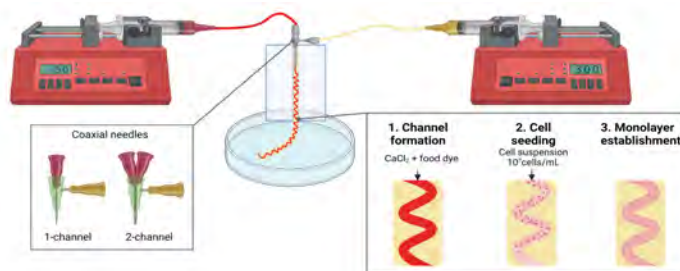
Introduction:

Despite increased global incidence of kidney failure, mechanisms of kidney disease are yet not fully understood. Among the different segments of the nephron, the proximal tubule (PT) is most susceptible for toxicant-induced injury because of its role in xenobiotic secretion and reabsorption. Moreover, genetic defects in transporters may lead to metabolic complications and tubulopathies. To gain insight in these diseases, it is of paramount importance to develop representative biomimetic *in vitro* models. The often applied 2D cell models are based on the use of PT epithelial cells (PTECs) for healthy stages. Genetic manipulations such as conditional immortalization and CRISPR-Cas9 have provided researchers with the tools to recreate cell models representative for diseased stages. Bioprinting offers new modeling alternatives to incorporate extracellular matrix (ECM) interactions as it has been repeatedly shown that both curvature and ECM composition are fundamental for the correct behavior of the PTECs. Extrusion co-axial bioprinting allows the fabrication of hollow channels within microfibers. Here, we apply co-axial printing to create a convoluted channel within a collagen-based microfiber to model the convoluted structure of the PT. Furthermore, we included a cystinosis-deficient (CTNS^{-/-}) cell line for modelling cystinosis, a currently incurable kidney disease.

Materials and Methods:

A bioprinting system consisting of syringe pumps, heaters, coaxial needles, and a silicon holder was designed. A gelatin-alginate-based bioink was formulated to allow printability while maintaining structural properties. Fine tuning of the composition, bioprinting temperature and feeding rate allowed an optimal bioink viscosity. Calcium chloride and microbial transglutaminase were used to stabilize the bioink. Conditionally immortalized PTECs, and CTNS^{-/-} were seeded to mimic two genotypes of PT (Fig. 1). (1,2) Immunofluorescent stainings for cytoskeleton organization (F-actin, Fig. 2), polarization markers (α -tubulin, NaK-ATPase), ECM production (collagen IV) and barrier formation (inulin-FITC leakage) were performed to evaluate the performance of the engineered proximal tubule. To study the stability of the hydrogel, a degradation assay was performed. One-way ANOVA and Tukey test were performed to assess significant differences.

Figure 1.



Results and Discussion:

The optimized bioprinting setup allows for the embedding of two hollow coiled channels within one cytocompatible hydrogel microfiber. Upon seeding, both healthy and CTNS^{-/-} cells formed a tight monolayer within the channel and showed polarization as indicated by staining for F-actin, NaK-ATPase and α -tubulin. Collagen-IV positive staining showed that cells started to deposit extracellular matrix into the tubular construct. The diffusion assay and degradation assay showed 65% permeability for a hydrogel environment of a diameter of 100 μ m on a transwell compared to the 0 μ m control (only transwell) ($P < 0.05$), and no significant degradation over 4 weeks ($P < 0.05$), respectively.

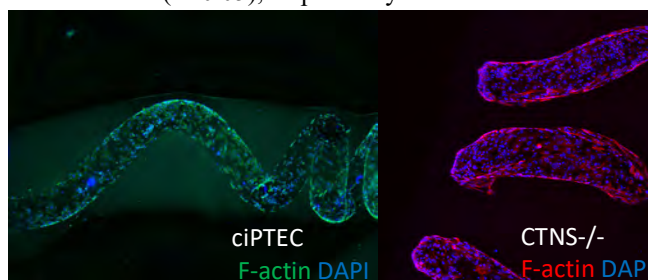


Figure 2.

Conclusions / Summary:

This printing device showed potential to mimic a 3D environment compatible with different PT cells. By further improving this setup, other diseases can be modelled to gain new insights in kidney disease mechanisms and progression.

Acknowledgements: Dutch Kidney Foundation, Utrecht Institute for Pharmaceutical Sciences, Materials Driven Regeneration

References:

1. Wilmer, Martijn J., et al. "Novel conditionally immortalized human proximal tubule cell line expressing functional influx and efflux transporters." *Cell and tissue research* 339.2 (2010): 449-457.
2. Jamalpoor, Amer, et al. "Cysteamine-bicalutamide combination therapy corrects proximal tubule phenotype in cystinosis." *EMBO Molecular Medicine* 13.7 (2021): e13067.

bFGF-Functionalized Polyisocyanopeptide Hydrogel for Tissue Regeneration of the Pelvic Floor

M.J.J. van Velthoven^{1,2}, E. Arendsen^{1,2}, A.N. Guddé³, R. Hammink¹, Z. Guler³, J.P.R.W. Roovers³, E.O. Oosterwijk², P.H.J. Kouwer¹

¹ Institute of Molecules and Materials, Radboud University, Nijmegen, The Netherlands ² Department of Urology, Radboud University Medical Center, Radboud Institute for Molecular Life Sciences, Nijmegen, The Netherlands ³ Department of Obstetrics and Gynaecology, Amsterdam University Medical Center, Amsterdam, The Netherlands

INTRODUCTION: Pelvic Organ Prolapse (POP) is characterized by the descent of the pelvic organs due to weakening of the pelvic floor. Up to 20% of the women get recurrence after surgery, implying that surgical outcomes are poor due to suboptimal wound healing[1]. Tissue engineering has shown great potential in stimulating regeneration by combining cells, biomaterials and biochemical cues. Polyisocyanopeptide (PIC) hydrogels are synthetic, thermosensitive and highly biomimetic, displaying stress-stiffening behavior similar to other biomacromolecules[2]. Furthermore, the PIC hydrogel can be functionalized with growth factors, like basic fibroblast growth factor (bFGF) to further promote cell proliferation and extracellular matrix (ECM) remodeling[3]. In this study, we developed a bFGF-functionalized hydrogel and investigate its wound healing capabilities *in vitro*.

METHODS: PIC polymers were synthesized and conjugated with a cell-adhesive peptide GRGDS as previously reported[4]. bFGF was reacted with DBCO-PEG4-NHS and Alexa647-NHS at 3 and 1.5 equivalent respectively in PBS. Next, the bFGF-DBCO was purified over a 10 kDa spin filter and conjugated to the PIC polymer overnight at 4°C (Fig. 1A). The bioactivity of PIC-bFGF was validated on 3T3 fibroblasts and human adipose-derived stem cells (ADSCs) using the CellTiter-Glo® assay. To assess its wound healing capabilities *in vitro*, the PIC-bFGF (50 ng/mL), encapsulated with ADSCs was evaluated at day 1, 7, 14 and 28. Cell viability was visualized with a LIVE/DEAD staining. ECM deposition was evaluated by quantifying (Sirius red staining) and visualizing (CNA-OG488) collagen and quantification of elastin (Fastin™ Elastin assay).

RESULTS: Dose-response curves were generated to validate the bioactivity of PIC-bFGF (Fig. 1B; $EC_{50} = 18.3$ ng/mL), showing a 3-fold induction in proliferation which is in line with the positive control whereby bFGF is added soluble to the PIC-RGD hydrogel (Fig. 1C; $EC_{50} = 3.7$ ng/mL). ADSCs ($EC_{50} = 17.9$ ng/mL) are highly viable in the PIC-bFGF (Fig. 1D). Furthermore, total collagen amount significantly increases up to day 7 ($p < 0.001$; data not shown) resulting in mature collagen network at day 14 (Fig. 1E). Preliminary data shows no significant increase in total collagen and elastin in the PIC-bFGF versus PIC-RGD yet.

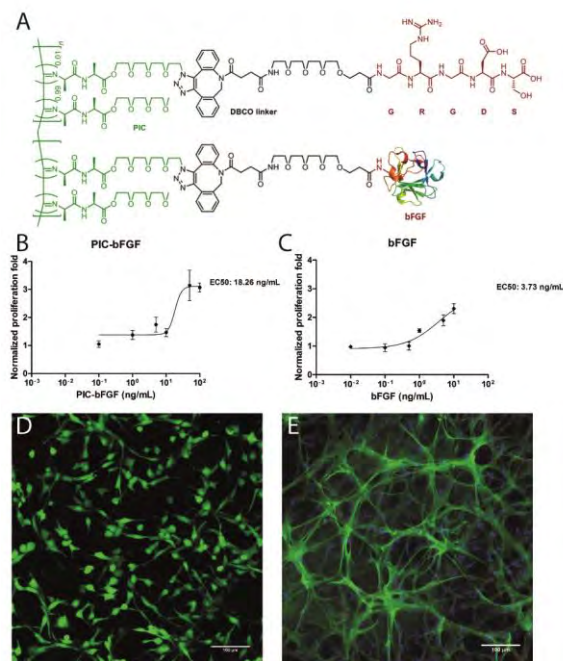


Fig. 1: Molecular structure of PIC-bFGF (A). Dose-response curves of PIC-bFGF (B) and soluble bFGF (C). Cell viability (D; live (green), dead (red)) and collagen production (E; collagen (green) F-actin (red) and nuclei (blue)) visualized via confocal microscopy.

DISCUSSION & CONCLUSIONS: PIC-bFGF is bioactive in both 3T3 and ADSCs. Therefore, the PIC-bFGF is very promising and will be studied to investigate whether wound healing can be promoted *in vivo*. Further research is ongoing to provide more insight in the promoting effect of PIC-bFGF versus PIC-RGD in ADSCs regarding ECM metabolism *in vitro*.

REFERENCES: ¹ Ismail S, Int Urogynaecol J. 2016; 27:1619-1632. ² Das R, Nat. Mater. 2016; 15: 318-325. ³ van Velthoven. 2022, manuscript in preparation. ⁴ Liu K, ACS. Appl. Mater. Interfaces 2020, 212: 56723-56730.

Labelling Limbal Stem Cells with Custom Nanoparticles to Track Corneal Regeneration

Arianne J.H. van Velthoven^{1,2}, Chloe A. Trayford¹, Sabine H. van Rijt¹, Vanessa L.S. LaPointe¹, Mor M. Dickman²

1. Department of Cell Biology–Inspired Tissue Engineering, MERLN Institute for Technology-Inspired Regenerative Medicine, Maastricht University, Maastricht, the Netherlands.

2. Maastricht University Medical Center+, University Eye Clinic Maastricht, Maastricht, the Netherlands.

The cornea is the transparent outer layer of the eye that covers the iris. The renewal and repair of the corneal epithelium depends on the epithelial stem cells present in the limbus (LESCs), which is located at the corneal scleral rim. Thermal or chemical ocular burns can destroy the limbus, causing a limbal stem cell deficiency (LSCD). LSCD results in conjunctivalization and neovascularization leading to pain and vision loss. Currently, treatment of unilateral LSCD involves transplantation of cultivated autologous limbal tissue onto the affected eye to restore a functional corneal epithelium. However, this stem cell–based therapy is hindered by a 66–77% success rate and requires a second procedure in many cases. Furthermore, the

mechanisms that underlie corneal regeneration after LES C transplantation are not clearly understood. To understand the mechanisms behind corneal epithelial regeneration, we use mesoporous silica nanoparticles with multimodal imaging capabilities to track transplanted LES Cs in vivo. Here, we validated the efficiency of this labelling and tracking method in vitro. We looked at the uptake efficiency of the particles in LES Cs and its effect on cellular behavior. Furthermore, we show the multimodal imaging properties of the particles using fluorescent imaging and optical coherence tomography. Our results link the regenerative potential of LES Cs to corneal regeneration post- engraftment.

Alignment of Keratocytes and Deposited Matrices in Concave, Micropatterned Environments

C. van der Putten^{1,2}, T.E. Woud^{1,2}, C.V.C. Bouten^{1,2} & N.A. Kurniawan^{1,2}

1. Soft Tissue Engineering and Mechanobiology, Department of Biomedical Engineering, Eindhoven University of Technology, PO Box 513, 5600 MB Eindhoven, The Netherlands
2. ICMS, Eindhoven University of Technology, 5600 MB Eindhoven, The Netherlands

Introduction | Worldwide, more than 23 million people are affected by loss of vision due to opacity in the corneal stroma¹. Currently, the most successful treatment option is a corneal transplantation, performed more than 65,000 times every year worldwide. Unfortunately, the demand for suitable donor tissue is still higher than the availability^{2,3}. In order to overcome this problem, alternatives for allogenic transplants need to be developed. A promising way to realize this is by mimicking the native structure of the cornea, which is crucial for proper optical and mechanical tissue function. The cornea mainly consists of highly organized collagen lamellae, maintained by keratocytes⁴. Therefore, many studies focused on the production of aligned collagen *in vitro* using contact-guidance cues such as structured culture substrates or aligned electrospun scaffolds to steer cell and collagen alignment. Although these studies show great potential, the *in vivo* environment is more complex with for example the curvature of the tissue also affecting cell and collagen alignment. Therefore, this study aims to combine both contact guidance and curvature guidance cues and study the alignment of keratocytes and the extracellular matrix. Ultimately, this may lead to a better understanding of the roles of environmental cues in the production of a native-like corneal stroma. Besides, upon understanding this approach may aid in the steering of cell and matrix alignment in more complex, representative *in vitro* environments.

Methods | PDMS cell culture chips containing a range of concave curvatures ($1/8000 \mu\text{m}^{-1} \leq \kappa \leq 1/250 \mu\text{m}^{-1}$) were produced using a negative mold. Next, chips were passivated using poly-L-lysine and mPEG-SVA and subsequently patterned (parallel lines or concentric circles) using an optics-based projection system (PRIMO, Alvéole), following a newly established protocol⁵. Next, a gelatin-fluorescein coating was applied to the surface of the substrates in order to induce a contact guidance response (see Figure 1). Primary keratocytes were isolated from donor material and cultured in DMEM/F12 supplemented with 5% FBS, 1% glutamax, 1% Penicillin/streptomycin, and 1 mM vitamin C. Cultures were fixed on day 1 and 7 to measure cell and collagen alignment.



Figure 1: 3D (left) and top down (right) visualization of a concave hemisphere ($\kappa=1/1000 \mu\text{m}^{-1}$) containing a circular pattern (lines: $20 \mu\text{m}$ wide and $20 \mu\text{m}$ gaps) of gelatin-fluorescein (green).

Results and Discussion | After 1 day, keratocytes on both circle and line patterns predominantly showed a contact guidance response on all curvatures (see Figure 2). No collagen was deposited yet after 1 day of culture. For the hemisphere with $\kappa = 1/1000 \mu\text{m}^{-1}$, the alignment response of keratocytes changed over the culture period of 7 days, indicating a reduction in the contact guidance response. Besides, no clear effect of curvature guidance was observed. We hypothesize that this reduction in cell alignment is due to the increased cell density within the fibrous matrix produced by the keratocytes themselves.

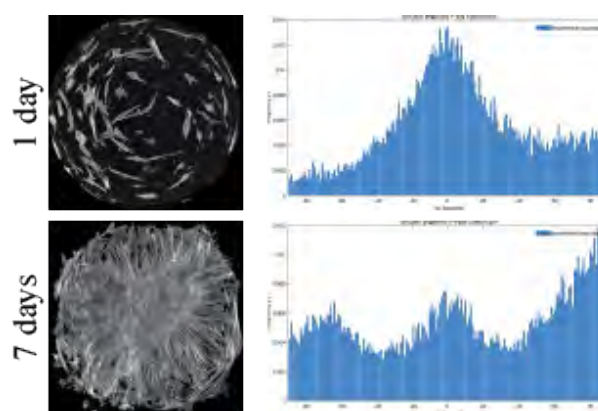


Figure 2: Maximum intensity projections and quantified alignment response of primary keratocytes cultured 1 and 7 days on patterned domes of $\kappa=1/1000 \mu\text{m}^{-1}$. X-axis from -90 to 90 degrees with respect to tangent of dome.

Conclusion and Outlook | The results indicate that the initial response of keratocytes can be steered in a desired direction using mainly contact guidance cues. However, upon increased proliferation, the population pressure of collective cell sheets appears dominant over the physical cues of the engineered multi-cue environments. Eventually, this study also may aid in the development of aligned sheets of collagen that can offer a solution to restore diseased corneas in patients suffering from corneal disease.

- [1] Hertsberg A.J. et al., Stem Cells in the Cornea, *Prog Mol Biol Transl Sci*, 134, 25-41, 2015
- [2] Tan D.T. et al., Corneal transplantation, *The Lancet*, 379(9827), 1749-1761, 2012
- [3] Williams K.A. et al., Prospects for genetic modulation of corneal graft survival, *Eye*, 23(10), 1904-1909, 2009
- [4] Reinstein D.Z. et al., Stromal Thickness in the Normal Cornea: Three-dimensional Display With Artemis Very High-frequency Digital Ultrasound, *J Refract Surg.*, 25(9), 776-786, 2009
- [5] van der Putten C. et al., Protein Micropatterning in 2.5D: An Approach to Investigate Cellular Responses in Multi-Cue Environments, *ACS Appl. Mater. Interfaces*, 13(22), 25589–25598, 2021

This work was performed under the framework of Chemelot InSciTe.

Cell Population Characterization of Enzymatically Isolated Articular Chondrocytes and Chondrons

M. van Mourik, G.H. Schuringa, C.C. van Donkelaar, J. Foolen, K. Ito

Orthopaedic Biomechanics, Dept. Biomedical Engineering, Eindhoven University of Technology,
P.O. Box 513, 5600 MB Eindhoven, The Netherlands

Introduction: In articular cartilage, chondrocytes are surrounded by a pericellular matrix (PCM), together, referred to as a chondron. Considered as the functional unit of articular cartilage, they are advantageous for cartilage regeneration. The method for enzymatic isolation of chondrons from articular cartilage described by Lee *et al* [1] is currently the golden standard for obtaining chondrons. However, this method results in a heterogeneous population of chondrons and chondrocytes [2]. Although this heterogeneity can influence their use, the properties and compositions of these cell populations have never been thoroughly characterized. The aim of this study is to compare enzymatic isolation methods for chondrons and characterize the results based on cell yield, efficiency, and structural quality of the PCM.

Methods: Articular chondrocytes and chondrons were enzymatically isolated from fresh bovine articular cartilage (n=3). Chondrocytes were isolated by overnight digestion at 37° C in 0.15% collagenase II and 0.01% hyaluronidase in DMEM, supplemented with 10% FBS and 1% pen/strep (Chy). Chondrons were isolated using an overnight or a 5-hour protocol, using 0.15% dispase and 0.1% collagenase II in DMEM, supplemented with 1% pen/strep (Chn ON) or 0.3% dispase and 0.2% collagenase in DMEM with 1% pen/strep (Chn 5H), respectively. Undigested tissue remnants were filtered out using a 70 µm and 100 µm cell strainer for the chondrocyte and chondrons digestion, respectively. All cells were washed twice with PBS, centrifuged at 150g for 5 min, and kept overnight in a loose pellet culture. For flow cytometry, cells were washed with 3% bovine serum albumin (BSA) in PBS and labelled with FITC-conjugated rabbit anti-collagen type VI polyclonal antibody at a dilution of 1:100 for 30 min. at 4° C. Flow cytometry was performed using a FACS Canto II and resulting data was analyzed using FlowJo. Data are presented as mean (± SD). For comparison of cell populations, a two-way ANOVA was performed with significance set as $p < 0.05$.

Results: For all isolations, a heterogeneous population of negatively and positively stained cells was found. The efficiency of Col-VI positive cells for Chy, Chn 5H and Chn ON was respectively 71% (± 12%), 93% (± 3.1%), and 82% (± 4.4%). However, within the Col-VI positive cells, two populations of high- and low-intensity staining

was found (Fig 1B). It was assumed that the high-intensity cells were intact chondrons and the low-intensity cells were chondrocytes with a partial PCM (partial chondrons). Single-cell and multicellular events were defined based on the relation between FSC-A and FSC-W, resulting in 20% (± 5.4%), 37% (± 4.5%), and 19% (± 8.9%) multicellular events in Chy, Chn 5H and Chn ON respectively. Intact chondrons were mainly found in the multicellular population, partial chondrons were found in both populations, and chondrocytes were mainly found in the single-cell population (Fig. 2). The percentage of partial chondrons in the multicellular population was found to be significantly lower in the Chn 5H digestion compared to the other digestions, while the percentage of intact chondrons for the Chn 5H was significantly higher in both the single-cell and multicellular populations compared to the other digestion methods (Fig 2B-C).

Discussion: This research showed that for both chondron and chondrocyte isolations, highly heterogeneous populations were obtained, which might influence the outcomes using these isolations. The golden standard five-hour digestion (Chn 5H) showed significant higher amounts of chondrons with an intact PCM in comparison with the overnight digestion. This was based on the assumption that high-intensity stained cell populations are intact chondrons, although the differences in intensities might also be due to zonal variation of the 3D morphology of chondrons [3]. However, due to the heterogeneity within the Col-VI positive cell populations, a more thorough characterization of these populations is necessary. The next step will be to obtain more insight into the properties of the observed cell populations and to improve the chondron population homogeneity using FACS.

Acknowledgements: This research was financially supported by the Gravitation Program “Materials Driven Regeneration”, funded by the Netherlands Organization for Scientific Research (024.003.013), and was performed under the framework of Chemelot InSciTe, supported by the partners of Regenerative Medicine Crossing Borders (www.regmedxb.com) and powered by Health-Holland, Top Sector Life Sciences & Health.

References:

- [1] Lee, G.M., *et al.* Osteoarthr Cartilage (1997)
- [2] Peters, H.C., *et al.* Tissue Engineering (2011)
- [3] Youn, I., *et al.* Osteoarthr Cartilage (2006)

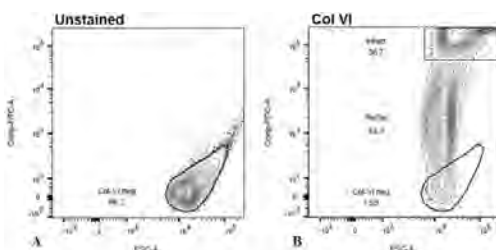


Figure 1: Flow cytometry data of unstained (A) and Col-VI stained (B) population of the 5-hour digestion protocol.

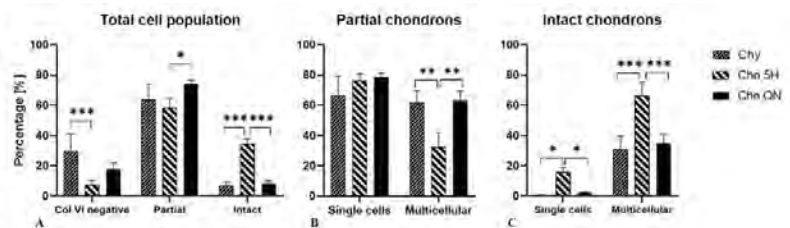


Figure 2: Percentages of Col VI negative cells, chondrocytes with partial PCM and intact chondrons of the total population (A). Differentiation of the percentages of chondrocytes with a partial PCM (B) and intact chondrons (C) within the single cell or multicellular population.

Efficacy of Diagnostic and Antimicrobial Capacity of Smart Triggered Release Systems for Medical Devices *In Vivo*

Nikitha Va vilthota, Gizem Babuccu, Martijn Riool, Sebastian A.J. Zaaij

Department of Medical Microbiology & Infection Prevention, Amsterdam institute for Infection and Immunity,
Amsterdam UMC, University of Amsterdam, Meibergdreef 9, 1105 AZ Amsterdam, The Netherlands

n.va.vilthota@amsterdamumc.nl

The use of biomaterials in modern medicine has overall improved patient care and quality of life. However, their usage is accompanied with additional complications specifically pertaining to that of infections. Furthermore, the presence of biomaterials in patients elevates susceptibility to infection. Biomaterial associated infections are the major cause for implant failure often leading to prolonged prescription of antibiotics, resulting in resistance or complete removal of implant with associated complications. Implant-associated infections are threatening the large-scale usage of biomaterials in medical practices.

Health care infections (HAIs) are the infections contracted in hospitals or other health care facility. They are severe global problem threatening the health, long term well-being of millions of people. The current antibiotic resistance in bacteria, possess an additional looming burden of HAIs, leading to worldwide concerns over the last decade. There is a urgent need to develop a novel strategy for early detection and treatment for HAIs.

In this light, the European Marie Skłodowska training network STIMULUS “Stimuli Responsive Materials for the Rapid Detection and Treatment of Healthcare Associated Infections” aims at creating medical devices that signal when an infection is present and thereby reduces the unnecessary prescription of antibiotics and hence the spread of antibiotic resistance. An important feature is the release of potent antimicrobials by an externally triggered stimulus to treat the infection.

The most common HAIs are urinary tract, wound site and respiratory tract infections. Particularly chronic skin wounds are painful, notoriously difficult to treat locally. Wound site infections apart from having numerous challenges to treat due to biofilm formation and antibiotic resistance can have debilitating effects on patients' health. The current project aims to study the diagnostic sensitivity, specificity, and performance for the detection of bacterial species in wound infections, and to evaluate the efficacy of novel antimicrobial systems to prevent or treat them will be evaluated in *in vivo* systems. Established mouse models of skin infection or subcutaneous implant infection will be used as platforms for these *in vivo* studies.

The objectives of this project include testing the models for smart triggered release systems – developed at the STIMULUS consortium partners – for novel antimicrobial peptides along with assessing the diagnostic capacity of these “theranostic” systems. Subsequently the following stages of the project include assessing the release of novel antimicrobial peptides against multi drug resistant bacteria.

The local and systemic environment of the host greatly influences the efficacy of the antimicrobial release systems. Detailed studies on cellular immune responses to these implants and the antimicrobial systems will be performed. Important immune mediators such as cytokines and their activity will be evaluated. Inflammatory mediators will potentially be used as stimuli for triggering the release of antimicrobial peptides in presence of bacterial infection. Ultimately, this type of smart triggered release systems will be used to detect, prevent, and treat bacterial infections.

Manipulation of Astrocyte Behavior on Graphene-based Biomaterials

K. Verstappen, A. Klymov, S.C.G. Leeuwenburgh, and X.F. Walboomers

Department of Dentistry-Regenerative Biomaterials, Radboud Institute for Molecular Life Sciences, Radboud university medical center;

Philips van Leydenlaan 25, 6525 EX Nijmegen, The Netherlands;

kest.verstappen@radboudumc.nl

Introduction

Due to their specific morphological, electrical and mechanical properties, graphene-based biomaterials have been shown to stimulate neuronal cell proliferation and differentiation as well as axonal outgrowth and signaling.¹ These features render this novel biomaterial a promising candidate for spinal cord regeneration. While most current research is focusing on the interaction between graphene and (reduced) graphene oxide and neuronal cells, its effect on glial cells like astrocytes, remains poorly understood. Being one of the main reasons for decreased neuronal regeneration in paralyzed patients,² in vitro evaluation of astrocyte response to any biomaterial of interest could (partially) predict the success of spinal cord regeneration therapies. Following spinal cord injury, resident astrocytes adopt a reactive phenotype in a process called astrogliosis.³ Activated astrocytes proliferate and migrate towards the site of injury, where they contribute to a cellular and biochemical barrier called the glial scar, which is advocated as the major factor contributing to inhibited regeneration.³ In fact, recent studies demonstrated that the binding of reactive astrocytes to collagen type I could accelerate this process.⁴

Materials and Methods

To investigate the ability to steer astrocyte behavior, the here presented study utilizes primary astrocytes for 2D and 3D culture using collagen type I (COL) or adipose-derived extracellular matrix (ECM) hydrogels, with or without the incorporation of graphene oxide (COLGO and ECMGO).

Results and Discussion

Reactivity- and proteoglycan-associated gene expression levels were significantly attenuated in primary astrocytes

cultured on graphene-based hydrogels, compared to the collagen type I control. Additionally, culturing primary astrocytes in 3D led to a similar but more pronounced attenuation of reactivity. Preliminary immunofluorescence stainings showed an increase of both astrocyte number as well as proteoglycan expression following extended culture periods (14 days in vitro) on adipose-derived ECM substrates, which could not be observed on graphene-based hydrogels.

Conclusion

These results indicate that the phenotype of astrocytes can be tuned by using graphene-based biomaterials. Currently, astrocyte/neuron co-culture models are being used to determine whether this altered proteoglycan-associated expression in turn affects neurite outgrowth. Future research will determine whether these biomaterials can be applied to create a pro-regenerative environment in vivo.

Acknowledgements

This project has received funding from the European Union's Horizon 2020 research and innovation program under grant agreement No829060.

References

1. O. Akhavan, *J. Mater. Chem. B* (2016); 4: 3169.
2. J. Silver and J.H. Miller, *Nature Reviews Neuroscience* (2004); 5: 146-156.
3. A. Alizadeh, S.M. Dyck, and S. Karimi-Abdolrezaee, *Front. Neurol.* (2019); 10: 282.
4. M. Hara, K. Kobayakawa, Y. Ohkawa, H. Kumamaru, K. Yokota, T. Saito, K. Kijima, S. Yoshizaki, K. Harimaya, Y. Nakashima, and S. Okada. *Nature Medicine* (2017); 23(7): 819-830.

Nanoparticle-based tracking and quantification of Col I and II in microtissues

Gerli Viilup, Sabine van Rijt

MERLN Maastricht University, Universiteitssingel 40, Maastricht, The Netherlands

Introduction: Osteoarthritis (OA) is a chronic and progressive joint disorder [1] characterized by degeneration and loss of articular cartilage [2, 3]. With the emergence of regenerative medicine, possible use of tissue-engineered implants can become a form of treatment in the future. Success of such treatment often depends on the quality of the implant characterized by the ratio of extracellular matrix (ECM) components (Col II/I) [4], which later determine the cartilage and bone production. Current methods in identifying collagen production in tissue constructs include use of antibody staining and collagen targeting peptide-modified (TP) nanoparticles focusing mainly on Col1 targeting [5]. Mesoporous silica based nanoparticles (MSNs) constitute a flexible platform for drug delivery and imaging in tissue engineering [6]. Here we report a novel way to image collagen I and II production in microtissues using mesoporous silica nanoparticles. In this study, we aim to follow collagen production in microtissue ECM over time, using MSNs of different size for enhanced tissue penetration.

Materials and Methods: Rhodamine B Isothiocyanate (RITC) was encapsulated in the MSN core and the nanoparticle surface modified with collagen targeting peptides (MSN-TP). In this particular study, *in vitro* model of collagen I gel interactions with MSN-Col1TP was imaged. Collagen gels were formed by mixing 3 mg/mL collagen I with 1x PBS buffer (pH=7.0, 100mM) and 0.1M NaOH at 37°C, overnight incubation. The targeting specificity was investigated through fluorescence microscopy. Additionally, nanoparticle concentration effects on hMSCs cellular aggregate formation and morphology were investigated up to 100 µg/mL.

Results and discussion: Fluorescence microscopy imaging of hMSCs cell aggregate interaction with MSNs (surface unmodified) showed no adverse of effects on cell morphology. *In vitro* studies showed collagen type I-specific targeting.

Conclusion: Using collagen I/II targeting peptide-modified and fluorescently labelled mesoporous silica nanoparticles, we aim to follow collagen production in microtissues over time. *In vitro* studies involving collagen gels have shown successful staining of collagen I fibers with nanoparticles. These results indicate that we are able to target collagen I specifically in *in vitro* models. The follow up study will be carried out for collagen II *in vitro* model. Additionally, we intend to image collagen in microtissues (grown from hPDSCs) and animal tissues.

Acknowledgements: This work is part of the JOINTPROMISE consortium funded by Horizon 2020 framework program, call SC1-BHC-07-2019 – Regenerative medicine: from new insights to new applications.

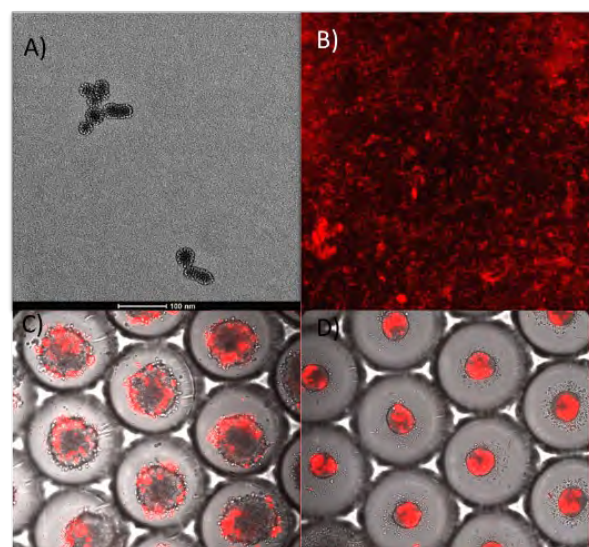


Figure 1. (A) TEM image of a 25 nm RITC modified MSN, (B) Col1TP-MSN labelled Col1 gel, (C) hMSC cell aggregate formation with fluorescently labelled MSNs (100 µg/mL) day 1, (D) day 7.

1. Thysen, S., F.P. Luyten, and R.J. Lories, *Targets, models and challenges in osteoarthritis research*. *Dis Model Mech*, 2015. **8**(1): p. 17-30.
2. Kalamegam, G., et al., *A Comprehensive Review of Stem Cells for Cartilage Regeneration in Osteoarthritis*. *Adv Exp Med Biol*, 2018. **1089**: p. 23-36.
3. Im, G.I. and T.K. Kim, *Regenerative Therapy for Osteoarthritis: A Perspective*. *Int J Stem Cells*, 2020. **13**(2): p. 177-181.
4. Chen, J.-L., et al., *Extracellular matrix production in vitro in cartilage tissue engineering*. *Journal of Translational Medicine*, 2014. **12**(1): p. 88.
5. Wahyudi, H., et al., *Targeting collagen for diagnostic imaging and therapeutic delivery*. *J Control Release*, 2016. **240**: p. 323-331.
6. Rosenholm, J.M., et al., *Mesoporous silica nanoparticles in tissue engineering--a perspective*. *Nanomedicine (Lond)*, 2016. **11**(4): p. 391-402.

Silk-based inks: from molecules to well-organized fibrous scaffolds

Martina Viola^{1,2}, Susanna Piluso, Marko Mihajlovic¹, Anne Metje van Genderen³, Jim de Ruiter⁴, Jos Malda², Tina Vermonden¹ and Miguel Castillo^{2,5}

¹ Department of Pharmaceutical Sciences (UIPS), Faculty of Science, Utrecht University, Utrecht, The Netherlands.

² Department of Orthopaedics, University Medical Center Utrecht, Utrecht, The Netherlands.

³ Department of Pharmacology, Utrecht University, Utrecht, the Netherlands.

⁴ Department of Inorganic Chemistry and Catalysis, Utrecht University, Utrecht, the Netherlands.

⁵ Department of Biomedical Engineering, Technical University of Eindhoven, Eindhoven, the Netherlands.

Silk as a material – from its unique mechanical properties to its biological properties – has been continually inspiring materials scientists, biologists and more recently tissue engineers. One open challenge in tissue engineering is to mimic the complex hierarchical structure of extracellular matrix (ECM) found in living tissues.^{1,2} In this project we aim to mimic the mechanical properties of collagen fibers within the cartilage tissue. To do this we have developed an alternative method of crosslinking silk fibroin (SF) from *Bombyx mori* cocoons, whose physicochemical properties have been thoroughly investigated.³ Significant efforts have been focused on reproducing the unique mechanical properties of natural silk fibers, but until now no method has managed to reproduce its elasticity and strength.

In this work we are developing an alternative method to process SF that induces a rearrangement of the secondary structure in the protein, such as to guarantee a level of elasticity that cannot be reached with other techniques. This material was also chosen for its inherent characteristic of forming fibrous structures.

In this regard, to induce the formation of fibrous structures we have chosen to process SF with electrohydrodynamic printing, an additive manufacturing technique that deposits polymer fibers on a computer-controlled collection plate, to form highly defined scaffold structures.

The feature that makes electrohydrodynamic printing an interesting biofabrication technique is the ability to fabricate well-organized fibrous scaffolds with resolutions (i.e. fiber diameter and pore size) not possible with conventional nozzle-based bioprinting processes.^{4,5} In this work, we have demonstrated the printability of SF with electrohydrodynamic printing. We adjusted the rheological properties by varying the concentration of SF (15% w/v) and the concentration of polyethylene oxide (2% w/v) (Mw: 600-1000 kDa), to obtain straight fibres in squared shaped laydown patterns with a fibre diameter of 10 to 20 μm and a minimum distance between fibres of 200 μm . Moreover, we demonstrated the stackability of the printed layers (up to 15). These scaffolds were physically crosslinked with a solution of sodium phosphate (1M) to make them stable in water and to induce elasticity in the fibres. We compared this

crosslinking method with the crosslinking with methanol, used several times in literature.

We have observed that the sodium phosphate crosslinking not only makes the fibres more elastic and less brittle, but also more stable and manageable in an aqueous environment.

The innovation that we want to propose with this project lies in this post-treatment to which the SF fibers are subjected, which not only guarantees the maintenance of the printed three-dimensional structure, but also induces innovative mechanical properties in the protein not yet observed with other crosslinking techniques.

Overall, the here developed materials have great potential to create a scaffold that manages to reproduce the internal collagen structure of cartilage. Our next steps will focus on reproducing both the hierarchical structure of cartilage from bottom to top, and the natural gradient in mechanical properties.

Email: m.viola@uu.nl

References

1. Hynes, R. O., The extracellular matrix: not just pretty fibrils. *Science* 2009, 326 (5957), 1216-1219.
2. Lutolf, M.; Hubbell, J., Synthetic biomaterials as instructive extracellular microenvironments for morphogenesis in tissue engineering. *Nature biotechnology* 2005, 23 (1), 47-55.
3. Koh, L.-D.; Cheng, Y.; Teng, C.-P.; Khin, Y.-W.; Loh, X.-J.; Tee, S.-Y.; Low, M.; Ye, E.; Yu, H.-D.; Zhang, Y.-W., Structures, mechanical properties and applications of silk fibroin materials. *Progress in Polymer Science* 2015, 46, 86-110.
4. Castillo, M.; van Mil, A.; Maher, M.; Metz, C. H.; Hochleitner, G.; Groll, J.; Doevendans, P. A.; Ito, K.; Sluijter, J. P.; Malda, J., Melt electrowriting allows tailored microstructural and mechanical design of scaffolds to advance functional human myocardial tissue formation. *Advanced Functional Materials* 2018, 28 (40), 1803151.
5. Monti, P.; Freddi, G.; Bertoluzza, A.; Kasai, N.; Tsukada, M., Raman spectroscopic studies of silk fibroin from *Bombyx mori*. *Journal of Raman Spectroscopy* 1998, 29 (4), 297-304.

Design of a 3D corneal stromal construct using supramolecular hydrogels functionalized with bioactive additives for encapsulation and recruitment of corneal keratocytes.

A.F. Vreken^{1,2,3}, J. Huang^{2,3}, P.Y.W. Dankers^{1,2,3}

¹Department of Biomedical Engineering, Laboratory for Cell and Tissue Engineering, ²Institute for Complex Molecular Systems,

³Department of Biomedical Engineering, Laboratory of Chemical Biology, Eindhoven University of Technology, PO box 513, 5600 MB Eindhoven, The Netherlands

Introduction | The cornea is a transparent avascular tissue which is responsible for refracting and transmitting light into the eye. About 90% of the cornea is composed of the stroma which exists of precisely arranged collagen fibrils. Between these collagen lamellae keratocytes can be found, which are mitotically quiescent cells.[1] In wound repair processes these keratocytes differentiate into a myo-fibroblastic phenotype. Lately, the idea of a bioengineered cornea has gained credibility in the field of ophthalmology. Synthetic hydrogels based on supramolecular moieties allow for material tunability by the incorporation of bioactive additives into the material which encourage the mimicking of the natural extracellular matrix. In this project, we aim to modify bioactive additives with ureido-pyrimidinone (UPy) moieties to design an *in-vitro* hydrogel-based 3D stromal construct for encapsulation and recruitment of corneal keratocytes. Hereby, a fully synthetic hydrogel based on an integrin binding peptide is compared with a hybrid hydrogel based on a collagen binding peptide and full length collagen protein.

Materials and methods | Diba *et al.* explored supramolecular hydrogels formed from molecules with bivalent (fig. 1A) and monovalent (fig. 1B₁) fourfold hydrogen bonding designs. These molecules self-assemble into supramolecular fibers and form a dynamic and biocompatible hydrogel network.[2] An integrin binding peptide, cRGDfk (fig. 1B₂) and a collagen type I binding peptide (fig. 1B₃) were synthesized and functionalized with UPy-moieties.[3] Both the cRGDfk peptide and the collagen binding peptide in combination with bovine collagen type I were incorporated as bioactive additives in a hydrogel with a bivalent and monovalent core. Subsequently, primary human keratocytes were cultured for several weeks in 3D. These primary keratocytes were treated with FBS to differentiate the cells into myofibroblasts and without FBS to differentiate the cells into keratocytes. Immunofluorescence and an enzyme linked immune-

sorbent assay were used to study the cellular behavior of the cells encapsulated within hydrogels.

Results and discussion | The ELISA revealed a decrease of interleukin-8 (IL-8) for the keratocytes and an increase in IL-8 for the myofibroblasts. (fig. 2A) Furthermore, immunofluorescence showed elongated cells for the cells treated as myofibroblasts and more spindle like phenotype was observed for the cells treated as keratocytes. (fig. 2B) These results indicate that both the fully synthetic hydrogel, as well as the hybrid hydrogel are biocompatible for the primary stromal cells. Moreover, a successful differentiation of the keratocytes was achieved for both hydrogels. More experiments are necessary to study possible differences between the two hydrogel compositions.

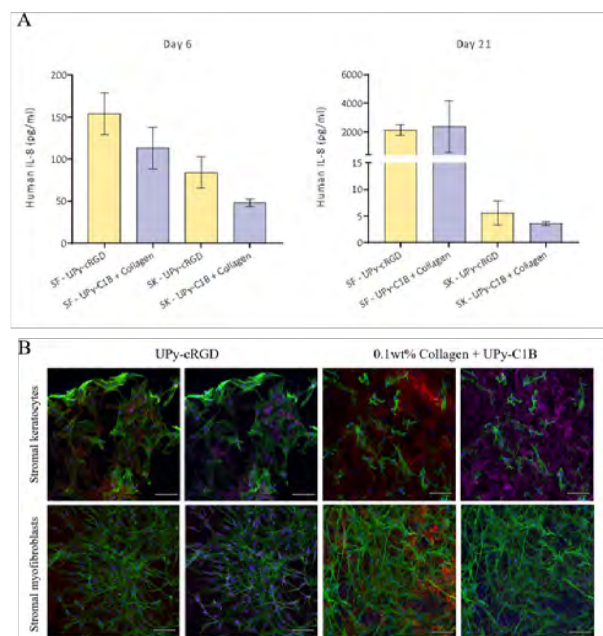


Figure 1. Cellular read-outs of encapsulated human primary stromal cells. **A.** Quantification of over-time human interleukin-8 secretion by primary keratocytes (SK) and myofibroblasts (SF), measured by an ELISA. **B.** Immunofluorescence of SK and SF after 21 days of encapsulation within the hydrogels; f-actin (green), nuclei (blue), collagen type I (red) and collagen type VI (purple). Scalebar 100µm.

Conclusion | We have successfully designed two 3D-hydrogelconstructs with biological properties to support the encapsulation of primary human keratocytes. Moreover, it was achieved to successfully guide differentiation of the encapsulated primary cells towards keratocytes and myofibroblasts. Next, more experiments are needed to explore the suitability of the studied hydrogels as a successful design of a stromal construct.

This work was performed under the framework of Chenelot InSciTe. [1] D.W. DelMonte *et al.*, "Anatomy and physiology of the cornea," *Journal of Cataract & Refractive Surgery*, Mar. 2011 | [2] M. Diba *et al.*, "Engineering the Dynamics of Cell Adhesion Cues in Supramolecular Hydrogels for Facile Control over Cell Encapsulation and Behavior," *Advanced Materials*, Sep. 2021 | [3] B.A. Helms *et al.*, "High-Affinity Peptide-Based Collagen Targeting Using Synthetic Phage Mimics: From Phage Display to Dendrimer Display," *Journal of the American Chemical Society*, Aug. 2009

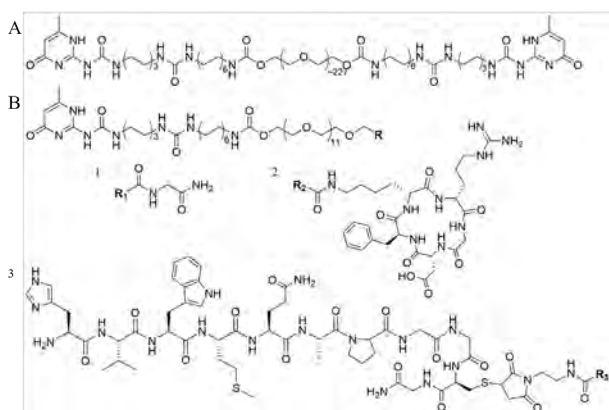


Figure 1. Chemical structures of used polymers. **A.** Bivalent UPy PEG_{10k}. **B.** Monovalent UPy polymer with various end groups (R), (1) Glycine, (2) cyclic RGDfk, (3) Collagen binding peptide end group.

A Bioinspired Strategy for Controlled Bio-functionalization of Polyacrylamide Hydrogels with Bioligands

A. Wolfel, M. Jin, J.I. Paez

Developmental BioEngineering, TechMed Centre and Molecules Centre, University of Twente, Drienerlolaan 5, 7522 NB Enschede, The Netherlands
a.wolfelsanchez@utwente.nl

Introduction: Understanding and controlling cell-materials interactions is key to modulate cell behavior in tissue engineered constructs. Polyacrylamide (PAM) hydrogels are used as 2D models for cell culture, allowing the study of cell response to specific biochemical and biophysical cues. PAM gels present advantages such as easy preparation, low cost, and compatibility with high-resolution and traction force microscopies. Because of their characteristic protein repellence, when used as biomaterials for the study of specific cell-materials interactions, PAM gels need to be biofunctionalized with cell-adhesive ligands in a controlled and tunable fashion. For this purpose, biofunctionalization strategies are necessary. Such strategies should ideally be user-friendly (e.g., involve few steps), inexpensive, and chemoselective (i.e., allow the controlled immobilization of the biomolecule to avoid unspecific binding that would lead to impaired functionality). Despite the effort achieved so far, current approaches to biofunctionalized PAM gels fail in some of the mentioned aspects [1]. Therefore, developing chemical strategies towards controlled PAM bioconjugation is of great interest.

In this work, we present our ongoing efforts in developing novel strategies that facilitate the biofunctionalization of PAM hydrogels with cell-adhesive ligands by means of a bioinspired coupling reaction: the luciferin-inspired click ligation [2]. We develop novel comonomers featuring a cyanobenzothiazole (CBT) group, which are compatible with PAM preparation. When copolymerized with acrylamide and a crosslinker via established protocols, PAM hydrogels with controlled mechanical properties are easily obtained. Pendant CBT moieties can later be used to covalently bind *N*-cysteine containing biomolecules in a single step, under physiological conditions, and at tunable concentrations.

Materials and Methods: ammonium persulfate (APS), *N,N,N',N'*-Tetramethyl ethylenediamine (TEMED), acrylamide (AM), *N,N'*-methylenebisacrylamide (BIS), were used as received. Hydrogel synthesis was performed by following an adapted protocol [1]. Comonomers were dissolved in a water:DMF mixture (60:40) and degassed before the addition of APS/TEMED. The curing mixture was spotted onto a hydrophobic glass slide and covered with a freshly prepared acrylated glass coverslip. PAM-CBT gels formed within 10 min, were rinsed with water and characterized by UV-Vis and fluorescence spectroscopies.

Results and Discussion: Novel CBT-AM comonomer was synthesized from inexpensive raw materials in three steps. Preliminary experiments indicated that CBT-AM is compatible with PAM free-radical polymerization, meaning that the CBT group of CBT-AM endures the

conditions used for PAM preparation. The pendant CBT groups in the hydrogel are then expected to remain available as anchoring sites for the chemoselective coupling of *N*-Cys-ligands. PAM hydrogels were prepared (Fig. 1A) at variable solid content (4-12 wt %) to adjust the biomaterial's mechanical strength to values representative of soft tissues ($G' \sim 1$ -50 kPa). The amount of CBT groups in the gel was varied by changing the content of CBT-AM comonomer between 0-5 mol%. Thin PAM-CBT hydrogels covalently attached to glass coverslips (15 mm diameter) were obtained in one step, and resulted translucent to the naked eye. The increasing amount of CBT-AM in the gels was proven by UV-Vis measurements of the thin films, thereby showing the increased absorbance at 320 nm, due to the inherent absorbance of CBT (Figure 1B). This result demonstrated the effective incorporation of the CBT-AM monomer by free radical polymerization. Furthermore, the previously reported fluorescent properties of CBT moiety was also evident in the hydrogels when irradiated at 320 nm (Figure 1C). This result supports the successful incorporation of CBT pendant groups to the hydrogel network, which can be used in a subsequent step for biofunctionalization.

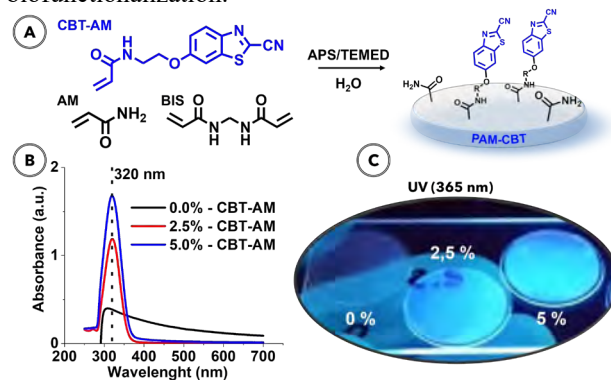


Figure 1. A) Reaction scheme showing preparation of PAM-CBT hydrogels. B) UV-Vis spectroscopy characterization of PAM-CBT gels. C) Pictures of fluorescent PAM-CBT gels attached to coverslips, when irradiated at 365 nm.

Conclusions: A novel comonomer compatible with free-radical polymerization was successfully synthesized and incorporated into PAM hydrogels. Ongoing work focuses in studying the reactivity of the immobilized CBT towards *N*-Cys-containing ligands such as fluorescent dyes and biofunctional molecules (e.g., cell-adhesive RGD peptide). We will study the effect of these ligands in cell behaviour. This strategy will be useful to implement bioinspired strategies for the biofunctionalization of tunable 2D-cell culture models.

References:

- [1] Farrukh, A. et al. *Angew. Chem. Int. Ed.* **2016**, *55*, 2092. [2] M. Jin, G. Kocer, J. I. Paez*, *ACS Appl. Mater. Interfaces* **2022**, in press, doi.org/10.1021/acsami.1c22186.

DNA Modified MSN Films as Versatile Biointerfaces to Study Stem Cell Adhesion Processes

X. Zhang, S. van Rijt

Department of Instructive Biomaterials Engineering, MERLN Institute for Technology-Inspired Regenerative Medicine, Maastricht University, P.O. Box 616, 6200 MD Maastricht, the Netherlands

Introduction

Stem cells, with an inherent ability to self-renew and the potential to differentiate into specialized cells, have great potential in the regenerative medicine field. However, an ongoing challenge in their clinical translation is control over their behavior once transplanted. In their natural environment, stem cell fate is regulated by their interaction with extracellular matrix (ECM), mainly through integrin-mediated cell adhesion. Integrin-mediated adhesion not only provide stem cells anchoring points but also directs their fate such as stem cell differentiation and self-renewal. As such, integrin-mediated stem cell adhesion processes are an important field of study to understand, predict and control stem cell behaviors. 2D biointerfaces that selectively present ECM ligands can be used as valuable tools to study and improve our understanding on stem cells adhesion processes. Mesoporous silica nanoparticles (MSNs) have promising characteristics to develop 2D biointerfaces, which include high surface area, mesoporous structure and high control over their size and shape. In this project, we aim to develop a new type of biointerface based on DNA functionalized mesoporous silica nanoparticles (MSN-DNA) to study stem cell adhesion.

Materials and Methods

MSN-ssDNA synthesis: MSN-NH₂ were synthesized based on a sol-gel co-condensation process [1]. To create the DNA modified MSN, MSN-NH₂ were modified with a Mal-PEG_n-NHS linker (n=6, 8 or 12) to form MSN-L. Then, a thiol functionalized ssDNA was grafted onto the PEG linker modified MSN (MSN-L) by thiol-maleimide reaction. DNA functionalized MSN (MSN-ssDNA) with varying PEG linker length were developed in the study and designated as MSN-L₆-ssDNA, MSN-L₈-ssDNA, MSN-L₁₂-ssDNA. MSN and MSN-ssDNA were characterized with Transmission electron microscopes (TEM).

MSN-dsDNA-RGD film preparation: To create the films, concentrated MSN-ssDNA nanoparticle suspension was spun over a plasma-treated coverslip. MSN-ssDNA films were characterized with Scanning electron microscope (SEM) and Water contact angle (WCA). Then, cell adhesion tripeptide RGD was conjugated to a complementary DNA strand, which could specifically bind to MSN-ssDNA to create MSN-dsDNA-RGD films. Finally, the morphology of human mesenchymal stromal cells (hMSC) on fabricated MSN films was analyzed by DAPI and phalloidin staining.

Result and Discussion

TEM images show that MSN-NH₂, MSN-L₆ and MSN-L₆-ssDNA have a spherical shape and a porous structure. DNA surface modification resulted in a less visible porous structure (Fig.1a and b). SEM showed that DNA modified MSN could be homogeneously spin coated to form a continuous layer of nanoparticles over the glass substrate (Fig.1c). The WCA measured on nanoparticles

coated glass was lower than that measured on plasma treated glass, which indicated an increase in surface hydrophilicity due to hydrophilic PEG linker and DNA modification (Fig.1d). Fluorescent microscopy images showed that MSN-dsDNA-RGD films could promote hMSCs adhesion and spreading, whereas MSN-dsDNA films without RGD resulted in poor cell spreading with round morphology, and low cell adhesion (Fig.2). In addition, we showed that cell adhesion to the films is PEG length-dependent.

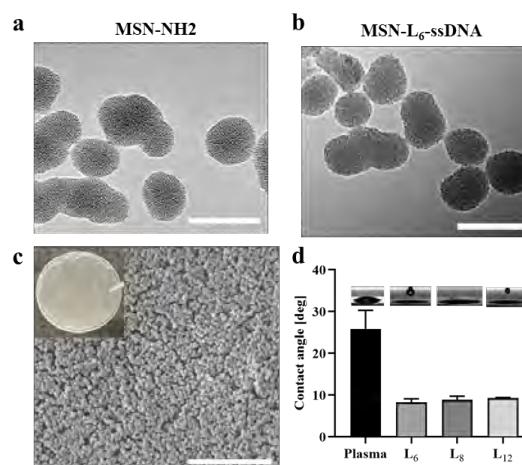


Fig.1 TEM images of a) MSN-NH₂ and b) MSN-L₆-ssDNA (scale bar=200 nm). c) SEM images of MSN-L₆-ssDNA films (scale bar=2 μm). d) WCA of glass surfaces before and after coating with different MSN-L-ssDNA.

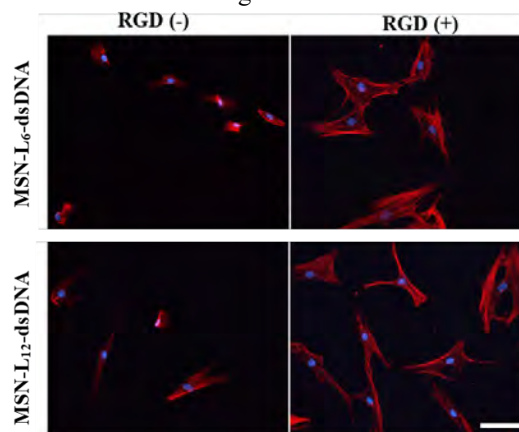


Fig.2 Representative fluorescence micrographs of hMSC cultured on MSN-L-dsDNA films with and without RGD for 1 day. Scale bar represents 100 μm.

Conclusion

In conclusion, DNA can be successfully surface grafted to MSN using various PEG linkers. MSN modified with PEG and ssDNA can be spin coated to create homogenous, stable and biocompatible films, which can be used as a novel and versatile 2D biointerface to study ligand-induced stem cell adhesion processes.

Reference

[1] Journal of the American Chemical Society 2009, 131, 11361.